Analysis of Tests of Subsurface Injection, Storage, and Recovery of Freshwater in Lancaster, Antelope Valley, California

U.S. Geological Survey
Water-Resources Investigations
Report 03-4061

Prepared in cooperation with the Los Angeles County Department of Public Works and the Antelope Valley-East Kern Water Agency

Analysis of Tests of Subsurface Injection, Storage, and Recovery of Freshwater in Lancaster, Antelope Valley, California

By Steven P. Phillips, Carl S. Carlson, Loren F. Metzger, James F. Howle, Devin L. Galloway, Michelle Sneed, Marti E. Ikehara, Kenneth W. Hudnut, *and* Nancy E. King

U.S. GEOLOGICAL SURVEY

Water-Resources Investigations Report 03-4061

Prepared in cooperation with the

LOS ANGELES COUNTY DEPARTMENT OF PUBLIC WORKS
ANTELOPE VALLEY–EAST KERN WATER AGENCY

7212-55

Sacramento, California
2003

U.S. DEPARTMENT OF THE INTERIOR

GALE A. NORTON, *Secretary*

U.S. GEOLOGICAL SURVEY

Charles G. Groat, *Director*

CONTRIBUTING U.S. GEOLOGICAL SURVEY STAFF

Technical Support

Michael R. Carpenter, Hydrologist
Art Clark and Central Region drill crew
Allen H. Christensen, Hydrologist
Wesley R. Danskin, Research Hydrologist
John R. Freckleton, Hydrologist
A. Scott Lewis, Hydrologic Technician
Tracy Nishikawa, Research Hydrologist
Donald R. Pool, Hydrologist
Diane L. Rewis, Hydrologist
Eric G. Reichard, Research Hydrologist
Francis S. Riley, Hydrologist

Editorial, Graphical and Text Preparation Team

Susan G. Davis, Production Editor
Myrna DeBortoli, Technical Editor
Mary Gibson, Editorial Assistant
David Uyematsu, Scientific Illustrator

Any use of trade, product, or firm names in this publication is for descriptive purposes only and does not imply endorsement by the U.S. Government.

For additional information write to:

District Chief
U.S. Geological Survey
Placer Hall—Suite 2012
6000 J Street
Sacramento, CA 95819-6129
http://ca.water.usgs.gov

CONTENTS

Abstract 1
Introduction 2
Description of Study Area 4
Acknowledgments 5
Geohydrologic Framework 6
Stratigraphy 6
Conceptual Layering of Aquifer System 8
Ground-Water Movement 10
Land Subsidence 11
Tests of Freshwater Injection 13
Preliminary Tests, 1994 13
Pilot Tests, 1996–98 18
Site Description 18
Test Procedure 18
Monitoring of Hydraulic Response 22
Historical Water Levels 22
Water-Level Network and Conditions Prior to Injection Testing 22
Water-Level Network Response to Injection Cycles 24
Water-Level Response Determined from Gravimetric Response 31
Monitoring of Subsidence-Related Effects 33
Borehole Extensometers 33
Continuous GPS 33
Spirit Leveling 37
Tiltmeters 37
Monitoring of Water Chemistry 37
Analysis of Injection Test Results 46
Hydraulic Properties 46
Aquifer-System Deformation and Subsidence-Related Properties 46
Uplift of Land Surface During Injection 46
Estimation of Subsidence-Related Storage Properties at the Extensometer Site 48
Areal Distribution of Subsidence-Related Storage Properties 50
Chemical Response 54
Potential for Mineral Precipitation 54
Recovery of Injected Water 54
Effects of Injection on Ground-Water Chemistry 55
Development of a Numerical Model of Ground-Water Flow in the Lancaster Area 56
Model Grid and Boundary Conditions 57
Initial Conditions and Temporal Discretization 62
Hydraulic Properties of the Aquifer System 62
Recharge and Discharge 64
Natural Recharge 64
Other Forms of Recharge 66
Ground-Water Extraction 70
Model Calibration and Sensitivity 71
Phase I Calibration 73
Phase II Calibration 75

Sensitivity Analysis 84
Appropriate Use and Improvement of the Ground-Water-Flow Model 90
Limitations of Numerical Models 90
Other Factors that Constrain Appropriate Use of the Model 90
Potential Improvements 91
Development of a Simulation/Optimization Model 92
Model Objective 93
Constraints on Water Supply and Demand 93
Imported Water-Supply Constraint 93
Ground-Water-Supply Constraints 94
Ground-Water Demand Constraint 97
Constraints on Hydraulic Head 98
Model Components and Conversion to Uniform Grid 100
Nonlinear Effects 101
Preliminary Simulation/Optimization (LANOPT) Model Results 102
Comparison of Simulation/Optimization (LANOPT) Model Results for Scenarios 103
Sensitivity Analysis of Simulation/Optimization (LANOPT) Model 113
Appropriate Use and Improvement of the Simulation/Optimization (LANOPT) Model 114
Assumptions Made during Model Development 114
Limitations Associated with the Software 115
Potential Improvements 117
Summary And Conclusions 118
References Cited 119

FIGURES

Figure 1. Map showing generalized surficial geology and location of study area and model area in Antelope Valley, California 3
Figure 2. Graph showing population of Lancaster and Palmdale, Antelope Valley, California, 1970 to 1999 5
Figure 3. Conceptual geologic cross section showing generalized alluvial fan lithology above the lacustrine unit, Antelope Valley, California 7
Figure 4. Cross section showing delineation of aquifers and lacustrine unit, Antelope Valley, California 9
Figure 5. Graph showing velocity log, during extraction, for Los Angeles County Department of Public Works (LACDPW) well 4-32 (7N/12W-27P2), Antelope Valley, California 10
Figure 6. Map showing ground-water-level contours based on data from wells perforated in the upper or upper and middle aquifers, April 1996, Lancaster, Antelope Valley, California..... 11
Figure 7. Map showing land subsidence (1930–92) determined from leveling and Global Positioning System surveys (Ikehara and Phillips, 1994) and from interferometric synthetic aperture radar (InSAR) from October 1993 to December 1995, in Lancaster, Antelope Valley, California 12
Figure 8. Map showing location of injection and extensometer sites, Lancaster, Antelope Valley, California 17
Figure 9. Diagram and map of injection site showing location of piezometers 7N/12W-27P5–P8 and Los Angeles County Department of Public Works (LACDPW) production wells 7N/12W-27P2–P3, Lancaster, Antelope Valley, California 19
Figure 10. Diagram and map of injection site showing location of piezometers 7N/12W-27F5–F8, extensometers 7N/12W-27F9–F10, and Los Angeles County Department of Public Works (LACDPW) production wells 7N/12W-27F2–F3, Lancaster, Antelope Valley, California 20
Figure 11. Graph showing time line of activities associated with injection cycles 1–3 at Lancaster, Antelope Valley, California 21
Figure 12. Graphs showing injection and extraction flow rates for wells 7N/12W-27P2 and -27P3 in Lancaster, Antelope Valley, California, 1996–98 23
Figure 13. Hydrograph showing periodic measurements in the injection wells (7N/12W-27P and 27P3) in Lancaster, Antelope Valley, California, March 1996 through June 1997 24
Figure 14. Hydrograph showing historical water levels in or near Lancaster and Palmdale, Antelope Valley, California, 1948–99 25
Figure 15. Map showing locations of nested piezometers and current or former extraction wells used in the ground-water-level monitoring network, Lancaster, Antelope Valley, California 26
Figure 16. Map showing water levels and approximate water-level contours near injection site, before injection cycle 2, Lancaster, Antelope Valley, California, November 1996 27
Figure 17. Hydrographs showing piezometers and wells closest to injection wells in Lancaster, Antelope Valley, California 28
Figure 18. Hydrograph showing variability in water-level response to injection cycle 2, Lancaster, Antelope Valley, California 31
Figure 19. Hydrographs showing water levels for the upper, middle, and deep aquifers at the injection and extensometer sites during injection cycle 3, Lancaster, Antelope Valley, California 32
Figure 20. Map showing locations of gravity stations, Lancaster, Antelope Valley, California 34
Figure 21. South–north profile showing change in gravity from pre-injection survey (November 1996) to post-injection survey (April 1997) near Lancaster, Antelope Valley, California 35
Figure 22. Graphs showing aquifer-system deformation and water levels during injection cycles 1–3, Lancaster, Antelope Valley, California in (*A*) the upper aquifer and middle aquifer above the lacustrine unit and (*B*) the lacustrine unit and upper part of the lower aquifer, 1996–98 36

Figure 23. Graph showing Change in land-surface elevation at the injection site from continuous Global Positioning System (GPS) daily solutions for selected periods of injection cycles 1–3, Lancaster, Antelope Valley, California 38
Figure 24. Map showing locations of bench marks used to monitor changes in land-surface altitude, Lancaster, Antelope Valley, California 39
Figure 25. Graph showing change in land-surface altitude of bench marks and gravity stations along the south–north survey line, 1995–98, Lancaster, Antelope Valley, California 40
Figure 26. Map showing locations of tiltmeters used to monitor land-surface deformation near Lancaster, Antelope Valley, California 41
Figure 27. Graphs showing magnitude (note variable scale) and direction of tilt recorded during injection cycle 2 at tiltmeters 1N, 2N, and 3N, Lancaster, Antelope Valley, California 42
Figure 28. Piper diagram showing chemical contrast between native ground water and injected water, Lancaster, Antelope Valley, California 43
Figure 29. Graph showing chloride concentrations in injected and extracted water during injection cycles 1–3, Lancaster, Antelope Valley, California 45
Figure 30. Graph showing trihalomethane (THM) concentrations in injected and extracted water during injection cycles 1–3, Lancaster, Antelope Valley, California 45
Figure 31. Continuous plot from April 1996 to December 1998 of depth to water (stress) versus compaction (strain) for (*A*) the upper and middle aquifers and (*B*) lacustrine unit plus upper part of lower aquifer, Lancaster, Antelope Valley, California 49
Figure 32. Borehole geophysical logs, well-construction diagrams, and lithologic logs for nested piezometers 7N/12W27-F5–F8 at the extensometer site, Lancaster, Antelope Valley, California 51
Figure 33. Map showing active region of the LAN model grid, Lancaster, Antelope Valley, California 58
Figure 34. Generalized sections *A–A´* from south to north and *B–B´* from northwest to southeast through injection site showing delineation of model layers for the Lancaster area (LAN) and regional (AV) models, Antelope Valley, California 59
Figure 35. Map showing lateral boundary conditions for layer 1 of the LAN model and 1996 water-level contours (modified from Carlson and others, 1998) used to define no-flow boundaries coincident with flowlines or ground-water divides, Lancaster, Antelope Valley, California 60
Figure 36. Maps showing contours of measured water levels for (*A)* spring 1983 (used as initial head values for both layers of the LAN model) and (*B*) April 1996 (modified from Carlson and others, 1998) in Lancaster, Antelope Valley, California 61
Figure 37. Graph showing estimated historical annual total and agricultural pumpage in the Antelope Valley ground-water basin, California 63
Figure 38. Map showing thickness of model layer 2, Lancaster, Antelope Valley, California 64
Figure 39. Maps showing distribution and values of hydraulic conductivity in the Lancaster-area (LAN) model, Antelope Valley, California. (*A*) initial values based on regional (AV) model (Leighton and Phillips, 2003), and (*B*) final calibrated values 65
Figure 40. Map showing distribution and magnitude of recharge in the Lancaster-area (LAN) model, upper and middle aquifers only, Antelope Valley, California 67
Figure 41. Graphs showing data and estimates for (*A*) recharge, (*B*) pumpage, (*C*) seasonal distribution of pumpage, and (*D*) a comparison of recharge and pumpage, in the model area, upper and middle aquifers only, Lancaster, Antelope Valley, California 69
Figure 42. Map showing locations of production wells included in the Lancaster-area (LAN) model in Lancaster, Antelope Valley, California 70
Figure 43. Map showing location of wells and piezometers used in model calibration, Lancaster, Antelope Valley, California 72

Figure 44. Diagram showing results of phase II calibration procedure for layer-1 hydraulic conductivity values (K_1), of (*A*) 12, (*B*) 15, and (*C*) 18 76
Figure 45. Diagram showing approximate predicted values of hydraulic conductivity (in foot per day) of layer 2 (K2) and effective vertical hydraulic conductivity (*KV*) compared to those determined from the phase II calibration procedure for layer-1 hydraulic conductivity (K1) of 8 feet per day 79
Figure 46. South-to-north profile with gravity-determined water-level changes compared to simulated injection mound geometries for a range of hydraulic conductivities, Lancaster, Antelope Valley, California 80
Figure 47. Contour map based on measured water levels and those simulated using the calibrated LAN model, Lancaster, Antelope Valley, California 81
Figure 48. Hydrographs of wells with long-term records during the calibration period, Lancaster, Antelope Valley, California 82
Figure 49. Hydrographs of wells and piezometers with dense data during injections tests, Lancaster, Antelope Valley, California 83
Figure 50. Plots showing sensitivity of calibrated hydraulic conductivities and simulated water levels near the injection site to changes in model variables, Lancaster, Antelope Valley, California 86
Figure 51. Graphs showing historical deliveries of State Water Project water by the Antelope Valley–East Kern Water Agency (AVEK), Lancaster, Antelope Valley, California 94
Figure 52. Map showing historical and recent land subsidence, and locations of Los Angeles County Department of Public Works (LACDPW) wells, Lancaster, Antelope Valley, California 95
Figure 53. Graphs showing water delivered in Lancaster by the Los Angeles County Department of Public Works (LACDPW) and projected ground-water demand used in the simulation/optimization model, Lancaster, Antelope Valley, California 99
Figure 54. Map showing location and dimensions of uniformly spaced model grid used in the simulation/optimization model, and simulated and measured water levels for April 1996, Lancaster, Antelope Valley, California 101
Figure 55. Hydrographs showing variable- versus uniform-grid results, Lancaster, Antelope Valley, California 102
Figure 56. Graphs showing graphical results from simulation/optimization (LANOPT) model for four hypothetical management scenarios, Lancaster, Antelope Valley, California 104
Figure 57. Graphs showing optimal well capacity used for injection and extraction for three hypothetical management scenarios for Lancaster, Antelope Valley, California 111
Figure 58. Graph showing optimal volumes of injection and extraction during the management period for three hypothetical management scenarios, Lancaster, Antelope Valley, California 112
Figure 59. Graph showing water-table results from linear optimization and the ground-water-flow model using optimal injection and pumping rates for scenario 4 (all existing and proposed wells for injection during six months of the year), Lancaster, Antelope Valley, California 116

TABLES

Table 1. Construction and other data for wells used in the study, Antelope Valley, California 14
Table 2. Range and comparison of hydraulic conductivity values estimated during phase II of the model calibration for Lancaster, Antelope Valley, California 78
Table 3. Estimated maximum and long-term capacities of existing and proposed potential injection/extraction wells in Lancaster, Antelope Valley, California 96
Table 4. Summary of simulation/optimization model objective and constraints, Lancaster, Antelope Valley, California 103
Table 5. Results from the simulation/optimization model for four hypothetical management scenarios for Lancaster, Antelope Valley, California, for management period 2000–2010 108
Table 6. Effect of proposed wells on the objective value (2,083 feet without proposed wells), Lancaster, Antelope Valley, California 113
Table 7. Effect of changes in optimization constraints on results from simulation/optimization (LANOPT) model of Lancaster, Antelope Valley, California, for management period, 2000–2010 114

CONVERSION FACTORS, VERTICAL DATUM, AND ABBREVIATIONS

CONVERSION FACTORS

Multiply	By	To obtain
acre	0.4047	hectometer
acre-foot (acre-ft)	0.001233	cubic hectometer
acre-foot per year (acre-ft/yr)	0.001233	cubic hectometer per year
centimeter (cm)	0.3937	inch
cubic foot per day (ft^3/d)	0.02832	cubic meter per day
foot (ft)	0.3048	meter
foot per day (ft/d)	0.0348	meter per day
foot per second (ft/s)	0.0348	meter per second
foot per day (ft/yr)	0.0348	meter per year
foot per year (ft/yr)	0.3048	meter per year
gallon per minute (gal/min)	0.06309	liter per minute
inch (in.)	25.4	millimeter
inch per year (in./yr)	25.4	millimeter per year
mile (mi)	1.609	kilometer
square miles (mi^2)	2.590	square kilometer

Temperature in degrees Celsius (^oC) may be converted to degrees Fahrenheit (^oF) as follows:

$$^oF=1.8\ ^oC+32.$$

Temperature in degrees Fahrenheit (^oF) may be converted to degrees Celsius (^oC) as follows:

$$^oC=(^oF-32)/1.8.$$

Changes in land-surface altitudes from differential-leveling surveys were measured in metric units and shown in this report as metric units so that comparisons can be made with Global Positioning System (GPS) data shown in this report. Coordinates determined by GPS surveying generally are reported in metric units. The industry standard for GPS usage is that field measurements are done in the metric system.

Specific conductance is given in microsiemens per centimeter at 25 degrees Celsius (µS/cm at 25°C).

Concentrations of chemical constituents in water are given either in milligrams per liter (mg/L) or micrograms per liter (µg/L).

VERTICAL DATUM

Sea level: In this report, “sea level” refers to the National Geodetic Vertical Datum of 1929 (NGVD of 1929)—a geodetic datum *derived* from a general adjustment of the first-order level nets of both the United States and Canada, formerly called Sea Level Datum of 1929.

Abbreviations

AFB	Air Force Base
AVEK	Antelope Valley–East Kern Water Agency
Br^-	bromide
$CHBr_3$	bromoform
$CHCl_3$	chloroform
Cl_2	chlorine gas
DBP	disinfection by-products
DOC	dissolved organic carbon
GPS	Global Positioning System
HOBr and OBr^-	hypobromous acid
HOC1 and $OC1^-$	hypochlorous acid
InSAR	Interferometric Synthetic Aperture Radar
LACDPW	Los Angeles County Department of Public Works
LAN	ground-water-flow model of the Lancaster area (simulated)
LANOPT	simulation/optimization model (modified version of the LAN model)
MODFLOW	modular three-dimensional dinite-difference ground-water-flow model
SCAG	Southern California Association of Governments
SCIGN	Southern California Integrated GPS Network
SWP	State Water Project
TDS	total dissolved solids
THM	trihalomethanes
USGS	U.S. Geological Survey

cm	centimeter
m	meter
mm	millimeter
mm/yr	millimeter per year
µGal	microgal

WELL-NUMBERING SYSTEM

Wells are identified and numbered according to their location in the rectangular system for the subdivision of public lands. Identification consists of the township number, north or south; the range number, east or west; and the section number. Each section is divided into sixteen 40-acre tracts lettered consecutively (except I and O), beginning with "A" in the northeast corner of the section and progressing in a sinusoidal manner to "R" in the southeast corner. Within the 40-acre tract, wells are sequentially numbered in the order they are inventoried. The final letter refers to the base line and meridian. In California, there are three base lines and meridians; Humboldt (H), Mount Diablo (M), and San Bernardino (S). All wells in the study area are referenced to the San Bernardino base line and meridian (S). Well numbers consist of 15 characters and follow the format 007N012W34B001S. In this report, well numbers are abbreviated and written 7N/12W-34B1. Wells in the same township and range are referred to only by their section designation, 34B1. The following diagram shows how the number for well 7N/1W-34B1 is derived.

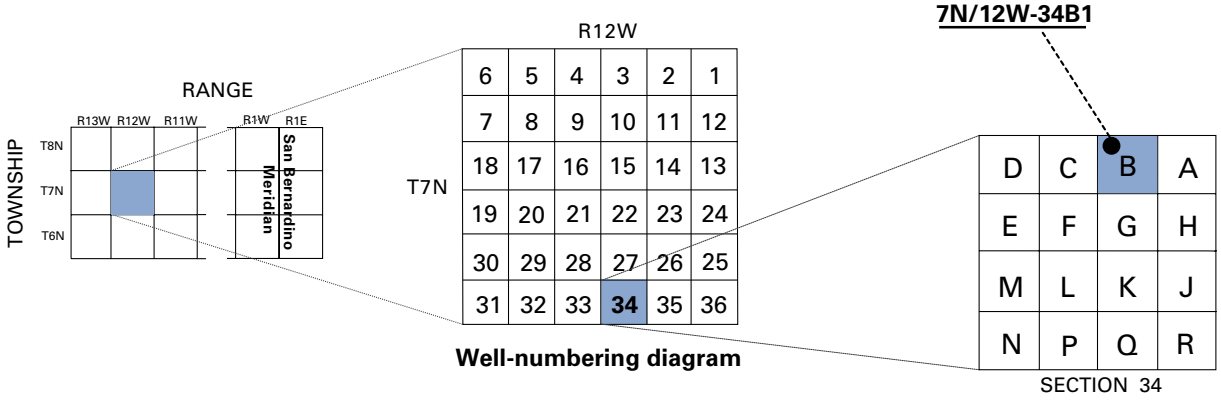

Well-numbering diagram

Analysis of Tests of Subsurface Injection, Storage, and Recovery of Freshwater in Lancaster, Antelope Valley, California

By Steven P. Phillips, Carl S. Carlson, Loren F. Metzger, James F. Howle, Devin L. Galloway, Michelle Sneed, Marti E. Ikehara, Kenneth W. Hudnut, *and* Nancy E. King

ABSTRACT

Ground-water levels in Lancaster, California, declined more than 200 feet during the 20th century, resulting in reduced ground-water supplies and more than 6 feet of land subsidence. Facing continuing population growth, water managers are seeking solutions to these problems. Injection of imported, treated fresh water into the aquifer system when it is most available and least expensive, for later use during high-demand periods, is being evaluated as part of a management solution. The U.S. Geological Survey, in cooperation with the Los Angeles County Department of Public Works and the Antelope Valley–East Kern Water Agency, monitored a pilot injection program, analyzed the hydraulic and subsidence-related effects of injection, and developed a simulation/optimization model to help evaluate the effectiveness of using existing and proposed wells in an injection program for halting the decline of ground-water levels and avoiding future land subsidence while meeting increasing ground-water demand.

A variety of methods were used to measure aquifer-system response to injection. Water levels were measured continuously in nested (multi-depth) piezometers and monitoring wells and periodically in other wells that were within several miles of the injection site. Microgravity surveys were done to estimate changes in the elevation of the water table in the absence of wells and to estimate specific yield. Aquifer-system deformation was measured directly and continuously using a dual borehole extensometer and indirectly using continuous Global Positioning System (GPS), first-order spirit leveling, and an array of tiltmeters. The injected water and extracted water were sampled periodically and analyzed for constituents, including chloride and trihalomethanes. Measured injection rates of about 750 gallons per minute (gal/min) per well at the injection site during a 5-month period showed that injection at or above the average extraction rates at that site (about 800 gal/min) was hydraulically feasible.

Analyses of these data took many forms. Coupled measurements of gravity and water-level change were used to estimate the specific yield near the injection wells, which, in turn, was used to estimate areal water-table changes from distributed measurements of gravity change. Values of the skeletal components of aquifer-system storage, which are key subsidence-related characteristics of the system, were derived from continuous measurements of water levels and aquifer-system deformation. A numerical model of ground-water flow was developed for the area surrounding Lancaster and used to estimate horizontal and vertical hydraulic conductivities. A chemical mass balance was done to estimate the recovery of injected water.

The ground-water-flow model was used to project changes in ground-water levels for 10 years into the future, assuming no injection, no change in pumping distribution, and forecasted increases in ground-water demand. Simulated ground-water levels decreased throughout the Lancaster area, suggesting that land subsidence would continue as would the depletion of ground-water supplies and an associated loss of well production capacity. A simulation/optimization model was developed to help identify optimal injection and extraction rates for 16 existing and 13 proposed wells to avoid future land subsidence and to minimize loss of well production capacity while meeting increasing ground-water demands. Results of model simulations suggest that these objectives can be met with phased installation of the proposed wells during the 10-year period. Water quality was not considered in the optimization, but chemical-mass-balance results indicate that a sustained injection program likely would have residual effects on the chemistry of ground water.

INTRODUCTION

Ground water is an important component of the water supply in Antelope Valley, California (fig. 1), accounting for about 60 percent of the supply in years that have normal rainfall and as much as 90 percent in times of drought (Templin and others, 1995). Lancaster, which had a population of about 126,900 in 1998, is the largest city in the valley followed closely by Palmdale (California Department of Finance, 1999, accessed June 1, 2000). Water delivered to Lancaster residents and businesses by the Los Angeles County Department of Public Works (LACDPW), Waterworks and Sewer Maintenance Division, represented about 26 percent of total water use in Antelope Valley in 1995 (Leighton and Phillips, 2003), of which about 50 percent was ground water (Los Angeles County Department of Public Works, unpublished data, 1998). The remainder of Lancaster's water supply is imported surface water from the State Water Project (SWP) treated to drinking-water standards by the Antelope Valley–East Kern Water Agency (AVEK). In recent years, the SWP generally was the primary source of water used in Lancaster (averaged 56 percent from 1995 to 1999). Use of ground water and water from the SWP varied with seasonal demand (Los Angeles County Department of Public Works, unpublished data, 1998).

Ground-water use in Antelope Valley in excess of recharge has caused ground-water levels to decline about 200 ft in the Lancaster area since the 1920s. Water levels presently are at or near historical lows (Carlson and others, 1998; Leighton and Phillips, 2003). Negative consequences of this decline include the depletion of ground-water resources, possible degradation of ground-water quality, and land subsidence. The depletion of ground-water resources, which in this case primarily is reflected in the lowering of the water table, has resulted in the withdrawal of water from older, deeply buried sediment. These sediments are less permeable and store less water than those already drained; thus, wells that are screened only within these older materials generally are less productive. Ground water drawn from deeper parts of the aquifer system generally is poorer in quality than water from the shallower parts. Several of the deeper wells in the Lancaster area recently have been shut down for exceedences of the current (1999) Environmental Protection Agency Maximum Contaminant Level for arsenic of 50 μg/L (Mustafa Ariki, Los Angeles County Department of Public Works, oral commun., 1999).

Measured land subsidence from ground-water withdrawal exceeded 6 ft in Lancaster from 1930 to 1992 (Ikehara and Phillips, 1994), and more recent evidence suggests that subsidence continues in this area (Galloway and others, 1998a). Negative consequences of land subsidence in Antelope Valley and similar areas include development of earth fissures; altered drainage gradients; increased flooding and erosion; failed well casings; structural damage to roads, buildings, pipelines, canals, homes, and other structures; and liability issues (Kennedy/Jenks Consultants, 1995; Prince and others, 1995; Galloway and others, 1999).

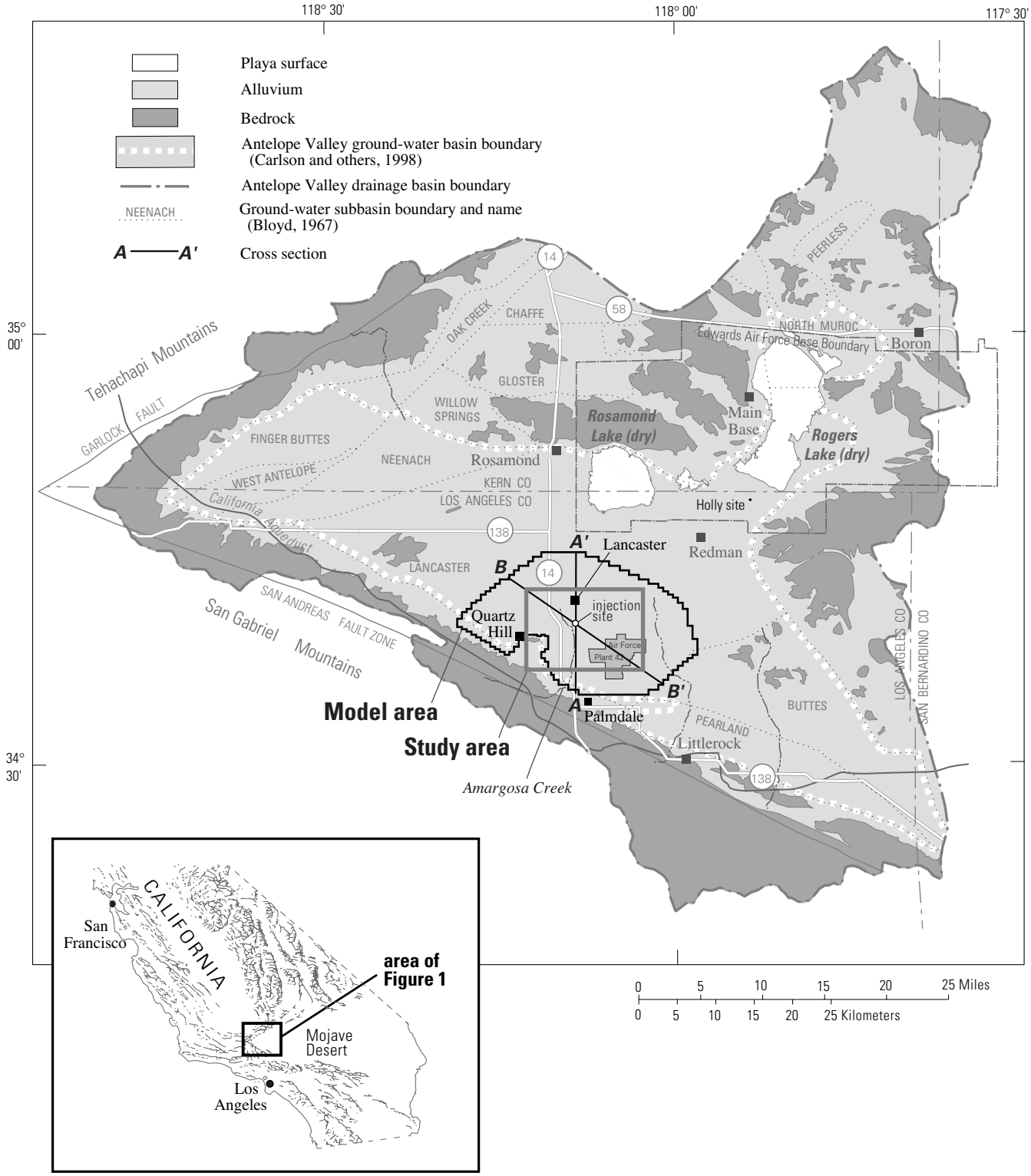

Figure 1. Generalized surficial geology and location of study area and model area in Antelope Valley, California.

(Modified from Londquist and others, 1993).

Facing future population growth and limited options for alternative water sources, water managers in Antelope Valley are seeking ways to make the best use of currently available resources. Injection of treated SWP water into the aquifer system during the winter (when it is most available) for later use in the summer (the peak demand period) is one potential element of a ground-water management plan. The U.S. Geological Survey (USGS), in cooperation with the LACDPW and AVEK, studied the feasibility of direct well injection through existing production wells and developed a simulation/optimization model to help evaluate the effectiveness of an injection program for halting the decline of ground-water levels and avoiding future land subsidence while meeting increasing ground-water demand.

The role of the USGS in this study was to collect and analyze hydraulic and aquifer-system deformation data, to develop a simulation/optimization model for use in designing and managing a larger scale injection program, and to determine the factors controlling the formation and fate of trihalomethanes (disinfection by-products) in the aquifer system. This report describes the analysis of hydraulic and deformation data and the development of a simulation/optimization model. Companion reports describe the data and the methods used to collect the data analyzed in this report (Metzger and others, 2002); the use of microgravity surveys to determine water-level changes (Howle and others, 2003); and the determination of the formation and fate of trihalomethanes (Fram and others, 2003; Fram and others, 2002).

This study was a cooperative effort between the USGS, LACDPW, and AVEK. The role of the LACDPW in this study was to conduct all engineering tasks required to convert existing production wells to injection/extraction wells; build the extensometer shelter; sample and analyze injected and extracted water during the injection tests; install tiltmeters and analyze resulting data; conduct repeat surveys for an extensive network of bench marks; and provide information for the simulation/optimization model. The role of AVEK in this study was to sample and analyze injected and extracted water during the tests, provide information for the simulation/optimization model, and provide the treated SWP water for the tests (more than 1,300 acre-ft).

Description of Study Area

Antelope Valley is the wedge-shaped western extension of the Mojave Desert, nestled between the Tehachapi and the San Gabriel Mountains to the northwest and southwest, respectively (fig. 1), and separated from the Mojave River Basin to the east by low-lying hills. The valley is topographically closed, with the valley floor ranging in altitude from about 3,500 ft adjacent to the foothills to about 2,270 ft at the playas. The climate in the valley is semiarid to arid, with less than 10 in./yr of rainfall (Rantz, 1969); the area has hot summers, cold winters, and high winds. Rainfall in Lancaster averaged 8 in./yr from 1974 to 1998 (Western Regional Climate Center, accessed July 10, 1999). The populations of Lancaster and Palmdale have grown rapidly during the past two decades, from a combined population of about 60,000 in 1980 to more than 250,000 in 1999 (fig. 2).

The Antelope Valley ground-water basin covers an area of about 940 mi^2 and is subdivided into seven ground-water subbasins (fig. 1). Previous investigators have defined the ground-water basin and subbasins therein on the basis of geologic, water-level, and other evidence of faults that act as partial barriers to ground-water flow (Thayer, 1946; Bloyd, 1967; Durbin, 1978; Nishikawa and others, 2001; Leighton and Phillips, 2003).

The study area is in the south-central part of the Antelope Valley ground-water basin, within the Lancaster subbasin (fig. 1). Included in the study area are most of the cities of Lancaster and Quartz Hill, and the western part of Air Force Plant 42. The aquifer system in the study area is characterized as three distinct aquifers: upper, middle, and lower (Nishikawa and others, 2001; Leighton and Phillips, 2003).

Running from south to north through the study area is the ephemeral Amargosa Creek (fig. 1). Although flow in this creek is infrequent, flashy, and ungaged, it is thought to be the third largest drainage from the San Gabriel Mountains within the Antelope Valley drainage basin (Durbin, 1978).

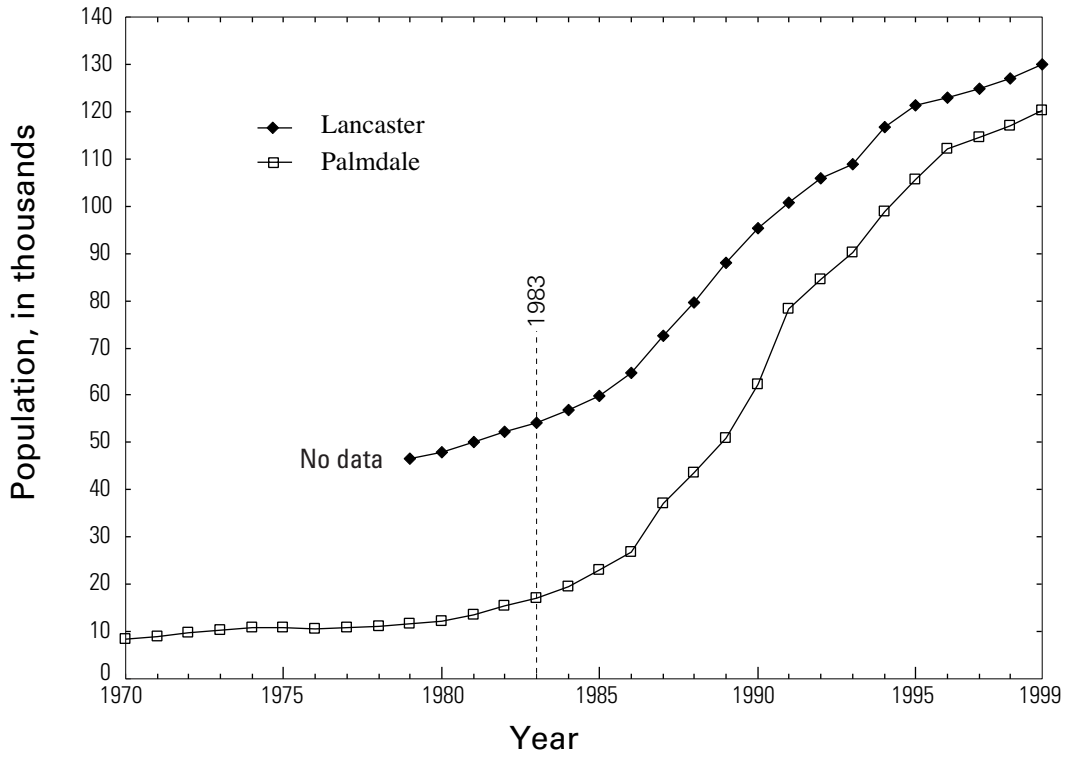

Figure 2. Population of Lancaster and Palmdale, Antelope Valley, California,1970 to 1999.

(California Department of Finance, accessed 1999. Yearly data plotted as January 1.)

Acknowledgments

The authors gratefully acknowledge the contributions of the LACDPW and AVEK toward the successful completion of this study. Individuals who provided assistance and support for this study include Eleni Hailu, Mustafa Ariki, Ramy Gindi, Dean Efstathiou, Joe Aja, Dan Jones, Kenneth Rosander, and Eugene Betts of the Los Angeles County Department of Public Works, and Wallace Spinarski and Russell Fuller of the Antelope Valley–East Kern Water Agency.

Field office personnel of the Los Angeles County Department of Public Works, Waterworks and Sewer and Maintenance Division, Lancaster, constructed a building to house the dual extensometer and shelters for two sets of nested piezometers, and kept the injection cycles running despite the various mechanical challenges that arose throughout the study.

Charles Peer, Gerald Campbell, and surveying crew of the Los Angeles County Department of Public Works Survey Division, assisted with the establishment and repeated surveying of the differential-leveling network. Robert Reeder and Darrel Bozarth of the Los Angeles County Department of Public Works, Survey Division, assisted in locating buried utilities and in organizing equipment, materials, and manpower for construction of the microgravity and differential-leveling networks.

Robert Larson of the Los Angeles County Department of Public Works, Materials Engineering Division, installed and operated the tiltmeter network.

Water-chemistry data and information on analytical methods were provided by Maureen Smith, Antelope Valley–East Kern Water Agency; Wilhelmina Solinap, Los Angeles County Department of Agricultural Commissioner and Weights and Measures, Environmental Toxicology Laboratory; and Ramy Gindi, Los Angeles County, Department of Public Works, Sewer and Maintenance Division.

Permission to access privately owned wells to measure water levels was provided by American Auto Sales Incorporated, the U.S. Department of the Air Force and Lockheed-Martin, the El Dorado Mutual Water Company, the West Side Park Mutual Water Company, and the White Fence Farms Water Company.

Tracy Nishikawa, Eric Reichard, John Freckleton, and Wesley Danskin provided technical assistance and constructive reviews of the optimization aspects of the modeling effort.

Francis Riley of the U.S. Geological Survey helped design the dual extensometer, provided guidance during its construction, and helped assemble the above-ground instrumentation. Diane Rewis assisted in the drilling effort and in establishing an electronic water-level monitoring network.

Donald Pool, U.S. Geological Survey, shared expertise in designing and implementing the microgravity surveys. Michael Carpenter, U.S. Geological Survey, provided useful insight regarding the performance characteristics of the particular gravity meter used in this study.

Kenneth Hudnut, U.S. Geological Survey, contributed the equipment and expertise for installing and operating a permanent continuous GPS station at the injection site, and processed the early data. Some of the GPS data was processed and provided by Jeffrey Behr, Southern California Earthquake Center. Additional GPS equipment was provided by Wayne Vallantine of the California Department of Transportation, Division 7.

Scott Lewis, U.S. Geological Survey, used ground-water chemistry data from the first two injection tests to estimate the percentage of injected water recovered.

GEOHYDROLOGIC FRAMEWORK

The San Gabriel Mountains along the southwestern margin of Lancaster subbasin were uplifted tectonically along the San Andreas Fault Zone about 1 to 2 million years ago and became the primary source of the Quaternary-age deposits that make up the aquifer system (Dibblee, 1967; Ponti, 1985). The Tehachapi Mountains were uplifted simultaneously along the Garlock Fault and became a secondary source of sediment (Dibblee, 1967). Prior to the uplift of these mountains, surface drainage was toward the ocean, and erosional degradation (transport of materials from the area, resulting in lesser slopes) occurred until drainage gradients were relatively small. Significant late-Tertiary deposition may have occurred on this surface (Reed, 1933; Dutcher and Worts, 1963; Dibblee, 1967). Uplift of the San Gabriel Mountains and the smaller Tehachapi Mountains, and probable downwarping in-between, formed the structurally closed Antelope Valley and greatly altered directions and patterns of Quaternary deposition in this area.

The rest of this section focuses on the Quaternary stratigraphy that forms the primary aquifer, the importance of stratigraphy in conceptualization of the aquifer system, ground-water movement, and land subsidence. More detailed accounts of the regional geologic history of Antelope Valley can be found in Thayer (1946), Hewett (1954a,b), Dutcher and Worts (1963), Dibblee (1967, 1981), Ponti (1985), and Londquist and others (1993).

Stratigraphy

About 5,000 to 10,000 ft of deposits of late-Tertiary and Quaternary deposits underlie the Lancaster area; these deposits are thickest in this part of the Lancaster subbasin (Mabey, 1960; Morin and others, 1990). The Quaternary deposits were formed by ephemeral streams emanating from the surrounding hills and mountains, depositing eroded material in alluvial fans. Modern alluvial fans are present in Antelope Valley (Ponti, 1985). If perennial streams were present in the geologic past, any fine-grained fluvial deposits are buried and not present at the land surface.

The existence of sand dunes in some parts of Antelope Valley is evidence that wind plays a role in the modern depositional environment. Little is known, however, about the presence and distribution of the older subterranean eolian (wind-laid) deposits.

Given the evidence of modern alluvial deposition and the lack of evidence for fluvial or substantial eolian deposits, the primary Quaternary depositional environment probably was alluvial. Alluvial fans are fan-shaped mounds that slope away from the mountains, often coalescing with adjacent alluvial fans or interfingering with intersecting fans. Alluvial fans have three parts: the fanhead at the highest altitude, the midfan, and the distal fan at the lowest altitudes (Blissenbach, 1954; Reineck and Singh, 1980). The texture of the alluvium varies with position on the fan as the stream gradient changes (fig. 3). The fanhead is characterized as a high-energy environment in which large stream gradients favor the transport and deposition of coarse-grained materials (gravel, sand), whereas the distal fan is characterized as a low-energy

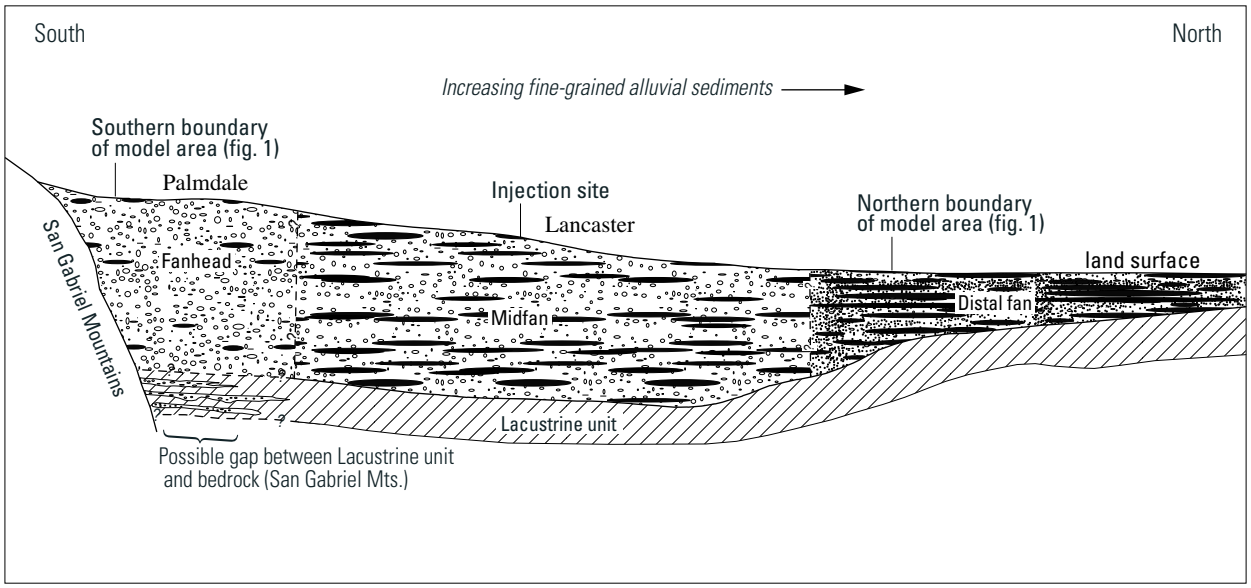

Figure 3. Generalized alluvial fan lithology above the lacustrine unit, Antelope Valley, California.

environment in which small gradients favor deposition of fine-grained materials (silt, clay). Unweathered (modern) alluvium ranges from about 4 percent silt and clay near the San Gabriel Mountains to 25 to 70 percent silt and clay in the sandy to silty loam soils typical of the more distal areas (Ponti, 1985). Texture also varies with depth below land surface and radial position on the fans, as rates of tectonic uplift, climatic conditions, and stream locations changed with time. Changing climatic conditions seem to be responsible for about six episodes of rapid alluvial fan aggradation (growth) during the upper Quaternary (Ponti, 1985). These episodes are marked by relatively rapid deposition followed by soil development and varying degrees of erosion prior to the next episode of deposition. The resulting alluvial strata are texturally and geometrically complex.

Interwoven with alluvial strata are lacustrine deposits associated with deposition of fine-grained materials at the bottom of areally extensive lakes and (or) marshes (Dibblee, 1967). These deposits are chemically reduced, indicative of a low-oxygen environment, and are characteristically grey to bluish- or greenish-grey. This is in contrast to the oxidized, brownish silty clays that comprise the modern playas (for example, Rogers and Rosamond Lakes). The primary lacustrine unit, referred to locally and by previous investigators (for example, Dutcher and Worts, 1963) as the “blue clay,” is present throughout most of the Lancaster subbasin; this unit is about 500 to 750 ft below land surface in the Lancaster area (fig. 3).

The elevation of the lacustrine unit increases to the north (fig. 3); the unit crops out west of the southern end of Rogers Lake on Edwards Air Force Base (AFB) (Nishikawa and others, 2001; Leighton and Phillips, 2003). This configuration of the lacustrine unit suggests northward migration of the lake or marsh with time and accumulation of material eroded from the San Gabriel Mountains (Dutcher and Worts, 1963). Paleomagnetic analyses of core samples from southern Lancaster were used to provide information on the age of the lacustrine unit. Core samples from depths of 345 and 450 ft below land surface show a magnetic reversal between these depths (Fram and others, 2002). The polarity was normal at a depth of 345 ft, but reversed at a depth of 450 ft, which was interpreted as the transition from the Brunhes to the Matuyama polarity chron. This transition occurred about 780,000 years ago; therefore, the lacustrine deposits, at a depth of more than 700 ft in the area, are older than that. In contrast, the lacustrine deposits on Edwards AFB interfinger with alluvial deposits less than 14,000 years old (Ponti, 1985).

Lithologic and geophysical logs of boreholes show little evidence of coarse-grained materials within the lacustrine unit at Edwards AFB and in the Lancaster area; however, lithologic logs for the Palmdale area show extensive interfingering of fine-grained lacustrine deposits and coarser grained alluvial deposits. The nature or presence of the lacustrine deposits at the contact between unconsolidated deposits and the foot of the San Gabriel Mountains is unknown; however, results of a ground-water-flow model of Antelope Valley suggest that this confining unit abuts the San Gabriel Mountains (Leighton and Phillips, 2003).

Many geophysical logs of boreholes in Antelope Valley suggest a disconformity between younger unconsolidated deposits and older, more compacted and indurated (hardened) deposits at an altitude of about 1,950 ft (Nishikawa and others, 2001; Leighton and Phillips, 2003).

Conceptual Layering of Aquifer System

The conceptual view of the aquifer system in Antelope Valley historically included two aquifers: an upper unconfined aquifer known locally as the "principal" aquifer and a "deep" aquifer overlain and confined by the thick, regionally extensive lacustrine unit where present (Durbin, 1978). The unconfined aquifer beyond the northern extent of the lacustrine unit (underlying part of Edwards AFB and northward) also was designated as the deep aquifer. Stratigraphic and other information collected for this study and other recent USGS studies in Antelope Valley (Nishikawa and others, 2001; Leighton and Phillips, 2003) has been used to change the historical conceptualization into three aquifers: upper, middle, and lower (fig. 4). In the study area, the lacustrine unit generally occupies the lower part of the middle aquifer, acting as a significant barrier to vertical flow between the middle and lower aquifers. Farther north, the lacustrine unit increases in elevation, forming a significant barrier to north–south ground-water flow within the middle and upper aquifers (fig. 4).

There are two key distinctions between the old and new conceptualizations of the aquifer system. The first is the recognition that the age of aquifer materials is a key factor controlling their hydraulic properties. Older materials have longer stress histories (compaction is more likely to have occurred) and are more likely to have undergone chemical cementation. Under the old conceptual model, surficial materials at Edwards AFB were considered part of the deep aquifer as were materials that started at a depth of about 900 ft below land surface in Lancaster. This configuration did not account for the differences in the age and depth of burial of the aquifer materials or the effects of these differences on hydraulic properties.

The second distinction between these conceptual models is a recognition that aquifer properties above the lacustrine unit in the study area vary significantly with depth. Geophysical evidence of such variations in the Lancaster and Edwards AFB areas suggests a disconformity (an erosional surface that separates the younger strata from parallel, underlying older strata) between the younger, unconsolidated deposits and the older, more compacted and indurated (hardened) deposits at an altitude of about 1,950 ft (Nishikawa and others, 2001; Leighton and Phillips, 2003). Other evidence includes greater hydraulic responses at depth to extraction and injection and results from a velocity log of one of the wells (7N/12W-27P2) used in the pilot injection tests. The velocity log was generated in 1998 during extraction using a dye-based method (Izbicki and others, 1999) and shows that most of the water produced from well 7N/12W-27P2 comes from the upper aquifer (fig. 5). The condition of the well screen and gravel pack may vary with depth, and thus, could have affected these results; however, the well screen (282–717 ft) was cleaned periodically during the project and inspected using a televiewer.

Aside from the physical evidence of variation in aquifer properties with depth, storage properties generally change with increasing depth from the water table in alluvial aquifers. At the water table, water drawn from the aquifer is obtained through drawdown of the water table and associated gravity drainage of the materials above the new water table. Water drawn at depth in an alluvial system cannot be immediately drawn from the water table because the vertical flow path is partly blocked by numerous overlapping bodies of fine-grained deposits. Instead, the immediate demand for water is met primarily through compaction of these deposits in response to decreased water pressure in pore spaces between grains of sediment. The storage values at depth, therefore, are much smaller than those at the water table.

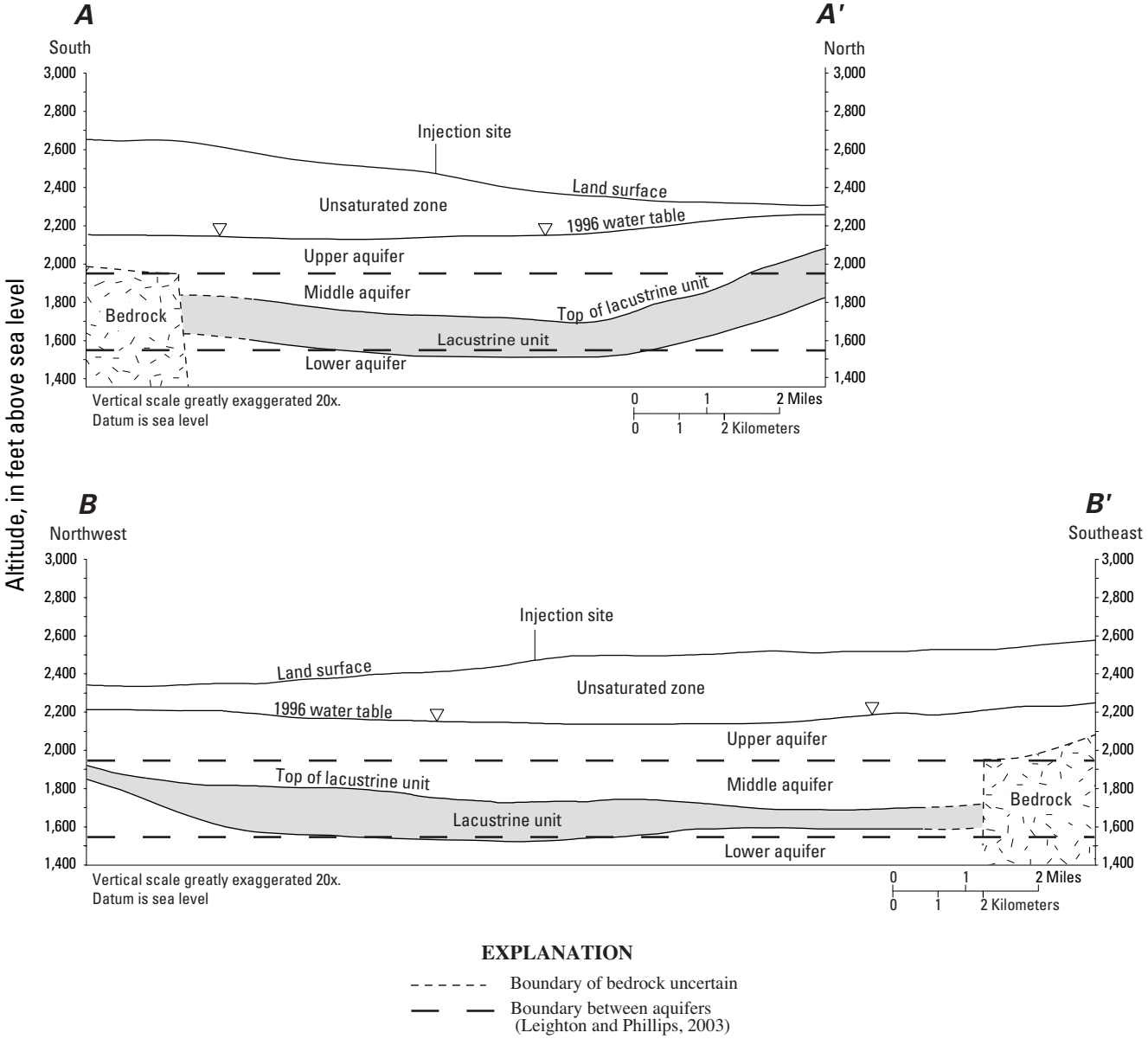

Figure 4. Delineation of aquifers and lacustrine unit, Antelope Valley, California.

Cross-section locations shown in figure 1.

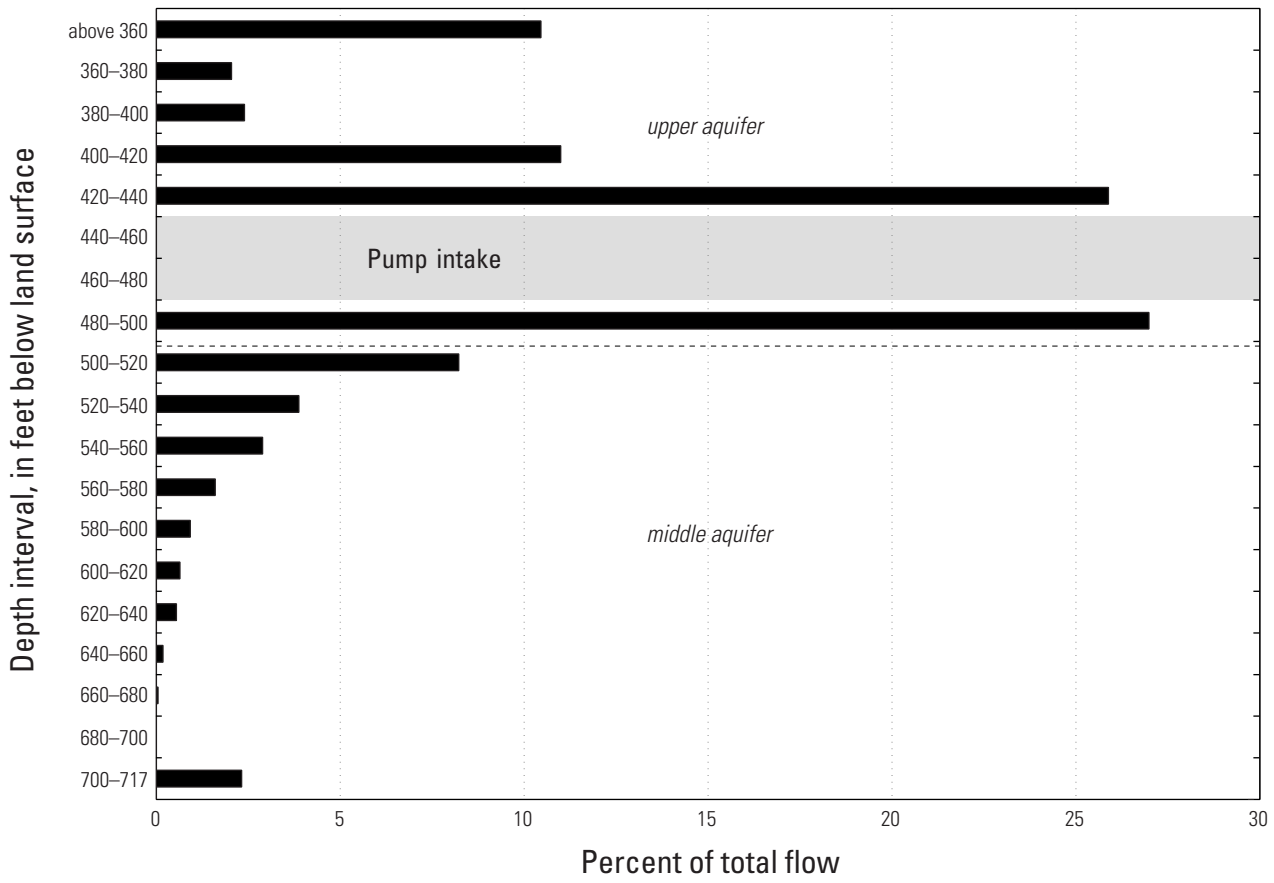

Figure 5. Velocity log, during extraction, for Los Angeles County Department of Public Works (LACDPW) well 4-32 (7N/12W-27P2), Antelope Valley, California.

Ground-Water Movement

Ground-water movement in the vicinity of the study area prior to significant development of ground water in the early 1900s was from the recharge zones where streams draining the San Gabriel and the Tehachapi Mountains enter the valley toward the playas in the northern part of the valley. Most of the discharge occurred as evapotranspiration within and surrounding these playas (Durbin, 1978; Leighton and Phillips, 2003). Since the post-World War II agricultural boom, ground-water movement has been toward the production wells, which is evident in the contour map of 1996 water levels in the vicinity of Lancaster and Palmdale (fig. 6). Note that ground-water movement generally is toward the urban areas of Lancaster and Palmdale where ground-water extraction in this part of the valley is concentrated.

Vertical ground-water movement in most of the Antelope Valley, including the Lancaster area, is poorly understood. At two sites in southern Lancaster, the measured gradients across the lacustrine unit ranged from 0.02 to 0.06 (upward) in April 1996 (relatively static conditions) prior to injection activity and from 0.03 (downward) to 0.06 (upward) in July 1996 (pumping conditions). These measurements were made in proximity to the production wells; it is not known if these measurements are representative of undeveloped areas.

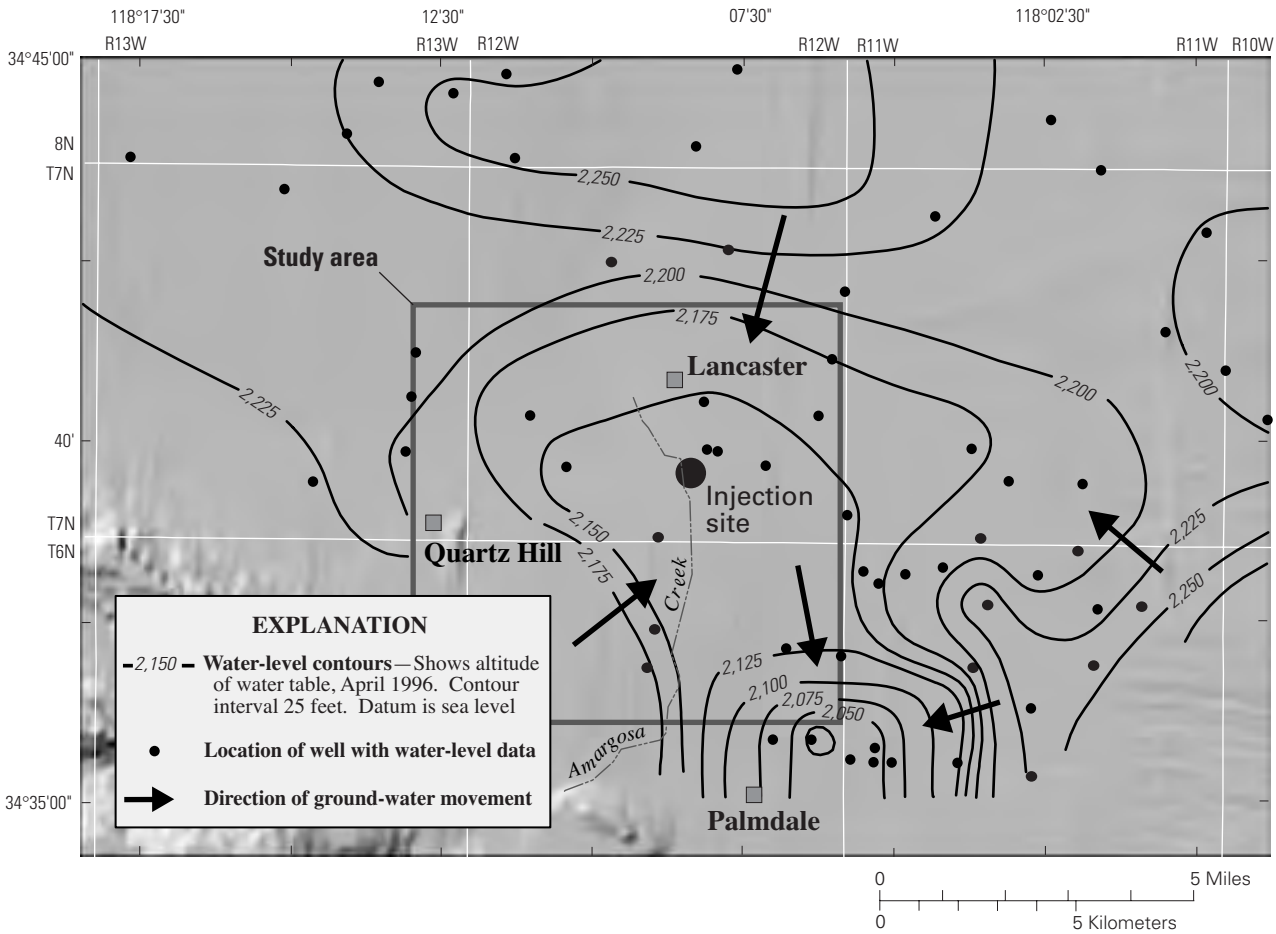

Figure 6. Ground-water-level contours based on data from wells perforated in the upper or upper and middle aquifers, April 1996, Lancaster, Antelope Valley, California.

(Modified from Carlson and others, 1998).

Land Subsidence

Global Positioning System (GPS) surveys and historical leveling data show that aquifer-system compaction from ground-water withdrawal caused more than 6 ft of land subsidence in Lancaster from about 1930 to 1992 and at least 1 ft of subsidence in an area of 290 mi^2 in Antelope Valley (Ikehara and Phillips, 1994; Galloway and others, 1998b). Galloway and others (1998a) used Interferometric Synthetic Aperture Radar (InSAR) to measure land subsidence at a high spatial resolution from 1993 to 1995; results indicated continued subsidence in the Lancaster area (fig. 7).

Negative consequences of land subsidence in Antelope Valley include altered drainage gradients; increased flooding and erosion; failed well casings; structural damage to roads and buildings; and development of earth fissures (Kennedy/Jenks Consultants, 1995; Prince and others, 1995; Dinehart and McPherson, 1998). Earth fissures on Edwards AFB have affected landings of space shuttles (Blodgett and Williams, 1992; Ward and Jachens, 1993). Fissures also have occurred in the eastern and northwestern parts of Lancaster (T.L. Holtzer and M.M. Clark, U.S. Geological Survey, unpublished data, 1981; Charles Swift, Geolabs–Weslake Village, written commun., 1991).

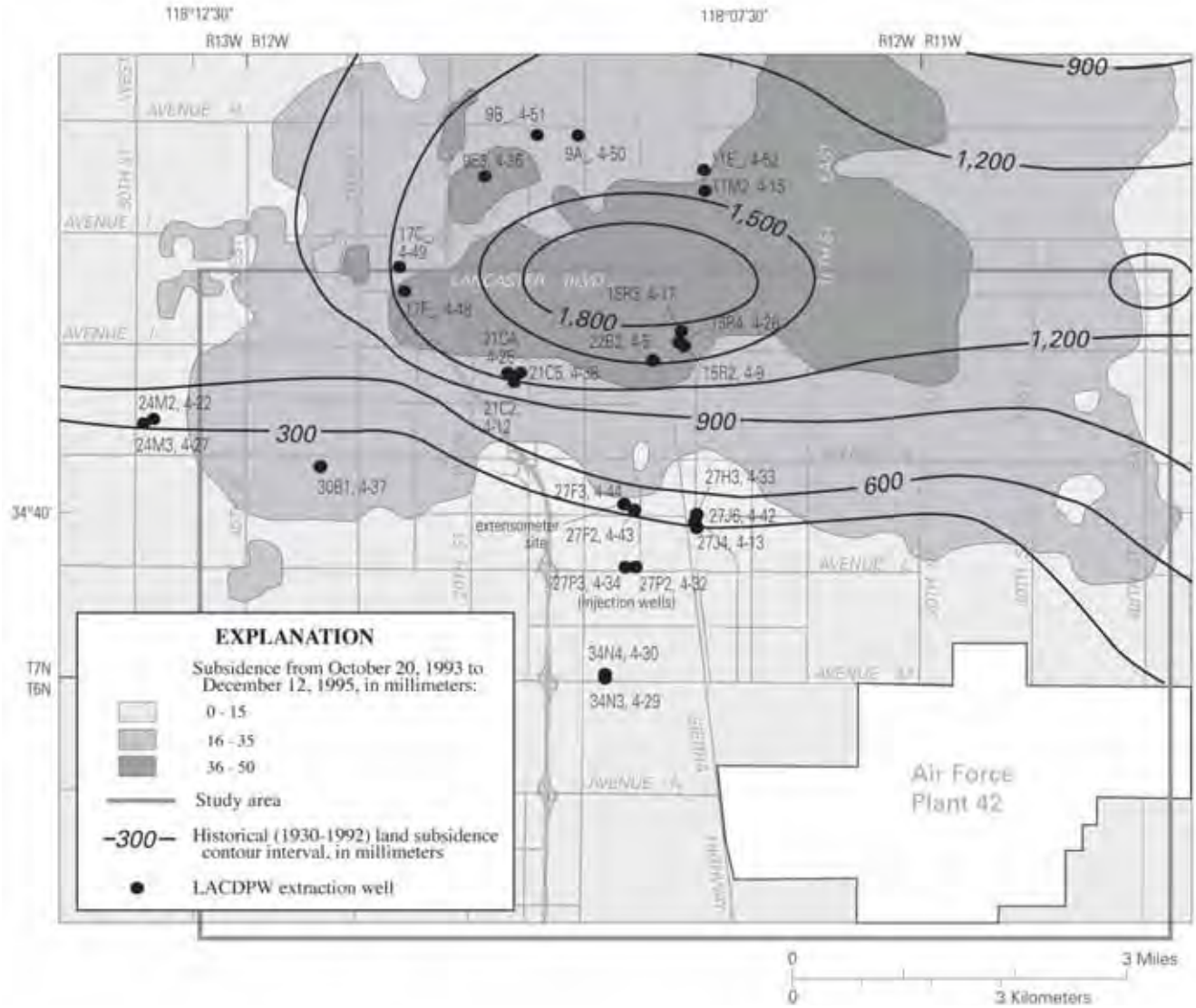

Figure 7. Land subsidence (1930–92) determined from leveling and Global Positioning System surveys (Ikehara and Phillips, 1994) and from interferometric synthetic aperture radar (InSAR) from October 1993 to December 1995, in Lancaster, Antelope Valley, California.

Also shown are Los Angeles County Department of Public Works (LACDPW) extraction wells.

All parts of an aquifer system are subject to compaction with ground-water withdrawal; however, the fine-grained deposits, or aquitards, are far more susceptible to permanent compaction that results in land subsidence than are the coarse-grained deposits.

The principle of effective stress (Terzaghi, 1925) describes the relation between changes in hydraulic head (expressed as pore pressure, p) and associated changes in effective (intergranular) stress (σ_e):

$$\sigma_e = \sigma_T - p \qquad (1)$$

where σ_T is the total stress caused by the overburden (weight of rock and water above the point of interest) and p is the pore pressure. With ground-water withdrawal, pore pressure decreases, effective stress increases proportionally, and the aquifer system deforms (compacts). For decreases in pore pressure to values higher than the previous lowest value (the preconsolidation head), deformation is elastic and the aquifer system recovers, or expands, when pore pressure again increases. If pore pressure decreases to below the preconsolidation head, effective stress exceeds the historical maximum, and compaction results in permanent deformation of the aquifer system.

Aquifer system deformation is expressed at the land surface as land subsidence during compaction and as uplift during expansion.

The above is a simplified explanation that does not always hold in practice because of the temporal aspect of compaction. When pore pressure decreases beyond its historical low, it takes time for pore pressures in the coarse-grained units and aquitards to equilibrate and for the associated compaction of the aquitards to take place. The time that this takes is a function of the vertical hydraulic conductivity and thickness of the aquitard; thin, permeable aquitards compact more quickly than thick, low-permeability aquitards. Thus, if pore pressure exceeds the preconsolidation stress for a relatively short period, the preconsolidation stress is not necessarily reset to the new low value; pore pressures only slightly below the original preconsolidation stress could trigger permanent compaction. Sneed and Galloway (2000) found that this *residual compaction* of thicker aquitards is a key element of subsidence at Edwards AFB; their report provides a more in-depth explanation of aquifer-system deformation.

Two conditions clearly need to be met for land subsidence to occur: hydraulic head must drop below the preconsolidation head, and compressible materials must be present. Where land subsidence has occurred and water levels have been measured, the preconsolidation head is relatively well understood. Where land subsidence has not occurred with water-level declines, either the preconsolidation head has not been exceeded or the materials are relatively incompressible. Fine-grained sediment such as silt and clay are the primary compressible materials in the Antelope Valley. The distribution of these materials and their compressibility is not well understood; however, the general distribution of fine-grained materials can be inferred from typical alluvial-fan stratigraphy (fig. 3). Accordingly, the aquifer system is likely to be coarser grained on the southern end of the study area nearest the San Gabriel Mountains and finer grained to the north.

The GPS and InSAR results for the study area (fig. 7) suggest that the potential for subsidence is high in central Lancaster where more than 6 ft had occurred between 1930 and 1992 and where the rates for 1993–95 were among the highest in the valley. These rates were similar to the average historical rates. GPS and InSAR results also suggest that the potential for subsidence decreases dramatically to the south; about 2 mi south of the area of maximum measured historical subsidence in Antelope Valley (central Lancaster) less than 1 ft of historical subsidence had occurred and the rates for 1993–95 were very low. Historical water-level declines in these areas are similar; thus, the sharp contrast in subsidence is likely tied to a difference in the total thickness and (or) the compressibility of fine-grained materials and (or) a difference in the stress history (preconsolidation head). The total thickness of the fine-grained materials may not be the sole reason for the contrast; significant silty and clayey materials were encountered while drilling boreholes in the southern area.

TESTS OF FRESHWATER INJECTION

Five injection tests were done for this study: two preliminary tests in 1994 to determine the feasibility of using existing wells for injection, and three pilot tests from 1996 to 1998 to assess the general feasibility of a multi-well injection program and the potential hydraulic, subsidence-related, and chemical effects of such a program.

Wells and piezometers in the study area often have multiple designations. Table 1 describes these designations, and includes basic well-construction information where available.

Preliminary Tests, 1994

The USGS, in cooperation with LACDPW and AVEK, tested the feasibility of injecting SWP water into the aquifer system at Lancaster through existing wells during spring 1994. Two wells in the Avenue K–8 and Division Street well field (fig. 8) were tested: well 7N/12W-27J5, an older abandoned production well screened in the upper and middle aquifers; and well 7N/12W-27J6, a newer active production well screened in the upper, middle, and lower aquifers (table 1). A total of more than 118 acre-ft of SWP water, treated to drinking-water standards by AVEK, was injected into the aquifer system through these wells during separate tests. Ground-water levels were measured in nine nearby wells. Velocity logs were obtained for four of the wells to determine interaquifer wellbore flow between the middle and deep aquifers. GPS surveys were done to monitor land-surface deformation during the tests.

Table 1. Construction and other data for wells used in the study, Antelope Valley, California

[State well number, as reported or determined: _, underscored where part of well number is unknown. See well-numbering system on page xi. See figures 15, 42, and 43 for location of wells. USGS, U.S. Geological Survey. USGS site identification number: The unique number for each site based on latitude and longitude of site, which is referenced to North American Datum of 1927 (NAD27); first six digits are latitude, next seven digits are longitude, and final two digits are a sequence number to uniquely identify each site; underscore indicates wells not canvassed and not in USGS digital database, information obtained from owner and (or) drillers' logs. Altitude of land surface in feet above sea level. Depth of well, well casing, and screened (perforated) interval in feet below land surface. Screened (perforated) interval: estimated where italicized. Aquifer zones: U, upper; M, middle; L, lower; inferred where italicized. —, no data available; ~, about]

State well number		USGS site identification number	Local well name	Land-surface altitude (feet)	Use of well	Year of con-struction	Depth drilled (feet)	Casing		Screened (perforated) interval (feet)	Aquifer zone perfo-rated
								Diameter (inches	Depth (feet)		
6N/11W	-1B1	343842117594001	3	2,500	Agricultural	1955	460	14	—	256-460	U
	-3C1	343845118015201	MW19	2,485	Observation	1995	341	4	335	290-335	U
	-3F_	—	—	—	Agricultural	—	—	—	—	*200-550*	*U*
	-3Q1	343754118013901	MW15	2,504	Observation	1995	330	4	330	285-330	U
	-4H1	343820118022601	—	2,489	Agricultural	1936	722	20	722	170-650	U,M
	-5G3	343826118035801	DW4-1	2,480	Industrial	1984	749	13	700	[1]420-700	U,M
	-5G4	343826118035601	DW4-2	2,480	Industrial	1984	742	13	670	[1]410-670	U,M
	-6F1	343822118051901	DW2-2	2,490	Industrial	1991	1,000	16	820	[1]400-800	U,M
	-6H3	343821118043601	DW3-1	2,484	Industrial/domestic	1971	800	16	800	400-800	U,M
	-6H4	343829118044101	DW3-3	2,479	Domestic/industrial	1986	810	16	800	500-800	U,M
	-8M_	—	3	—	Agricultural	—	—	—	—	*200-451*	*U*
	-8R3	343700118034302	4	2,523	Agricultural	1946	709	16	708	252-708	U,M
	-9D1	343752118031201	MW4	2,498	Observation	1988	334	4	334	289-334	U
	-9H1	343717118023201	—	2,513	Agricultural	1948	500	8	500	200-500	U
	-9P1	343700118031101	1	2,523	Agricultural	1946	652	—	652	537-652	U,M
	-9Q1	343700118024001	—	2,526	Agricultural	1937	—	10	566	486-566	U
	-11C1	343751118005801	MW18	2,513	Observation	1995	340	4	335	290-335	U
	-15A1	343700118012801	MW16	2,537	Observation	1995	334	4	331	281-331	U
	-16D_	—	MW3	2,523	Observation	—	—	—	—	*300-350*	*U*
	-16J1	343628118022701	—	2,547	Unused/observation	1964	630	14	630	322-630	U,M
	-17_	—	—	—	Agricultural	—	—	—	—	*200-600*	*U,M*
	-17A_	—	5	—	Agricultural	—	—	—	—	*200-600*	*U,M*
	-17D1	343647118041601	DWX-2	2,531	Industrial	1988	600	11	600	*200-600*	*U,M*
	-18A_	—	—	—	Agricultural	—	—	—	—	*500-800*	*U,M*
	-18H1	343644118044701	—	2,534	Domestic/industrial	1982	800	14	800	500-800	U,M
	-19C_	—	8A	2,568	Public supply	1987	1,030	16	960	560-940	U,M,L
	-19E5	343554118053401	2A	2,584	Public supply	1968	915	16	900	[1]450-900	U,M
	-19E6	343545118052701	3A	2,586	Public supply	1960	868	16	848	396-848	U,M
	-19F1	343542118050701	4A	2,571	Public supply	1970	838	16	838	480-830	U,M
	-19F2	343554118050501	7A	2,563	Public supply	1985	1,020	16	920	570-900	U,M
	-19G1	343542118044801	24	2,569	Public supply	1985	950	16	920	570-900	U,M
	-19L_	—	23A	2,579	Public supply	1991	900	16	840	600-840	U,M
	-20A1	343559118033701	—	2,564	Agricultural	1960	—	—	600	*200-600*	*U,M*
	-20A_	—	—	—	Agricultural	—	—	—	—	*200-600*	*U,M*
	-20D1	343554118043001	MW2	2,558	Observation	1989	540	6	540	480-540	U
	-20G2	343542118034101	10	2,568	Public supply	1956	694	16	694	310-694	U,M
6N/12W	-5J_	—	3	2,565	Public supply	—	—	—	—	*288-504*	*U*
	-9H3	343727118085202	—	2,610	Public supply	1992	1,015	16	910	500–900	U,M,L
	-12M2	343717118063601	DW8-1	2,560	Industrial	1976	810	14	801	500–801	U,M
	-12R1	343711118054001	DW7-1	2,538	Industrial	1951	—	16	800	380-800	U,M

Table 1. Construction and other data for wells used in the study, Antelope Valley, California—*Continued*

State well number	USGS site identification number	Local well name	Land-surface altitude (feet)	Use of well	Year of con-struction	Depth drilled (feet)	Casing		Screened (perforated) interval (feet)	Aquifer zone perfo-rated
							Diameter (inches	Depth (feet)		
6N/12W -13N1	343609118063801	15	2,591	Public supply	1960	880	16	800	420-800	U,M
-15H_	—	34-6	2,620	Public supply	1988	1,074	16	1,050	500-1,050	U,M,L
-16A2	343655118090001	—	2,640	Public supply	—	([2])	—	([2])	*388-800*	*U,M*
-23A1	343600118064901	6A	2,598	Public supply	1983	1,030	16	1,010	480-1,010	U,M,L
-24A3	343558118055001	14A	2,579	Public supply	1965	900	16	900	450-900	U,M
-24C1	343600118061001	11A	2,585	Public supply	1963	1,275	16	1,275	504-900	U,M
7N/11W -8M1	344229118042901	1	2,372	Public supply	1962	605	14	600	310-*600*	U,*M*
-8M2	344229118043101	2	2,372	Public supply	—	—	—	—	*290-600*	*U,M*
-18R_	—	4-58	2,396	Public supply	1989	—	16	1,240	400-1,220	U,M,L
-18R_	—	4-59	2,397	Public supply	1989	1,260	16	1,240	400-1,220	U,M,L
-20G_	—	4-54	2,414	Public supply	1988	1,210	16	1,200	300-1,200	U,M,L
-20G_	—	4-55	2,416	Public supply	1989	1,208	16	1,200	360-1,200	U,M,L
-27Q1	343939118013701	—	2,463	Unused/observation	—	650	14	650	300-650	U,M
-33A1	343926118024001	3	2,461	Agricultural	—	—	—	—	374-770	U,M
-33J2	343859118024002	2	2,471	Agricultural	1963	770	16	770	*374-770*	*U,M*
-33N1	343847118032001	—	2,473	Destroyed in 1996	—	—	20	[3]351	—	U
-33Q1	343846118025301	—	2,468	Agricultural	—	700	16	700	318-700	U,M
7N/12W -9A_	—	4-50	2,321	Public supply	1989	754	16	510	280-500	U,M
-9B_	—	4-51	2,316	Public supply	1989	885	16	510	[1]250-490	U,M
-9E3	344239118094201	4-36	2,318	Public supply	1973	515	16	500	140-490	U,M
-11E_	—	4-52	2,340	Public supply	1988	1,175	16	1,000	240-980	U,M,L
-11M2	344240118074301	4-15	2,338	Public supply	1959	705	14	600	[1]180-525	U,M
-13F1	344151118061901	1	2,382	Agricultural	1948	552	12	552	175-*552*	U,*M*
-15R2	344123118075501	4-9	2,386	Industrial	1953	670	14	670	466–670	U,M
-15R3	344130118075701	4-17	2,375	Public supply	1958	1,227	14	1,227	[1]480–1,227	U,M,L
-15R4	344125118075801	4-26	2,384	Public supply	1965	700	14	693	235–693	U,M
-17C_	—	4-49	2,319	Public supply	1988	1,160	16	1,150	320-1,140	U,M,L
-17F_	—	4-48	2,324	Public supply	1988	1,135	16	1,110	320-1,100	U,M,L
-19R1	344030118110001	—	2,386	Unused/observation	—	400	12	400	100-400	U
-21C2	344107118092401	4-12	2,357	Public supply	1955	639	14	639	300–639	U,M
-21C4	344109118092601	4-25	2,359	Public supply	1964	800	14	640	200–640	U,M
-21C5	344109118092201	4-38	2,358	Public supply	1974	750	16	733	210–720	U,M
-22B2	344120118081301	4-5	2,375	Public supply	1947	578	14	552	192–552	U,M
-22K1	344043118080301	—	2,407	Abandoned/ observation	—	400	8	—	—	U
-26K3	343951118065902	4-31	2,459	Abandoned	1969	770	16	687	310–674	U,M
-27F1	344004118082401	—	2,444	Abandoned	—	—	—	([4])	—	U,M
-27F2	344005118081801	4-43	2,445	Public supply	1988	1,210	16	1,202	400–1,202	U,M,L
-27F3	344006118082601	4-44	2,440	Public supply	1988	1,220	16	1,202	400–1,202	U,M,L
-27F5	344005118082201	5K8-PZ1	2,441.6	Piezometer	1996	1,183	2	935	905–925	L
-27F6	344005118082202	5K8-PZ2	2,441.6	Piezometer	1996	1,183	2	735	705–725	M
-27F7	344005118082203	5K8-PZ3	2,441.6	Piezometer	1996	1,183	2	535	505–525	M
-27F8	344005118082204	5K8-PZ4	2,441.6	Piezometer	1996	1,183	2	425	395–415	U
-27F9	344005118082205	5K8-EX1	2,441.6	Extensometer	1996	735	7	725	—	—

Table 1. Construction and other data for wells used in the study, Antelope Valley, California—*Continued*

State well number	USGS site identification number	Local well name	Land-surface altitude (feet)	Use of well	Year of con-struction	Depth drilled (feet)	Casing		Screened (perforated) interval (feet)	Aquifer zone perfo-rated
							Diameter (inches	Depth (feet)		
7N/12W -27F10	344005118082206	5K8-EX2	2,441.6	Extensometer	1996	1,205	7	1,190	—	—
-27H1	344004118075901	—	2,449	Abandoned/ observation	1949	500	14	500	189–500	U
-27H3	344008118074701	4-33	2,443	Public supply	1971	730	16	710	260–700	U,M
-27H5	344003118074801	DK8-PZ1	2,449	Piezometer	1992	1,120	2	1,120	1,080–1,100	L
-27H7	344003118074803	DK8-PZ3	2,449	Piezometer	1992	1,120	2	724	684–704	M
-27J4	344002118074701	4-13	2,448	Public supply	1956	1,108	14	[5]1,102	[5]362–1,102	U,M
-27J5	343903118074801	4-8	2,449	Abandoned	1953	700	14	700	350–700	U,M
-27J6	344003118074901	4-42	2,449	Public supply	1987	1,174	16	1,150	400–1,140	U,M,L
-27P2	343943118081801	4-32	2,463	Public supply	1969	735	16	727	282–717	U,M
-27P3	343943118082101	4-34	2,462	Public supply	1972	740	16	720	280–710	U,M
-27P5	343943118081701	5L-PZ1	2,462.7	Piezometer	1998	918	2	910	890–910	L
-27P6	343943118081702	5L-PZ2	2,462.7	Piezometer	1998	918	2	560	540–560	M
-27P7	343943118081703	5L-PZ3	2,462.7	Piezometer	1998	918	2	460	440–460	U
-27P8	343943118081704	5L-PZ4	2,462.7	Piezometer	1998	918	2	390	330–370	U
-30B1	344028118112601	4-37	2,387	Public supply	1974	652	16	610	260–600	U,M
-30J_	—	8	—	Public supply	—	—	—	—	*260-610*	*U,M*
-32A1	343936118100201	—	2,450	Public supply	1947	540	12	—	*210-437*	*U*
-33R3	343848118085203	—	2,519	Public supply	1993	824	16	780	440–760	U,M
-34B1	343931118081601	—	2,475	Abandoned	1953	425	8	—	—	U
-34N3	343848118083801	4-29	2,522	Public supply	1967	792	14	740	350–728	U,M
-34N4	343851118083801	4-30	2,517	Public supply	1968	800	16	770	350–760	U,M
-35G2	343912118071102	2	2,497	Public supply	1956	630	—	559	307-*559*	U
7N/13W -14D1	344207118140801	3	2,351	Public supply	1941	500	14	480	321-*480*	U,*M*
-14D2	344207118140802	4	2,352	Public supply	1941	500	—	488	321-488	U,M
-23R1	344029118131301	—	2,384	Public supply	1950	437	12	437	199-*437*	U,*M*
-24M2	344044118125701	4-22	2,372	Public supply	1951	593	14	593	167-593	U,M
-24M3	344042118130001	4-27	2,375	Public supply	1965	602	14	575	150-575	U,M
-25M2	344003118120502	5	~2,415	Public supply	—	590	—	590	300-590	U,M
-26J2	344000118130601	—	2,417	Public supply	1957	606	14	606	288-606	U,M
-26J_	—	—	—	Public supply	—	—	—	—	*250-501*	*U,M*
-34A_	—	2	—	Public supply	—	—	—	—	*250-475*	*U*

[1]Not continuous.
[2]Depth, obtained from owner, is approximately 800 feet below land surface.
[3]Destroyed in 1996.
[4] Depth at least 750 feet below land surface; sounded March 1996.
[5]Well casing filled with gravel to about 700 feet below land surface in early 1990s.

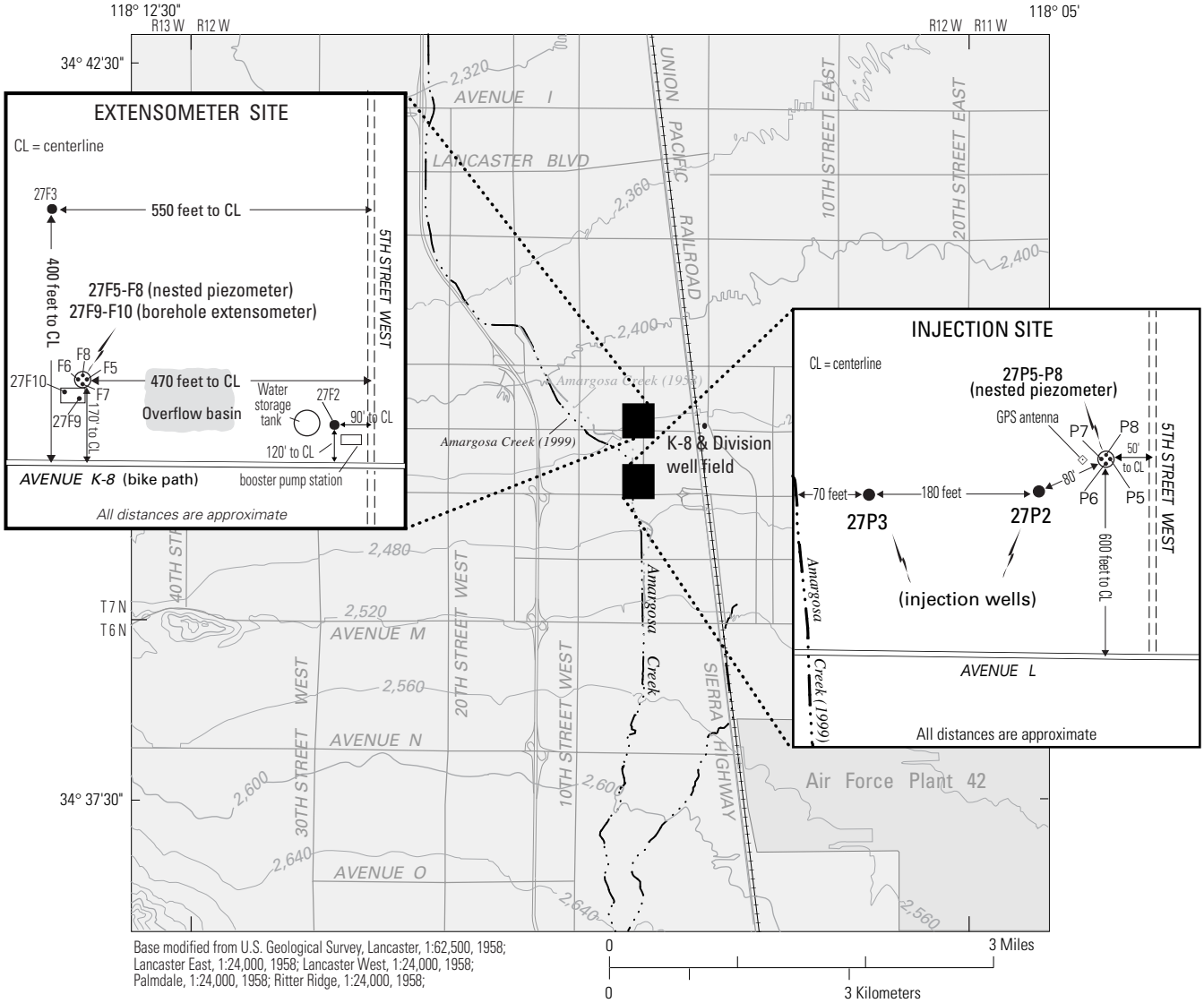

EXPLANATION

2,560 **Land-surface altitude**—Contour interval 40 feet, dashed interval 20 feet. Datum is sea level

Figure 8. Location of injection and extensometer sites, Lancaster, Antelope Valley, California.

GPS, global positioning system.

Key results of these preliminary tests indicated that

(1) unrestored abandoned wells may not be suitable for injection because of large head losses caused by encrusted well screens and gravel packs (for example, the water level in the injection well had to be near land surface to achieve reasonable injection rates);

(2) the lower aquifer accepted only 17 percent of the water injected into well 7N/12W-27J6, coupled with large increases in pressure, suggesting this aquifer has low transmissivity and very low storativity (generally a poor set of conditions for aquifer injection, storage, and recovery); and

(3) both injection tests appeared to cause temporary, measurable changes in land-surface elevation.

These findings influenced the selection of the site used in the pilot tests and the data-collection efforts for these tests. Wells at the new site were in the upper and middle aquifers, active, and far from structures that may be damaged by fluctuations in land-surface elevation.

Pilot Tests, 1996–98

The USGS, in cooperation with LACDPW and AVEK, conducted three pilot injection tests from 1996 to 1998 to assess the general feasibility of a multi-well injection program and to determine the potential hydraulic, subsidence-related, and chemical effects of such a program. The first test, which included about 1 month of injection, was a warm-up for the subsequent long-term test, which involved 5 months of injection. Determination of the hydraulic feasibility and the effects of injection was the primary purpose of these two tests. Secondary goals included measurement of aquifer-system deformation and collection of water-chemistry data. The primary goal of the third pilot test was to determine the factors controlling the formation and fate of trihalomethanes.

Site Description

Selection of the site for the pilot injection tests was based on the results from the preliminary tests, the accessibility of AVEK (injection) water, and the relative dependence on the wells during periods of high water demand. The site selected, referred to herein as the injection site (fig. 8), has two relatively new production wells (7N/12W-27P2 and 27P3) screened only within the upper and middle aquifers and one nested piezometer (7N/12W-27P5–8) established in 1998 for this study (fig. 9). The injection site is surrounded by undeveloped land, which minimized potential damage from land-surface deformation, and is near a source of AVEK water. There was enough redundancy in the system of wells, pipelines, and storage tanks to likely avoid unscheduled extraction at or near the site during the tests.

An extensometer site was established about 0.5 mi north of the injection site (fig. 8) for measuring aquifer-system deformation during the pilot tests and for subsequent long-term subsidence monitoring. This site consists of a paired dual-borehole extensometer and one nested piezometer constructed in 1995 for this study. Near this site are two production wells (7N/12W-27F2 and 27F3) that are open to the upper, middle, and lower aquifers (fig. 10).

Test Procedure

One or both of the production wells at the injection site were used during the three pilot injection tests. Each of these tests, referred to herein as cycles, involved several stages:

(1) pre-injection water-level recovery prior to the start of the test;

(2) injection;

(3) storage period; and

(4) extraction.

The first of these tests began in April 1996 and involved 28 days of injection. The second and the third tests were conducted in 1996–97 and 1998 and involved 5 and 1.5 months, respectively, of injection. Figure 11 shows a time line depicting the various stages and monitoring activities of these tests.

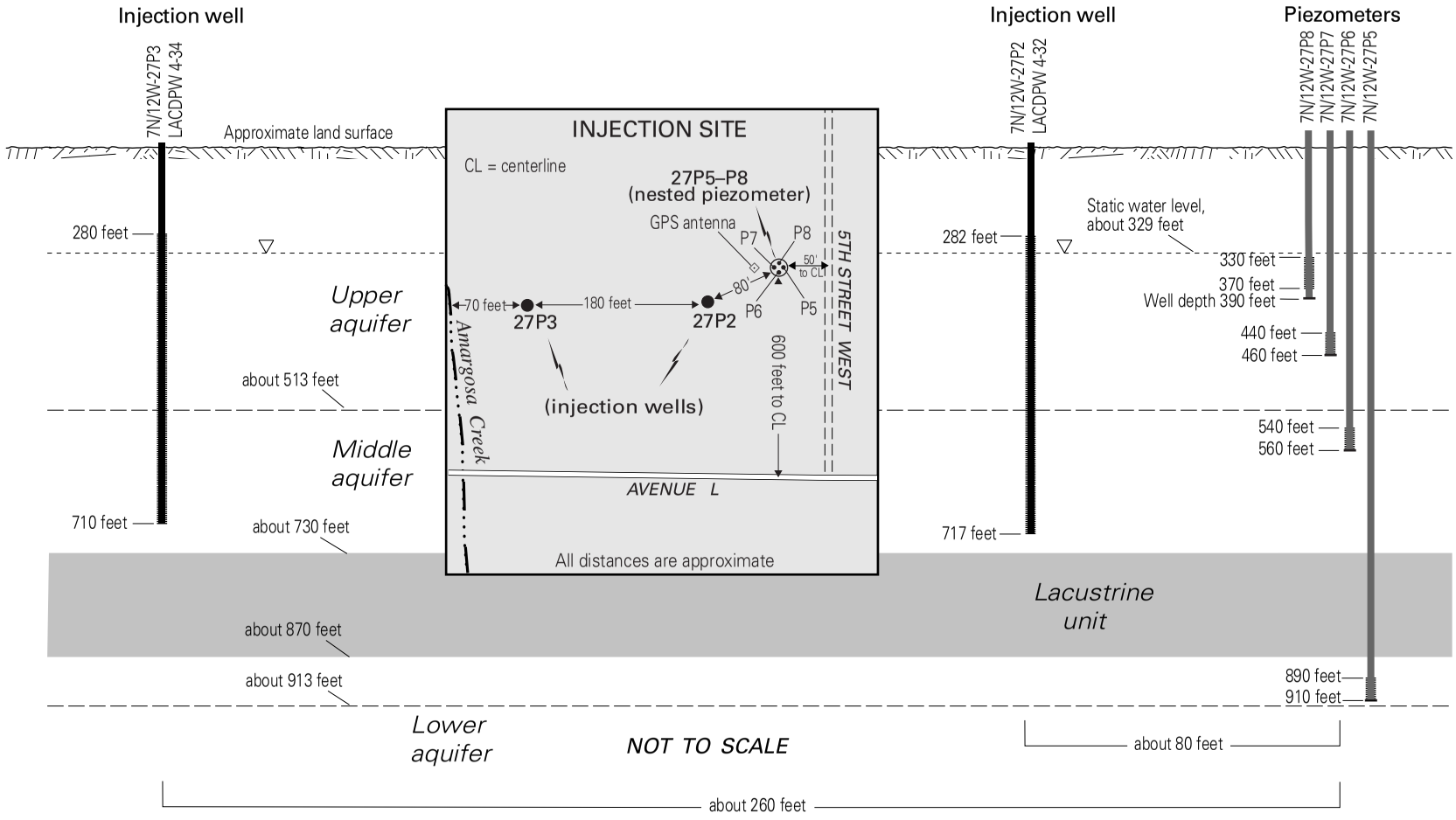

Figure 9. Location of piezometers 7N/12W-27P5–P8 and Los Angeles County Department of Public Works (LACDPW) production wells 7N/12W-27P2–P3, Lancaster, Antelope Valley, California.

Diagram is not to scale, but does identify depths from land surface and distances between well. Map show relative locations. GPS, global positioning system.

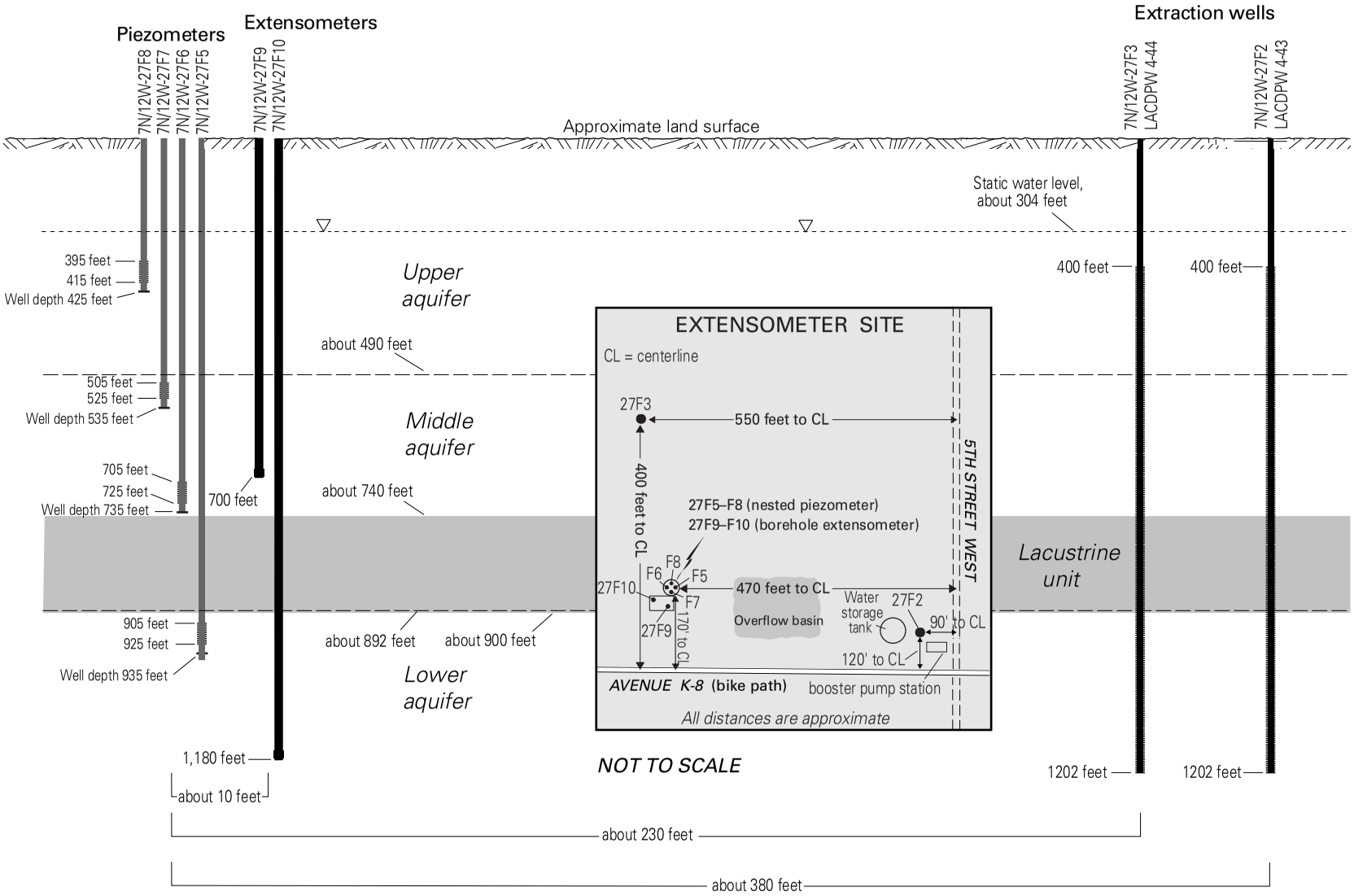

Figure 10. Location of piezometers 7N/12W-27F5–F8, extensometers 7N/12W-27F9–F10, and Los Angeles County Department of Public Works (LACDPW) production wells 7N/12W-27F2–F3, Lancaster, Antelope Valley, California.

Diagram is not to scale, but does identify depths from land surface and distances between well. Map shows relative locations.

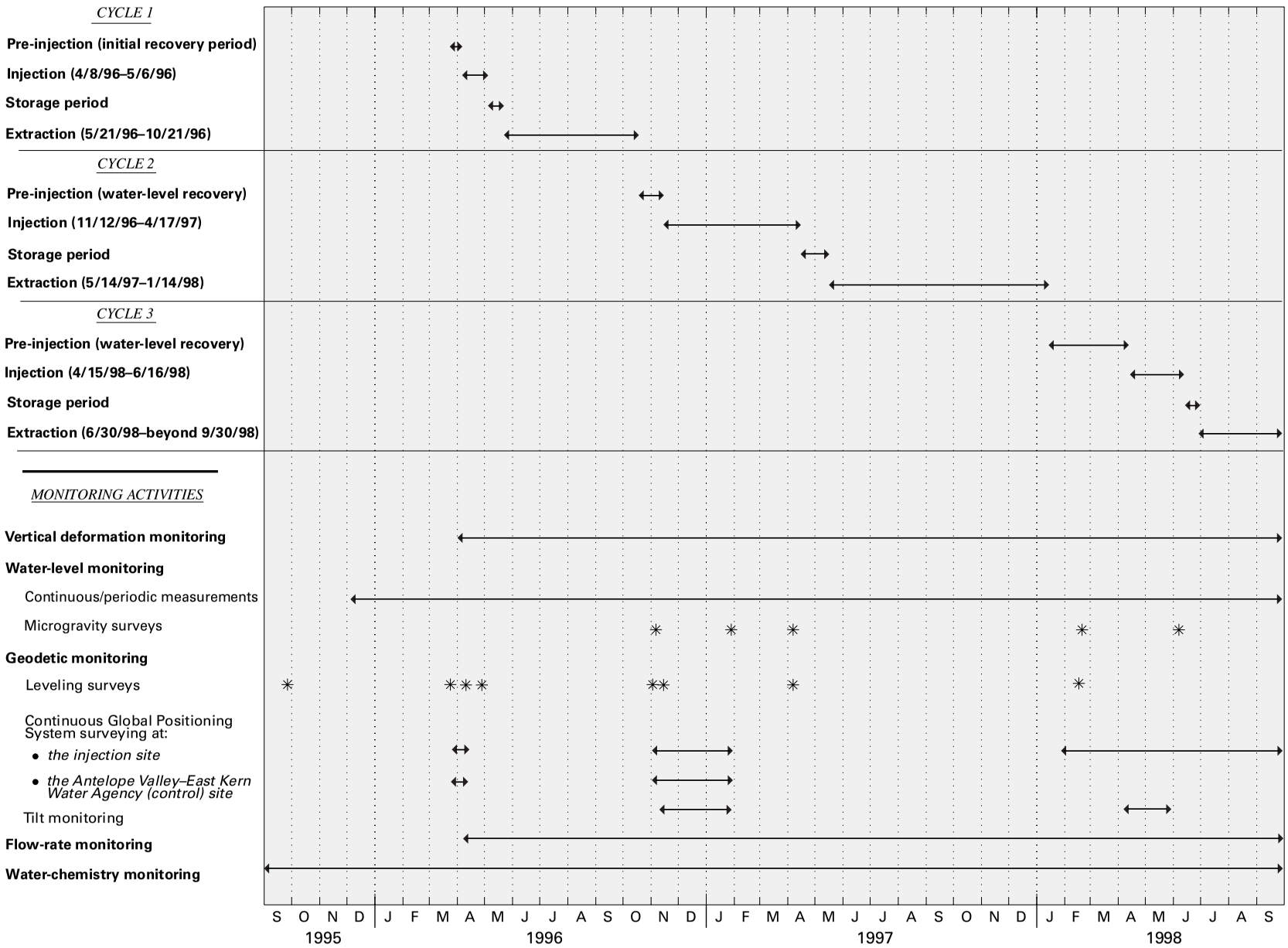

Figure 11. Time line of activities associated with injection cycles 1–3 at Lancaster, Antelope Valley, California.

Injection was accomplished by conveying AVEK water into the injection wells either through a 4-inch conductor pipe (with pump removed) or through the pump column with the electric turbine in place on the wellhead (unlocked so it could spin). A series of valves were used to reduce system pressure prior to release into the wells, and the wells were gravity-fed. Injection and extraction rates were measured continuously using an inline flow meter for each well and recorded on a data logger. Injection rates were held somewhat steady at about 750 gal/min per well, and extraction rates averaged about 850 gal/min per well during cycles 1 and 2 and about 450 gal/min during cycle 3 (fig. 12). The highest measured water level in either injection well during injection was about 185 ft below land surface (fig. 13), which indicates that 750 gal/min was easily accommodated and may not represent the maximum attainable rate in these wells.

The pre-injection recovery period ranged from 1 to 12 weeks; this stage of the pilot injection test allowed water levels and aquifer-system deformation to stabilize prior to injection and reach quasi-static conditions. This helped distinguish between the hydraulic response to the cessation of extraction and to the onset of injection. The storage period followed injection and ranged from 2 to 4 weeks. This period allowed water levels and aquifer-system deformation to stabilize, and provided time for specific chemical reactions (formation of trihalomethanes) to occur prior to extraction.

Data collected to document the hydraulic, subsidence-related, and chemical response to the injection cycles are described in the rest of this section of the report and analyses of these data are discussed in the following section. The timing of the injection cycles and the associated sampling is shown in figure 11.

Monitoring of Hydraulic Response

The hydraulic response of the aquifer system to stresses during the injection cycles was determined directly by measuring water levels in wells and piezometers and indirectly by measuring changes in gravity. Following is a discussion of historical water levels and a description of the water-level network used for this study, the response of water levels in this network during the injection cycles, and the use of microgravity surveys to estimate water-level changes in the absence of wells.

Historical Water Levels

Water levels in Antelope Valley are lower than they were prior to ground-water development in the valley in the early 1900s. Water levels in the study area were affected primarily by agricultural activity through the 1960s, but now are controlled largely by pumping for urban use (Templin and others, 1995; Leighton and Phillips, 2003). Water levels near Lancaster and Palmdale declined about 110 and 185 ft, respectively, since about 1965 (fig. 14). Longer term records show drawdowns exceeding 200 ft in the Lancaster area and 300 ft in the vicinity of Palmdale since the early 1900s.

Water-Level Network and Conditions Prior to Injection Testing

The water-level network established for this study consists of 13 active or abandoned production wells, 2 nested piezometers installed by the USGS for a previous study, and 2 sets of 4 nested piezometers installed for this study (table 1; fig. 15) (Metzger and others, 2002). The areal distribution of the wells in this network is not ideal; more than 70 wells known to exist at one time within 2 mi of the injection wells were either destroyed, inaccessible, or could not be found. The screened intervals vary from 20 ft in most of the piezometers to 300 to 400 ft in most of the wells.

Water levels in all the network piezometers and wells were measured periodically using a calibrated electric sounder or a graduated steel tape. Continuous measurements were made at most of the piezometers and at one well. The measurements were collected with pressure transducers and recorded electronically. Metzger and others (2002) describe the methods and protocol used in collecting these data and present a complete tabular (except for continuous data) and graphical record of the measurements.

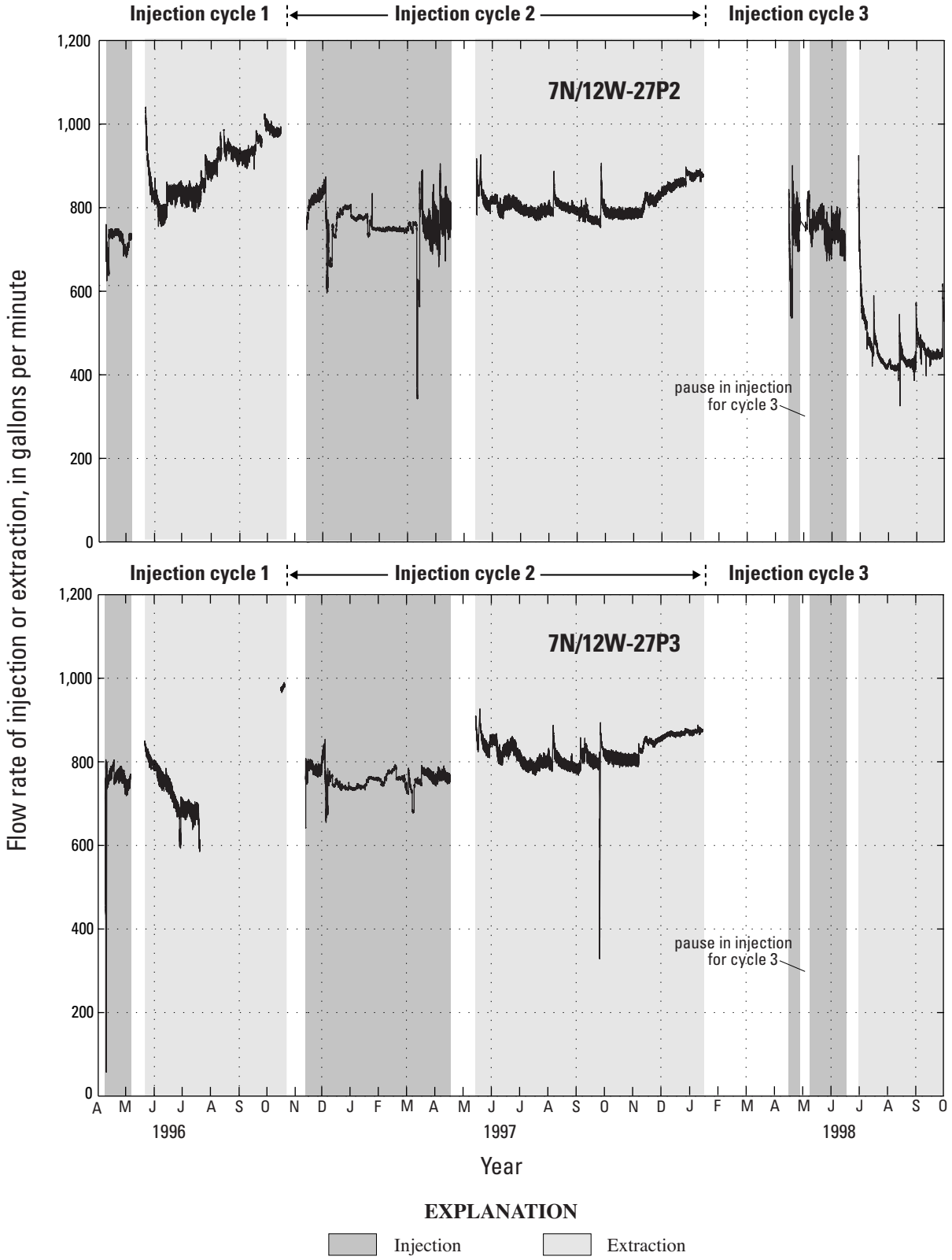

Figure 12. Injection and extraction flow rates for wells 7N/12W-27P2 and -27P3 in Lancaster, Antelope Valley, California, 1996–98.

Breaks in graphs indicate wells were not in use.

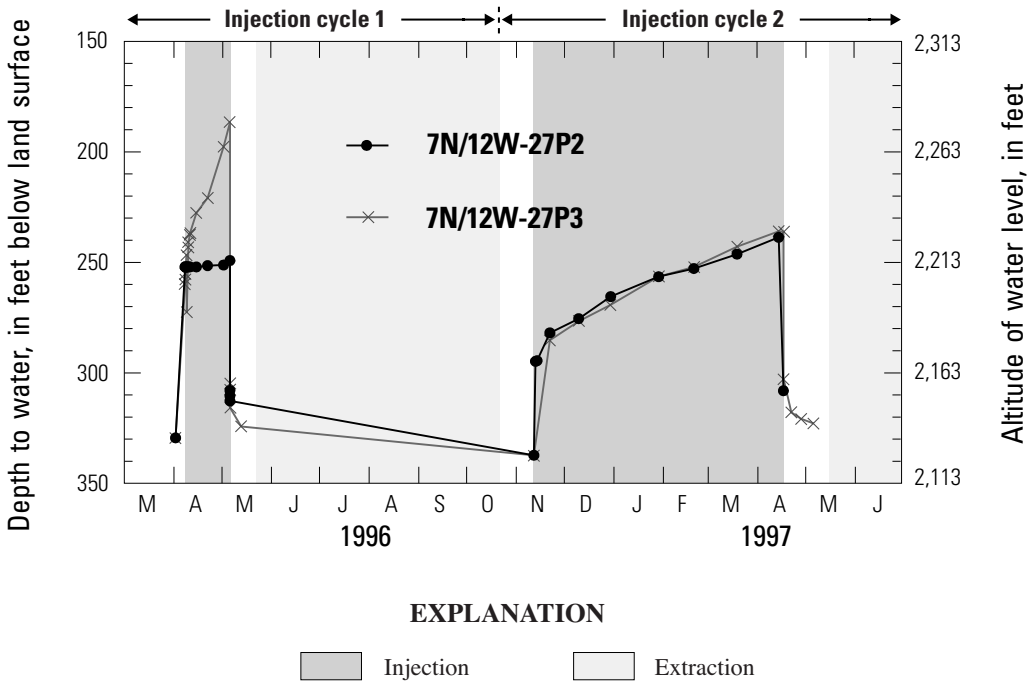

Figure 13. Periodic measurements in the injection wells (7N/12W-27P and 27P3) in Lancaster, Antelope Valley, California, March 1996 through June 1997.

November 1996 water-level data for the study area are depicted in figure 16. All the wells in this figure are screened in the upper aquifer, but some are also screened in the other aquifers; therefore, the water levels shown on figure 16 may not represent the water table. These data were collected 3 weeks after extraction ceased in local LACDPW wells following a 5- or 6-month period of relatively high extraction rates. The water-level contours on figure 16 are for November 1996, and therefore are not entirely representative of conditions prior to injection testing because the first cycle involved injection during April 1996 and extraction from late May through mid-October. Because water levels were not available for the four wells south of well 7N/12W-34B1 prior to the April 1996 injection, the November 1996 data provide a more comprehensive view. These contours show ground-water movement toward the injection site in the Lancaster area and southeastward flow south of Lancaster toward Palmdale. Although there are no data between wells 7N/12W-34B1 (just south of the injection site) and 6N/12W-12M2 (at Air Force Plant 42), the water-level contours indicate that a ground-water flow divide may exist between these wells. On the other hand, the April 1996 data prior to injection show water levels 4 to 9 ft higher in the northern area; later water-level measurements for well 6N/12W-12M2 show little seasonal variation (2 ft maximum change from November 1996 through May 1998), suggesting that a very shallow southward gradient may exist during periods of low extraction rates (relatively high water levels) in Lancaster.

Water-Level Network Response to Injection Cycles

Measured water levels in the network piezometers and wells closest to the injection wells are shown on the hydrographs in figure 17 (locations shown in figure 15). An inspection of these hydrographs reveals that quantifying the difference between normal seasonal water-level recovery and that caused by injection is not possible using water-level data alone because subannual data were not available for the area near the injection site prior to the first injection cycle and because a full water-level recovery did not take place prior to subsequent injection cycles. However, continuous and periodic water-level data recorded during the injection cycles shows qualitatively that the hydraulic response to injection was significant (for example, wells 7N/12W-27F6, 34B1, and 27H7).

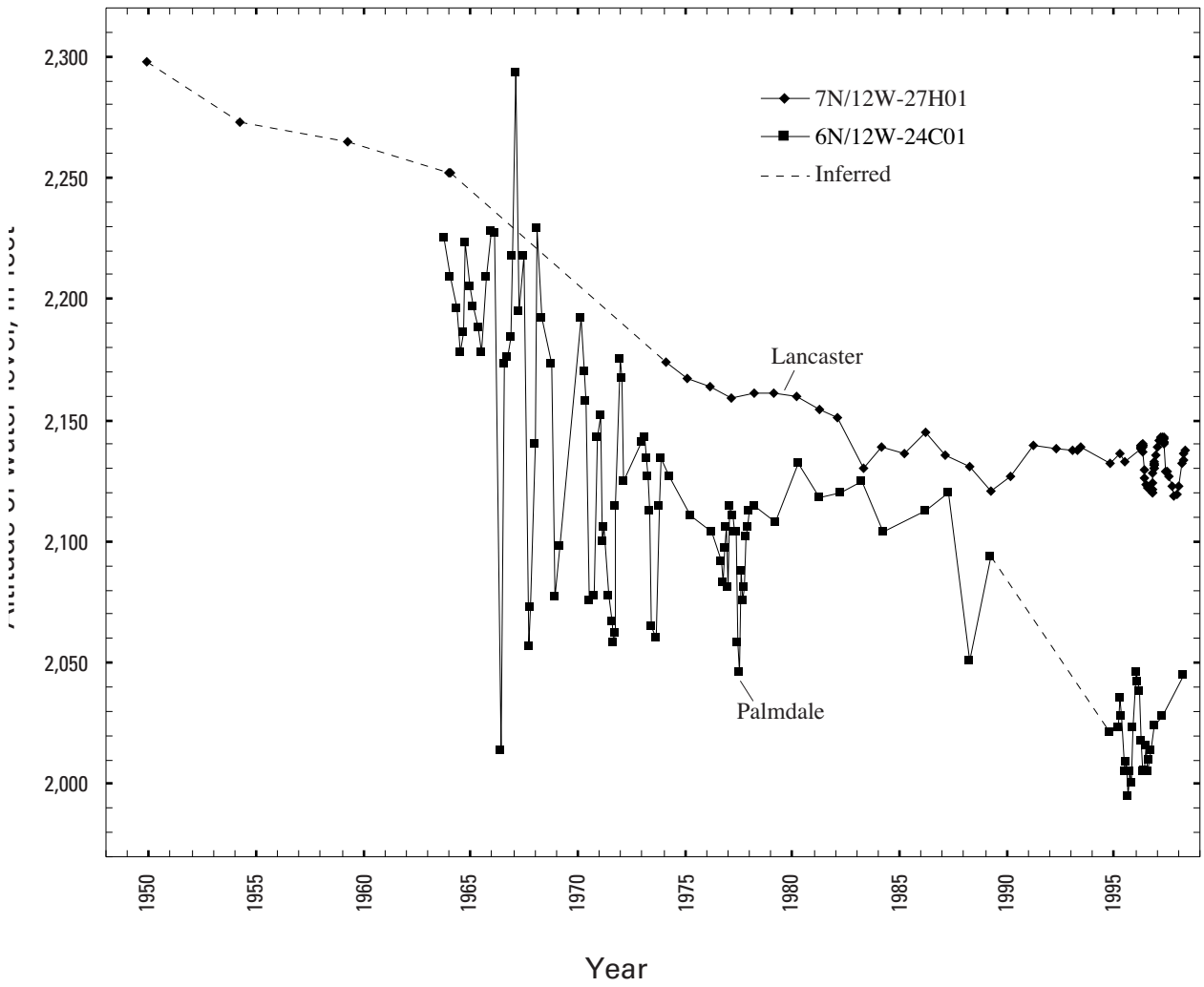

Figure 14. Historical water levels in or near Lancaster and Palmdale, Antelope Valley, California, 1948–99.

Continuous water levels just above the lacustrine unit measured at well 7N/12W-27F6 during the cycle-2 injection at the extensometer site, about 2,270 ft north of the injection wells, are shown in figure 18. The rate of recovery clearly had slowed prior to the start of injection, but it quickly recovered at the onset of injection as indicated by a rapid increase in head of about 6 ft. Well 7N/12W-27H1, about 2,800 ft northeast of the injection wells, also responded rapidly to injection, though with less magnitude. Water levels in wells more than 1 mi away from the injection wells did not appear to be affected immediately, if at all, by injection; for example, well 7N/12W-26K3, which is 1.2 mi to the east of the injection wells, did not respond perceptibly to injection. Water-level responses to the cessation of injection were similar for the three wells (fig. 18).

Continuous water-level data from the nested piezometers screened in the upper and middle aquifers show an increased response to injection and extraction with increased depth in the system (fig. 19*A*, *B*). Vertical hydraulic gradients above the lacustrine unit generally shift from upward during injection and recovery periods to downward during withdrawal.

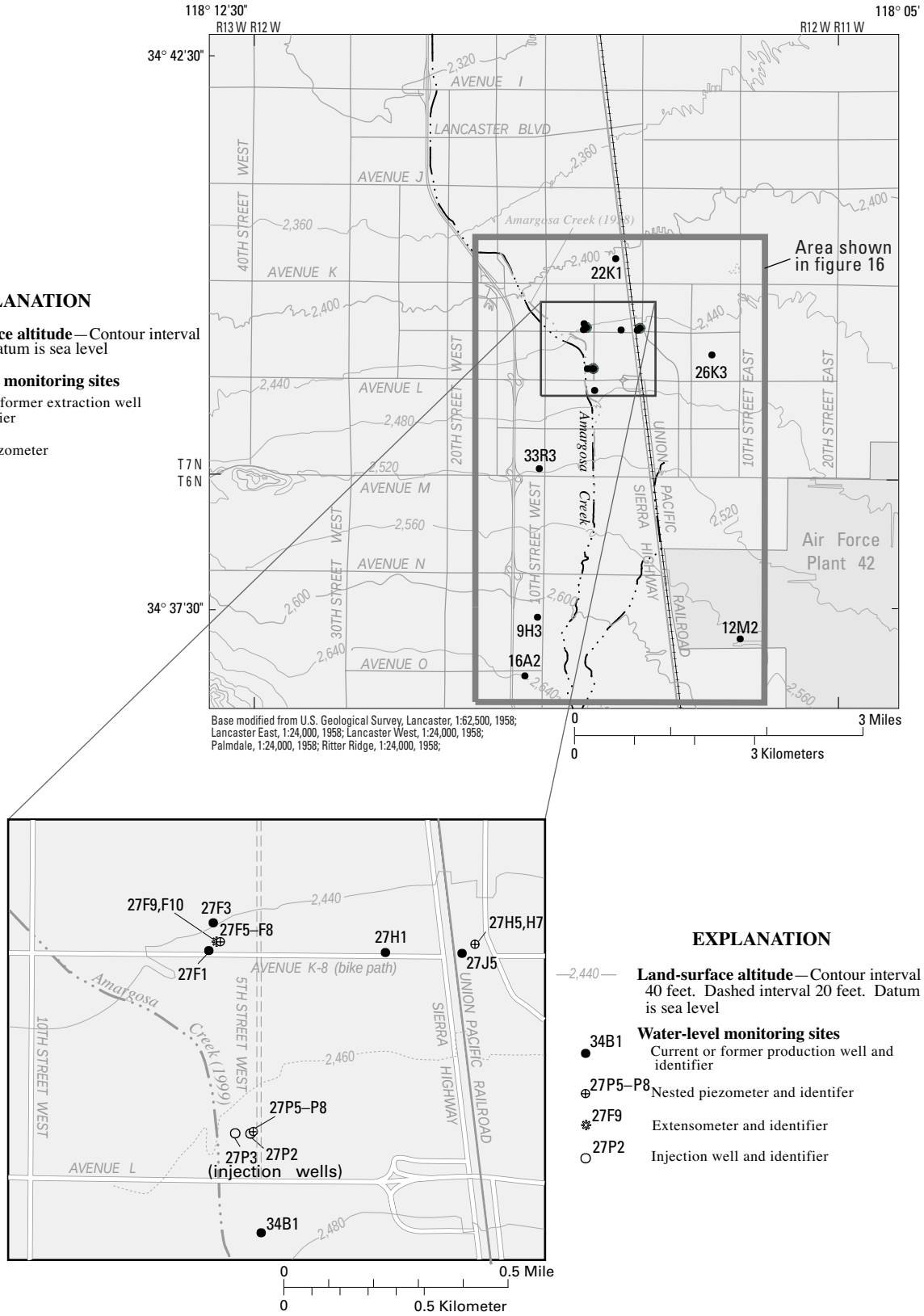

Figure 15. Locations of nested piezometers and current or former extraction wells used in the ground-water-level monitoring network, Lancaster, Antelope Valley, California.

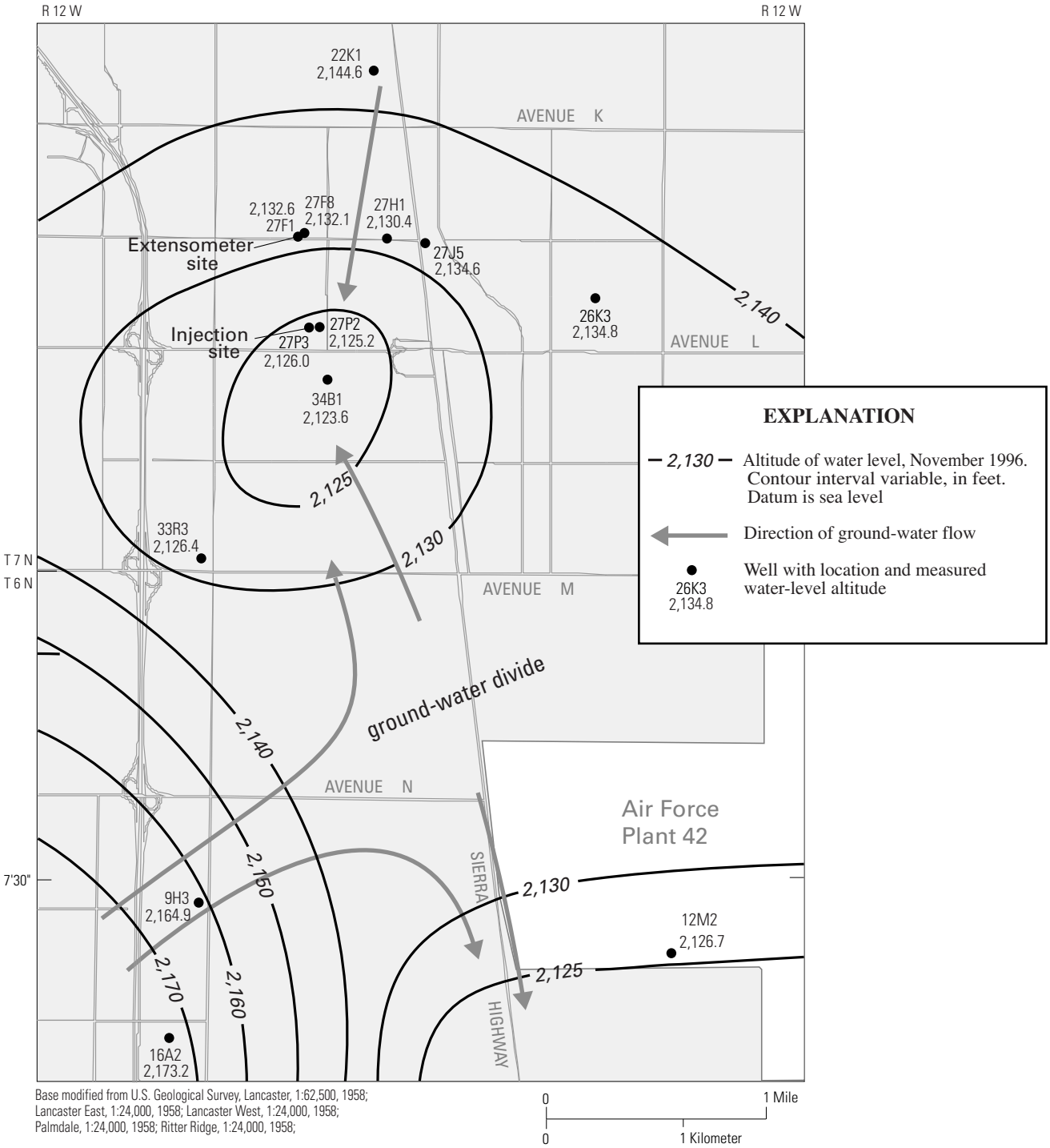

Figure 16. Water levels and approximate water-level contours near injection site, before injection cycle 2, Lancaster, Antelope Valley, California, November 1996.

All wells perforated in the upper aquifer; some also perforated in other aquifers (see table 1). Areal extent shown in figure 15.

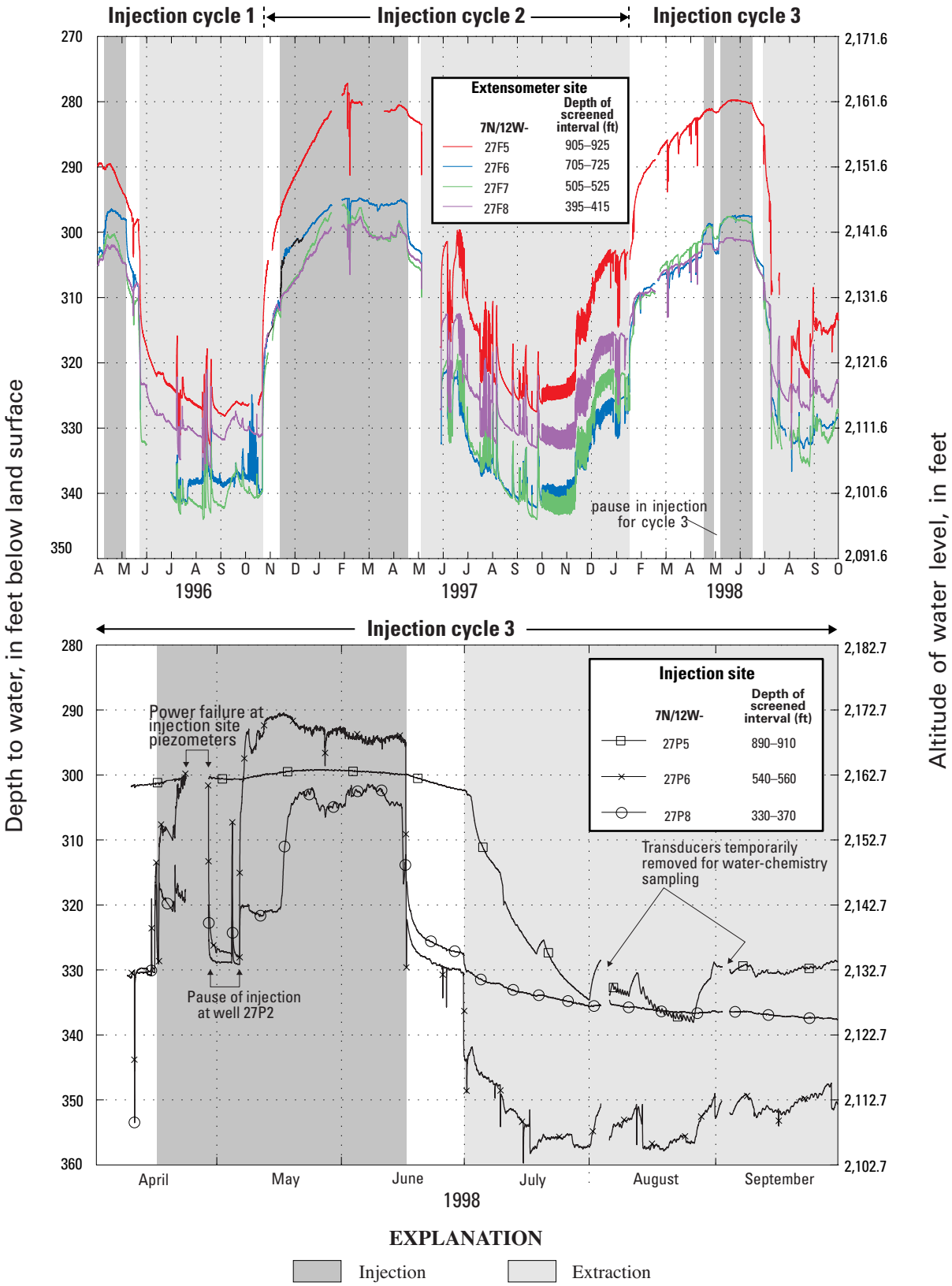

Figure 17. Piezometers and wells closest to injection wells in Lancaster, Antelope Valley, California.

Unlabeled discontinuities in data are gaps in data collection. Aquifers associated with extensometer- and injection-site piezometers are shown in figures 9 and 10 (ft, foot).

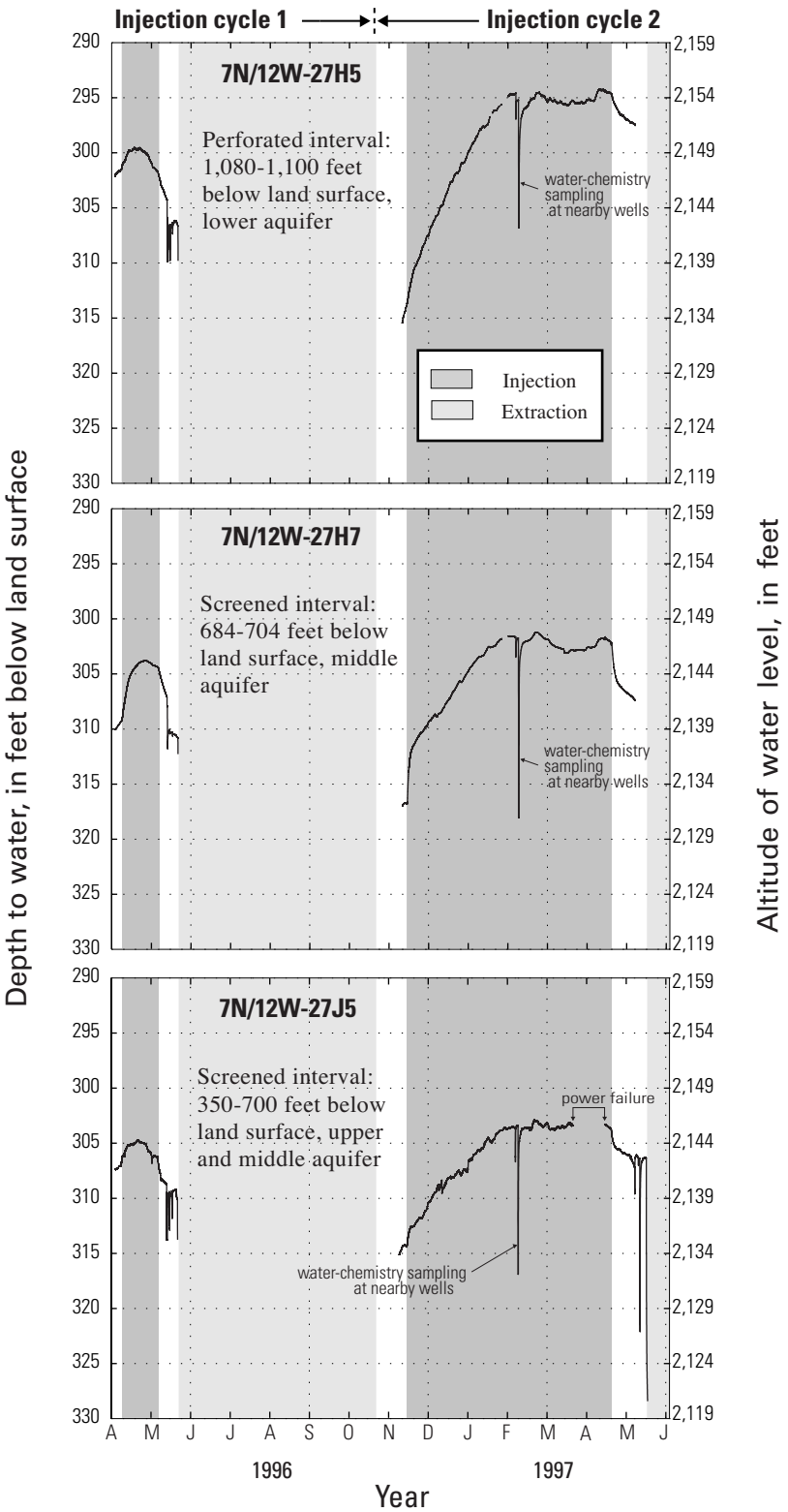

Figure 17.—*Continued.*

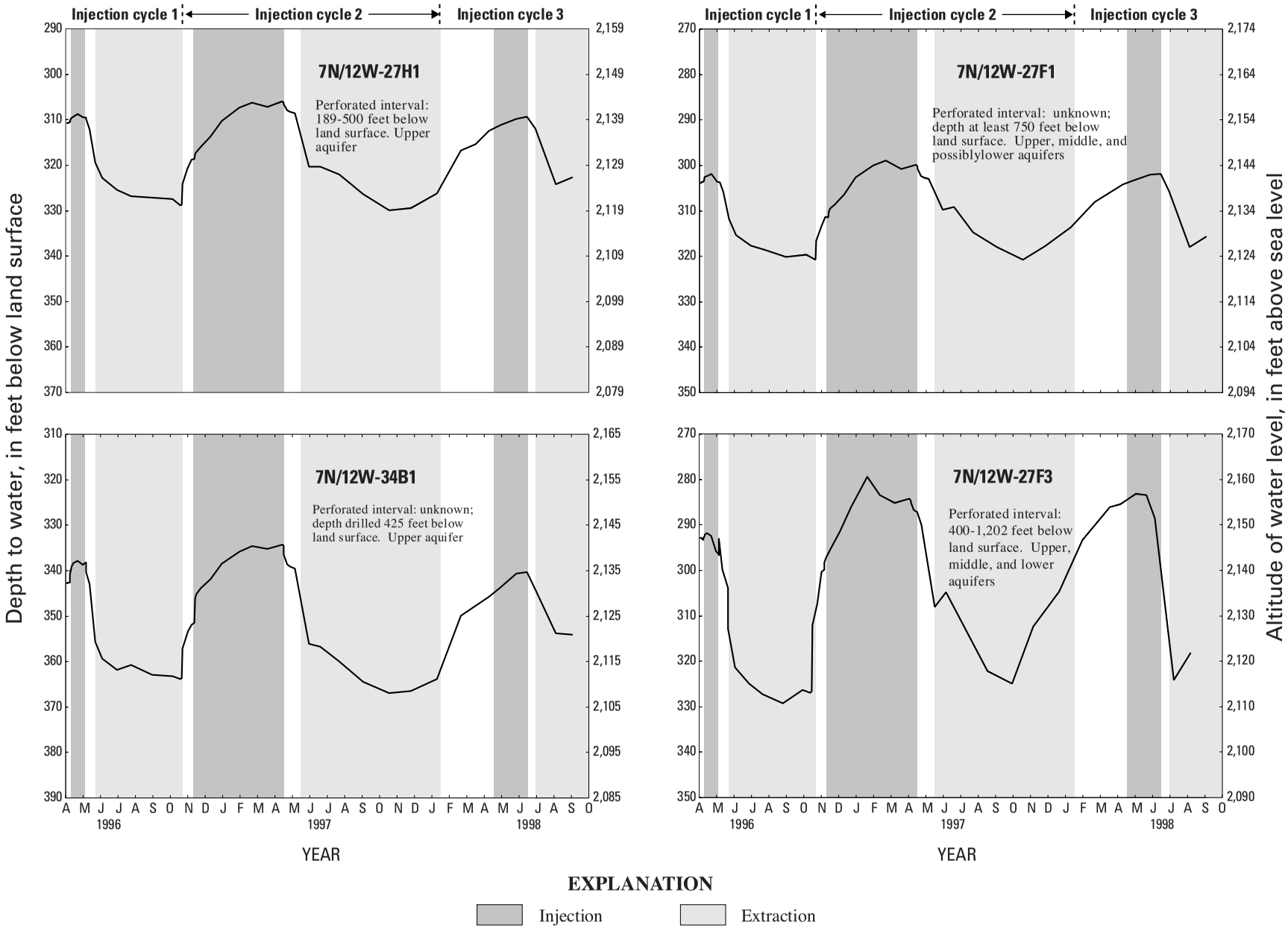

Figure 17.—*Continued.*

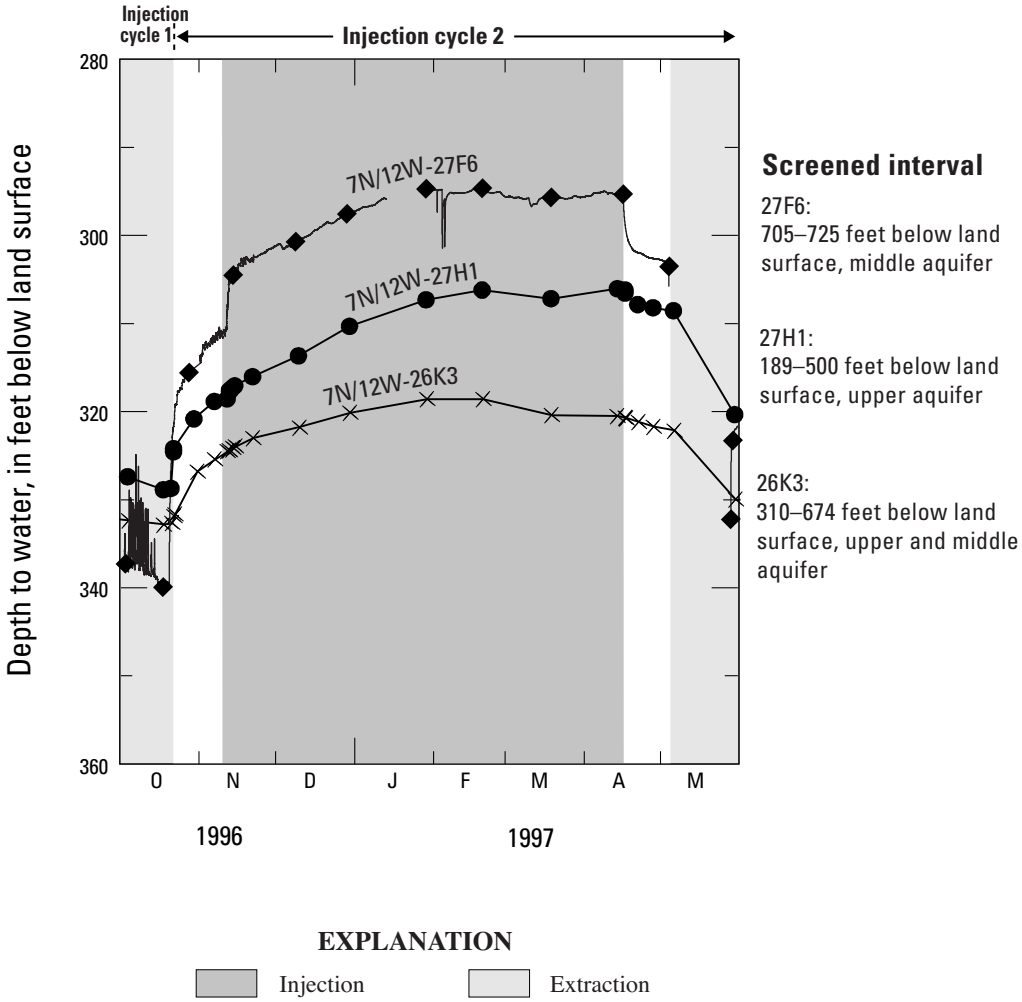

Figure 18. Variability in water-level response to injection cycle 2, Lancaster, Antelope Valley, California.

Wells shown are not at the same location or altitude (see figure 15).

Water levels for the upper, middle, and deep aquifers at the Water levels in the lower aquifer at the injection and extensometer sites responded similarly during the cycle-3 injection (fig. 19*C* and *D*, respectively). Responses to injection and during the storage period were highly subdued replicas of those in the middle aquifer. At the extensometer site, the head in the lower aquifer consistently exceeded that in the middle aquifer by 15 to 20 ft, maintaining an upward gradient. The greater head response in the middle aquifer at the injection site caused vertical gradients to reverse (to downward) during injection. The head responses during extraction were similar in magnitude to those in the middle aquifer, which is in sharp contrast to the subdued responses during injection and storage. This anomaly was caused by extraction, which started about July 9, 1998, from other nearby LACDPW wells to meet high water demand; it is clearly visible in the hydrographs for the extensometer site and for the lower aquifer at the injection site (fig.19*B, C, D*).

Water-Level Response Determined from Gravimetric Response

Microgravity surveys conducted during cycle 2 were used to estimate changes in water-table altitude during the injection tests (Howle and others, 2003). The surveys were done as an alternative to installing many additional monitoring wells for measuring ground-water levels. A rise or decline in the water table causes a net change in mass proportional to the volume of water that fills or drains pore spaces in the sediment.

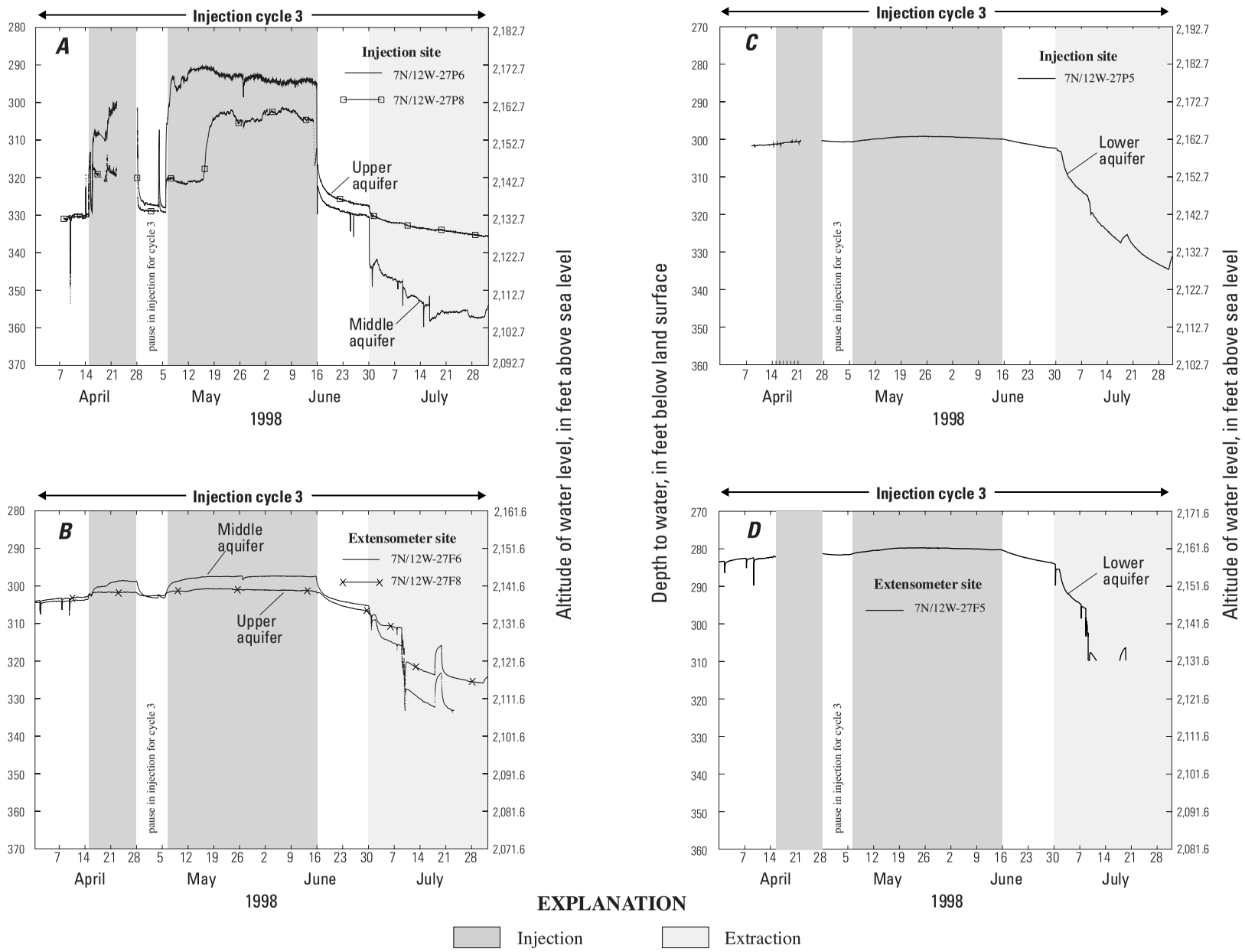

Figure 19. Water levels for the upper, middle, and deep aquifers at the injection and extensometer sites during injection cycle 3, Lancaster, Antelope Valley, California.

This mass change causes a small but measurable change in gravity. Precise measurements of gravity [determined from the microgravity surveys conducted at the gravity-station monitoring network (fig. 20)] were made before (November 1996 was the baseline) and during injection. The resulting gravity changes were used to estimate water-level changes at each gravity station based on a value of specific yield (0.13) determined from simultaneous water-level and microgravity measurements at well 7N/12W-34B1 (Howle and others, 2003). This well is adjacent to gravity station G5S (fig. 20). A more detailed account of the theory for using microgravity surveys for determining water-level changes is given in Howle and others (2003). See Pool and Hatch (1991) and Pool and Eychaner (1995) for descriptions of similar applications.

The gravimetric response measured at the gravity stations along the central south–north survey line is shown in figure 21. The gravity response to injection was greatest near the injection wells and generally decreased with distance from the wells. The response along the west–east survey line was more complex; Howle and others (2003) provides a more detailed account.

Monitoring of Subsidence-Related Effects

Two forms of land-surface deformation were studied during the injection tests: land subsidence and temporary uplift of the land surface with the onset of injection. Although historical land subsidence was small at the injection site, it was substantial a short distance to the north (fig. 7); therefore, it was important to monitor the effects of injection activities on land subsidence. A temporary uplift of the land surface was measured using occasional static GPS measurements during the preliminary injection tests at the Avenue K–8 and Division Street well field in 1994. Maximum uplift and areal distribution of uplift were unknown; uplift measured during the preliminary injection tests, however, was about 4 to 6 cm. The error associated with the static GPS measurements is unknown.

Several methods were used to measure land-surface deformation during the injection cycles; they include borehole extensometry, continuous GPS, spirit leveling, and high-precision tiltmeters. These methods are described in detail by Metzger and others (2002).

Borehole Extensometers

A dual borehole extensometer was constructed about 0.5 mi north of the injection wells (fig. 8) to measure land-surface deformation during and beyond this study. A borehole extensometer is a device for establishing a reference point at the bottom of a borehole and measuring the vertical position of this reference point with respect to the land surface. As the intervening part of the aquifer system compacts, the reference point and land surface converge. At the extensometer constructed for this study, counter-weighted pipes rest on concrete plugs (the reference points) at the bottom of two boreholes of different depths [see Metzger and others (2002) for design details]. The movement of these pipes relative to land surface was measured to determine the compaction or expansion of the aquifer system. This set of pipe extensometers measures deformation continuously from about 15 ft below land surface (avoiding near-surface effects caused by temperature variation and shrink/swell of clays) to 700 and 1,180 ft. The 16- to 700-ft interval represents most of the upper and middle aquifers, and the difference between these measurements and those of the 16 to 1,180 ft interval represents the interval from 700 to 1,180 ft, which contains the entire lacustrine unit, other materials in the upper part of the lower aquifer, and the remainder of the middle aquifer. The extensometers are paired with four nested piezometers screened at various depths within this interval (fig. 10). This pairing provides simultaneous, continuous measurement of stress (water-level change) and strain (aquifer-system deformation) (fig. 22).

Continuous GPS

A permanent antenna mount for a continuous GPS site was established about 65 ft from injection well 7N/12W-27P2 (fig. 8). Continuous GPS was used to obtain continuous measurements of land-surface elevation near the injection wells to better understand the magnitude and transient nature of land-surface uplift with the onset of injection. The GPS data were collected at intervals of 30 to 120 seconds using slightly different equipment and procedures for the different cycles, as described in Metzger and others (2002).

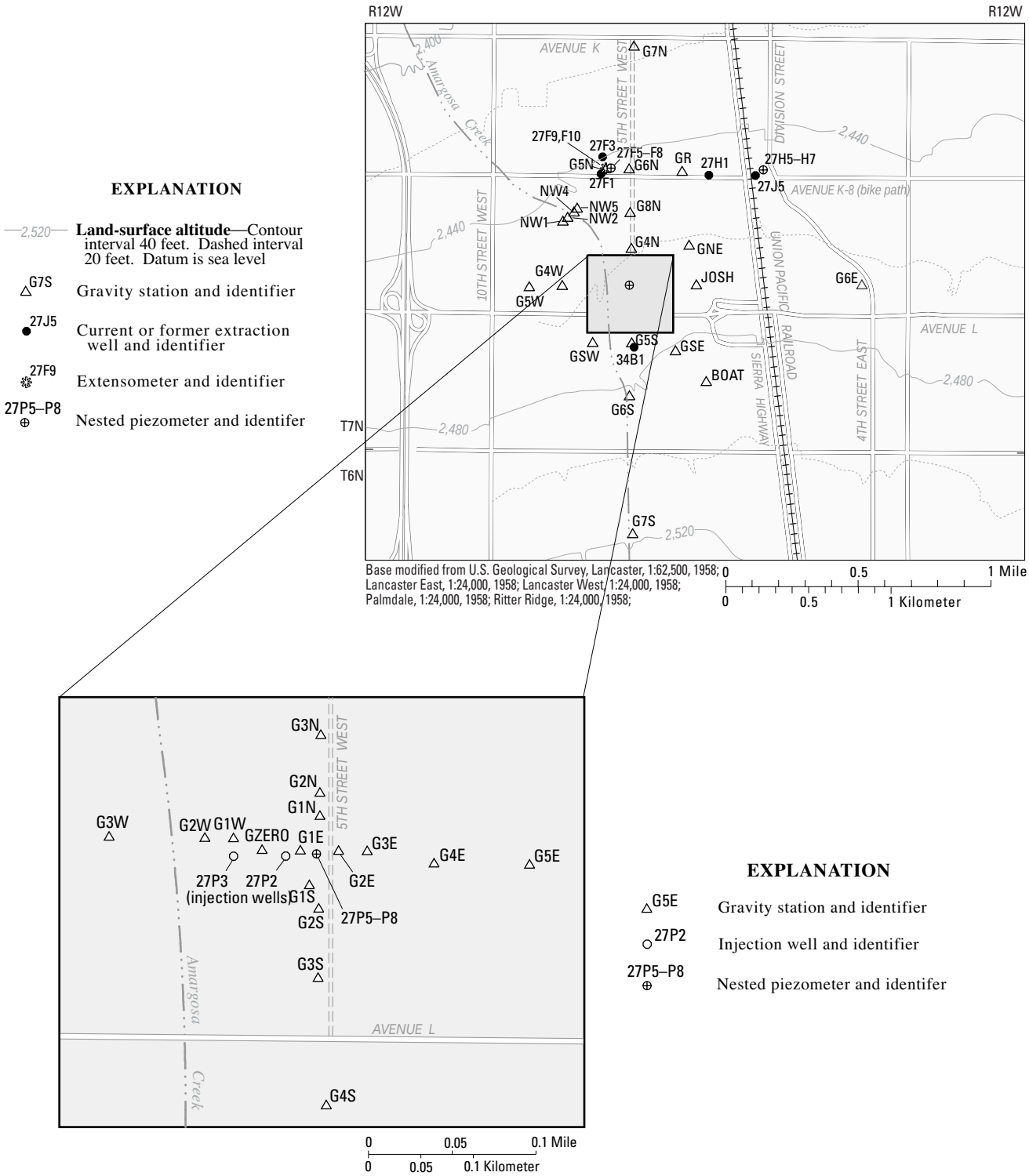

Figure 20. Locations of gravity stations, Lancaster, Antelope Valley, California.

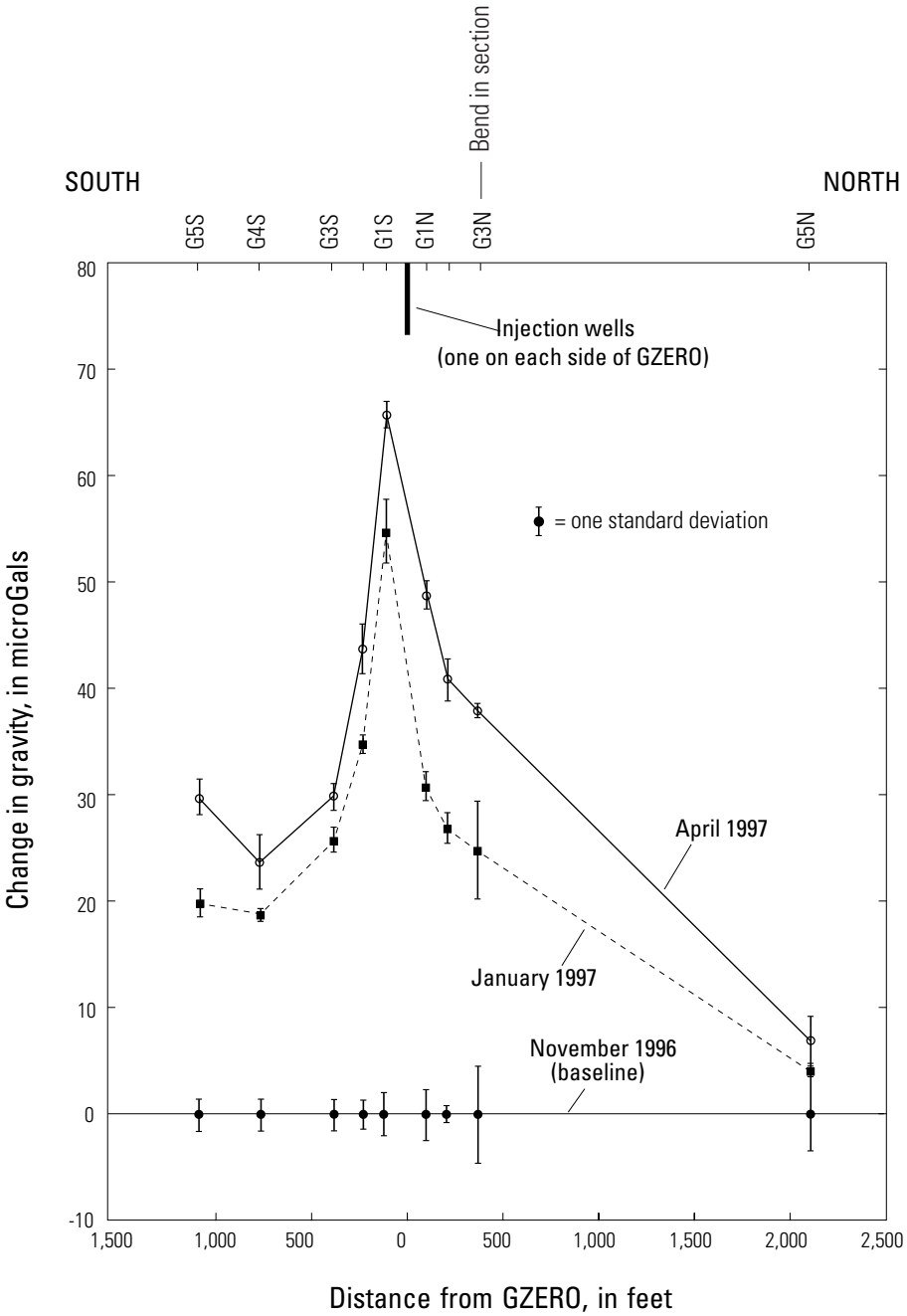

Figure 21. Change in gravity from pre-injection survey (November 1996) to post-injection survey (April 1997) near Lancaster, Antelope Valley, California.

Continuous GPS data collected during the first and third cycles were analyzed using GAMIT/GLOBK software (Herring, 1998; King and Bock, 1998), using methods described by Behr and others (1998). The data collected from the Lancaster injection site (LINJ) were used to calculate a position relative to three Southern California Integrated GPS Network (SCIGN) continuous-GPS stations—Chilao Flat (CHIL), Holcomb Ridge (HOLC), and Table Mountain (TABL). Data from the second cycle were collected from LINJ and from a temporary control site established at AVEK headquarters on Quartz Hill, a prominent bedrock outcrop, and analyzed using methods similar to those described in Ikehara and Phillips (1994).

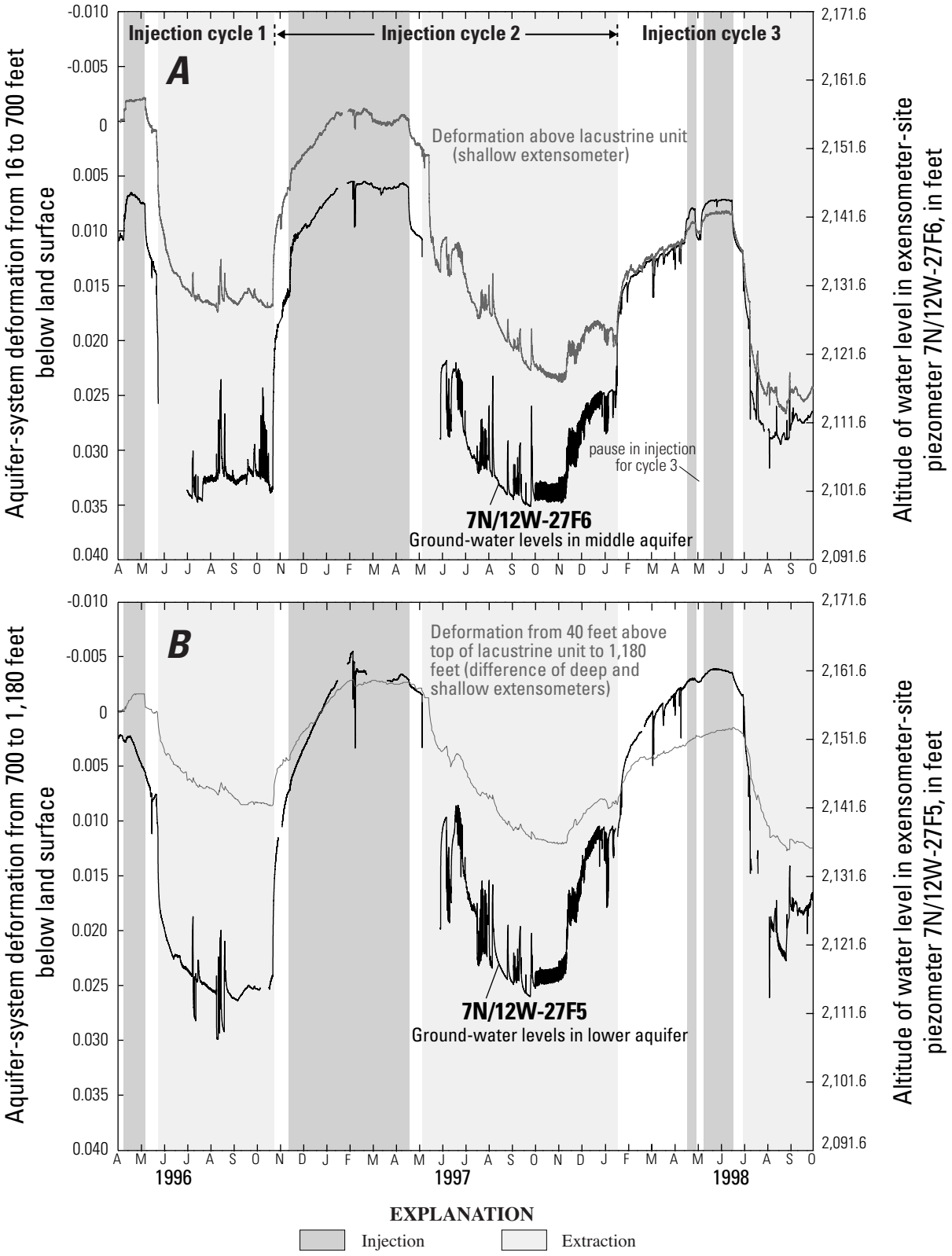

Figure 22. Aquifer-system deformation and water levels during injection cycles 1–3, Lancaster, Antelope Valley, California in (*A*) the upper aquifer and middle aquifer above the lacustrine unit and (*B*) the lacustrine unit and upper part of the lower aquifer, 1996–98.

Breaks in graphs indicate wells were not in use.

The continuous GPS data were processed to estimate absolute station positions in a global reference frame. Precise ephemerides (satellite orbits) generated by the International GPS Service (Beutler and Neilan, 1997) and UT1/polar motion estimates provided by the U.S. Naval Observatory were used to provide optimal estimates of the satellite positions and orientation of the global reference frame. Daily and sub-daily positions were estimated from data recorded every 30 to 120 seconds; the sub-daily solutions, however, did not provide additional relevant information and were associated with greater error. Daily solutions for all three cycles are shown in figure 23.

Spirit Leveling

Spirit-leveling surveys were done in the vicinity of the injection and extensometer sites to document the areal nature of land-surface deformation during injection. The monument array installed and used for the leveling surveys consists of more than 120 bench marks generally spaced 40 m (131 ft) apart (fig. 24). Static GPS was used to determine the altitude of bench mark ZERO. The horizontal locations of the remaining bench marks were determined by fast-static GPS using bench mark ZERO as a reference (Metzger and others, 2002). All the surveys were done to first-order accuracy using laser leveling methods without temperature corrections (Federal Geodetic Control Subcommittee, 1984).

For the first injection cycle, it was assumed that the temporal pattern of uplift would be similar to that observed during the preliminary tests in 1994, which indicated that maximum uplift may occur after the first week of injection. Accordingly, leveling took place during the seventh and eighth day of injection. However, the initial continuous GPS results from the first cycle indicated that uplift may have occurred within 48 hours of the onset of injection, and therefore, leveling for the second cycle was done during the first 2 days of injection. Leveling was not done for the third cycle except at the gravity monuments, which was done well into the test.

Leveling results in the form of change from the initial survey (September 25–28, 1995) are shown in figure 25 for selected periods for the bench marks along the south–north survey line; results of all the surveys are given in Metzger and others (2002). The primary assumption made from the results shown in figure 25 was that the southernmost bench mark, measured during successive surveys, was vertically stable between the surveys.

Using the assumption that the southernmost bench mark is vertically stable, results of the surveys for the first injection cycle indicate that uplift near the injection wells is less than 2.0 mm (0.006 ft) 7 and 21 days from the start of injection. Longer term results, through cycle 2, show little or no uplift at the injection site and generally more variability toward the northern end of the survey line (fig. 25).

Tiltmeters

High-precision tiltmeters were used by Robert Larson, LACDPW Materials Engineering Division, to characterize the shape and estimate the extent of land-surface uplift during cycle 2 injection. Data were obtained from three tiltmeters installed north of injection well 7N/12W-27P3 at distances of 134, 305, and 1,323 ft from the well (fig. 26). The magnitude and direction of tilt for each tiltmeter during the first 2 months of the cycle 2 injection are shown in figure 27.

Monitoring of Water Chemistry

Ground-water and injection-water chemistry was monitored to estimate the percentage of injected water recovered and the related residual effects of injection on ground-water chemistry. All water-chemistry data collected and analyzed prior to and during the first two injection tests are included in Metzger and others (2002). This discussion focuses on these two tests. Data collected for the third test, which involved a typical source of water, are included in Fram and others (2002) and analyzed by Fram and others (2003); the analytical methods are described in these reports.

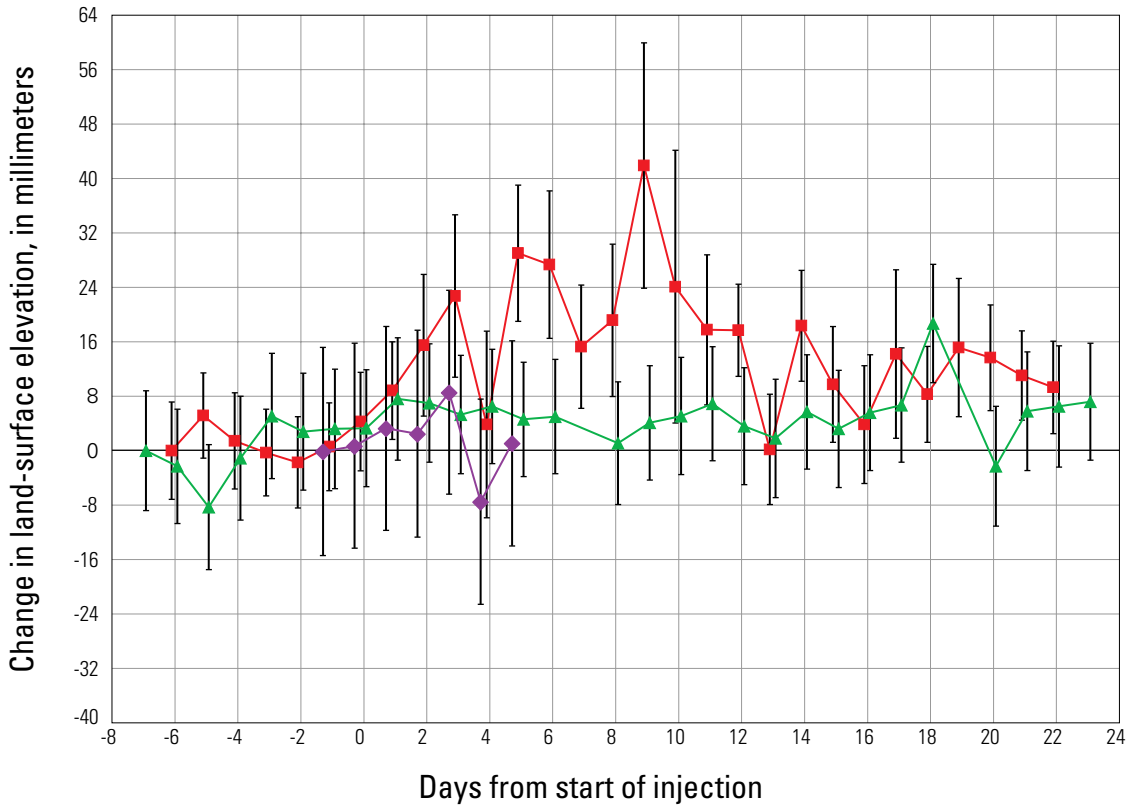

EXPLANATION

Daily solution with error bar showing one standard deviation:

Cycle 1 for April 7–13, 1996.
(Maximum uncertainty ± 16 millimeters)

Cycle 2 for November 6–December 4, 1996.
(Maximum uncertainty ± 19 millimeters)

Cycle 3 for April 9–May 9, 1998.
(Maximum uncertainty ± 9 millimeters)

Figure 23. Change in land-surface elevation at the injection site from continuous Global Positioning System (GPS) daily solutions for selected periods of injection cycles 1–3, Lancaster, Antelope Valley, California.

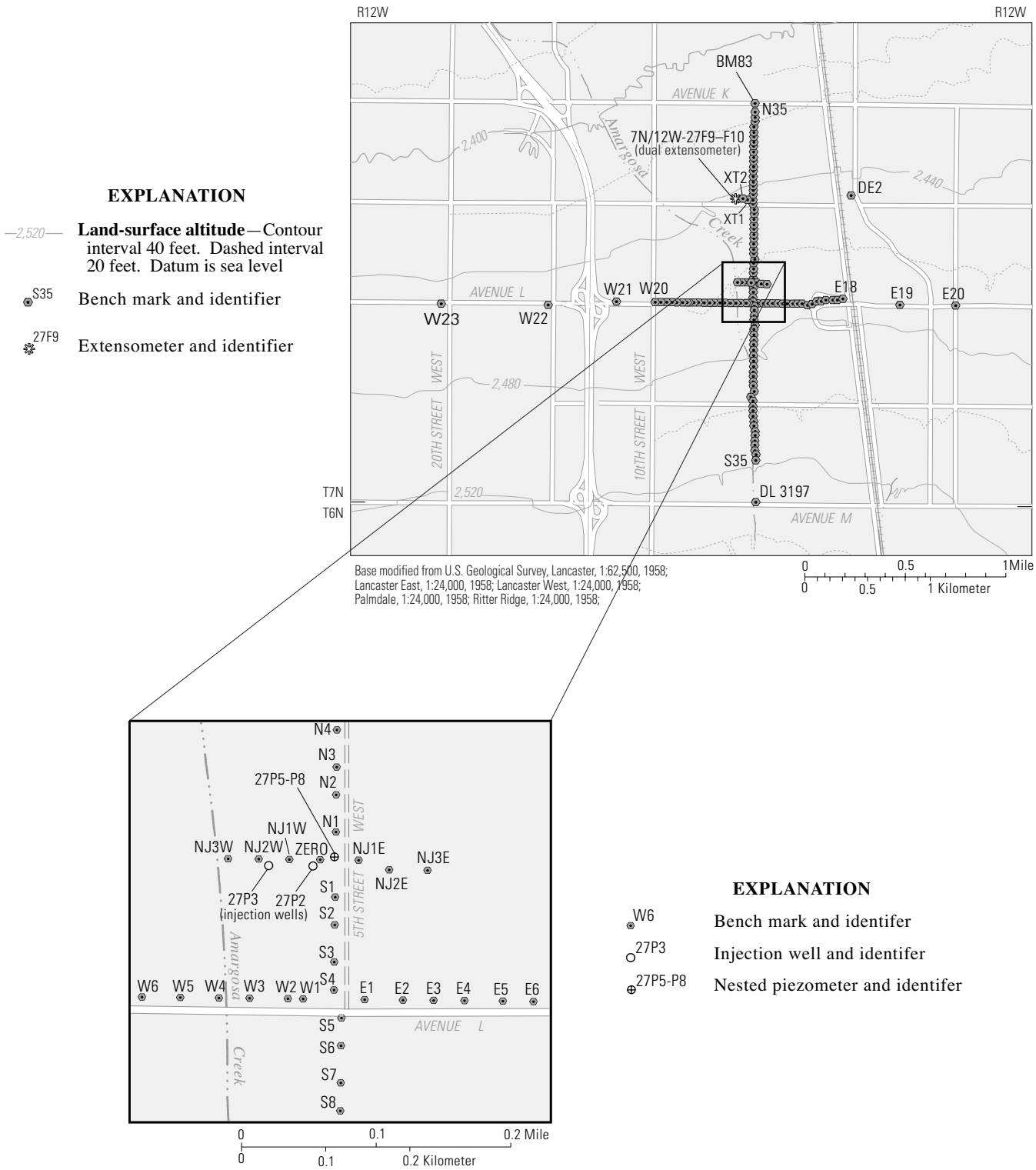

Figure 24. Locations of bench marks used to monitor changes in land-surface altitude, Lancaster, Antelope Valley, California.

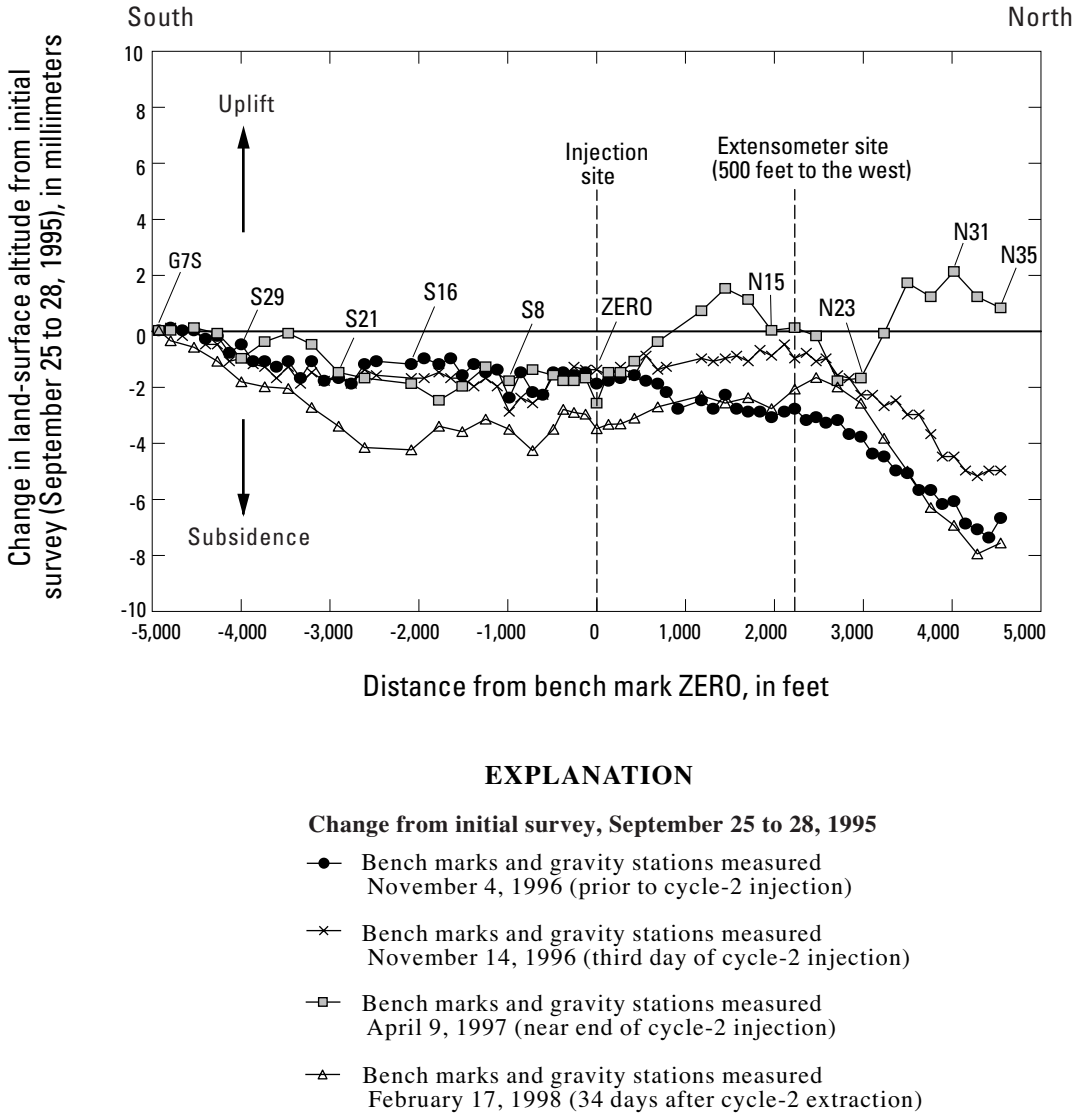

Figure 25. Change in land-surface altitude of bench marks and gravity stations along the south–north survey line, 1995–98, Lancaster, Antelope Valley, California.

See figure 20 for location of gravity station and figure 24 for location of bench marks.

Ground-water quality for pre-injection conditions was established by sampling the injection wells and other nearby production wells 1 year prior to the first pilot test and by analyzing field parameters, major ions, selected trace metals, and total trihalomethanes. Wells that penetrate the lower aquifer had a much higher salinity (total dissolved-solids concentrations of 314 to 630 mg/L) than those in the upper and middle aquifers (150–248 mg/L), and the pH ranged from 7.6 to 8.4. Major ion concentrations varied with depth and location (fig. 28). Sodium and potassium were the dominant cations in all wells, but the anions ranged from bicarbonate in the upper and middle aquifers to sulfate and chloride in wells that included the lower aquifer. Arsenic concentrations ranged from 4 to 51 µg/L; the larger concentrations were from the deep wells. Trihalomethanes were not detected.

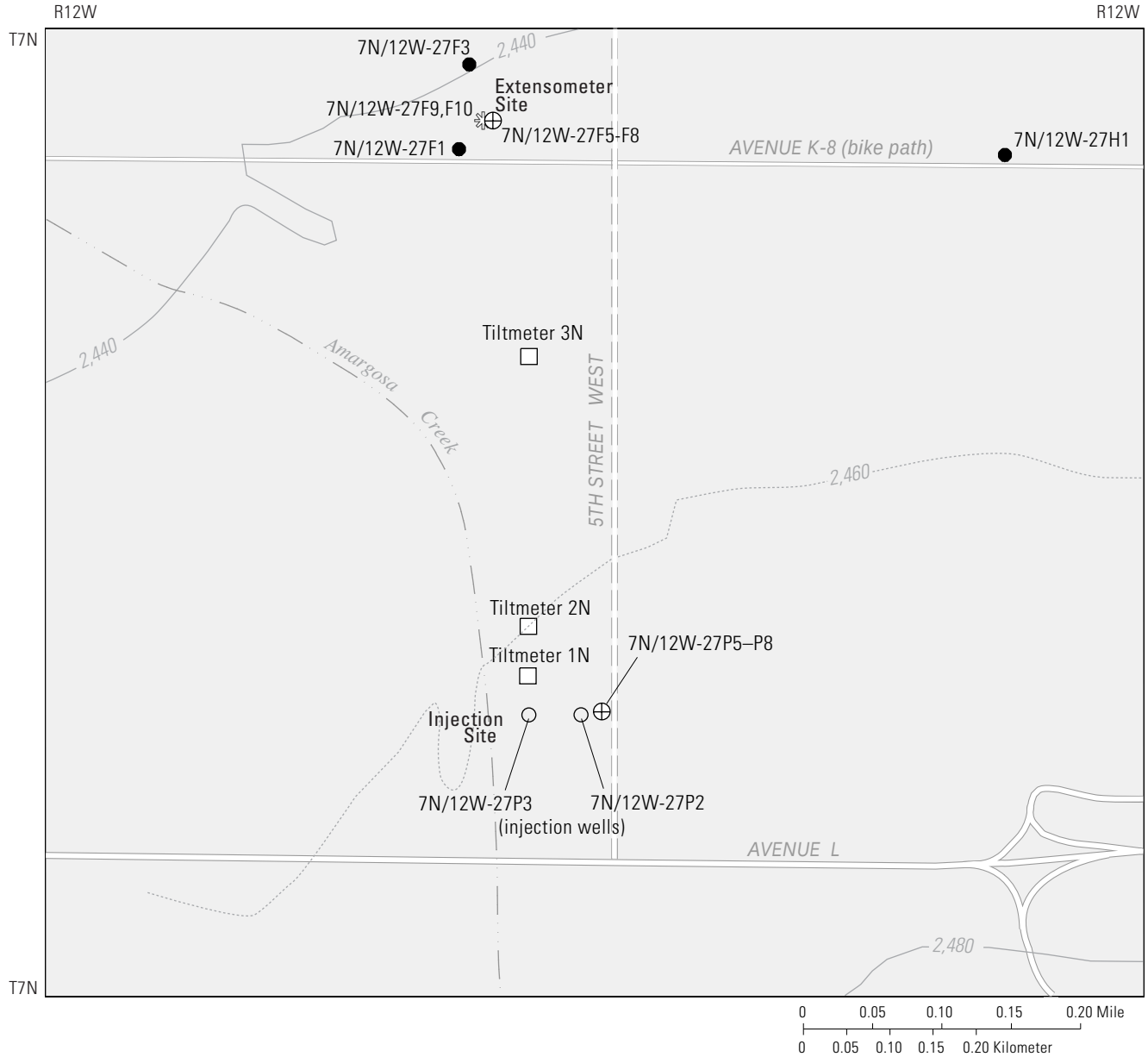

EXPLANATION

2,480	**Land-surface altitude**—Contour interval 40 feet. Dashed interval 20 feet. Datum is sea level
1N	**Tiltmeter and identifier**
27F3	**Water-level monitoring sites** Current or former extraction well and identifier
27P5-P8	Nested piezometer and identifer
27F9	**Extensometer and identifier**
27P2	**Injection well and identifier**

Figure 26. Locations of tiltmeters used to monitor land-surface deformation near Lancaster, Antelope Valley, California.

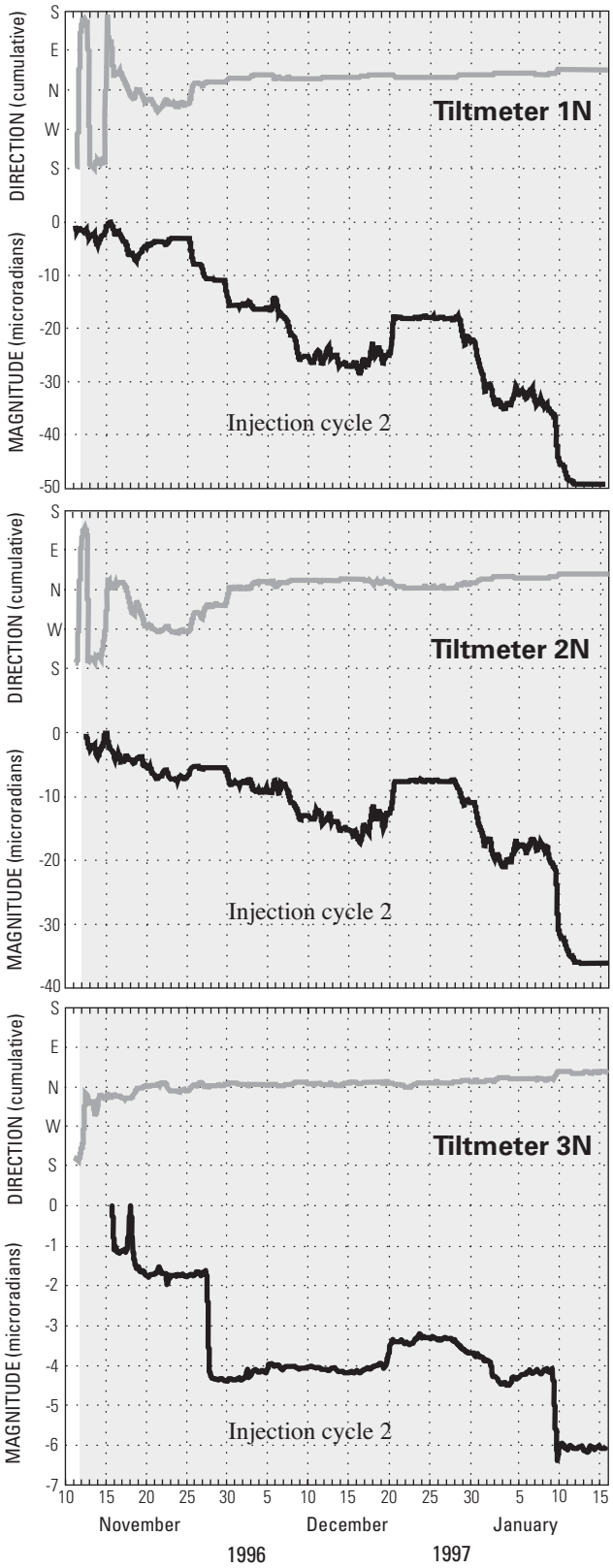

Figure 27. Magnitude (note variable scale) and direction of tilt recorded during injection cycle 2 at tiltmeters 1N, 2N, and 3N, Lancaster, Antelope Valley, California.

(From Robert Larson, Los Angeles County Department of Public Works, Materials Engineering Division, written commun., 1997)

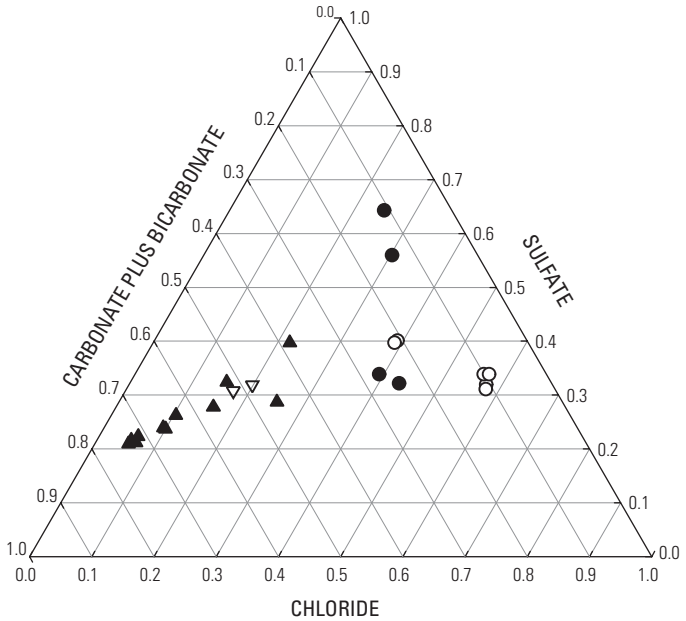

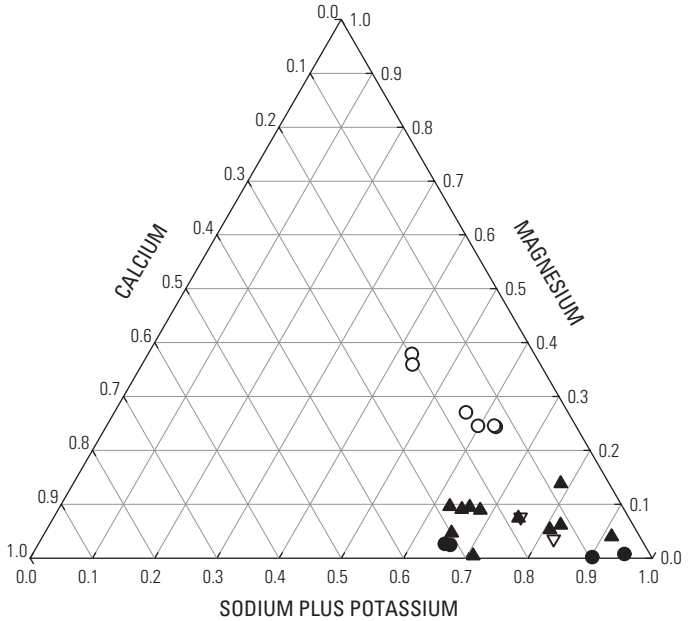

EXPLANATION

▲ **Ground water**—Upper and middle aquifers

● **Ground water**—Upper, middle, and lower aquifers

▽ **Ground water**—Injection wells 7N/12W-27P2–P3 (upper and middle aquifers)

○ **Injection water**—Cycle 2

Figure 28. Chemical contrast between native ground water and injected water, Lancaster, Antelope Valley, California.

The injected water originated as surface water in reservoirs north of the Antelope Valley and was imported from the Sacramento–San Joaquin Delta via the California Aqueduct. All water was treated to meet the drinking-water standards by AVEK. Imported water is delivered to most Lancaster residents during the late autumn, winter, and early spring, and generally is blended with ground water during the rest of the year. The injection water type was indeterminate, with sodium and potassium the dominant cations and chloride the dominant anion (fig. 28). The total dissolved solids (TDS) ranged from 94 to 326 mg/L, and the pH ranged from 6.7 to 7.1.

There were some differences in the major-ion and trace-metal concentrations in the native ground water and the injected water. The concentrations of magnesium, potassium, sulfate, and chloride in injected water were greater than those in the native ground water, but the nitrate concentrations were lower. The only trace metal regularly detected in the injected water was zinc, which was not detected in the native ground water. Arsenic was not detected (<2 μg/L) in the injected water.

Water delivered by AVEK contains disinfection by-products (DBPs) not found in native ground water. Trihalomethanes (THMs) are DBPs formed from dissolved organic carbon (DOC) and bromide, both present in the imported SWP water, and chlorine gas (Cl_2), used for disinfection. Cl_2, which is added at the end of the treatment process, reacts with water to form HOCl and OCl^- (hypochlorous acid). HOCl and OCl^- reacts with dissolved bromide (Br^-) to form HOBr and OBr^- (hypobromous acid). The hypochlorous and hypobromous acid species then react with DOC to form THMs and other DBPs (Fujii and others, 1998; Fram and others, 2003):

$$\text{DOC} + \text{HOCl} + \text{OCl}^- + \text{HOBr} + \text{OBr}^- \longrightarrow \text{THMs} + \text{other DBPs} \qquad (2)$$

The THMs produced range from chloroform ($CHCl_3$) to bromoform ($CHBr_3$). The Maximum Contaminant Level for total THMs in drinking water was recently lowered by the U.S. Environmental Protection Agency from 100 to 80 μg/L (U.S. Environmental Protection Agency, accessed October 2002).

The chemistry of the water injected into the aquifer system during the injection tests was variable owing to, in part, changes in water sources. The sources of the SWP water primarily were the Sacramento–San Joaquin Delta during the first two injections tests (there was a brief switch to San Luis Reservoir in March 1997) and from Lake Isabella during the third test. Figures 29 and 30 show measured concentrations of chloride and THMs, respectively, for all three injection cycles. Chloride concentrations in weekly samples of the injected water during cycles 1 and 2 ranged from 4.7 to 94 mg/L, with a median of 53 mg/L. THM concentrations in the injection water during the same period ranged from 21 to 62 μg/L, with a median of 37 μg/L. Chloride and THM concentrations were notably affected by the brief switch in water sources in March 1997. Median chloride and THM concentrations in injected water during cycle 3 were lower at 9 mg/L and 29 μg/L, respectively.

The initial concentrations of the THMs in extracted ground water following the injection and storage periods of the first two injection cycles were much higher than the maximum measured concentrations in the injected water). The peak THM concentration in the water extracted from injection well 7N/12W-27P2 during cycles 1 and 2 was 127 μg/L compared with the maximum measured concentration of 62 μg/L in the injected water. In contrast, the maximum chloride concentration in well 27P2, early in the extraction period of cycle 2, was 61 mg/L, which is close to the median concentration for the injected water during that cycle (56 mg/L) and consistent with the final chloride concentration measured during injection (57 mg/L; fig. 29). Chloride concentrations in ground water collected early in the extraction period of the first injection cycle exceed those measured during injection (fig. 29); however, given the extreme variability of the chloride concentrations in the injected water and only a weekly sampling rate, it is assumed that the extremes were not represented in the four samples taken during the cycle-1 injection period. The THM concentrations in the extracted water during the third injection cycle also increased during the storage period, but concentrations generally were lower (during injection) than those during the previous injection cycles (fig. 30). However, the chloride concentrations, unlike those during the previous cycles, generally were lower than those in the native ground water during injection but increased toward background concentrations during extraction (fig. 29).

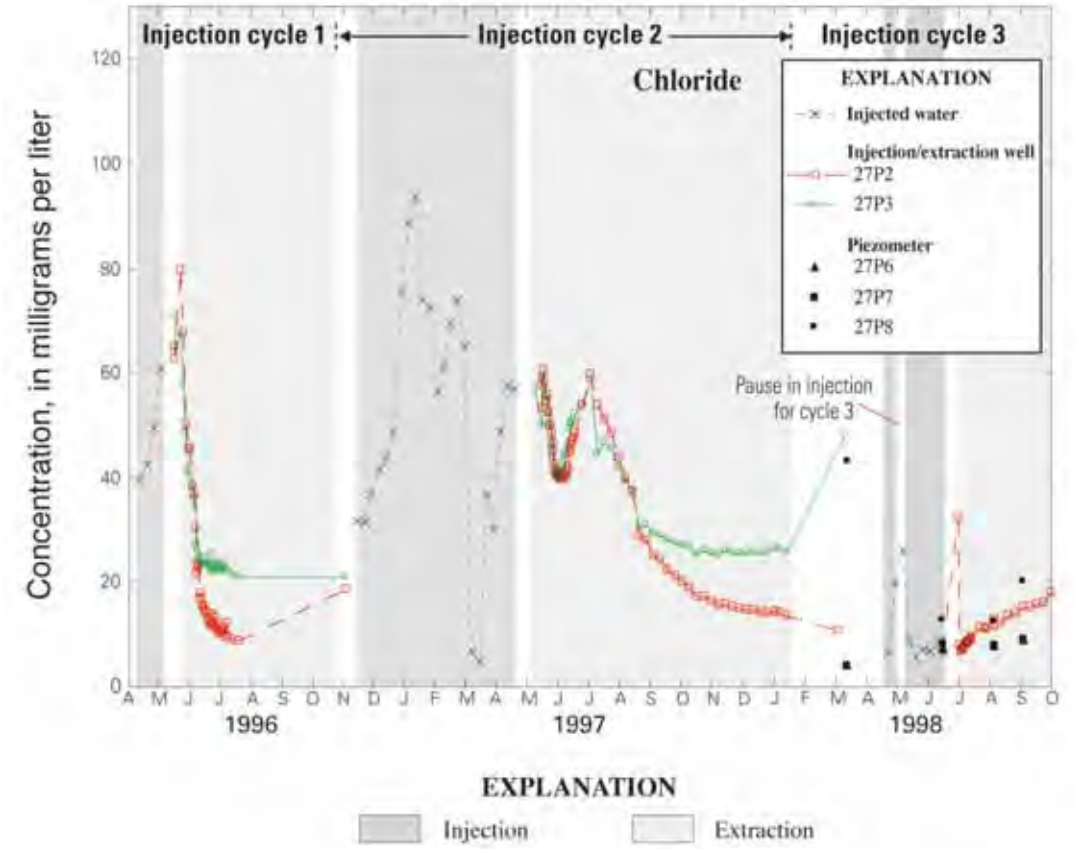

Figure 29. Cloride concentrations in injected and extracted water during injection cycles 1–3, Lancaster, Antelope Valley, California.

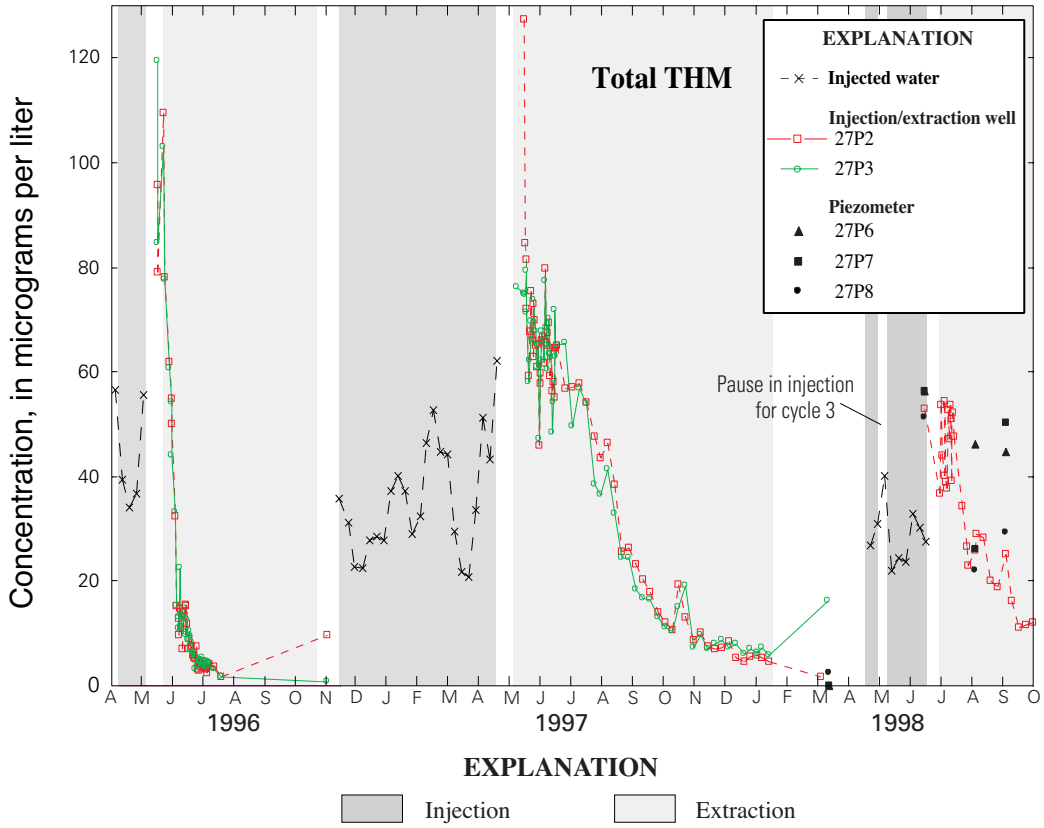

Figure 30. Trihalomethane (THM) concentrations in injected and extracted water during injection cycles 1–3, Lancaster, Antelope Valley, California.

ANALYSIS OF INJECTION TEST RESULTS

Aquifer-system properties of interest in this study include those affecting the hydraulic and subsidence-related responses to injection. A combination of analyses were used to estimate some of these properties, which were then tested and further refined through development of a simulation model. Water-chemistry data were analyzed to determine the chemical responses to injection.

Hydraulic Properties

Hydraulic properties of an aquifer system are physical characteristics that govern the capacity of the system to store and transmit water. For this study, these characteristics include storage coefficient, hydraulic conductivity, and transmissivity. Aquifer-test analyses can provide estimates of these properties. Such analyses were attempted to estimate hydraulic conductivity and transmissivity using water-level data from the injection-site piezometers during cycle 3; however, the unusual delayed water-level response in the shallow piezometer (7N/12W-27P8) during May 1998 (fig. 19) and the lack of water-level measurements for the injection well (owing to technical difficulties) severely limited the viability of analytical approaches. Instead, these values were estimated through calibration of the model.

The storage coefficient is the volume of water an aquifer releases from or takes into storage per unit surface area of the aquifer, per unit change in head. In the unconfined part of the system, removal of water from storage is manifested as a corresponding drop in the water table. This release of water from gravity drainage is described by the specific yield.

Specific yield was measured at one location in the study area where simultaneous measurements of water levels and gravity were available (Howle and others, 2003). Water levels were measured in well 7N/12W-34B1 prior to (h_o) and during injection (h_i), and corresponding microgravity measurements (g_o and g_i, respectively) were made at gravity monument G5S (fig. 20). The change in gravity was converted to a change in water mass (Δm_w):

$$\Delta m_w = \frac{g_i - g_o}{12.77} \tag{3}$$

where gravity is in μGals and Δm_w is in feet of water (12.77 μGals is the mass equivalent of 1 ft of water). Specific yield (S_y) was then calculated as follows (Howle and others, 2003):

$$S_y = \frac{\Delta m_w}{h_i - h_o} \tag{4}$$

The resulting value of specific yield was about 0.13 at well 7N/12W-34B1, which is within the range of typical values (0.02–0.30) for unconfined aquifers (Fetter, 1994).

The storage coefficient decreases deeper in the aquifer system as cumulative fine-grained sedimentary layers, typical of alluvial deposits, effectively reduce the hydraulic connection to the water table. Thus, when water is removed from deeper parts of the system, the water is not provided by drainage of the water table but primarily by deformation of the aquifer-system matrix. This dependence on the elastic properties of the aquifer system associated with confined aquifers effectively lowers the storage coefficient, which is now governed by the elastic skeletal specific storage and aquifer thickness. The observed increase in hydraulic response to stress with depth (fig. 19*A*, *B*), despite strong evidence that less water is produced from deeper parts of the aquifer system (fig. 5), is indicative of confined conditions.

Aquifer-System Deformation and Subsidence-Related Properties

The objectives of measuring aquifer-system deformation and associated deformation of the land surface included determining the spatial and temporal nature of land-surface uplift during injection and the subsidence-related properties of the aquifer system.

Uplift of Land Surface During Injection

An apparent uplift of the land surface of 4 to 6 cm was measured using static GPS during preliminary injection tests at the Avenue K–8 and Division Street well field. Although some uplift was anticipated because of the elastic nature of the aquifer-system materials, 6 cm was more than expected. Spirit leveling, tiltmeters, and continuous GPS were used at the current injection site to better understand the spatial and temporal nature of this apparent uplift.

Leveling results suggest that uplift occurred during injection but that this uplift probably was small [less than about 3 mm (0.01 ft)] during the first few weeks of injection at bench mark ZERO (fig. 25), which is about 30 ft northeast of injection well 7N/12W-27P2 . Note, leveling was done only periodically and, thus, larger elevation changes between surveys may have been missed. The assumption of stability of the southernmost bench marks included in successive surveys may be a source of error, particularly for the shorter surveys. However, comparisons of the results of the leveling surveys that included bench mark GS7, almost 5,000 ft south of the injection wells (fig. 25), appear to be valid, as the measured elevation changes from the spur line to the deep extensometer agree with the extensometer measurements from each of the surveys (within 0.3 to 0.6 mm [0.001–0.002 ft]). Only the survey lines that include bench mark GS7, which are consistent with respect to changes at the extensometer, are shown in figure 25.

Results from the tiltmeter array (fig. 27) show northward tilt during cycle 2 in all three tiltmeters, the most distant at about 1,320 ft from injection well 7N/12W-27P3 (fig. 26). The meters closest to the injection well tilted the steepest away from the well, suggesting a concave-upward shape to the deformation. Rough estimates of uplift at well 7N/12W-27P3 can be calculated using the tilt data and making assumptions about the distribution of tilt between meters. Assuming the tilt between meters is best represented by that at the meter farthest from the injection well results in a minimum estimate of about 6 mm (0.02 ft) of uplift by January 16, 1997 (after just more than 2 months of injection during cycle 2). Assuming the tilt between meters is best represented by the average tilt at adjacent tiltmeters results in a higher estimate of about 11 mm (0.04 ft) of uplift during the same period. These estimates assume negligible uplift at the outermost meter and no increase in tilt over the 134 ft between the innermost meter and the injection well; uplift may have been greater than estimated if these assumptions are not correct.

Tilt increased at a fairly constant rate during the measured period suggesting a slow, steady rate of uplift. Uplift as of November 14, 1996 (the third day of the cycle-2 injection) was calculated, as described in the previous paragraph, for comparison with leveling results; however, early data were not available for tiltmeter 3N (farthest from the injection well; fig. 27). It was assumed that the ratio of uplift between tiltmeters 1N and 2N and between tiltmeters 2N and 3N remained constant during injection; uplift from tiltmeters 2N and 3N was estimated from this ratio calculated as of January 16, 1997. The resulting high-end estimate of uplift on November 14, 1996, at injection well 7N/12W-27P3 was about 0.6 mm, which agrees well with the leveling results at bench mark ZERO [uplift of about 0.5 mm (0.002 ft)] (fig. 25).

The continuous GPS results by themselves suggest that about 42 mm (±18 mm) (0.14 ft ± 0.06 ft) of uplift may have occurred at the injection site during the first 9 days of the cycle-2 injection, followed by a decrease to the average (of a noisy signal) of about 10 mm (0.03 ft) above the pre-injection baseline (fig. 23). Leveling and tiltmeter results, however, do not support these GPS results. Leveling on November 14, 1996, indicates uplift of about 0.5 mm (0.002 ft) from the pre-injection baseline compared with about 16 mm (±11 mm) (0.05 ft ± 0.04 ft) indicated by GPS. The continuous tiltmeter record for the cycle-2 injection period suggests a slow, steady uplift; this contrasts sharply with the relatively extreme rise and fall suggested by the GPS data. GPS surveys can be influenced by several factors including changes in weather, stability of the control station(s), regional tectonic activity, and changes in the status of the GPS satellites. A weather front came through during the early part of the cycle-2 injection, and the antenna at the control station was found to have slipped downward 3 cm (prior to the apparent maximum uplift), but it is not known if either of these factors or other factors significantly influenced the results.

Combined results from the geodetic measurements described previously indicate there was uplift of the land surface during injection. This uplift was measured most accurately by the extensometers, followed by spirit leveling, which added a second dimension that proved to be very useful for interpretation. The tiltmeter data were used to determine the general shape and extent of deformation, but the continuous GPS data were too noisy to be of use for this study. None of these results differentiate between uplift caused by injection and that caused by normal water-level recovery from seasonal pumping. Examination of data from the shallow borehole extensometer and of associated water-level data shows that water levels and coupled aquifer-system deformation had not stabilized prior to the start of the cycle-2 injection (fig. 22*A*). Accordingly, uplift of the land surface during the cycle-2 injection likely was related to both injection and normal water-level recovery from seasonal pumping.

Estimation of Subsidence-Related Storage Properties at the Extensometer Site

Simultaneous measurement of aquifer-system deformation and water-level changes at the dual borehole extensometer provided the information needed to determine the subsidence-related storage properties of the aquifer system at the extensometer site. The elastic properties were used in a model, which is described later in this report, and although the model does not simulate inelastic deformation, these properties were estimated for the benefit of future investigations. Note that the excellent agreement between the land-surface changes at the extensometer site measured by leveling surveys and the deformation measured by the deep extensometer suggests that there was little or no deformation below the deep extensometer (1,180 ft).

The aquifer-system properties that govern the response (compaction or expansion) of the system to applied stress are components of the aquifer-system storativity. Storativity of a confined aquifer, which describes conditions in deeper parts of the aquifer system in the study area, consists of three components: elastic skeletal storage coefficient, inelastic skeletal storage coefficient, and storage derived from the compressibility of water. The elastic skeletal storage coefficient represents the amount of water yielded from fully recoverable (elastic) deformation of the aquifer-system skeleton (sediment). When deformation exceeds the elastic range and results in permanent rearrangement of the aquifer-system skeleton, the amount of water yielded is greater than that within the elastic range, and is represented by the inelastic skeletal storage coefficient. The amount of water yielded from the compression or expansion of water is relatively small and, in most cases, can be ignored.

Continuous measurements of water-level change (stress) and aquifer-system deformation (strain) can be used to determine individual components of aquifer-system storativity. Elastic and inelastic storage coefficients were estimated using an established graphical method (Riley, 1969). This method is similar to the approach taken to determine the coefficients of compressibility from stress/strain relations derived from laboratory consolidation tests. Applied stress (hydraulic head) is plotted on the *y*-axis and vertical strain (displacement) on the *x*-axis. A change in water level (hydraulic head) represents a change in applied stress, which is equivalent to the change in effective stress on a confined aquifer system with a constant total stress (eq. 1). Riley (1969) showed that for aquifer systems where pressure equilibration can occur rapidly between aquifers and aquitards, the inverse slopes measured from the predominant linear trends in the stress/strain trajectories represent measures of the skeletal storage coefficients.

Stress/strain diagrams for the period April 1996 through December 1998 were constructed for the aquifers above and below the lacustrine unit at the extensometer site. Aquifer-system deformation in the upper and middle aquifers was measured by the 700-ft (shallow) extensometer; deformation that occurred at the extensometer site in the depth interval 700 to 1,180 ft below land surface was deduced by computing the difference between the daily deformation measurements from the shallow and deep (1,180 ft) extensometers. These deformation timeseries data were matched with water-level timeseries data from the appropriate piezometers (fig. 22) to produce stress/strain diagrams representative of these intervals of the aquifer system (fig. 31).

The closed loops evident in the stress/strain diagrams (fig. 31) are indicative of cyclical loading in the elastic, or recoverable, range of deformation. The linear trend evident from the recovery segments of the closed loops represents the elastic behavior of the skeletal component of the system. The inverse slope of this linear trend (chosen subjectively) represents the elastic skeletal storage coefficient, which is about 4.5×10^{-4} for the upper and middle aquifers and 2.6×10^{-4} for the lower aquifer.

Inelastic compaction is evident both in the stress/strain diagrams (fig. 31) and in plots of water levels and deformation with time (fig. 22). Horizontal offsets of the large loops in the stress/strain diagrams indicate inelastic compaction on the order of the offsets, or about 0.008 ft in the upper and middle aquifers and 0.004 ft in the lower aquifer from 1996 to 1997. Similar offsets (about 0.007 ft in the upper and middle aquifers and 0.003 ft in the lower aquifer) are shown in the compaction record on figure 22) despite the recovery of water levels close to those of the previous year.

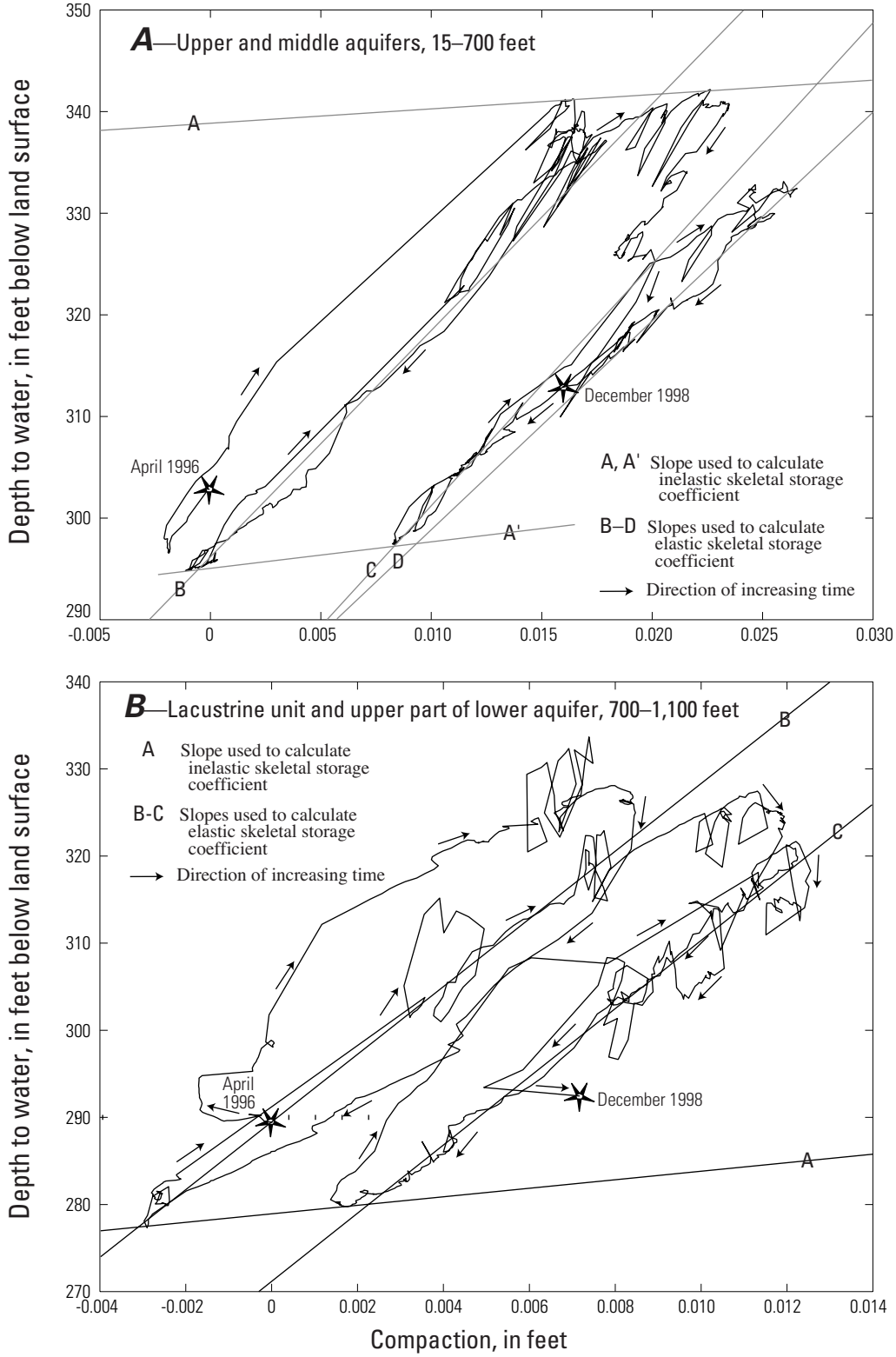

Figure 31. Continuous plot from April 1996 to December 1998 of depth to water (stress) versus compaction (strain) for (*A*) the upper and middle aquifers and (*B*) lacustrine unit plus upper part of lower aquifer, Lancaster, Antelope Valley, California.

Measured inelastic compaction, though small, allows estimation of the inelastic skeletal storage coefficient. A linear trend between successive annual loops in the stress/strain plots represents inelastic behavior of the skeletal component of the aquifer system (Riley, 1969). The inverse slope of this linear trend represents the inelastic skeletal storage coefficient, which is about 7.0×10^{-3} for the upper and middle aquifers and 2.0×10^{-3} for the lower aquifer. Because only 2.5 years of data were available, only two full loops could be plotted on in the stress/strain diagram; therefore, the slope drawn for this linear trend is somewhat subjective.

The estimated specific storages at different depths at the extensometer site were compared. The elastic specific storage was calculated using the entire thickness of the saturated materials within the extensometer range, which is about 385 ft for the 700-ft extensometer and 480 ft for the 1,180-ft extensometer (after the thickness of the 700-ft extensometer is subtracted). The inelastic specific storage was calculated using the combined thickness of the fine-grained materials in these intervals, which were estimated from the geophysical logs to be about 176 and 280 ft for the shallow (20 ohm-meters resistivity or less) and deep (10 ohm-meters resistivity or less) intervals, respectively. The resistivity values were selected by comparing the lithologic and geophysical logs. From shallow to deep, the calculated elastic specific storages are about 1.2×10^{-6} and 5.4×10^{-7} per foot and the calculated inelastic specific storages are about 4.0×10^{-5} and 7.1×10^{-6} per foot. The decrease in elastic and inelastic storage values with depth is consistent with the consolidating effects of deeper burial and more advanced induration (cementation), which was noted during drilling and observed indirectly on the velocity log (fig. 5).

Areal Distribution of Subsidence-Related Storage Properties

An understanding of the areal distribution of subsidence-related storage properties can aid in managing land subsidence in Lancaster and surrounding areas. Information regarding the areal distribution of these properties can be gained by comparing calculated values for the Lancaster area with those from a study of the Holly site at Edwards AFB (Sneed and Galloway, 2000) and by examining the spirit leveling data. Storativity at the Holly extensometer site, which is about 20 mi northeast of Lancaster on Edwards AFB, was estimated by Sneed and Galloway (2000) using stress/strain analyses and detailed one-dimensional simulations of compaction. The Holly extensometer measures aquifer-system deformation to a depth of 840 ft, which is similar in thickness to the 700-ft interval measured by the shallow extensometer in Lancaster. A fundamental difference in the geology of the two sites is that the lacustrine unit is at depths greater than 700 ft below land surface at Lancaster but at depths of only 140 ft below land surface at Holly.

The elastic specific storage based on the 700-ft extensometer in Lancaster (1.2×10^{-6}) is consistent with that determined at the 840-ft Holly extensometer (1.7×10^{-6}) (Sneed and Galloway, 2000). Estimates of inelastic specific storage at the Holly site ranged from 4.0×10^{-5} per foot for aquitards less than 18 ft thick to 3.5×10^{-4} per foot for thicker aquitards. The lithologic and geophysical logs of the borehole for nested piezometers 7N/12W-27F5–8 at the extensometer site in Lancaster (fig. 32) suggest that the aquitards are relatively thin above the lacustrine unit. The associated inelastic specific storage is 4.0×10^{-5} per foot, which equals that calculated by Sneed and Galloway (2000) for relatively thin aquitards. This estimate of inelastic specific storage is small compared with that reported for other aquitards (Riley, 1998).

Although the estimates of elastic and inelastic storage for the relatively thin aquitards at the Holly and the Lancaster sites agree well, the estimates of inelastic storage for thick aquitards is 200 times smaller at the Lancaster site (7.1×10^{-6} per foot) than at Holly (3.5×10^{-4} per foot). Sneed and Galloway (2000) concluded that delayed drainage of the thick aquitards is responsible for most of the ongoing land subsidence at the Holly site. In contrast, the lacustrine unit at the Lancaster extensometer site appears to be less responsible for subsidence than the thinner aquitards. The extensometer data for Lancaster show that only about one third of the inelastic compaction measured at this site is occurring in the interval containing the lacustrine unit (fig. 22).

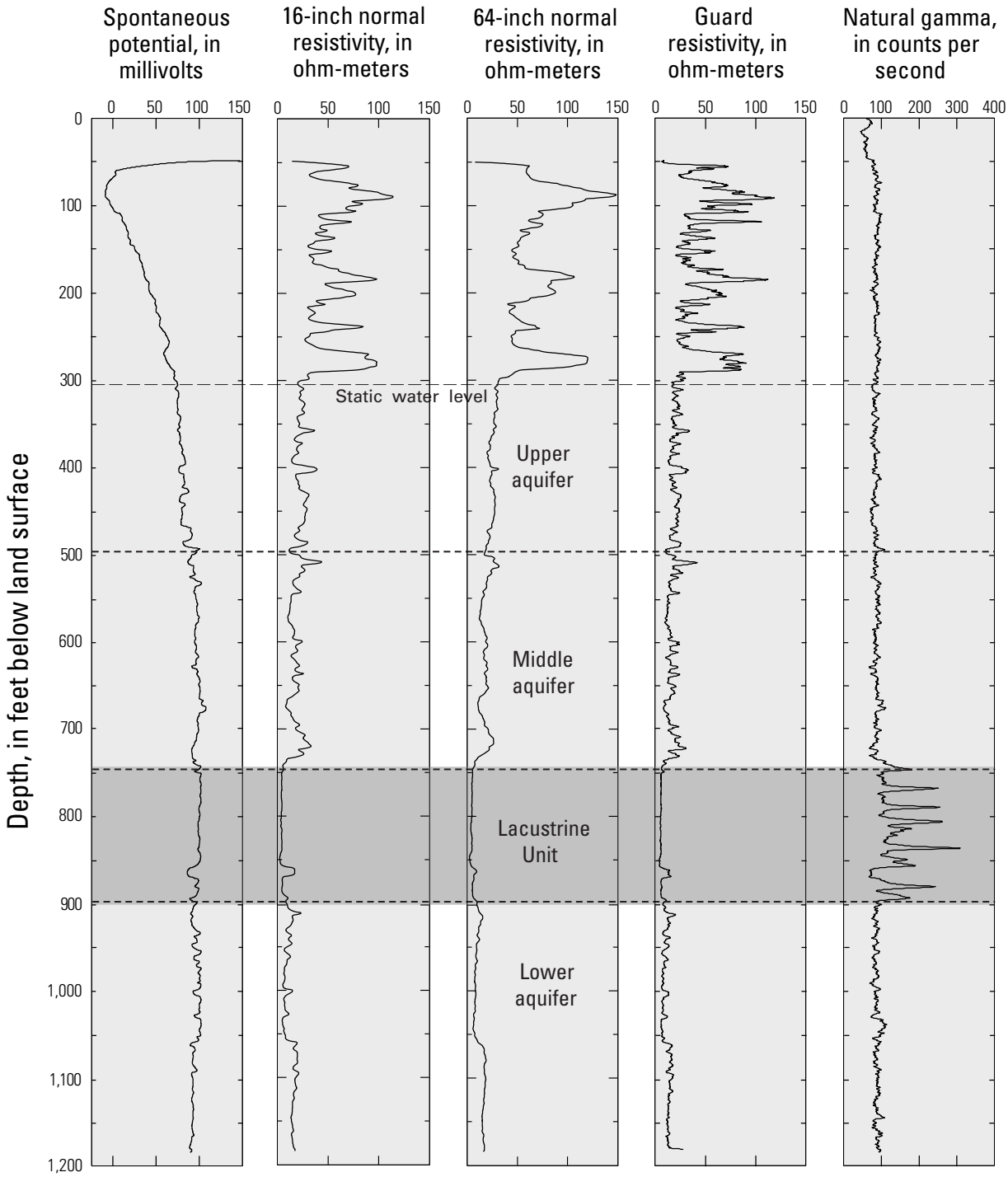

Figure 32. Borehole geophysical logs, well-construction diagrams, and lithologic logs for nested piezometers 7N/12W27-F5–F8 at the extensometer site, Lancaster, Antelope Valley, California.

The color of the samples are described using numerical color designations from Munsell soil-color charts (Munsell Color, 1975).

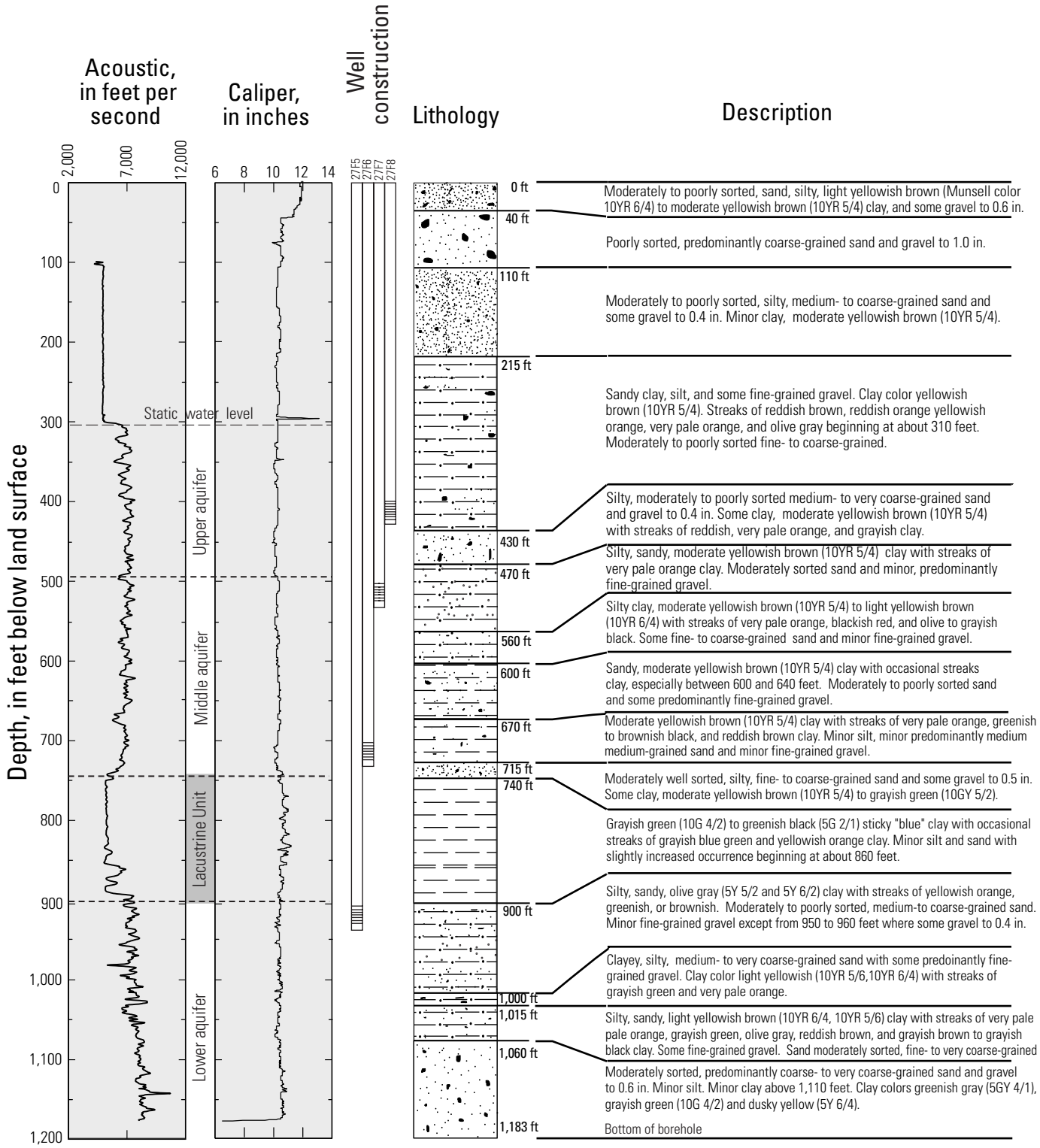

Figure 32.—*Continued*.

The contrast in the inelastic storage of the thick confining unit at Lancaster and at the Holly site may be related to differences in the depth of burial and the relative age of the thick aquitard. The top of the lacustrine unit is more than 700 ft below land surface at the Lancaster site but only 140 ft below land surface at Holly. The greater the depth of burial of the confining unit, the greater the total stress and corresponding stress on the aquifer matrix (effective stress, eq. 1) and the lower the potential for future strain (compaction).

The relative age of lacustrine deposits at the Lancaster and the Holly sites may be an important control on their compressibility because the older materials have longer stress histories and have been in contact with older, more saline water for a longer time (higher potential for cementation). The rising of the lacustrine unit toward the land surface from south to north has been interpreted as northward migration of an ancient lake or marsh associated with the uplift of the San Gabriel Mountains and associated development of alluvial fans (Dutcher and Worts, 1963). This interpretation suggests that the lacustrine deposits in the southern part of Antelope Valley may be significantly older than those in the northern part. Paleomagnetic data and alluvial sequence dating strongly support this interpretation and indicate that the lacustrine unit in Lancaster probably is at least 765,000 years older than that at Edwards AFB (Fram and others, 2002; Ponti, 1985).

Borehole acoustic logs of the extensometer site in Lancaster (fig. 32) and of two sites near Holly suggest that more compaction and (or) cementation of the lacustrine unit has occurred at the Lancaster site than at the Holly site. Sound travels relatively slowly through unconsolidated materials and speed increases with higher consolidation whether by compaction or cementation. Acoustic logs of the two boreholes near the Holly site show low velocities (average of about 4,650 ft/s) within the lacustrine unit (Londquist and others, 1993; Rewis, 1993) compared with that measured at the Lancaster site (about 5,260 ft/s). These relatively high velocities in the lacustrine unit at the Lancaster site are a clear indication of greater consolidation.

Leveling data from this study provide indirect evidence of the local variability of the skeletal storage properties. Figure 25 shows the results from a series of leveling surveys completed along the south–north survey line; the results are expressed as differences from the initial survey on September 25–28, 1995, and the survey on November 27, 1996. The initial survey was done near the end of a typical 6-month extraction period and therefore represents relatively low water levels and associated land-surface elevations. Note that although the November 4, 1996, survey followed about 2 weeks of water-level recovery from the 1996 extraction season, the elevation of almost all the bench marks were lower those than during the initial survey, and by significantly different amounts. This suggests that inelastic compaction may have occurred between these surveys and that stresses and (or) skeletal storage properties vary along this line.

Stresses along the survey line during this study were limited to extraction and injection at the injection site and to minor extraction at the extensometer site. No other significant production wells were active along the line or within about 1.4 mi north or south of the end points of the survey line. Although water-level measurements are not available near the end points of the survey line, it is reasonable to assume that changes in water levels at the end points were smaller than those at bench marks closer to the wells. Most of the land-surface change between the first two (and subsequent) surveys occurred at the northern end of the survey line, more than 4,000 ft from the injection site, suggesting that variability in skeletal storage properties was the controlling factor.

A fourth survey (April 9, 1997) was done after 146 days of the cycle-2 injection. Results of a comparison of the initial survey (September 25–28, 1995) with those from the April 9, 1997, survey show that land-surface elevations recovered along parts of the northern end of the survey line but had little change at the southern end (fig. 25). This suggests that the elastic skeletal specific storage is greater at the northern end. The final survey on February 17, 1998, was done about 1 month after the end of an unusually long period (8 months) of continuous extraction at the injection site. Despite 1 month of recovery, these elevations were significantly lower than previous measurements along most of the line. This suggests that inelastic compaction occurred during the extended extraction period.

The leveling data show a clear trend of generally increasing temporal and spatial variability in land-surface elevation from south to north (fig. 25); arguments based on these data have been made herein for a corresponding increase in the skeletal components of storage. Measurements of land subsidence from 1993 to 1995, made using InSAR (fig. 7), show an increase in subsidence just north of the extensometer site, which supports this argument.

A key component of aquifer-system deformation that has not been discussed is the preconsolidation head and its distribution within the aquitards. Johnson (1911) mapped the area of historically flowing wells in Antelope Valley that may be associated with high preconsolidation heads. Heads likely were high in the aquitards throughout this area, and today may have relatively high residual heads in their interior (Sneed and Galloway, 2000). The southern boundary of the area of historically flowing wells is roughly coincident with Avenue K, which is the northern extent of the survey line. Therefore, it is possible that long-term dewatering of aquitards, preferentially in the northern area, may be at least partly responsible for the observed increase in inelastic compaction in that area.

The overall trend of increasing variability in land-surface elevation from south to north is conspicuously broken at the injection site and possibly broken at the extensometer site (fig. 25). Long-term extraction from wells in these areas may have resulted in preferential aquifer-system compaction in the vicinity of these wells. Laboratory studies have shown that skeletal storage properties of aquifer-system materials decrease with increased applied stress (Poland, 1984). It is possible, therefore, that the areas nearest the extraction wells have relatively low skeletal storage values.

Chemical Response

The potential chemical responses to injection of imported water into native ground water were analyzed prior to injection to determine the likelihood of precipitation of minerals that could clog the screens of the injection wells. Water-chemistry data collected during cycles 1 and 2 were used to estimate the amount of injected water recovered during extraction and, in turn, the effects of injection on ground-water chemistry. The results from these analyses led to a more detailed investigation of the chemical response during cycle 3 (Fram and others, 2002; Fram and others, 2003), and are presented here as background for that work.

Potential for Mineral Precipitation

If mixing of native ground water and injection water were to cause precipitation, there could be temporary or permanent losses in well capacity from accumulation of mineral coatings on the well screen and within the gravel pack and aquifer system. A geochemical equilibria model, PHREEQE (Parkhurst and others, 1980), was used to evaluate the potential for mineral precipitation from the mixing of these waters. Ground-water samples that were collected from the injection wells prior to injection (Metzger and others, 2002) and a random sample of AVEK (imported) water were used for this analysis. Results of the equilibria model indicate that the mixing of these waters would not cause precipitation (Scott Hamlin, U.S. Geological Survey, written commun., 1996); however, the full range of chemical conditions later observed in imported and extracted water during that study was not addressed.

Recovery of Injected Water

If a substantial volume of injected water cannot be recovered during the extraction period of a seasonally operated injection program, the injected water could have a residual effect on the chemistry of the ground water. Water-chemistry data collected during the cycle-2 injection, which involved about 5 months of injection, were used to calculate a mass balance and associated residuals.

The mass-balance calculations of chloride in wells 7N/12W-27P2 and 27P3 were used to estimate the residual concentrations during the second cycle. Chloride generally is conservative in ground-water systems; the mean concentration of chloride in the injected water during this cycle exceeded that in ground water (figs. 28 and 29). It was assumed that chloride concentrations in the extracted water that exceeded the concentrations in ground water indicated the presence of injected water.

The baseline chloride concentration in ground water in well 7N/12W-27P2 was assumed to be that at the end of cycle-1 extraction (about 8.7 mg/L in July 1996) rather than that measured in April 1995, which was 1 year prior to the first injection test (about 14 mg/L). The difference in these concentrations suggests that chloride concentrations in native ground water may be sensitive to pumping conditions: April represents the end of a long period of recovery, while July is well into the high-extraction period. Baseline concentrations in well 7N/12W-27P3 were 21 mg/L for the two periods.

The mass of chloride injected was determined from weekly samples of AVEK water collected at the injection site and from continuous measurements of injection rates. The mean chloride concentration of injection water was calculated by dividing the total mass of chloride injected by the total volume of water injected. Similarly, the mean daily to weekly chloride concentrations of extracted water was determined from daily to weekly samples of extracted water (fig. 29) and from continuous measurements of extraction rates. Using the following equation, the mean injected chloride concentration and the daily to weekly estimates of extracted chloride concentrations were used to calculate the volume of injected water for each daily or weekly sampling period needed to raise the chloride concentration of ground water to that in the measured volume of extracted water:

$$V_{inj} = \frac{[chloride]_{extr} - [chloride]_o}{[chloride]_{inj} - [chloride]_o} \times V_{extr} \qquad (5)$$

where

V_{inj} is the volume of injected water in the extracted volume during the period;

$[chloride]_{extr}$ is the concentration of chloride in extracted water during the period;

$[chloride]_{inj}$ is the mean concentration of chloride during cycle-2 injection;

$[chloride]_o$ is the baseline concentration of chloride in ground water; and

V_{extr} is the total volume of water extracted during the period.

Results from the mass-balance calculations suggest that about 50 percent of the injected water was recovered during the cycle-2 extraction, split about evenly between the two wells (7N/12W-27P2 and 27P3). The cycle-2 injection test involved 156 days of injection followed by 243 days of extraction; about 156 percent of the total volume injected was extracted (injected and native ground water). The accuracy of this estimate may have been affected by the high variability of the chloride concentrations in the injected water and in the ground-water samples and is dependent on the assumption that chloride is conservative in this system.

The third injection cycle was designed, in part, to address the issues of recovery of injected water more quantitatively. A conservative tracer, sulfur hexafluoride, was added to the injection water. Results of the tracer experiment indicate that there was extensive mixing between the injected water and the native ground water. Analytical modeling of the mixing process indicate that this mixing was the primary cause of the incomplete recovery of injected water (Fram and others, 2003).

Effects of Injection on Ground-Water Chemistry

Results of the mass-balance calculation, the tracer experiment, and analytical modeling indicate that seasonal operation of an injection program likely would have a residual effect on the chemistry of ground water for the same chemical and hydrologic conditions and for a similar ratio of injection to extraction volume. Results from an analytical mixing model, assuming complete mixing, are in agreement with this conclusion (Fram and others, 2003). Although both the imported water and the native ground water are of drinking-water quality and are delivered to customers in Lancaster, the imported water used during the first two injection cycles contained constituents, in addition to chloride and THMs, with concentrations greater than those in the native ground water. On the other hand, the imported water contained some constituents with lower concentrations than those in ground water including arsenic, which is a constituent of concern locally.

Determining the potential long-term effects of injection on ground-water chemistry was beyond the scope of this study; but results of a qualitative analysis of chemistry data collected for this study do provide some insight on those effects. There are many significant differences between the chemical composition of the native ground water and that of the injected water including differences in pH, several major ions, trace metals, and THMs. Early in the extraction period of cycle 2, the chemistry of the extracted water was similar to the median chemistry of the injected water, as might be expected. By the end of 243 days of extraction, the chemistry of the extracted water was similar to that of the native ground water, with some exceptions: the extracted water had a lower pH (7.5) than the native ground water (8.3), possibly owing to geochemical reactions; and the THM concentration in the extracted water was 4.6 µg/L but was not detected in the native ground water

(Metzger and others, 2002). These exceptions suggest that the injection water remained in the aquifer system, as is also indicated by the results of the mass-balance calculations. The similarities between the extracted water and the native ground water near the end of cycle 2 suggest that the rate of recovery of the remaining injected water was relatively slow by the end of the extraction period.

A large-scale injection effort using existing wells likely will involve equivalent periods of injection and extraction, which could affect the ability to recover injected water. Assuming that about 1 month is needed for maintenance, monitoring, and any physical modification required for switching between injection and extraction leaves about 5.5 months (166 days) each available for injection and extraction. The change in concentrations of many of the constituents is large for this period, particularly for THMs (fig. 30). For example, during the cycle-2 injection, total THMs concentrations decreased from 127 to 8.8 µg/L during the 166-day extraction period, but only to 4.6 µg/L during the remaining 77 days of the full 243 days of extraction. The rates of change for the other constituents were similarly reduced, suggesting that continued extraction beyond 166 days achieved only a minor recovery of the injected water.

THMs represent a change in ground-water chemistry because the native ground water had no detectable concentrations. For example, during cycle 2, the THM concentrations increased almost twofold in the extracted water compared with the concentrations in the injected water (fig. 30). A decrease in the measured concentrations of free chlorine, from 0.30 to 0.80 mg/L (median 0.52 mg/L), in the injected water to below the detection limit in the extracted water suggests that the THMs continued to form in the aquifer system after injection. A comparison of the median concentrations of the THM species in injected water to those of extracted water early in the extraction period suggests preferential growth of the chlorinated species within the ground-water system: chloroform concentrations increased by 179 percent compared with bromoform, which increased only 38 percent. The controls on THM formation in the aquifer system after injection during cycle 3 are discussed in detail by Fram and others (2003). A key finding from their work is that THMs do not undergo biodegradation by aquifer bacteria under the aerobic conditions present at the injection site and that THMs do not adsorb the aquifer sediments from this site.

DEVELOPMENT OF A NUMERICAL MODEL OF GROUND-WATER FLOW IN THE LANCASTER AREA

A numerical model of three-dimensional ground-water flow in the Lancaster area (the area surrounding the injection site) from 1983 to 1998 was developed to aid in the analysis of the hydraulic data collected during the injection tests, and as part of a simulation/optimization model for use in planning and managing a potential larger scale injection program. A USGS finite-difference model code [MODFLOW (McDonald and Harbaugh, 1988), with the PCG2 numerical solver (Hill, 1990)], was used to develop this model, which simulates transient three-dimensional ground-water flow in an 11- by 19-mi area surrounding the injection site (figs. 1 and 33). MODFLOW calculates directions and quantities of ground-water flow, and their associated effects on ground-water levels using input that describes the interaction between the modeled volume and its surroundings (boundary conditions); the state of the aquifer system at the start of the simulation (initial conditions); hydraulic properties of the aquifer system; and natural or artificial stresses affecting the aquifer system (for example, recharge from streams, or discharge from ground-water pumping). Simulated ground-water levels, streamflow, recharge rates, and (or) other indicators of the state of the aquifer system are compared with measured values to evaluate the accuracy of the simulation.

Although subsidence is a significant hydraulic process in the Lancaster area, it was not simulated in this model because additional subsidence was not considered an acceptable outcome of future ground-water management. Water levels were controlled in subsidence areas during management optimization simulations to avoid additional subsidence. The model, as discussed in this section of the report, was used to synthesize available hydraulic data and to estimate lesser known hydraulic properties that control the behavior of the aquifer system. Application of the model as a planning tool in the form of a simulation/optimization model is discussed in the section “Development of A Simulation/Optimization Model.”

Three models are discussed often in this report. One is a previously published model of ground-water flow and aquifer-system compaction (land subsidence) for the Antelope Valley ground-water basin (fig. 1), herein referred to as the AV model. This model was developed for another study and is documented in a report by Leighton and Phillips (2003). The ground-water-flow model of the Lancaster area, discussed in this section of the report, is referred to as the LAN model. A simulation/optimization model discussed later in this report, which incorporates a modified version of the LAN model, is referred to as the LANOPT model.

Sources of model input and measures of the state of the aquifer system include information gathered for this study, described earlier in this report, and by Howle and others (2003) and Metzger and others (2002); results from previous hydrologic studies, including Bloyd (1967), Londquist and others (1993), Templin and others (1995), Carlson and Phillips (1998), Carlson and others (1998); ground-water pumpage and well-construction data, as well as other data provided by the LACDPW; and results from previous regional-scale models of Antelope Valley (Durbin, 1978; Leighton and Phillips, 2003).

Model Grid and Boundary Conditions

The model grid serves to divide the conceptual aquifer system into discrete three-dimensional blocks, or cells. Hydraulic properties and stresses are assigned to each cell. Hydraulic head and flow directions and rates are calculated for each cell on the basis of the input values and the simulated interactions with neighboring cells. Data collected during the injection tests were from wells that are densely spaced within a small area near the injection wells, where the hydraulic response to injection was greatest, and are more sparsely spaced with increasing distance from the injection site. Accordingly, the model grid (fig. 33) was constructed with relatively small cells at the injection site (about 100 ft on each side), increasing in cell size (by a factor of 1.1) with distance from the injection site, to a maximum dimension of about 1,980 ft. The resulting grid is 77 rows by 101 columns, some of which are inactive (rows 1 and 2 and 75 through 77, and columns 1 through 3 and 99 through 101).

The model domain was divided vertically into two layers at an altitude of 1,950 ft. Vertical discretization was required to adequately represent the contrast between younger, unconsolidated materials in the upper aquifer and the underlying older, more compacted and indurated (hardened) materials in the middle aquifer (fig. 34) (Leighton and Phillips, 2003). The lower aquifer and lacustrine unit were not included in the LAN model. The lacustrine unit, which was assumed to act as a significant barrier to both vertical and horizontal flow, formed the impermeable bottom and (or) sides of model cells, as appropriate. The specified thicknesses of model layers 1 and 2 were variable and dependent on the altitudes of the water table (variable in time and space), the lacustrine unit, and bedrock (fig. 34). The lateral extent of layer 2 is smaller than that of layer 1 because the aquifer system thins along the margins of the model area with rising bedrock to the south and the rising lacustrine unit to the north (figs. 33 and 34).

Boundary conditions are used to describe the hydraulic interaction across model boundaries. Ideally, model boundaries are placed far enough away from the area of interest to minimize their possible effects on the numerical solution on that area and reasonably represent true hydrologic conditions. For the LAN model, the lateral boundaries that parallel bedrock outcrops along the San Gabriel Mountains and Quartz Hill were assumed to be no-flow boundaries because the hydraulic interaction with bedrock probably is small (fig. 35). Interbasin subsurface ground-water flow into the model area from the upgradient Pearland and Buttes subbasins (fig. 1) was represented by a specified flux boundary in layer 1 (layer 2 not present) (fig. 35), and is based on the results from the AV model (Leighton and Phillips, 2003). Heads were specified in layer 1 along a stretch of the northern boundary to account for southward flow from a broad ground-water mound between Lancaster and Rosamond (Carlson and others, 1998). Measured water levels in wells within the ground-water mound decreased by 5 ft or less during the simulation period; accordingly, the specified heads were held constant with time. The remaining lateral boundaries, to the northwest and east, are represented as no-flow boundaries based on the flowlines and ground-water divides determined from contour maps of ground-water levels in 1983 and 1996 (Carlson and others, 1998) (fig. 36*A*, *B*) and from results of the regional simulations (Leighton and Phillips, 2003). All lateral boundaries for layer 2 were no-flow. The upper boundary condition is the water table.

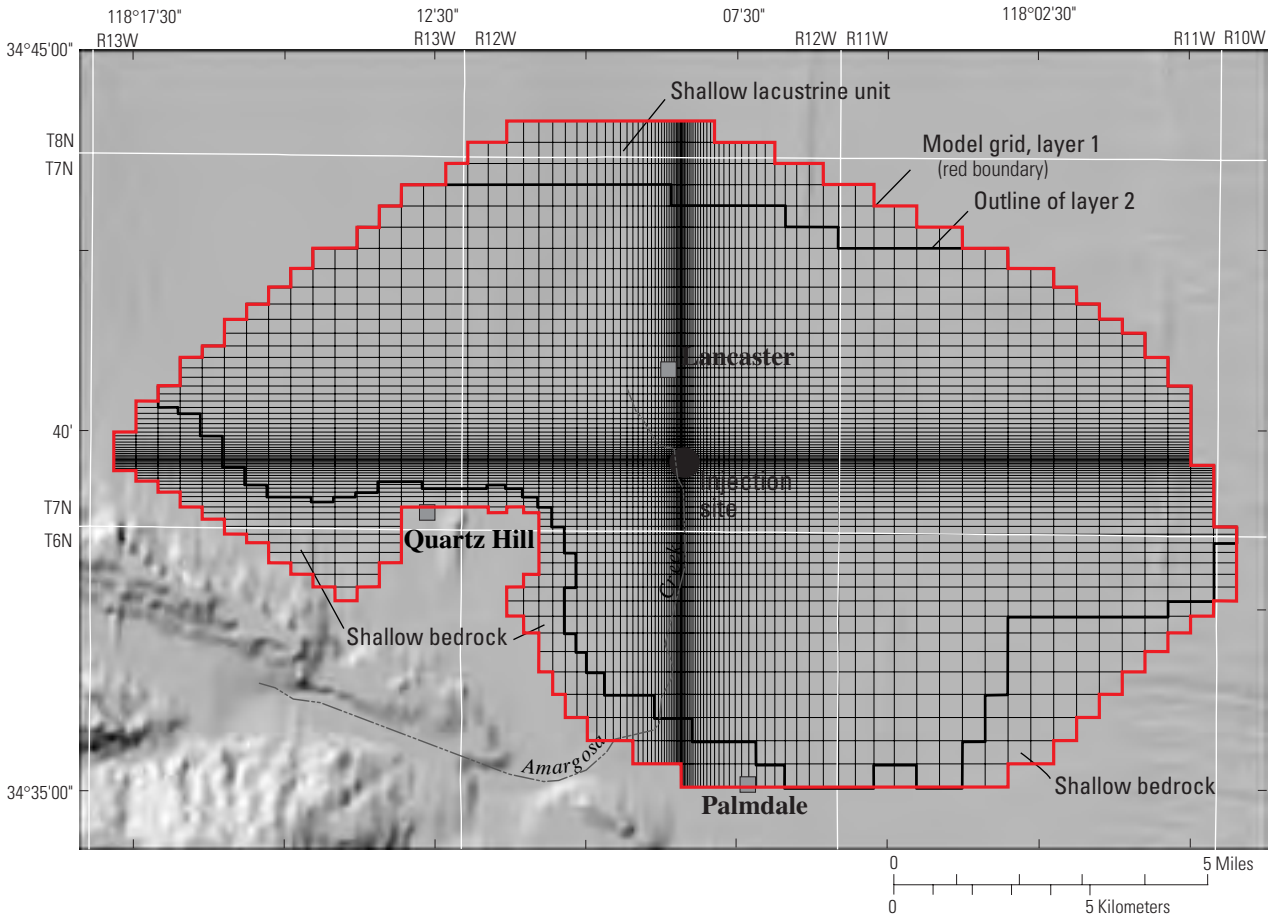

Figure 33. Active region of the LAN model grid, Lancaster, Antelope Valley, California.

Cells increase in size outward from about 100 feet square at injection site to maximum dimension of about 2,000 feet. Rows and columns are numbered sequentially from the northwest corner of the grid.

The lacustrine unit is not simulated in the LAN model, because vertical flow across the lacustrine unit was assumed to be negligible (a no-flow boundary). Although flow across the lacustrine unit likely does occur, and certainly occurs through production wells screened both above and below this unit and over much larger periods than simulated, such flow probably is small during the periods simulated. Information necessary for simulating the lower aquifer (particularly the transmissivity and lateral boundary conditions) and for assessing model performance in the lower aquifer is lacking. The AV model includes the lower aquifer, but the calibration of that aquifer was poorly constrained in the area of the LAN model (Leighton and Phillips, 2003). The upper boundary of the LAN model is the water table, a free surface.

The assumption of no flow across lateral boundaries defined by flowlines and ground-water divides was tested because of uncertainty in the water-level contour maps potential for variations in flow directions with depth, and possible movement of these features during the calibration period. Fluxes through these boundaries were simulated for the period 1983 to 1995 using the AV model (Leighton and Phillips, 2003). Results showed minor flow through most of the flowline boundaries, but relatively significant flow from the LAN model area toward the east, an agricultural area. This eastward flow ranged from about 2,300 to 900 to acre-ft/yr, decreasing essentially linearly with time, and averaged 1,600 acre-ft/yr. The steady decrease in eastward flow is related to the eastward migration of the ground-water-flow divide along that boundary (fig. 36), which parses the recharge from the southeastern boundary into eastward and westward flow. Recharge along the eastern third of the southeastern boundary was reduced by these transient amounts from 1983 to 1995 (assuming linear decrease) to compensate for the portion that leaves the model area through the eastern boundary. Eastward flow from 1996 to 1998 was assumed to be 900 acre-ft/yr.

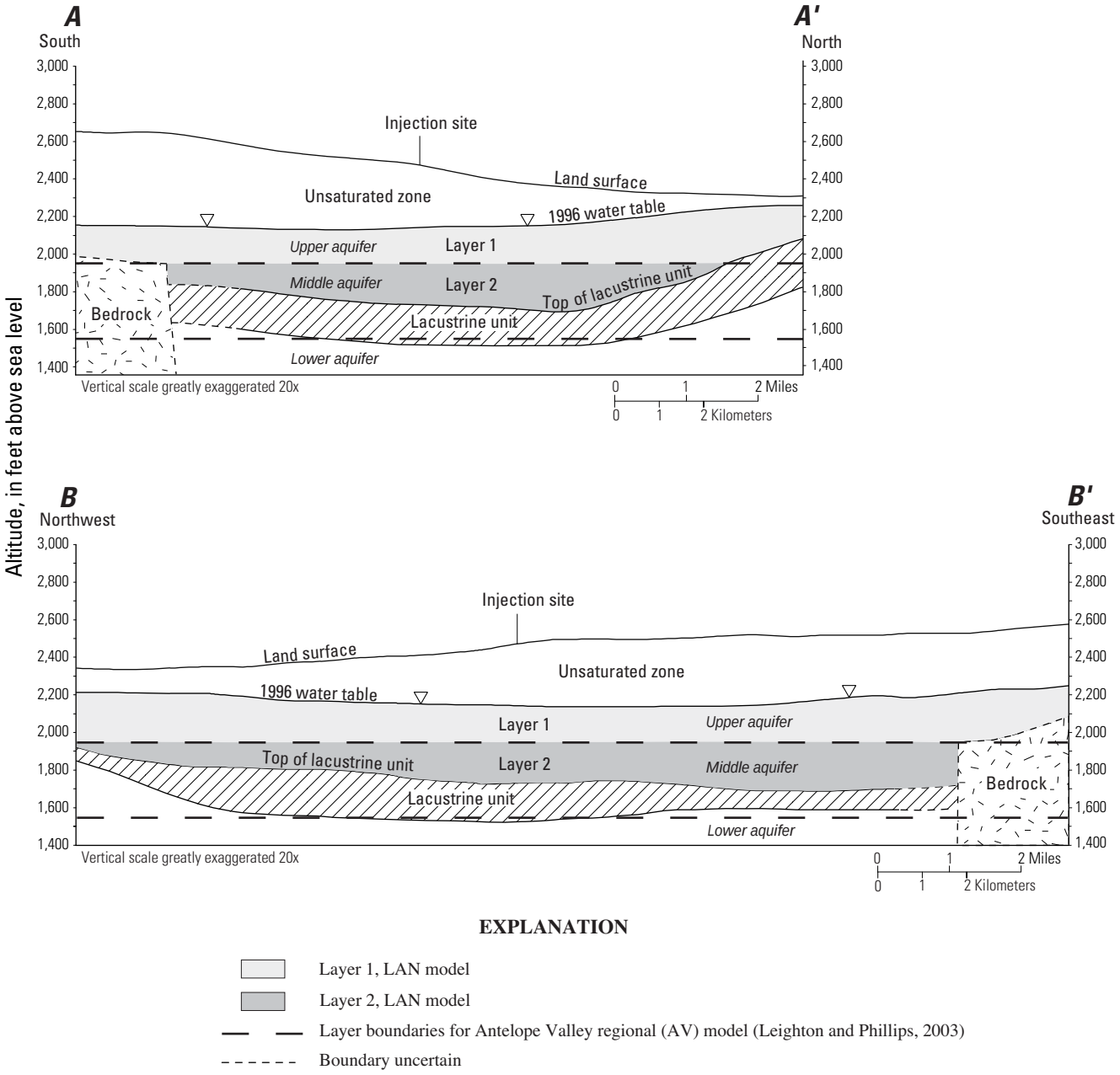

Figure 34. Generalized sections *A-A′* from south to north and *B-B′* from northwest to southeast through injection site showing delineation of model layers for the Lancaster area (LAN) and regional (AV) models, Antelope Valley, California.

Cross-sections locations shown in figure 1.

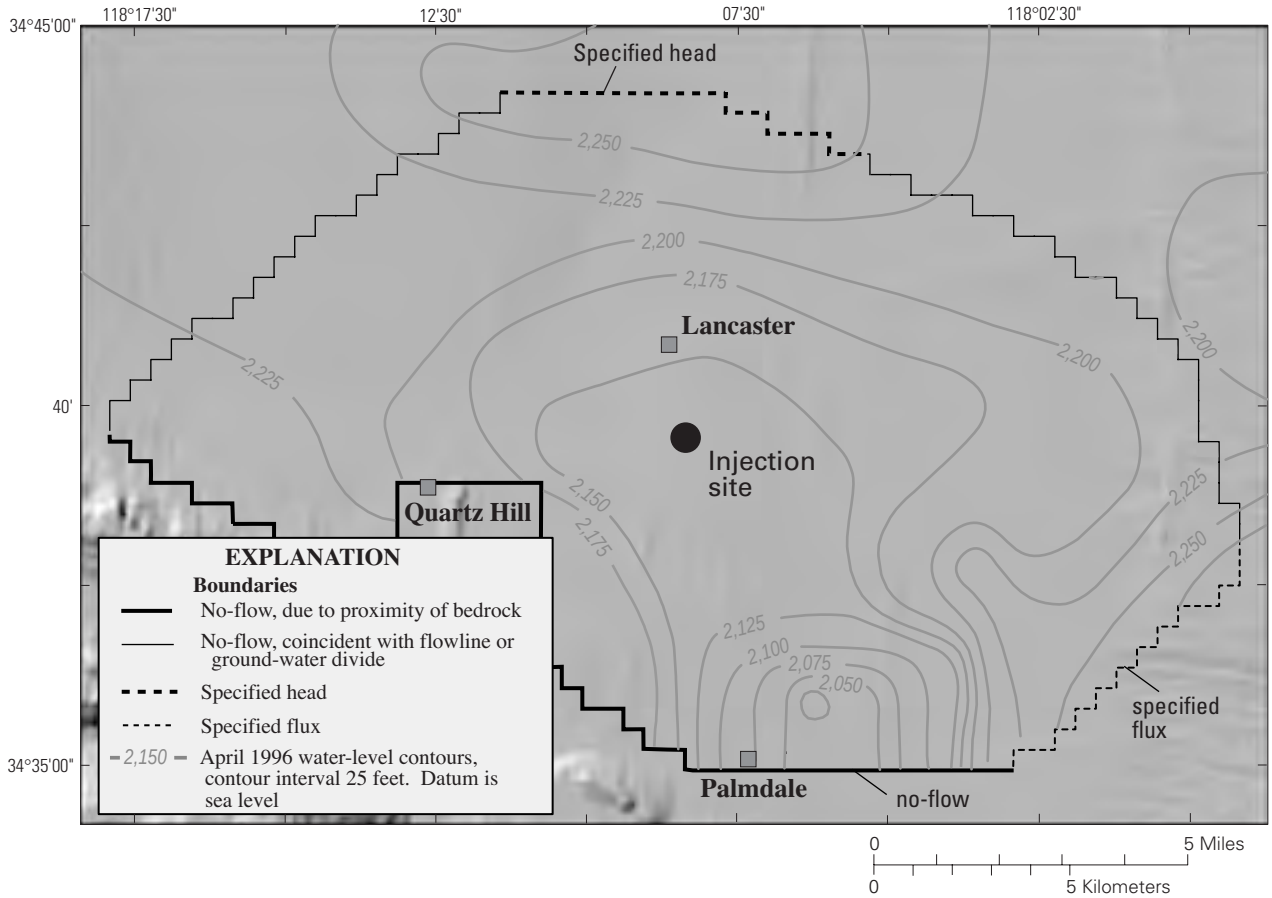

Figure 35. Lateral boundary conditions for layer 1 of the LAN model and 1996 water-level contours (modified from Carlson and others, 1998) used to define no-flow boundaries coincident with flowlines or ground-water divides, Lancaster, Antelope Valley, California.

All lateral boundaries for layer 2 are no-flow.

Initial Conditions and Temporal Discretization

Ideally, transient models are developed by initially simulating the aquifer system during a period when it is in equilibrium (a steady-state model) and then incorporating the output as the initial condition for the transient simulation. It was not possible to use this methodology for this study because the system has not been in equilibrium since predevelopment and because the boundary conditions changed dramatically from predevelopment to the present. However, hydraulic parameters were available from the AV model (Leighton and Phillips, 2003) that was calibrated. The AV model included a steady-state model representing predevelopment conditions (prior to 1915) and transient conditions (1915–95). Parameters from the AV model were used initially in this model and adjusted as necessary to calibrate the LAN model. Although significant adjustments were made to individual parameters, the calibrated bulk properties were similar.

Spring 1983 measured water levels (fig. 36*A*) were used for the initial condition in the LAN model because the spring season generally represents recovered conditions prior to the summer pumping season. In addition, water-level data for 1983 are relatively plentiful and well distributed (Carlson and others, 1998), and 1983 represents a short-term quasi-steady-state condition, falling between the end of an agricultural decline and the beginning of rapid urban expansion (figs. 2 and 37) (Templin and others, 1995; Leighton and Phillips, 2003). Although the measured water levels for 1983 do not indicate ideal steady-state conditions throughout the model area, the long-term hydrograph of well 7N/12W-27H1, which is within 0.5 mi of the injection and extensometer sites, suggests that this is a reasonable approximation in the area of interest (fig. 14).

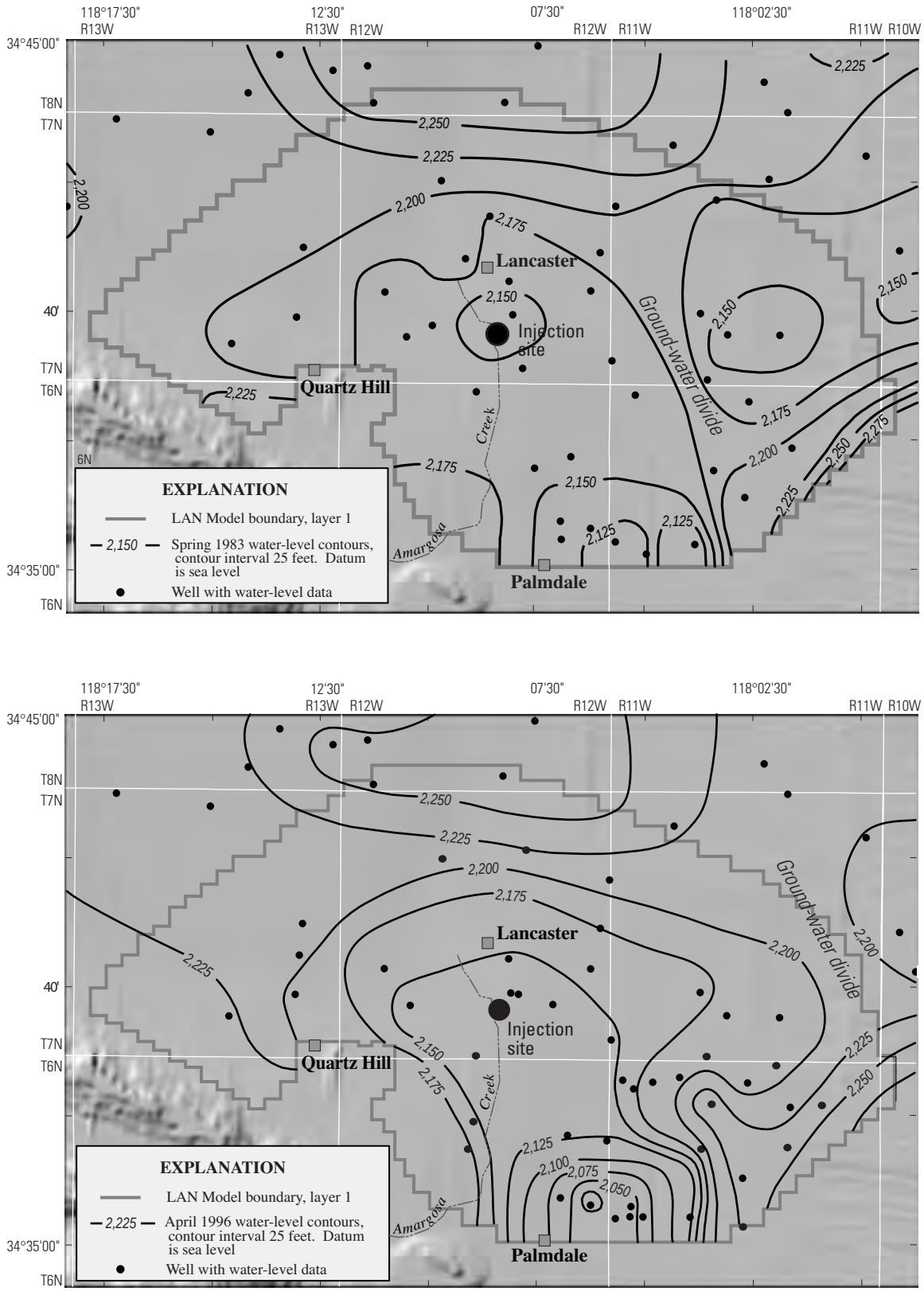

Figure 36. Contours of measured water levels for (*A*) spring 1983 (used as initial head values for both layers of the LAN model) and (*B*) April 1996 (modified from Carlson and others, 1998) in Lancaster, Antelope Valley, California.

Spring 1983 water-level data were used to develop a contour map (fig. 36*A*), which, in turn, was used to assign initial head values for every cell in the model. Owing to a lack of distributed depth-specific data, it was assumed that heads in layers 1 and 2 were equal. Recent water-level data from the nested piezometers installed for this study (fig. 17) indicate this is a reasonable assumption for spring conditions prior to the injection tests.

The simulation period for the LAN model is May 1983 through August 1998. This time period was divided into 185 monthly segments (30.4375 days each) called stress periods. Extraction and injection rates, as well as other stresses, are defined for each stress period. Given that most of the pumpage data was available as monthly totals and that the shortest injection cycle was 1 month in duration, this level of temporal discretization was considered appropriate. To ensure numerical accuracy of the solution, each stress period was divided into 15 time steps; the length of each time step was increased by a factor of 1.2 from that of the previous step.

Hydraulic Properties of the Aquifer System

The hydraulic properties of an aquifer system are the physical characteristics that govern the capacity of the system to store and transmit water. For this study, these characteristics are defined by the storage coefficient, hydraulic conductivity, and transmissivity. The storage coefficient is the amount of water taken into or released from the system per foot of water-level change. In the unconfined part of the system, removal of water from storage is manifested as a corresponding decline in the water table. This release of water from gravity drainage, termed the specific yield, was calculated for this study from coupled microgravity and water-level measurements (Howle and others, 2003) to be about 0.13 near the injection wells. As in the AV model (Leighton and Phillips, 2003), this was assumed constant across the model area in layer 1.

The storage coefficient decreases with increasing depth in an alluvial aquifer system because the cumulative fine-grained sedimentary layers, typical of alluvial deposits, effectively reduce the hydraulic connection to the water table. Thus, when water is removed from deeper parts of the system, this water is not from water-table drainage, but primarily from deformation of the aquifer-system matrix. This dependence on the elastic properties of the aquifer system dramatically lowers the storage coefficient, which is then governed by the specific storage and layer thickness. A specific storage of 1.2×10^{-6} per ft was used in the LAN model, which is the elastic skeletal specific storage determined from the stress/strain analysis at the extensometer site. The storage coefficient for layer 2 was the product of specific storage (assumed to be the same everywhere) and actual layer thickness (fig. 38). Values of storage coefficient ranged from 3.8×10^{-5} to 3.5×10^{-4}.

The inelastic component of storage was not simulated in the LAN model. A primary goal of ground-water management is to avoid subsidence; therefore, the inclusion of subsidence in the LAN model was not needed. The effects of ignoring inelastic compaction as a source of water in the LAN model vary with areal location. Measured inelastic compaction was small at the extensometer site (fig. 22), totaling about 0.01 ft in the upper and middle aquifers from 1996 to 1997. If this compaction is assumed to ultimately contribute water to the water table, the equivalent water-table increase from water derived from compaction would be about 0.08 ft/yr at a specific yield of 0.13. In central Lancaster, where the measured total subsidence rate was about 2 cm (0.066 ft) per year from 1993 to 1995 (fig. 7), the equivalent water-table increase would be about 0.34 ft/yr if it is assumed that about two thirds of the compaction occurred in the upper and middle aquifers (as at the extensometer site). Water from compaction could have a greater effect on water-level changes in the middle aquifer, but induced flow between the upper and middle aquifers would dampen large changes.

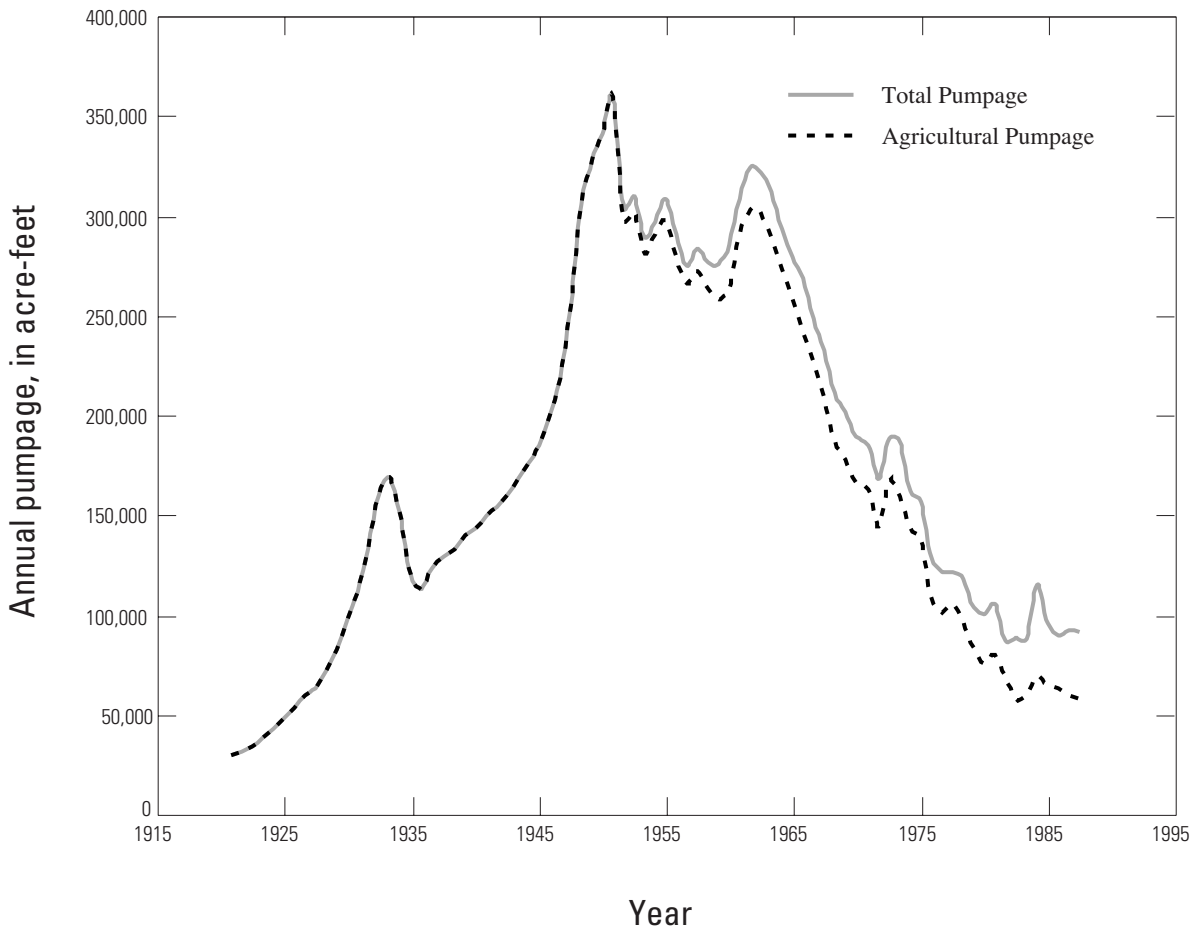

Figure 37. Estimated historical annual total and agricultural pumpage in the Antelope Valley ground-water basin, California.

(From Leighton and Phillips, 2003).

The ability of aquifer-system materials to transmit water is defined by their horizontal and vertical hydraulic conductivities. Horizontal transmission of water is defined by the transmissivity, which is the product of horizontal hydraulic conductivity and saturated thickness of the aquifer. Initial horizontal hydraulic conductivity values (fig. 39) used in the LAN model were based on those used in the AV model (Leighton and Phillips, 2003), which, in turn, were, for the most part, based on specific-capacity data from Bloyd (1967) for wells throughout the region. The vertical hydraulic conductivities also initially were based on conductivity values used in the AV model, for which the ratio of horizontal to vertical hydraulic conductivity (vertical anisotropy) was assumed to be 100:1, but were adjusted during calibration.

Recharge and Discharge

Recharge and discharge refer to the replenishment and loss of water to and from the ground-water system. During the calibration period (1983–98) of the LAN model, recharge in the Lancaster area occurred by natural and artificial means and discharge occurred primarily by ground-water extraction. Simulated recharge was varied annually, depending on the contributions from local runoff, interbasin flow, agricultural return flow, and infiltration of treated wastewater and discharge was varied monthly according to measured and estimated ground-water pumpage.

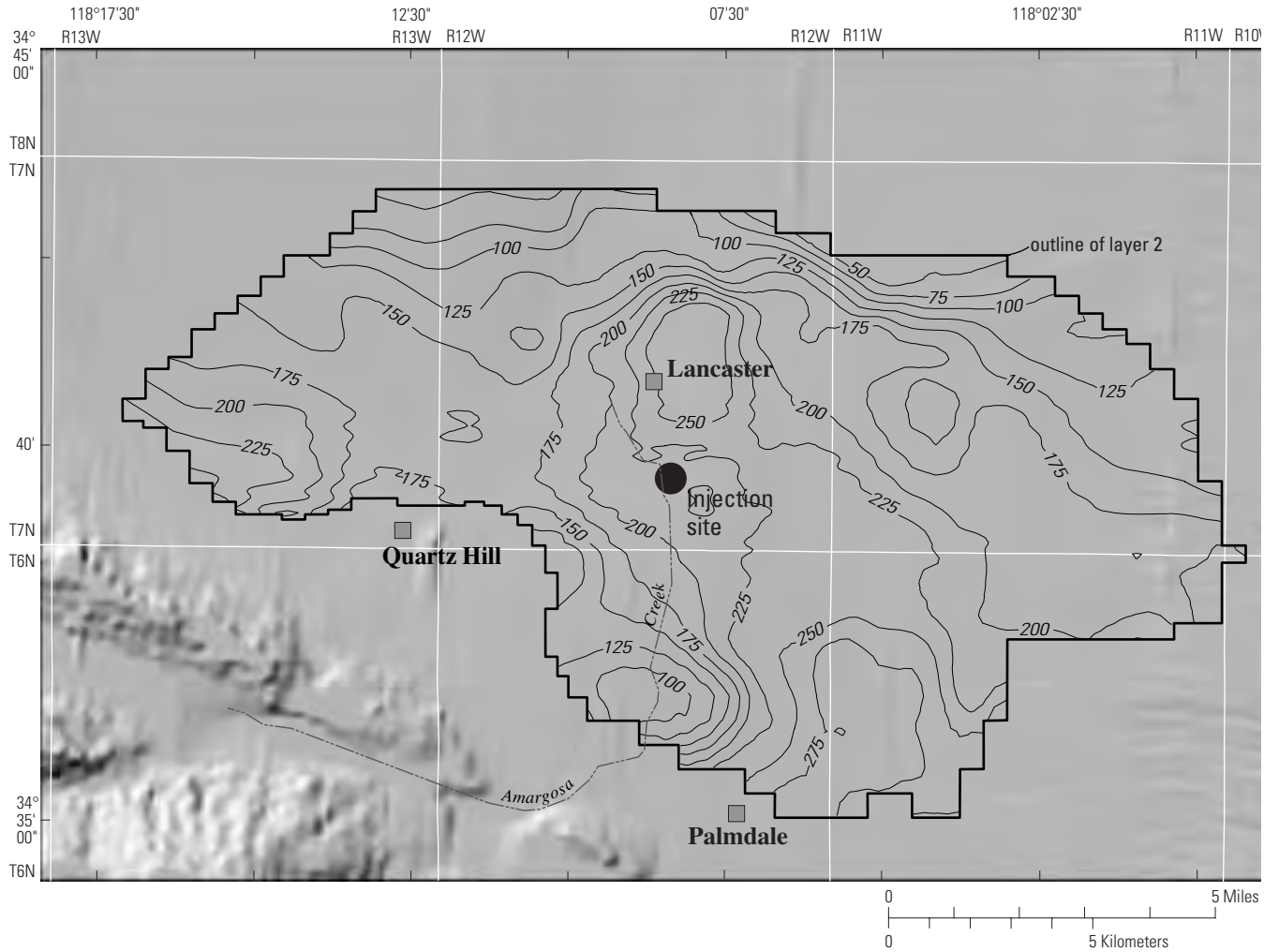

Figure 38. Thickness of model layer 2, Lancaster, Antelope Valley, California. Thickness contours are in feet.

Natural Recharge

Natural recharge in Antelope Valley is believed to occur primarily through infiltration of runoff from the surrounding mountains, concentrated in stream channels along the mountain front (Thompson, 1929; Bloyd, 1967; Durbin, 1978). Aquifer materials generally are coarser at the heads of alluvial fans and are associated with relatively high infiltration rates. Aquifer materials are finer downgradient from the heads of the alluvial fans and less runoff infiltrates.

A primary source of natural recharge within the model area is Amargosa Creek, which lies in the central part of the southern boundary of the model (fig. 40). Flow in Amargosa Creek is ephemeral and flashy; however, there is a lack of information on the timing, duration, and volume of flow. Studies of recharge processes in the Mojave River Basin, the adjacent basin east of Antelope Valley, have shown that downward flow of infiltrated runoff through large thicknesses of alluvial materials can take from decades to centuries to reach the water table (Izbicki and others, 1998; Izbicki, 1999). Downward movement of water is slowed by multiple laterally extensive, flat-lying, fine-grained layers upon which perched water spreads laterally, effectively diffusing the recharge spatially and temporally. Thus, although there is extreme short-term and annual variability in runoff, this variability likely is damped by the time infiltrated runoff becomes recharge to the water table. Owing to the lack of flow measurements on Amargosa Creek and the results of Izbicki's work, recharge from Amargosa Creek was assumed constant with time. Recharge initially was specified at 662 acre-ft/yr, as in the regional AV and Durbin (1978) models, and then adjusted to 2,835 acre-ft/yr during calibration of the LAN model to

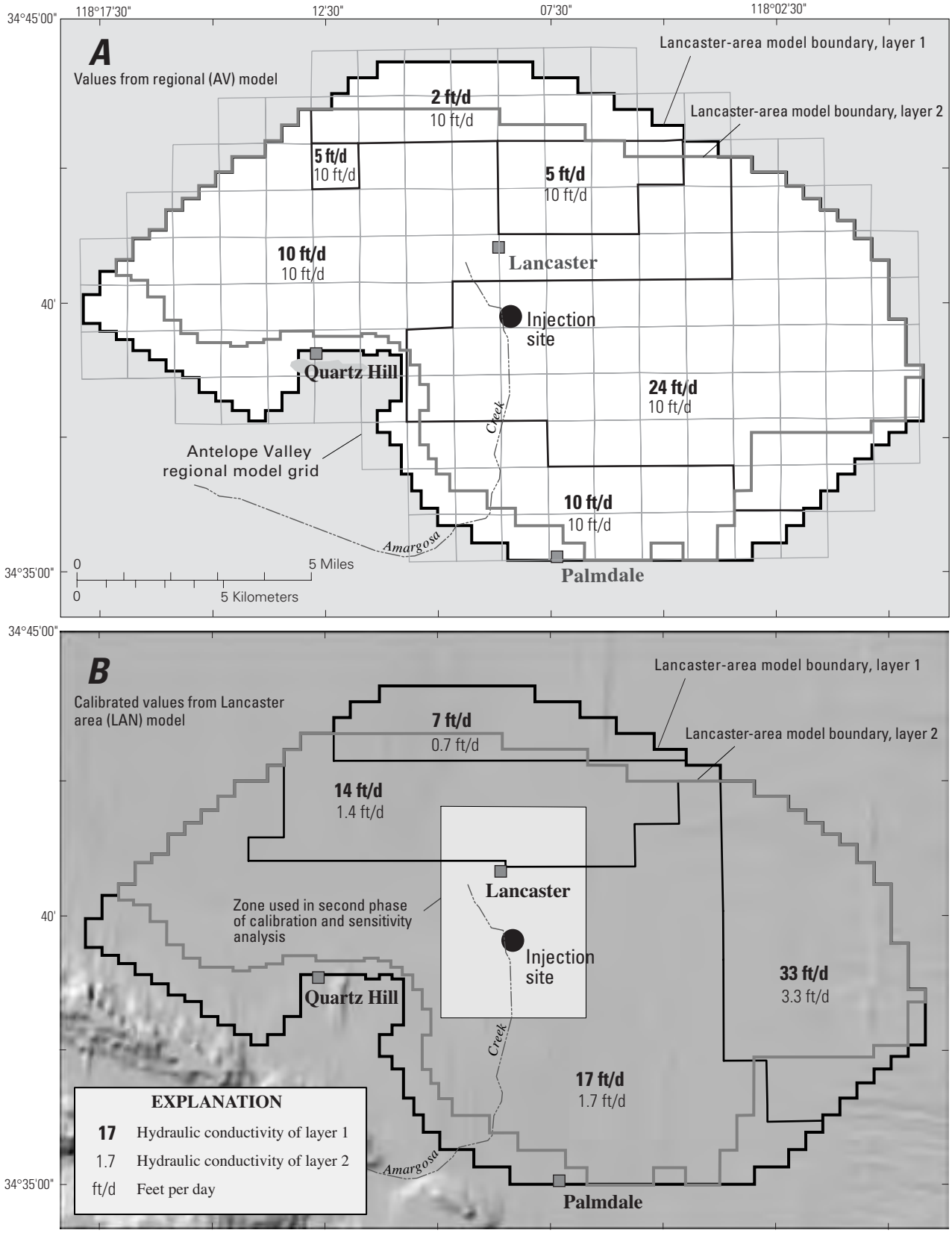

Figure 39. Distribution and values of hydraulic conductivity in the Lancaster-area (LAN) model, Antelope Valley, California. (*A*) initial values based on regional (AV) model (Leighton and Phillips, 2003), and (*B*) final calibrated values.

match the measured hydraulic gradient in wells on the Amargosa alluvial fan. These regional models also included recharge along the San Gabriel Mountains west of Amargosa Creek (fig. 40) to account for flow from many of the smaller intermittent streams in this area. Recharge from these smaller streams to the LAN model was specified as about 1,300 acre-ft/yr (same value specified in the regional models) and was not adjusted during calibration of the LAN model.

The southeastern specified-flux boundary represents the natural recharge upgradient of the model area that enters the model area as subsurface interbasin flow into the Lancaster subbasin from the Pearland and Buttes subbasins (fig. 40). Little Rock and Big Rock Creeks recharge the Pearland and Buttes subbasins; any recharge from these creeks that is not consumed or retained within these basins flows downgradient to the Lancaster subbasin; some of the flow enters the model area. This interbasin flow into the model area was estimated by the AV model as varying by less than 8 percent from 1983 to 1995, at an average rate of about 7,650 acre-ft/yr (Leighton and Phillips, 2003). This estimate was based on constant annual rates of recharge from Little Rock and Big Rock Creeks during this period and on variable rates of extraction in the area. Flows in these creeks, and associated recharge, were not constant during this period that includes both drought and relatively wet conditions. The estimated average annual recharge represents average conditions based on reasons similar to those described for constant recharge from Amargosa Creek.

Simulations of the AV model suggested that net eastward flow was occurring through the eastern boundary of the LAN model area. This flow decreased from about 2,290 acre-ft in 1983 to 900 acre-ft in 1995, averaging 1,636 acre-ft/yr. The specified interbasin flow (recharge) through the eastern third of the southeastern boundary was reduced by these rates, linearly distributed on an annual basis, to compensate for the effect of the eastward migration of the ground-water flow divide that straddles the eastern boundary. Thus, net outward flow through the eastern boundary, in the form of discharge (or diverted recharge), was accounted for through a reduction in recharge from the adjacent southeastern boundary.

Other Forms of Recharge

In addition to artificial recharge by injection (only from the injection project within the LAN model area), other forms of recharge in the LAN model area include agricultural return flow (agricultural recharge), infiltration of secondary-treated wastewater ponded near the southeastern boundary (wastewater recharge), and southward flow through the northern boundary. The distribution and rates of agricultural and wastewater recharge are shown in figure. 40. Agricultural recharge was specified for current and former agricultural areas to account for irrigation water that percolates past crop roots through the unsaturated zone and reaches the water table, which was assumed to be 30 percent of total irrigation (Leighton and Phillips, 2003). Most of the irrigation water in these areas was ground water pumped from local wells, but the area along the western boundary (fig. 40) was irrigated using imported water provided by AVEK. Leighton and Phillips (2003) incorporated a delay of 10 years between the onset of irrigation and the onset of agricultural recharge, and between the cessation of irrigation and the cessation of agricultural recharge, to improve the match between stimulated and measured water levels in agricultural areas in the AV model. Therefore, recharge was specified for some formerly irrigated lands and for several areas where farming continues. Irrigation returns were specified annually through 1995 using the same rates as those in the AV model and were assumed to remain at the 1995 rate from 1996 to 1998.

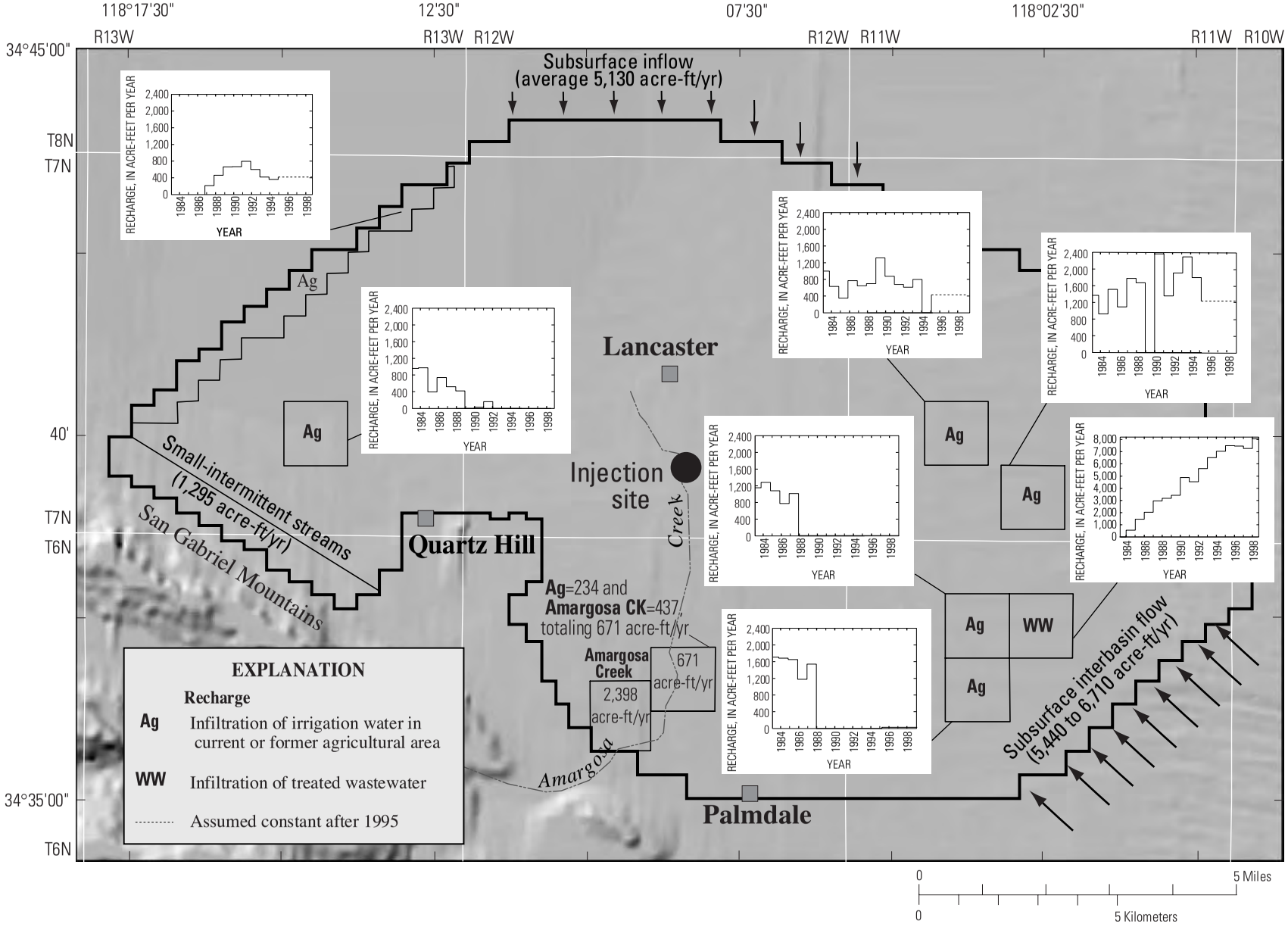

Figure 40. Distribution and magnitude of recharge in the Lancaster-area (LAN) model, upper and middle aquifers only, Antelope Valley, California.

Secondary-treated wastewater from the Palmdale Wastewater Reclamation Plant has been ponded on Los Angeles Department of Airports property since 1984 as a means for disposal. On the basis of field evidence, ongoing studies (Jose Saez, Los Angeles County Sanitation Districts, unpublished data, 1999), and mass-balance calculations from inflow volume and pan evaporation rates, these ponds are assumed to contribute recharge to the aquifer system. The mass-balance calculations were based on inflow volumes from 1984 to 1998 (David Lambert, Los Angeles County Sanitation Districts, unpublished data, 1996, 1998), a pan evaporation rate of 114in./yr (Bloyd, 1967), and pond acreages. Prior to 1997, about 58 acres were ponded (David Lambert, Los Angeles County Sanitation Districts, written commun., 1996). In 1997, pond acreage increased to about 400 to 500 acres; however, the larger ponds were seldom fully wetted. Records of the wetted areas of the larger ponds are not available; therefore, it was assumed that, on average, about twice the area of the old pond was wetted from 1997 to 1998. Calculated wastewater recharge increased from about 1,457 to 8,064 acre-ft from 1985 to 1998 (fig. 40), which correlates well with population growth in Palmdale (about 23,150 to 117,100) for the same period (fig. 2). Because this source of water is continuous and essentially constant and the rate of infiltration per acre is much greater than that for agricultural recharge, it was assumed for both the AV and the LAN models that the delay between infiltration through the bottom of the pond and water-table recharge was less than 1 year.

The northern boundary of the LAN model area straddles a broad ground-water mound between Lancaster and Rosamond to the north (Carlson and others, 1998). Simulated southward flow from this mound in the LAN model, through the specified-head boundary, averages 5,130 acre-ft/yr (fig. 40). This mound is in an area that historically had not been developed, except for a few homesteads which had flowing wells (Johnson, 1911); this area has remained undeveloped. Because there are limited potential sources of recharge in the area, the ground-water mound probably is a remnant of past hydraulic conditions rather than a feature fed by recharge. Any simulated recharge from the northern boundary probably represents ground-water storage released during a slow northward retreat of the mound as widening cones of depression from the Lancaster area draw water southward. The specified-head boundary is a surrogate for this process, which cannot be simulated at this subregional scale.

A summary of estimated recharge from all sources considered is shown in figure 41*A*. Potential recharge that was assumed to be insignificant include upward flow from the lower aquifer, direct infiltration of precipitation, and urban sources. Although annual precipitation is small in the Lancaster area, even a small amount of rainfall reaching the water table over a large area would constitute a significant volume of recharge. However, given the very dry nature of desert soils, it commonly has been assumed that infiltrated precipitation is held in tension in near-surface soils and later evaporates rather than moves downward (Snyder, 1955; Durbin, 1978).

Potential urban sources of recharge in the model area primarily include infiltration of irrigation water from urban landscaping and from pipe leakage. Grass lawns, for example, have irrigation requirements similar to alfalfa. The average home owner or municipal caretaker may irrigate a lawn more than the average farmer irrigates alfalfa, but because of thatch buildup in lawns, runoff to storm drains, and other factors, recharge from this source may be equal to or less than that from agriculture. Leakage from water-delivery, storm-drain, and sewer pipes can be a substantial component of recharge in some areas (Phillips and others, 1993). Positive, but low (0.05–0.11 mg/L), measurements of methylene-blue-active substances [an indicator of sewage source (Phillips and others, 1993)] from wells near the intersection of Avenue J and Sierra Highway (fig. 7) suggest that recharge from sewer-pipe leakage in this area may be small; concentrations in all other wells tested were below the detection limits (less than 0.05 mg/L) for this substance. A determination of recharge from these sources is beyond the scope of this work; however, it is important to recognize that these potential sources of recharge are not accounted for in the model.

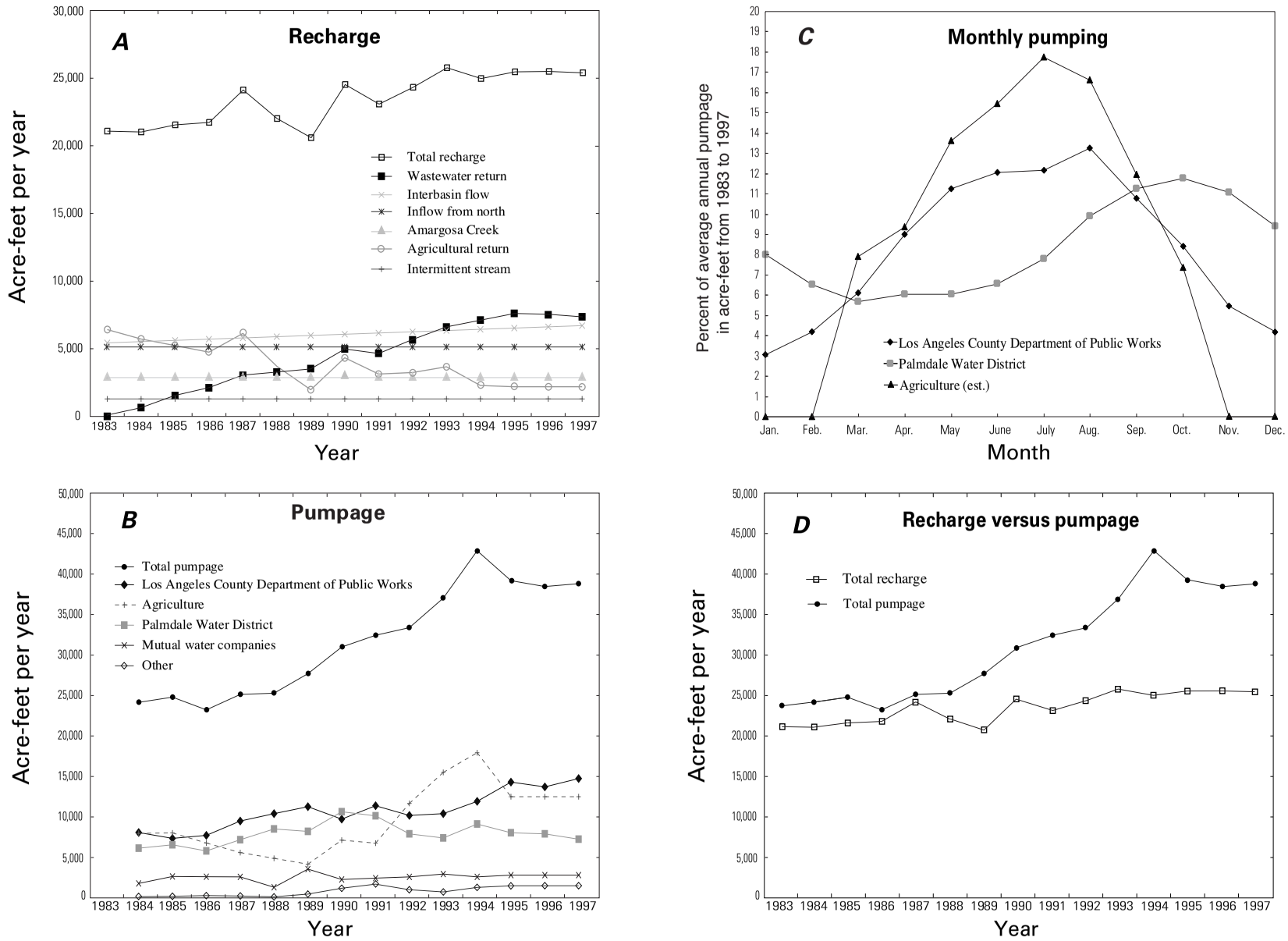

Figure 41. Data and estimates for (*A*) recharge, (*B*) pumpage, (*C*) seasonal distribution of pumpage, and (*D*) a comparison of recharge and pumpage, in the model area, upper and middle aquifers only, Lancaster, Antelope Valley, California.

Ground-Water Extraction

Ground-water pumpage data were gathered and compiled from several sources (Templin and others, 1995; Leighton and Phillips, 2003; and individual water purveyors). Figure 42 shows the location of the known production wells in the model area; construction information for these wells is given in table 1. Well depths are known for 70 of the 85 known production wells, and the screened intervals are known for 68 of the wells. Figure 41*B* shows annual ground-water pumpage for various groups of wells and total pumpage from 1983 to 1997. The sharp increase in pumpage during the late 1980s corresponds with increased agricultural use and rapid population growth in the area during that period (fig. 2). Pumpage plateaued during the early 1990s, which corresponds to water shortages and associated water conservation efforts during the 1987–92 drought; pumpage increased after the drought.

Monthly meter readings were available for all the LACDPW and Palmdale Water District wells in the model area and account for most of the annual pumpage (fig. 41*B*). Because only annual pumpage data were available from all the other entities, the monthly distribution of pumpage for these wells was estimated. Because most of the urban suppliers in this group used little imported SWP water, it was assumed that the temporal distribution of ground-water pumpage for these suppliers would be similar to that of the Palmdale Water District, which had less seasonal variation in pumpage during most of the simulation period than that of LACDPW, which used SWP water extensively during the winter (fig. 41*C*).

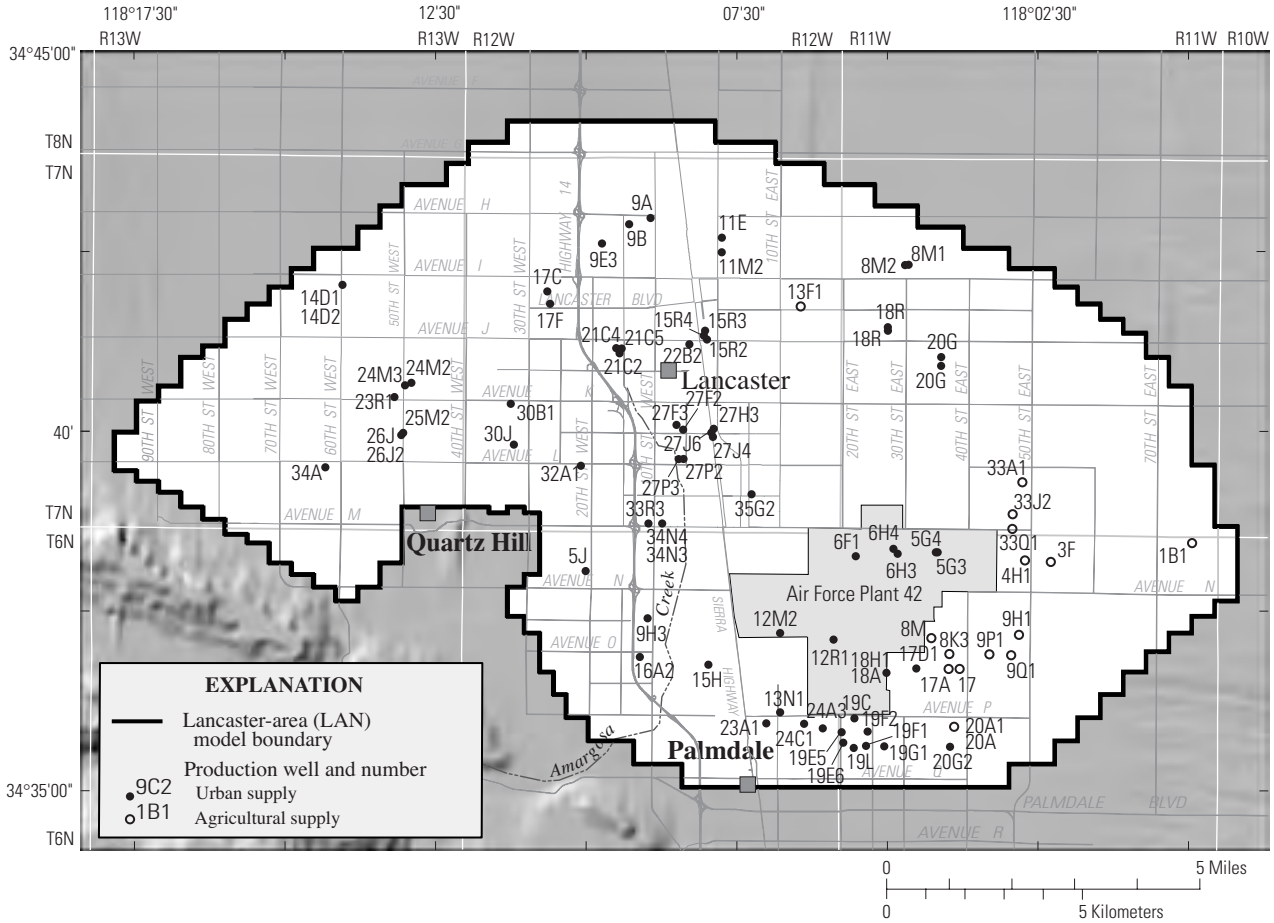

Figure 42. Locations of production wells included in the Lancaster-area (LAN) model in Lancaster, Antelope Valley, California.

Agricultural pumpage is the least understood category of ground-water usage in the Antelope Valley (Templin and others, 1995; Leighton and Phillips, 2003). Although estimates of agricultural water use were available from recordations provided to the State Water Resources Control Board, comparisons of these data with land-use information and crop production reports suggest that these data are incomplete (Templin and others, 1995; Leighton and Phillips, 2003). Leighton and Phillips (2003) estimated agricultural pumpage from land-use data, crop acreages, and estimated crop water demands and irrigation efficiencies. Annual agricultural pumpage values from the AV model for the area of the LAN model (fig. 41*B*) were divided evenly among the 17 known agricultural wells in the area (fig. 42). There may be additional agricultural wells in this area, but they likely would be near the known agricultural wells. Although this method results in an areawide average annual extraction value for each well, which ignores local variability, it produces a more reasonable total annual variability that agrees with known crop acreages. This method also concentrates the pumpage in areas with dense concentrations of agricultural wells, which seems appropriate assuming that the known distribution of wells reasonably represents the true distribution.

Data on the monthly distribution of agricultural pumpage were not available; therefore, the distribution was estimated using the monthly reference evapotranspiration for alfalfa (University of California Cooperative Extension, 1994) for March through October (fig. 41*C*). Alfalfa, which was the dominant crop in Antelope Valley, generally is not irrigated during the other months of the year. Although other crops were grown in the area of the LAN model, there is little information on the areal distribution by crop type; therefore, it was assumed that the monthly irrigation schedule for alfalfa (timing only, not volume) is representative of all crops grown in the area.

Monthly extraction rates for each well were assigned to the row and column in the model grid that coincides with the location of the well. Extraction rates for some model cells represent more than one well.

Pumpage from wells screened in the upper and middle aquifers was apportioned by the transmissivity of layers 1 and 2. The transmissivity of the upper aquifer (layer 1) changes in response to water-level changes because the aquifer is unconfined. These changes in transmissivity cause changes in the vertical distribution of flow into a well. Pumpage was redistributed vertically for 3 time intervals during the simulation (1983–1987, 1988–1992, and 1993–1996) to account for temporal changes in transmissivity.

For wells that are also screened in the lower aquifer, which was not simulated in the LAN model, the pumpage was reduced by the percentage of effective transmissivity attributed to the lower aquifer prior to distributing it to model layers. This effective transmissivity was calculated from the screened interval within the lower aquifer and the assumed hydraulic conductivity of this aquifer. The value of horizontal hydraulic conductivity used in the AV model for the lower aquifer was constant, 2.0 ft/d; however, that model was relatively insensitive to this value (Leighton and Phillips, 2003). This value was initially used for the entire area of the LAN model, but was increased to 7.0 ft/d for the northern part of the model area on the basis of relative well capacities and borehole flow data (described later in this report). The pumpage attributed to the lower aquifer in the calibrated LAN model was 13 percent of the total pumpage.

Ground-water recharge and pumpage in the model area during the calibration period are shown in figure 41*D*. A comparison of these data suggests a near-equilibrium condition from the beginning of the calibration period through about 1988, followed by depletion of ground-water storage through the end of the calibration period.

Model Calibration and Sensitivity

Model calibration involves adjusting the initial input values within reasonable ranges to obtain good agreement between simulated and measured (or estimated) values. Calibration of the LAN model was achieved in two phases: a trial-and-error process (phase I), followed by a more systematic parameter estimation process (phase II) that also served as a sensitivity analysis. The trial-and-error process is useful for learning about the aquifer system, and sometimes it is the only means available or practical for model calibration. Results from this process, however, can be non-unique and difficult to interpret. It was used for this study to determine the general sensitivity of the model results to changes in the conceptual model and reasonable ranges of input parameter values for the next phase of calibration. A more systematic approach

was used in phase II to address the uniqueness of the calibration results and to determine the sensitivity of model results to values not thoroughly considered during the trial-and-error calibration. In keeping with this approach, results from the trial-and-error process are discussed in general terms in the phase I section of the report. Presentations of model fit (hydrographs and water-level) are given in the phase II section.

The calibration criteria was various forms of hydraulic head. Hydraulic head was the only measured dependent value simulated, which is not ideal for model calibration. Preferably, calibration would include both head and flow, but no measurements of dependent flow were available. Simulated and measured water-table altitudes were compared using a contour map of the 1996 water table (fig. 36); hydrographs of 10 wells that, for the most part, show annual water-level changes throughout all or most of the calibration period; hydrographs of 5 piezometers and 3 wells that were measured frequently during the injection tests; and hydrographs of 20 wells with short-term records. The locations of all the wells used in model calibration are shown in figure 43. Simulated hydraulic gradients from the upper aquifer (water table) to the middle aquifer were compared with the measured hydraulic gradients in nested piezometers.

Although it was considered important to simulate the measured heads and flow directions near the outer margins of the LAN model, the primary focus during calibration was the central part of the model. This area of the model includes the injection site for this pilot study and is the area where a larger scale injection program may be implemented.

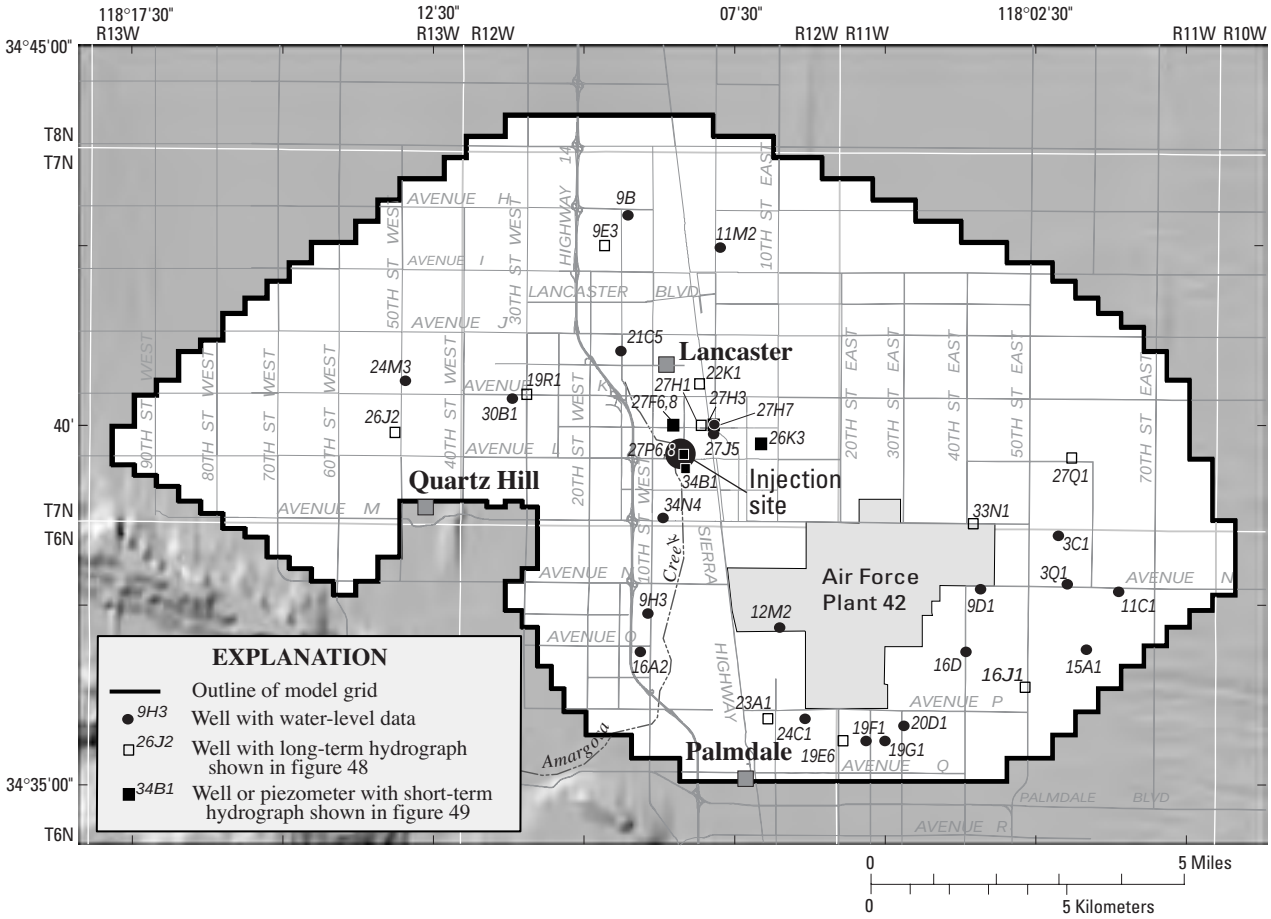

Figure 43. Location of wells and piezometers used in model calibration, Lancaster, Antelope Valley, California.

Phase I Calibration

For the first phase of calibration, a trial-and-error approach was used to determine the general sensitivity of the model results to changes in the conceptual model and to determine reasonable ranges of the parameter values for the next phase of calibration. Values considered during the phase I calibration included the hydraulic conductivity of layer 1 (K_1), transmissivity of layer 2 (T_2), leakance (λ) between layers, specific yield (S_y), specific storage (S_s), the vertical distribution of ground-water pumpage, and recharge. All these hydraulic parameters, except leakance, are described in detail earlier in this report. The ability of aquifer-system materials to transmit water vertically is described by the leakance (λ):

$$\lambda = \frac{KV}{b} \tag{6}$$

where

KV is the effective vertical hydraulic conductivity between layers 1 and 2 (L/t), and

b is the thickness between the midpoints of layers 1 and 2 (L).

Parameters values were adjusted by trial and error within reasonable ranges of measured values, when available, and of the calibrated values from the AV model (Leighton and Phillips, 2003). Measured values were available for S_y and S_s for individual sites. S_y was assumed to be 0.13 throughout the LAN model area; this value was based on the calculated value from simultaneous measurements of gravity and water-level change (Howle and others, 2003) and on the successful use of this value in the AV model (Leighton and Phillips, 2003). Although evidence presented earlier suggests variability in the elastic skeletal specific storage, which comprises the S_s of the LAN model, information needed for determining the areal distribution of this variability was not available. The AV model simulated subsidence measured at bench marks in the Lancaster area reasonably well. The calibrated value for compaction in the Lancaster area reasonably matched the measured value using a constant elastic skeletal specific storage of 1.7×10^{-6}, which is essentially identical to that calculated from the stress/strain diagrams using data from the Lancaster extensometer site (1.2×10^{-6}). Therefore, S_s was assumed to be 1.2×10^{-6} throughout the model area and the storage coefficient for each cell in layer 2 was calculated as the product of S_s and the thickness of the middle aquifer at the cell location. Values of S_y and S_s were varied during the first phase of calibration but ultimately were returned to 0.13 and 1.2×10^{-6}, respectively.

Measurements were not available for K_1, T_2, and λ, and therefore the calibrated values from the AV model were used as the initial values in the LAN model. The AV-model values of T_2 and λ were not directly applicable to the LAN model, however, because these values were affected by the thickness of layer 2, which was different in the two models (fig. 34). Instead, the AV-model values for K_2 and *KV* for the appropriate thicknesses were used in the LAN model.

The initial values for K_1 (based on the calibrated value from the AV model) are shown in figure 39. Values of K_1 were varied widely during calibration of the LAN model to determine the overall sensitivity, but generally were narrowed for the injection site to the range of values for nearby cells in the AV model (10–24 ft/d). Results from the AV model (fig. 39*A*) show that hydraulic conductivity decreases with increasing distance from the San Gabriel Mountains, the primary source of the aquifer materials, along the south–southwestern border of the LAN and AV models. However, a relatively low value of K_1 was required during calibration of the AV model for the Palmdale area to match the measured water-level declines; a low value of K_1 also was required during the first phase of calibration of the LAN model. It was assumed that because of the relatively large depth to the water table in the Palmdale area (fig. 36) and the corresponding increase in age and induration of the saturated materials, a relatively low hydraulic conductivity occurs in this area. A decrease in S_y would have partly offset the decrease in K_1; however, it was assumed that S_y is constant.

Another anomaly in the distributed K_1 values in the AV model is the easternmost zone (fig. 39*A*) which had the highest hydraulic conductivity (24 ft/d), which includes an area relatively far from the San Gabriel Mountains. A high hydraulic conductivity was required for the southern part of this zone to transmit underflow from the southeast without generating simulated heads that were much higher than those measured in this area, where the water table is relatively shallow. The simulated heads in the northern part of this zone were relatively insensitive to hydraulic conductivity in both the AV and the LAN models; therefore, the actual K_1 may be lower than that shown in figure 39 for the northern part of the easternmost zone.

The hydraulic conductivity of layer 2 (K_2) in the AV model was constant at 10.0 ft/d in the LAN model area, and transmissivity varied with the thickness of the model layer. The initial transmissivity of layer 2 of the LAN model was calculated using a value of 10 ft/d for K_2 and the appropriate layer thickness for each model cell. The T_2 was calibrated in the vicinity of the injection and extensometer sites on the basis of the measured water levels in the piezometers screened only within the middle aquifer. Results of the first phase of calibration showed that values of K_2 considerably smaller than those of K_1 were required to produce satisfactory results for these locations; this differs from results of the AV model, particularly if the ratio of K_1:K_2 is assumed to be consistent throughout the model area. Results of the phase I calibration suggested that the total transmissivity of layers 1 and 2 in the LAN model needed to be approximate to that in the AV model for most areas.

The leakance (λ) between the upper and middle aquifers in the AV model for the Lancaster area was based on a ratio of K_1:*KV* of about 100:1. For the LAN model, the value of *KV* was also linked to K_1; thus, their areal distribution was the same (fig. 39*B*). The ratio of K_1:*KV* was varied during the phase I calibration. The measured vertical gradients were best simulated with ratios greater than 100:1, and *KV* was not linearly related to K_1. These *KV* values were divided by the thickness between the midpoints of layers 1 and 2 to calculate λ for every cell.

The vertical distribution of ground-water pumpage was calculated for each well on the basis of the calculated effective transmissivity of each layer in the LAN model that each well is screened in and of the lower aquifer. The lower aquifer was not simulated in the LAN model, so these calculations were external to the model. The vertical distribution of pumpage was affected during calibration by changes in K_1 and K_2 and by the hydraulic conductivity assigned to the lower aquifer for the calculations. The hydraulic conductivity of the lower aquifer initially was assumed to be 2.0 ft/d throughout the LAN model area, as in the AV model. It was increased to 7.0 ft/d in the northern part of the LAN model area during the second phase of calibration.

Ground-water recharge was the only stress that was changed in magnitude during the phase I calibration. Recharge from Amargosa Creek was adjusted, and the effects of a previously ignored potential source of recharge was examined. The only known estimate of recharge from Amargosa Creek (about 662 acre-ft/yr) was by Durbin (1978); he based the estimate on the channel geometry method. This method is subject to large variation between estimates, particularly for desert environments where flashy runoff regularly alters and (or) leaves the channel. The calibrated value (2,835 acre-ft/yr) was based on the measured hydraulic gradient between wells 6N/12W-16A2 and 9H3, which have similar depths and are similarly constructed (table 1); these wells are about 1.5 and 2.2 mi north of the point where Amargosa Creek enters the model area, respectively (fig. 42). No other means was found to match this gradient and the water-table altitude without a substantial increase in recharge. Prior to increasing recharge, initial heads were checked and adjusted slightly where Amargosa Creek enters the model area. Amargosa Creek, which is ungaged, is the third largest drainage from the San Gabriel Mountains in Antelope Valley; for comparison, the estimated total recharge from the two larger drainages averages 16,200 acre-ft/yr (Leighton and Phillips, 2003).

The calibrated value for recharge from Amargosa Creek (2,835 acre-ft/yr) exceeds the previous estimate (662 acre-ft/yr) by Durbin by a factor of 4. It is possible that any simulated recharge that exceeds the estimated channel capacity of Amargosa Creek may occur as infiltration of precipitation falling on the coarse-grained fanhead where Amargosa Creek enters the valley and (or) by ground-water movement through coarse materials beneath the streambed.

It initially was assumed that no flow occurred between the middle or upper aquifer and the lower aquifer through the lacustrine unit. During calibration, this assumption was relaxed, and recharge was added to the middle aquifer as if upward flow were occurring. Water levels were sensitive to this potential source of recharge; however, the effects were not beneficial enough to warrant the uncertainty introduced from estimating the magnitude and distribution of upward and, at times, downward flow. The small measured vertical gradients suggest that flow across the lacustrine unit probably is a minor source of water. Data required for simulation of the lower aquifer in this area are lacking.

Results of the phase I calibration suggested that a reasonable match between simulated and measured heads for most of the model area could be obtained using reasonable values for the calibration parameters and the existing conceptual model. However, an excellent match was not obtained at the extensometer and injection sites for any one set of parameters. Two specific difficulties in matching measured water levels were identified: a good match of both high (at peak injection) and low (during the August pumping season) water levels could not be made at the extensometer site nor could a good match be made for water levels in the middle aquifer at the extensometer and the injection sites with the same set of parameters. The phase I calibration was useful for determining the gross sensitivity of the model results to the input variables, and, in turn, for developing an approach for the next phase of calibration and the sensitivity analysis.

Phase II Calibration

A systematic approach was developed for the second phase of calibration using what was learned during the phase I calibration. The primary assumption made in the transition was that the storage properties (S_y and S_s) are constant throughout the model area. This assumption was based on the results of the AV model, in which this parameter was constant throughout the area of the LAN model (Leighton and Phillips, 2003) and on the results of the phase I calibration. Results from the phase I calibration showed that the simulated long-term water-level changes are sensitive to the S_y where water-level changes are greatest and that a value of 0.13 provides a reasonable match to measured water-level changes. Although the value of elastic S_s estimated from the stress/strain analysis was consistent with that used throughout the AV model and with that determined at the Holly site at Edwards AFB (Sneed and Galloway, 2000), there is abundant evidence that the elastic S_s varies spatially. There is not enough information, however, to quantify the distribution of elastic S_s throughout the model area. Simulated heads are relatively insensitive to reasonable changes in this value. The assumption that storage properties are uniform and known reduced the calibration variables to three parameters: K_1, K_2 (used to calculate T_2), and *KV* (used to calculate λ). Pumpage, recharge, and the model geometry were unchanged.

For a given value of K_1, K_2 and *KV* were varied systematically for specified ranges within a zone surrounding the injection site (fig. 39*B*). This zone was designed to be large enough to minimize effects of the "boundary conditions" outside the zone (areas with unchanging parameters), and small enough to avoid relatively drastic effects, such as dewatering of the upper aquifer, in some parts of the model with some combinations of these three parameters.

The upper and lower bounds of K_2 considered initially in the phase II calibration were about 15 and 1 ft/d, respectively; these values were based on results from the AV model (Leighton and Phillips, 2003) and from the phase I calibration of the LAN model. The bounds of *KV* were less constrained, so a larger range (0.001–1.0 ft/d) was explored. K_1 was adjusted within the range of 12 to 18 ft/d.

The error associated with simulations using each combination of K_1, K_2, and *KV* was quantified by comparing 3 measured and simulated conditions: water-table rise during injection, and vertical gradients during injection and extraction. These errors were calculated for the injection and extensometer sites; however, only those for the injection site are presented because measured and simulated responses at the extensometer site to stresses at the injection site were insufficient (particularly at the water table) for use in this calibration procedure.

The errors associated with water-table rise and seasonal vertical gradients were plotted in 2-dimensional space (K_2 and *KV*) and contoured to form an error surface. This error surface reveals the shape and position of lines of zero error (fig. 44). Each point along these 3 lines of zero error represents a combination of parameters that results in zero error between measured and simulated values. The combination of parameters that best simulates the 3 conditions (water-table rise during injection and vertical gradients during injection and extraction) is at the intersection of the 3 lines. The location of these intersections is sensitive to the value of K_1 associated with each error surface (fig. 44).

The error in simulated water-table rise generally was sensitive to K_1 and K_2 and relatively insensitive to *KV*; the lines of zero error are subhorizontal in figure 44. The error in simulated vertical gradient was very sensitive to *KV* and mildly sensitive to K_1 and K_2; it is shown as vertically oriented contours in figure 44. These different sensitivities to the parameters help to constrain the location of the intersection of these zero-error lines.

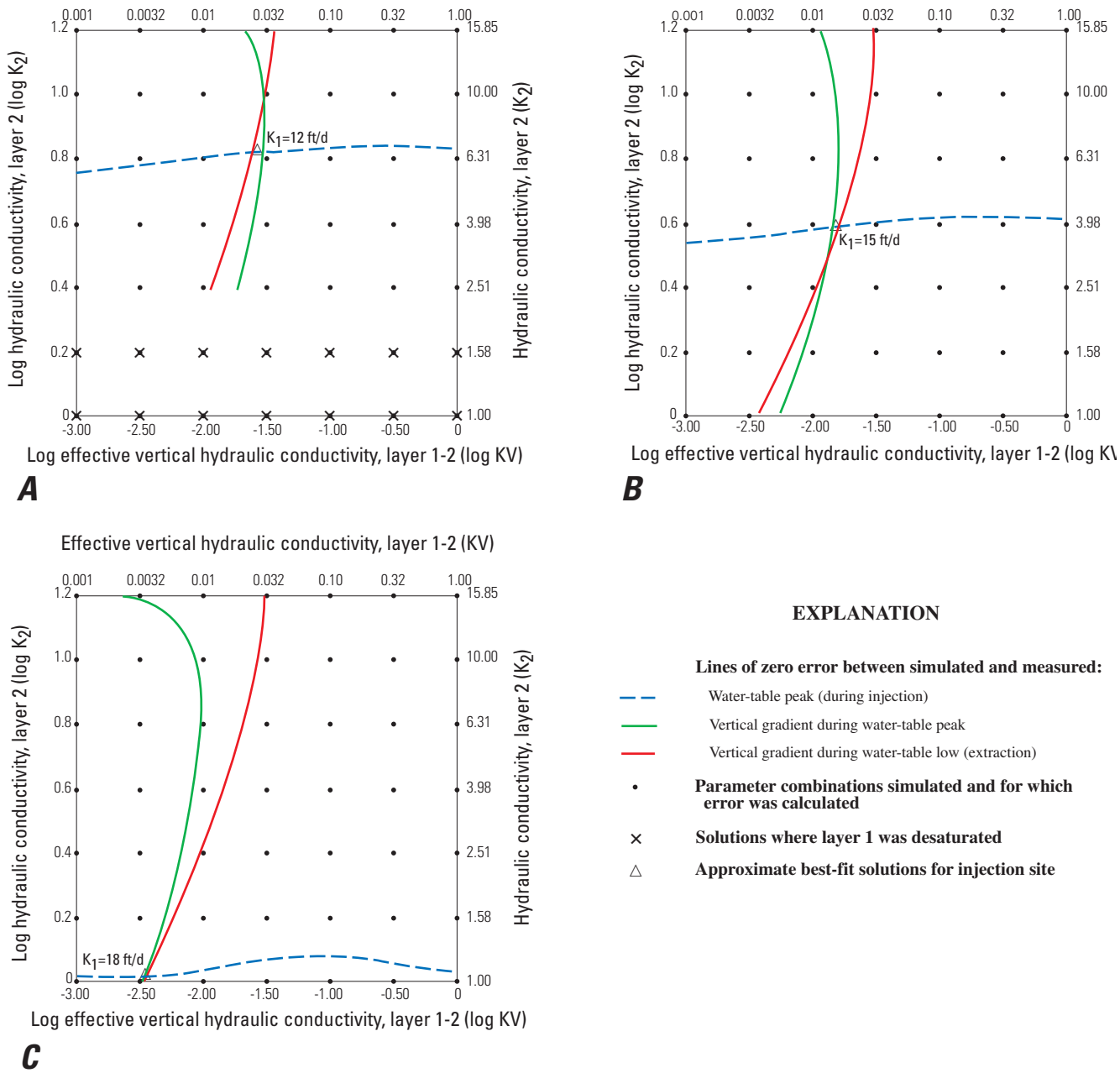

Figure 44. Results of phase II calibration procedure for layer-1 hydraulic conductivity values (K_1), of (*A*) 12, (*B*) 15, and (*C*) 18 ft/d.

The curved lines in the diagram represent approximate parameter combinations that result in zero error between simulated and measured water-table rise during injection or between simulated and measured vertical gradients at the injection site during injection cycle 3. All values of hydraulic conductivity are in foot per day (ft/d).

There was a separation between the zero-error lines representing the vertical gradients at the injection and extensometer sites. Those for the extensometer site are not shown in figure 44, but were offset to the right (indicating a higher *KV*) and roughly parallel to those for the injection site. This separation is likely related to the inability to match the measured water levels in the middle aquifer at both sites with one set of parameters, as was noted during the phase I calibration. Simulations that matched the measured conditions at the injection site are associated with low hydraulic heads (about 20 ft lower than the measured value) in the middle aquifer at the extensometer site during the pumping season. Simulated conditions in the upper aquifer at the extensometer site reasonably matched the measured conditions year round. Calibration results indicate that an increase in the vertical hydraulic conductivity of at least one order of magnitude in the vicinity of the extensometer site over that for the injection site may correct this problem. There is no apparent justification, however, for increasing *KV* to the north, where fine-grained materials would be expected to increase, or for increasing it by such a large amount across a short distance (about 0.5 mi). This inability to match measured conditions in the middle aquifer at both sites is insensitive to the other parameters considered in the calibration procedure: K_1 and K_2.

A probable explanation for the inability to match simultaneously the water levels in the middle aquifer at both the extensometer and injection sites is that the effects of inelastic compaction were not simulated. Inelastic compaction measured by the shallow extensometer from 1996 to 1997 was about 0.007 ft, which yielded an equivalent amount of water. This amount is conservative because the shallow extensometer does not include the lower 40 ft of the middle aquifer (fig. 10), which contains fine-grained materials (fig. 32), and because compaction of the upper part of the lacustrine unit also would yield water to the middle aquifer. The deep extensometer includes both of these intervals. About 0.003 ft of additional compaction was recorded at this extensometer during the same period. The 20 ft of excess drawdown simulated for the same period multiplied by the specific-storage value used in the LAN model (1.2×10^{-6}/ft) and the thickness of the middle aquifer at the extensometer site (about 250 ft) yields 0.006 ft of water. The general agreement between the magnitude of inelastic compaction and the amount of water associated with excess simulated drawdown suggests that the simulation of too much drawdown in the middle aquifer at the extensometer site was probably caused by the use of a constant specific-storage value and the associated effect of omitting water contributed from inelastic compaction of the aquifer system.

Leveling data and simulated water levels for the only other local piezometer screened within the middle aquifer support the above argument. The leveling data suggest that little or no inelastic compaction occurred at the injection site and corroborate data from the extensometer; therefore, the assumption of constant storage appears to be valid for the injection site. The simulated water levels that match those measured at the injection site also match those at piezometer 7N-12W-27H7, in the Avenue K–8 and Division Street well field about 0.5 mi east of the extensometer site. Like the injection site, Avenue K–8 and Division Street is distant (relative to the extensometer site) from areas where significant subsidence was measured from 1993 to 1995 (fig. 7).

A comparison of the results of the phase I and phase II calibrations yielded quantitative information on qualitative relationships. A comparison of the parameter values at the approximate intersections of zero-error lines for the cycle-3 injection (shown as triangles on figure 44) reveals some predictability in the behavior of the model. Table 2 shows the parameter values at these intersections and key consistent relations between the parameters. Note that the sum of K_1 and K_2, which are proportional to transmissivity because the thicknesses of layers 1 and 2 are similar, is essentially constant at an average of about 19 ft/d. This makes intuitive sense, as these are the only significantly variable components of the overall transmissivity of the system—changes in this transmissivity would cause either an overestimation or an underestimation of head without changes in storage and (or) stresses to compensate. K_2/KV is fairly constant and averages about 272 (table 2). These observations suggest that given a value of K_1, K_2, or *KV*, one can predict the other two values that will result in zero (or very low) error. This was tested by predicting the zero-error values of K_2 and *KV* for a K_1 of 8.0 ft/d and comparing the result with that for K_1 values of 12, 15, and 18 ft/d.

Table 2. Range and comparison of hydraulic conductivity values estimated during phase II of the model calibration for Lancaster, Antelope Valley, California

[All values are in feet per day]

Hydraulic conductivity of model layer 1 (K_1)	Hydraulic conductivity of model layer 2 (K_2)	Effective vertical hydraulic conductivity between model layers 1 and 2 (*KV*)	Hydraulic conductivity of model layers 1 and 2 (K_1+K_2)	Hydraulic conductivity of model layer 2/effective vertical hydraulic conductivity between model layers 1 and 2 (K_2/*KV*)
12	6.51	0.026	18.5	250
15	3.92	.014	18.9	280
18	1.06	.0037	19.1	286

The values of K_2 and *KV* were predicted using the values of K_1+K_2 and K_2/*KV* for a K_1 of 12 ft/d (table 2), rather than using average values, because the line connecting the zero-error solutions (fig. 44) is not quite linear. Accordingly, the estimated values of K_2 and *KV* were 10.5 and 0.042 ft/d, respectively. The predicted and the simulated values were almost identical (fig. 45).

An infinite set of parameter values, such as those shown in table 2, can produce simulated water levels that match those measured at the injection site, as long as the relations noted above hold. Given no additional information, any single solution within this set is clearly non-unique. Additional information, however, is available to help constrain the parameter values including information from the velocity log of injection well 7N/12W-27P2 (fig. 5) and from microgravity results. The velocity log shows that about 12 percent of the volume extracted from well 7N/12W-27P2 came from the middle aquifer (fig. 5). Assuming that the condition of the well screen and the error associated with the data-collection method was uniform with depth, this result can be used to estimate the relative hydraulic conductivities of the upper and middle aquifers at the injection site. Taking into account the relative saturated screened intervals during the velocity logging, it was assumed that K_2 is about 10 percent of K_1 in the vicinity of the injection site.

Howle and others (2003) compared water-table changes calculated from the measured changes in gravity and a specific yield (0.13) with those simulated using a simplified ground-water-flow model of the upper aquifer. Several values of hydraulic conductivity were used in the simulation, and the results were superimposed onto those from the gravity analysis (fig. 46). The hydraulic conductivity for the upper aquifer that best matches the results from the gravity analysis is about 18 ft/d.

Combining the results of these independent analyses, a K_1 of about 18 ft/d and a K_2 for layer 2 that is 10 percent of that for layer 1 are indicated. Accordingly, if K_1 is 18 ft/d, the sum of K_1 and K_2 would be 19.8 ft/d, which slightly exceeds the ideal value of 19.1 (table 2). The estimated K_2 value from the calibration procedure for a K_1 of 18 ft/d is about 1.06 (fig. 45), somewhat lower than 1.8 ft/d (10 percent of 18 ft/d). If K_1 is reduced from 18 to 17 ft/d, the sum of K_1 and K_2 would be 18.7 ft/d, which is closer to the ideal value of 19.1 ft/d. The value of *KV* associated with a K_1 of 17 ft/d, calculated from the average value of K_2/*KV* (table 2), is 0.006 ft/d. The intersection of these calculated K_2 (1.7 ft/d) and K_v (0.006 ft/d) values for a K_1 of 17 ft/d plots very close to where the zero-error solution of the calibration procedure would be for the same K_1 value (fig. 45). Although there are potential errors inherent in both of the independent estimates used to narrow the infinite set of parameters, the close match of the values calculated using the relations shown in table 2 to those from the calibration results is compelling enough to put this forward as the preferred set of parameters (K_1 of 17 ft/d, K_2 of 1.7 ft/d, and *KV* of 0.006 ft/d).

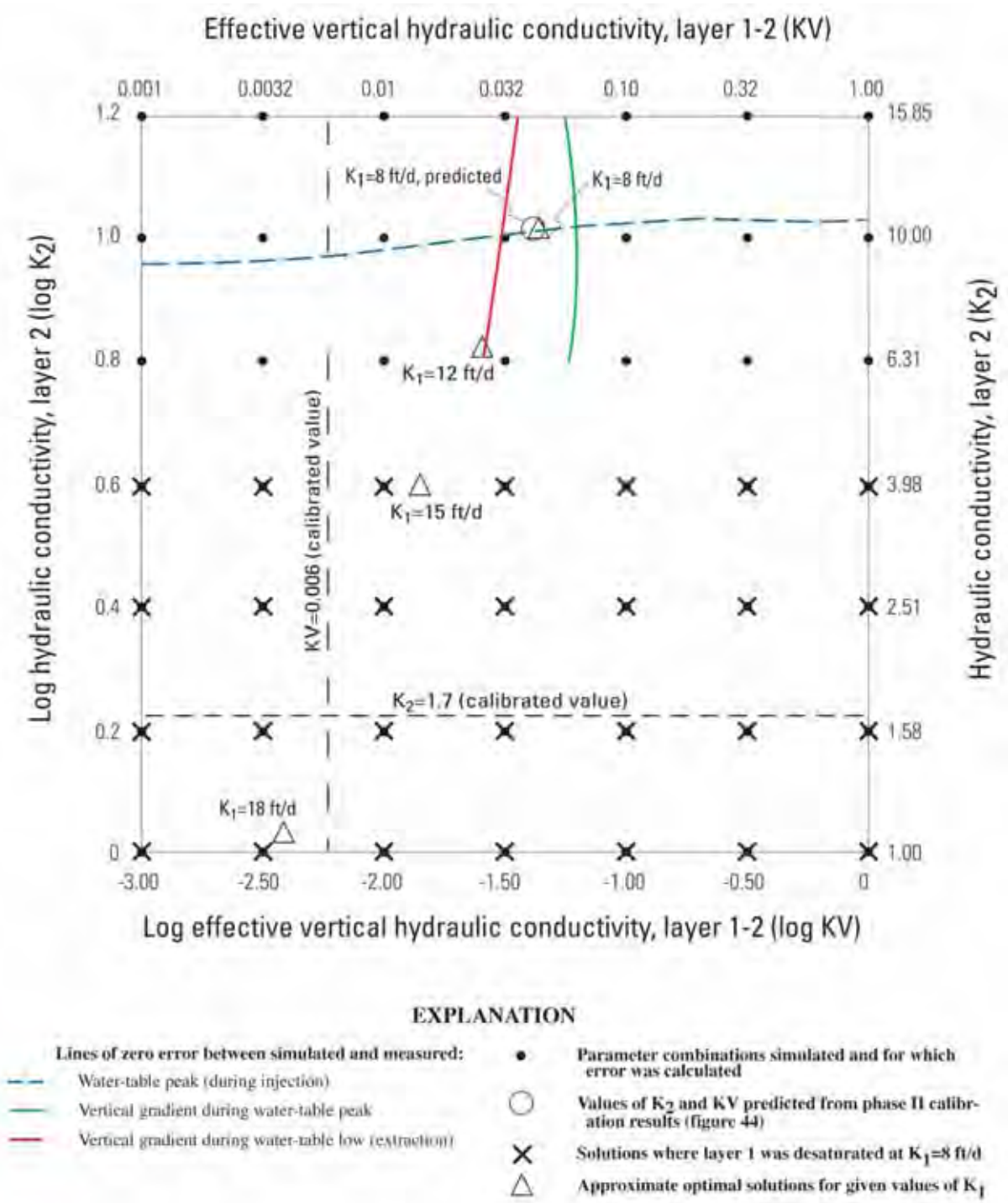

Figure 45. Approximate predicted values of hydraulic conductivity (in foot per day) of layer 2 (K_2) and effective vertical hydraulic conductivity (*KV*) compared to those determined from the phase II calibration procedure for layer-1 hydraulic conductivity (K_1) of 8 feet per day.

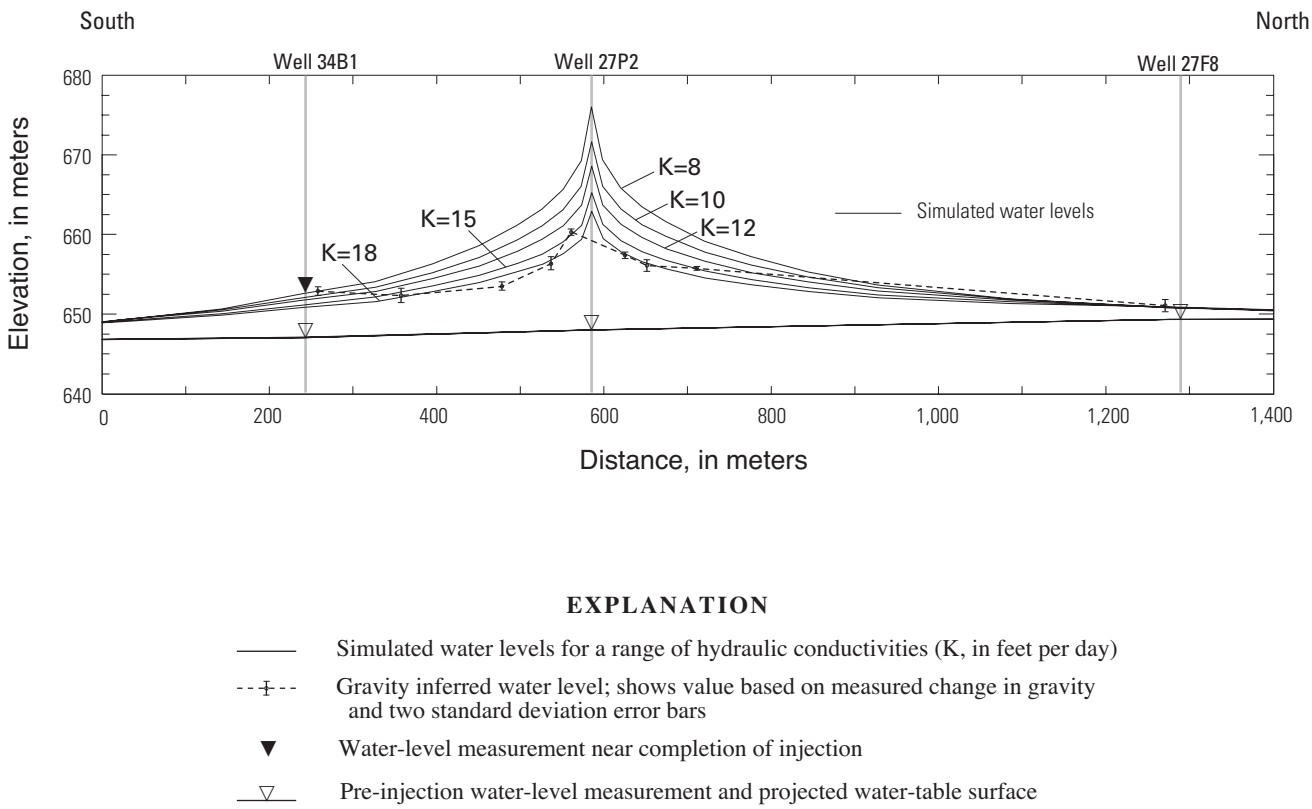

Figure 46. South-to-north profile with gravity-determined water-level changes compared to simulated injection mound geometries for a range of hydraulic conductivities, Lancaster, Antelope Valley, California.

The simulations were done using a simplified one-layer model representing only the upper aquifer (from Howle and others, 2003).

Phase II calibration involved changing parameters only within the zone (figure 39*B*) surrounding the injection and extensometer. Results of periodic tests showed the zero-error solution for this zone was insensitive to the same changes outside this area. Using the preferred set of parameters, the same ratio of K_1/K_2 and K_2/KV was used for the entire model area, while maintaining the same sum of K_1 plus K_2 generated during the phase I calibration (fig. 39*B*). This was done as an attempt to retain the relative differences in transmissivity inferred by the AV model and the phase I calibration of the LAN model while incorporating what was learned at the smaller scale.

Results from the calibrated LAN model are shown in figures 47–49. Contours of the simulated water levels for April 1996 compare well with the contours based on the measured water levels, particularly those in the Lancaster and Palmdale areas (fig. 47). The simulated values for the long-term water-level trends closely match the measured values throughout the model area (fig. 48). Short-term seasonal water levels measured during the injection tests also were simulated reasonably well (fig. 49).

A comparison of input values for the LAN model with those for the AV model for the same areas (Leighton and Phillips, 2003) shows that most of the values are similar, but that there also are some significant differences. Storage properties are essentially identical except for inelastic skeletal specific storage, which was simulated in the AV model but not in the LAN model. Pumpage and recharge from interbasin flow, small intermittent streams, and infiltration of treated wastewater and agricultural irrigation are essentially the same, though the distribution was slightly different in some cases. Recharge related to southward flow from the ground-water mound through the northern boundary of the LAN model was smaller than that simulated by the AV model. However, the northward retreat and degradation of the simulated mound in the AV model was much

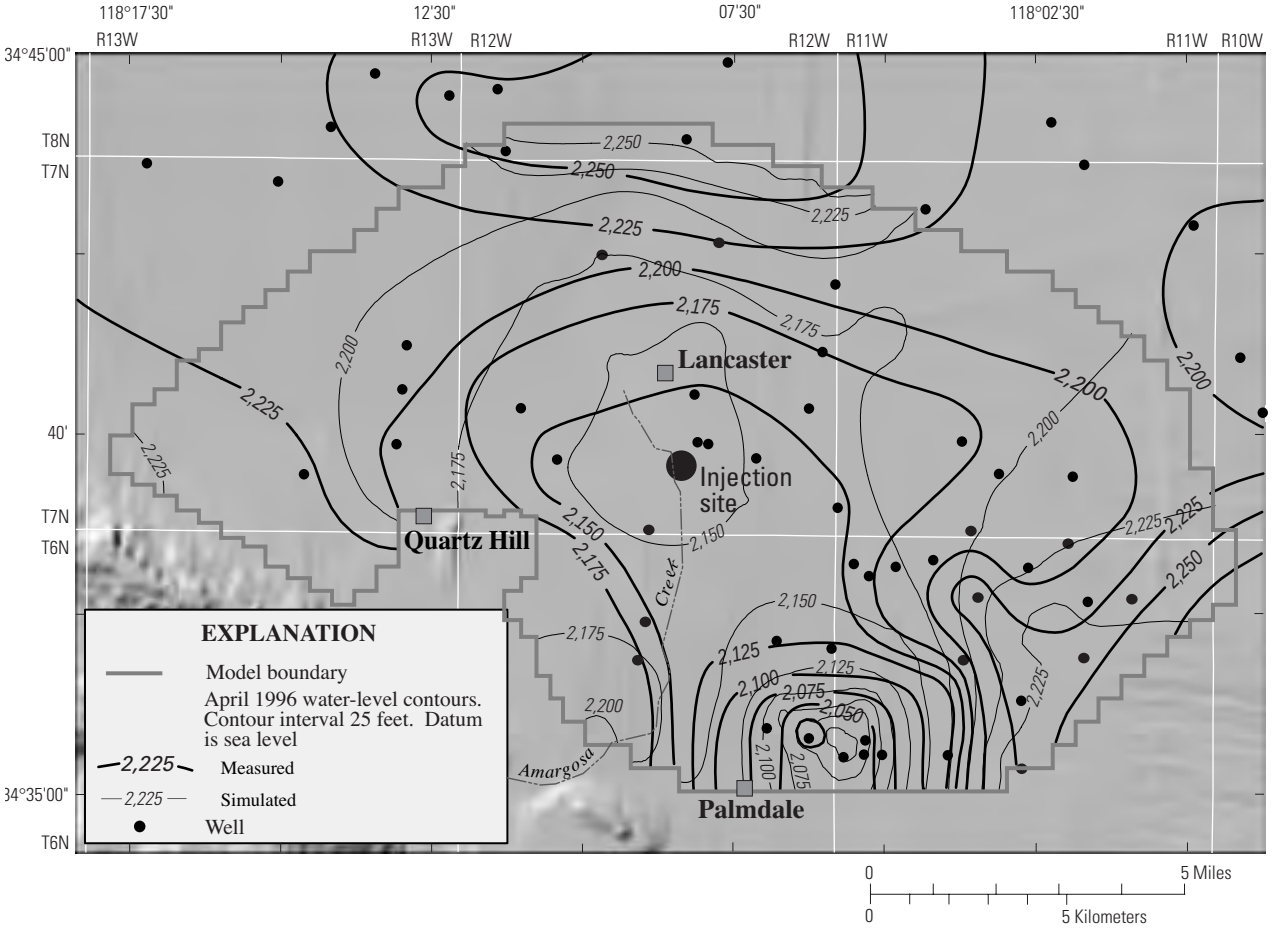

Figure 47. Contour map based on measured water levels and those simulated using the calibrated LAN model, Lancaster, Antelope Valley, California.

more rapid than measured; thus, the ground-water mound in the AV model was much farther north and smaller in magnitude than it should have been by 1983. Similarly, specified recharge from Amargosa Creek was much greater in the LAN model than in the AV model, but heads in this area were simulated too low in the AV model.

There are significant differences in the calibrated hydraulic conductivities of the two models, but the total transmissivities are comparable. The hydraulic conductivity for the upper aquifer generally is greater in the LAN model than in the AV model and that for the middle aquifer is lower (fig. 39). In the vicinity of the injection site, K_1 and K_2 are 17 and 1.7 ft/d, respectively, in the LAN model; K_1 ranges from 10 to 24 ft/d and K_2 is 10 ft/d in the AV model. K_1 in the LAN model is within the range of values used in the vicinity of the injection site in the AV model, and the sum of K_1 and K_2 (proportional to the transmissivity, as thicknesses are similar) for the LAN model (18.7 ft/d) is near the low end of that for the AV model (20 ft/d). Vertical hydraulic conductivities near the injection site are 0.006 and about 0.10 ft/d in the LAN and AV models, respectively. The vertical hydraulic conductivity for the AV model was assumed, and was not adjusted from calibration of that model; however, the calibration was poorly constrained in the vertical dimension.

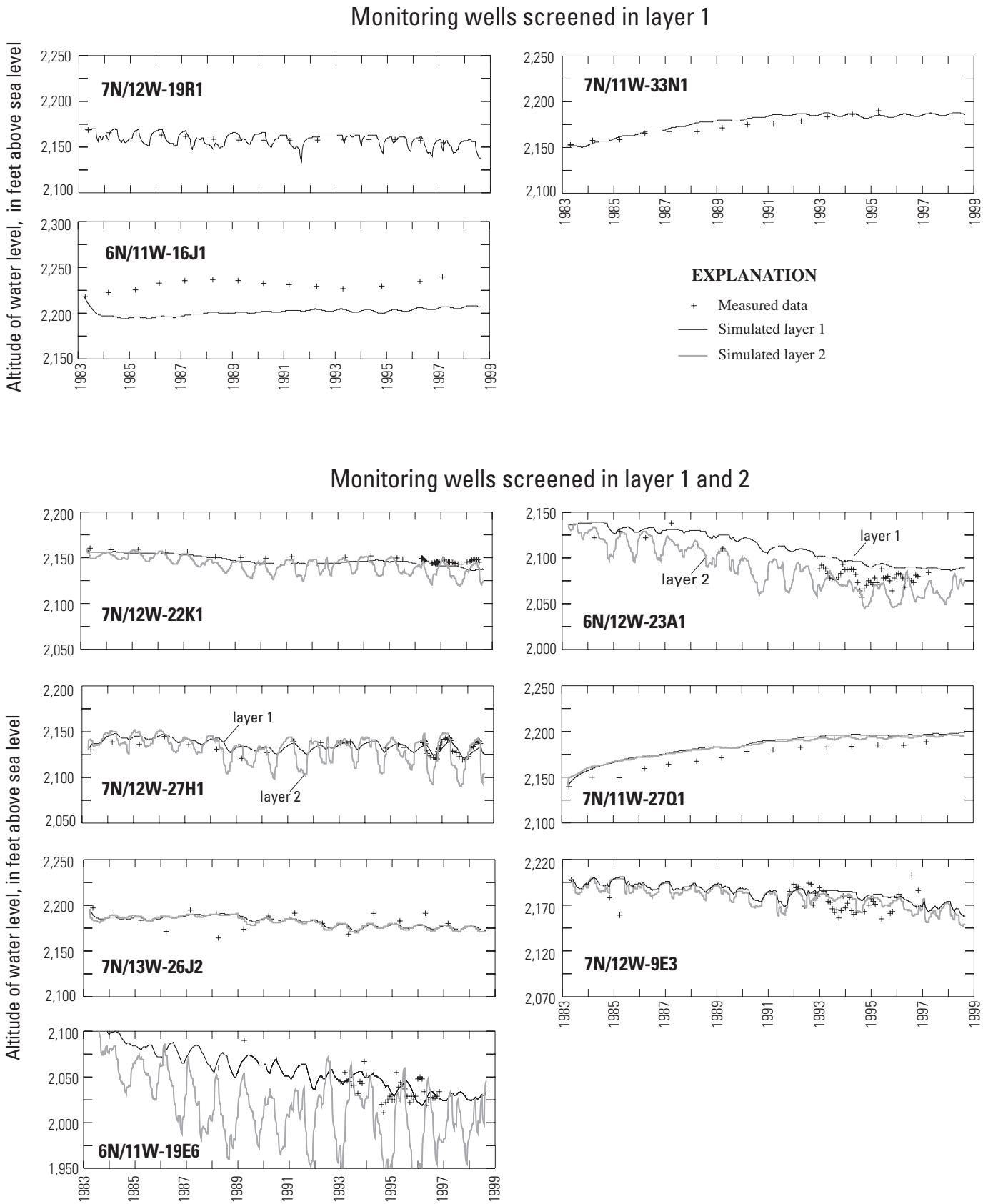

Figure 48. Hydrographs of wells with long-term records during the calibration period, Lancaster, Antelope Valley, California.

Simulated results from phase II calibration of the Lancaster-area (LAN) model are shown only for the model layers included in the screened interval of the well. Well locations shown in figure 43.

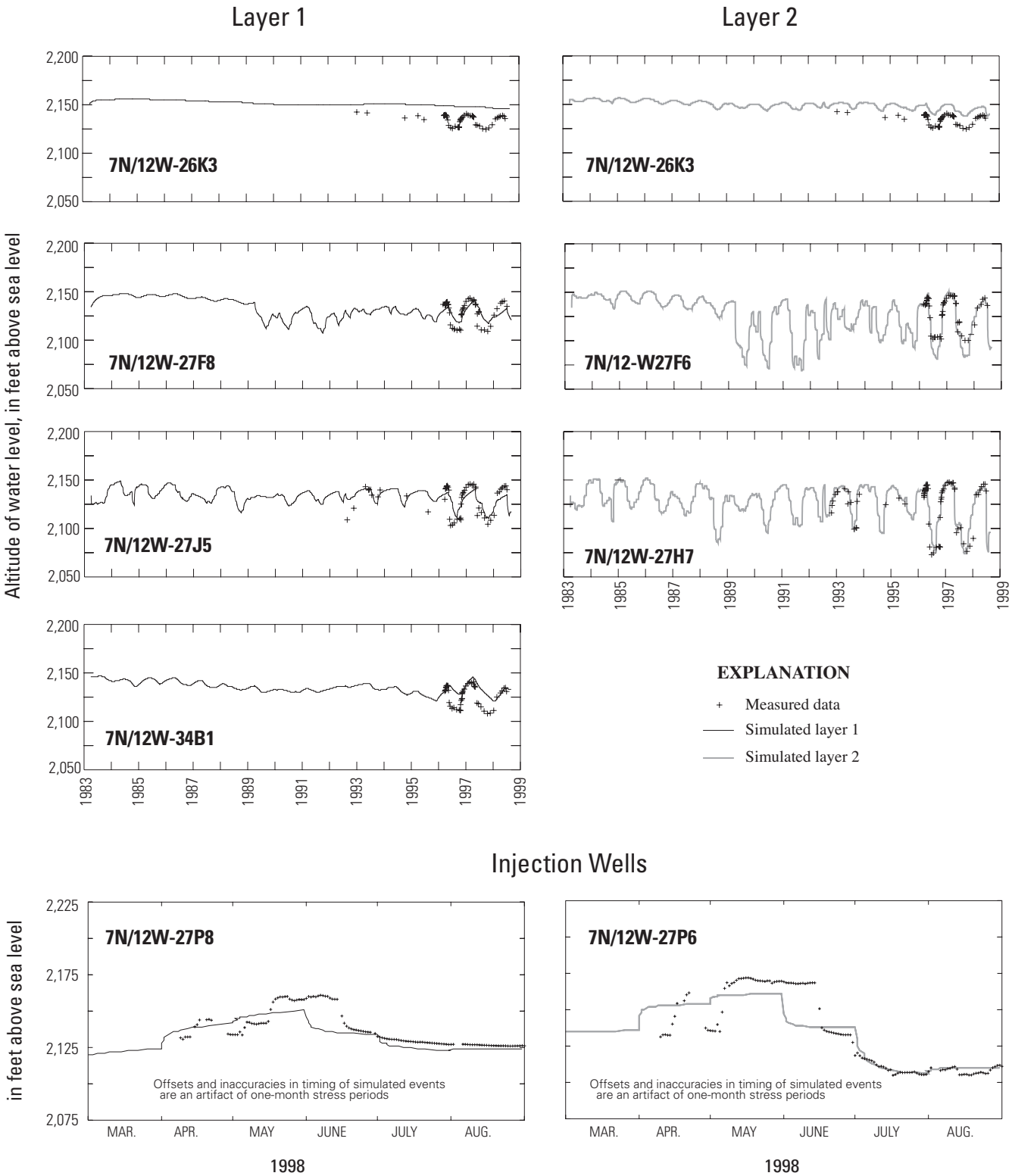

Figure 49. Hydrographs of wells and piezometers with dense data during injections tests, Lancaster, Antelope Valley, California.

Simulated results from phase II calibration are shown only for the model layers included in the screened interval of the well or piezometer. Well locations shown in figure 43.

The phase II calibration of the LAN model provided qualitative and quantitative improvements over the phase I calibration. The systematic parameter estimation procedure clarified the effects of not simulating aquifer-system compaction in subsiding areas; this procedure resulted in a more justifiable set of model parameters and, thus, in good model performance. The uniqueness of the parameter set was addressed, and the procedure developed aided in the remainder of the sensitivity analysis. Key findings are as follows:

- Simulation of inelastic storage, which was not simulated in the LAN model, likely would enable close simulation of measured head changes at both the injection and the extensometer sites; this was not feasible using justifiable changes of parameters in the current model.
- The sum of the estimated hydraulic conductivities of layers 1 and 2 of the LAN model, which are proportional to the transmissivities of those layers in the vicinity of the injection site, is about the same as the low end of the range for these in the AV model (20 ft/d).
- The hydraulic conductivity of layer 2 is about 10 percent of that for layer 1 in the vicinity of the injection site.
- The ratio of the hydraulic conductivity of layer 2 to the equivalent vertical hydraulic conductivity between layers 1 and 2 is about 270 in the vicinity of the injection site.

Sensitivity Analysis

A sensitivity analysis is a means for determining the sensitivity of model results to parameters in the model. The phase II calibration, for example, constituted a sensitivity analysis of the hydraulic conductivities specified in the model (K_1, K_2, and *KV*). Although other aspects of the ground-water system were represented in the model, not all were addressed or fully explored during calibration, including some of the boundary conditions, most system stresses (recharge and pumping), and storage values. The sensitivity of the model results to some of these aspects of the model was evaluated using plots of model error, like those in figure 44 (hereinafter referred to as sensitivity plots), generated using the same procedure developed for the phase II calibration, and hydrographs showing the effects of changes in the calibrated model. The sensitivity plots reflect relative head changes, whereas the hydrographs show error in absolute head; combined, they are effective tools for determining the effects of adjusting various model input. In addition, the sensitivity plots show quantitatively the effects of these adjustments on the preferred set of hydraulic conductivity parameters. For example, if reducing recharge in an area of the model causes substantial changes in head at the injection site, the zero-error lines on the sensitivity plots would shift, indicating a new set of parameters that would best fit the changed hydrologic regime.

Sensitivity is discussed in this report with respect to the central part of the model unless noted otherwise. Unreasonable changes in head in other areas generally are noted, but the focus of this analysis is on the area surrounding the injection site.

Hydrographs of the shallow and deep piezometers at the extensometer and injection sites and of well 7N/12W-27H1, which is within 0.5 mi of these sites and has the most complete long-term water-level record in the vicinity were used for the sensitivity analysis. The hydrographs were used to determine the effects of changes in the LAN model on simulated short- and long-term system behavior. Simulated hydrographs were interpolated from cell centers to measurement locations (Hanson and Leake, 1999). The sensitivity plots were based on the LAN model, modified as described on the plots.

For the no-flow boundary conditions, the lateral flowline boundaries were tested using the AV model, and the assumption of no flow through the lacustrine unit was tested during the calibration of the LAN model. Results from the AV model suggest that significant flow occurred through the eastern boundary of the LAN model during the calibration period and that this flow decreased significantly with time. This transient flow through the eastern boundary was accounted for in the LAN model by altering the specified flux (recharge) through the adjacent southeastern boundary.

The northern specified-head boundary, which represents the water-table mound between Lancaster and Rosamond, provided 22 percent of the average annual recharge to the model area. The simulated water levels near the injection site were relatively insensitive to this source of water. Conversion to a no-flow boundary caused large water-level declines (not shown) in the northern area of the LAN model, as expected, but much smaller declines near the injection site (fig. 50*A*). The sensitivity of the estimated hydraulic conductivities near the injection site to the specified-head boundary was varied. Conversion to a no-flow boundary resulted in an increase in the estimated value of K_2, by a factor of 1.2, but essentially no change in *KV*.

The southeastern specified-flux boundary, which represents subsurface interbasin flow from the Pearland and the Buttes subbasins, provided an average of 26 percent of the annual recharge to the LAN model area. The volume of flow crossing this boundary simulated by the AV model was 7,650 acre-ft/yr (Leighton and Phillips, 2003); this volume was reduced in the LAN model by an average of 1,636 acre-ft/yr (21 percent) to compensate for flow exiting the model area through the eastern boundary. To test the sensitivity of the LAN model results to these recharge estimates, the flux through the southeastern boundary was reduced and increased annually by an average of about 40 and 85 percent, respectively. Although the simulated water levels near the southeastern boundary were sensitive to these changes (for example, increased 20 to 60 ft with increased recharge), the hydrographs fig. 50*B*) show that the simulated water levels near the injection site were essentially unaffected. The sensitivity plot shows very little change in the estimated hydraulic conductivities from those in the LAN model. Because the sources of recharge from treated wastewater and from agriculture generally are close to the southeastern boundary and because the average volumes of recharge from these sources are smaller than those from the southeastern specified-flux boundary, it was assumed that the sensitivity to these sources of recharge is similar to that for the southeastern flux.

The intermittent-stream recharge specified west of Quartz Hill is relatively small and remote from the Lancaster area; recharge from this source was not considered important with respect to model sensitivity. Amargosa Creek, however, is a significant source of recharge and is relatively close to Lancaster (fig. 40). The calibrated recharge from Amargosa Creek (2,835 acre-ft/yr) was reduced and increased by about 50 and 100 percent, respectively, which resulted in small, but noticeable changes in the model results (fig. 50*C*). The long-term hydrograph responded to these changes, but the difference in water levels simulated by the calibrated LAN model was less than about 6 ft during the 15-year period. The hydrographs of the piezometers show similar variability. The sensitivity plot also responded, indicating that minor adjustments in the parameter values would be required to match the measured water levels if large adjustments were made to simulated recharge from Amargosa Creek (fig. 50*C*). Note that such changes in recharge would alter the water-level altitude and hydraulic gradient in the vicinity of wells 6N/12W-16A2 and 9H3. As discussed in the phase I Calibration section, hydraulic conditions at these wells were very sensitive to recharge from Amargosa Creek.

The sensitivity of the model results to errors in ground-water pumpage was not tested. Urban ground-water pumpage was metered, and therefore any errors were assumed to be small. Agricultural pumpage, though not metered, was estimated from crop demand (Leighton and Phillips, 2003) and is remote from the area of interest.

The storage properties of the aquifer system (S_y and the elastic component of S_s) were varied during the phase I calibration of the model, but were assumed for the calibrated LAN model to be constant in the model area as had been assumed for the AV model (Leighton and Phillips, 2003). Results of the phase I calibration indicate that simulated hydraulic head throughout most of the model is insensitive to reasonable changes in the elastic component of S_s, but that simulated heads in the middle aquifer were very sensitive to S_s in areas where inelastic compaction occurred. Inelastic compaction was not accounted for in the LAN model, but is a source of water in the real system. Storage in the upper aquifer was large (0.13) relative to inelastic S_s (about 4.0×10^{-5}/ft); thus, the sensitivity of simulated hydraulic head to inelastic compaction in layer 1 would be very low. Elastic S_s in the middle aquifer (1.2×10^{-6}/ft), however, was more than 30 times smaller than the inelastic S_s, which may have resulted in a significant overestimation of drawdown for areas where inelastic compaction occurred. The oversimulation of drawdown in layer 2 at the extensometer site may be accounted for by inelastic aquifer-system compaction. A quantitative sensitivity analysis of the effects of inelastic compaction on the total S_s is not straightforward because the S_s is head-dependent (different above and below the pre-consolidation head) and, therefore, an analysis was not done.

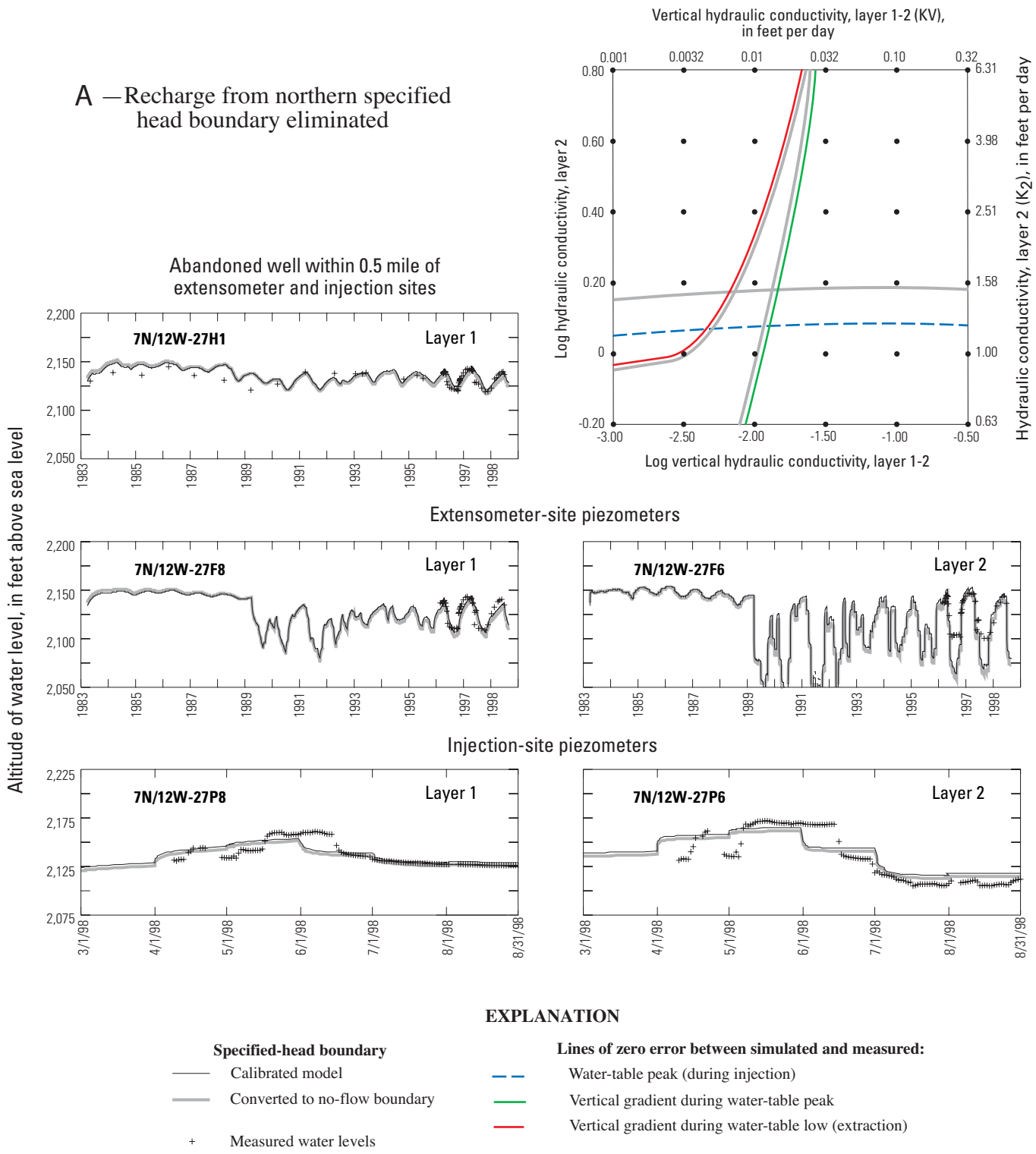

Figure 50. Sensitivity of calibrated hydraulic conductivities and simulated water levels near the injection site to changes in model variables, Lancaster, Antelope Valley, California.

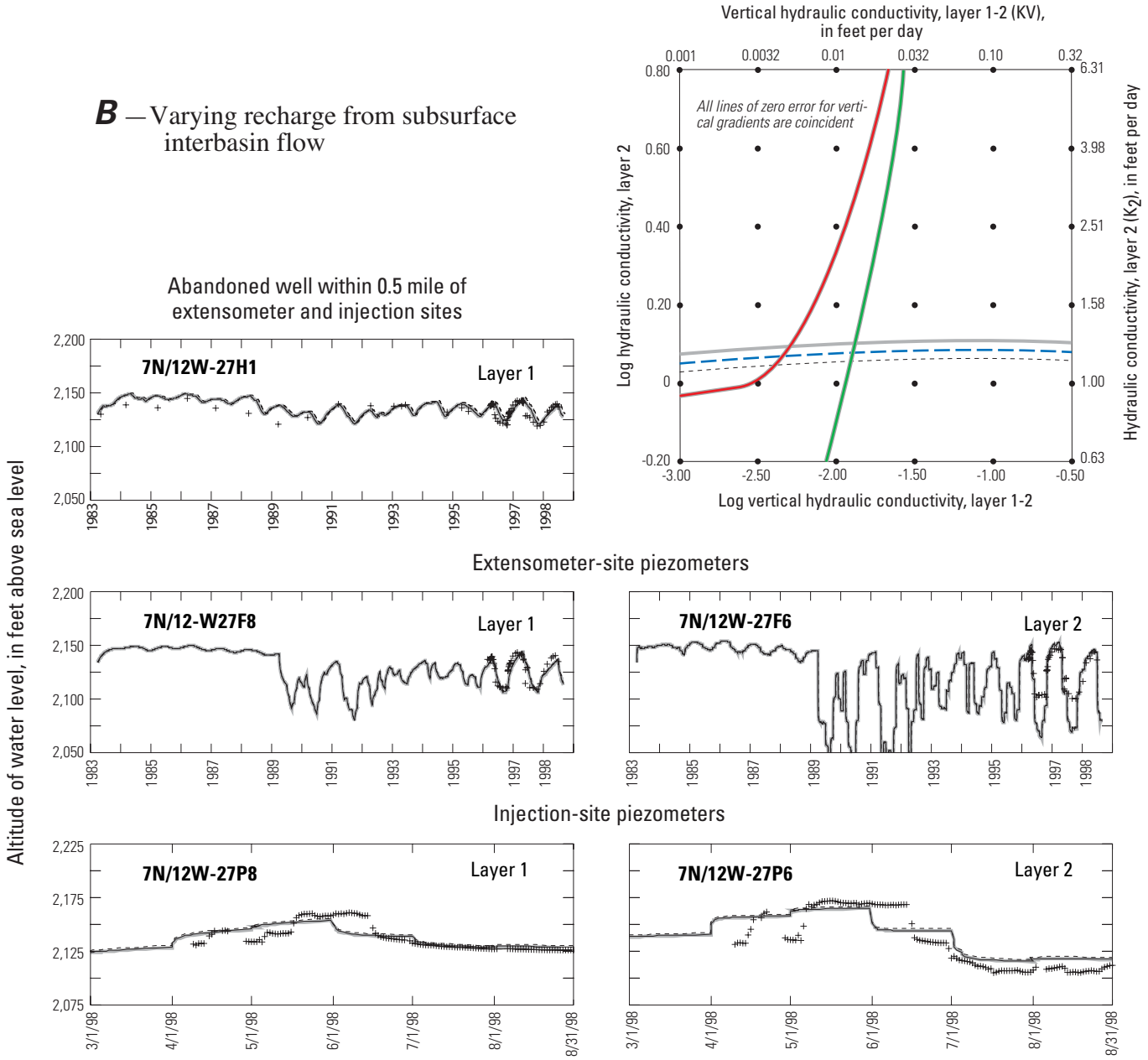

EXPLANATION

Recharge from subsurface interbasin flow along southeastern boundary

- Calibrated model
- Reduced by 37.9–42.4 percent per year
- Increased by 75.9–93.6 percent per year

Lines of zero error between simulated and measured:

- Water-table peak (during injection)
- Vertical gradient during water-table peak
- Vertical gradient during water-table low (extraction)

+ Measured water levels

Figure 50.—*Continued.*

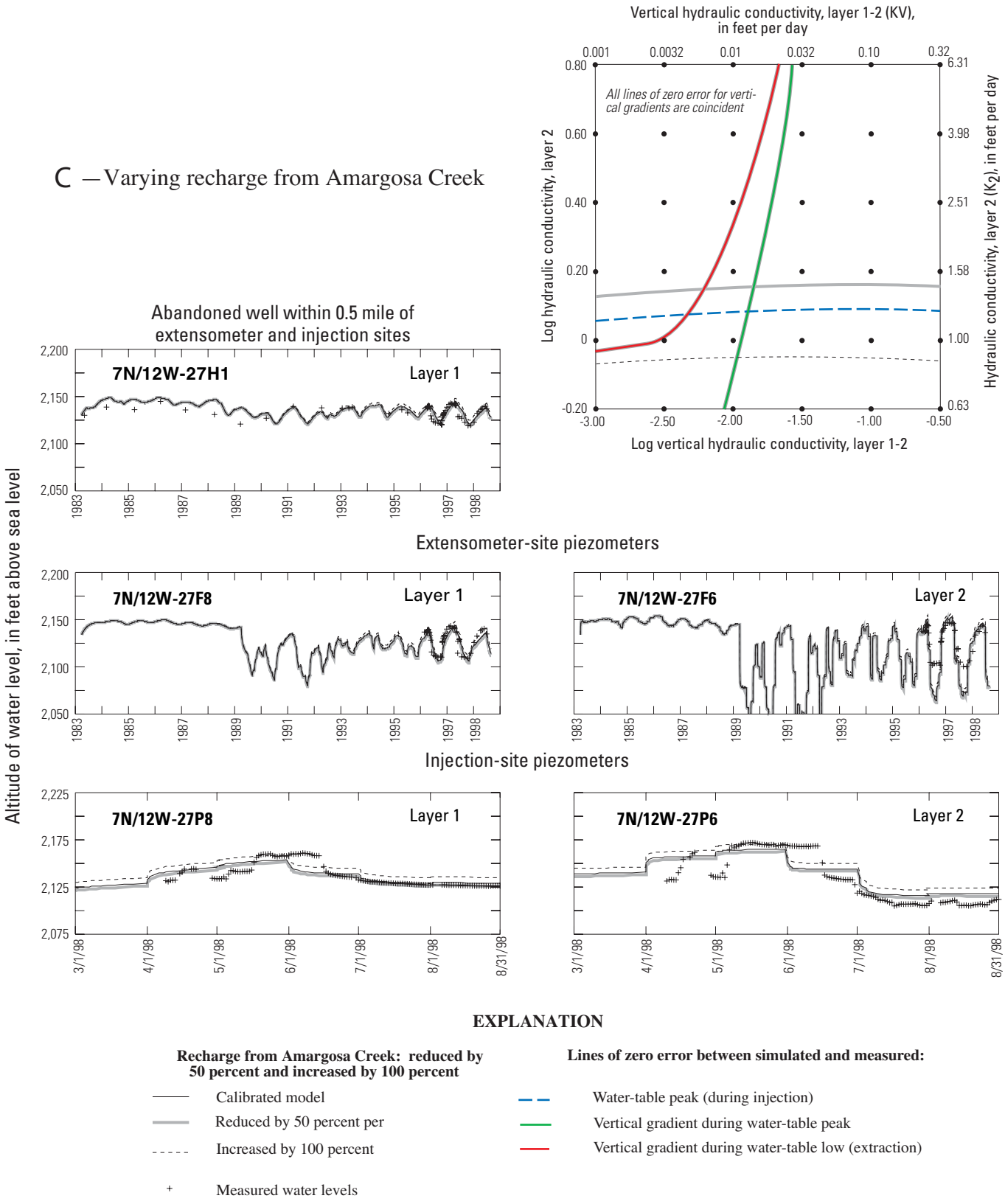

Figure 50.—*Continued*.

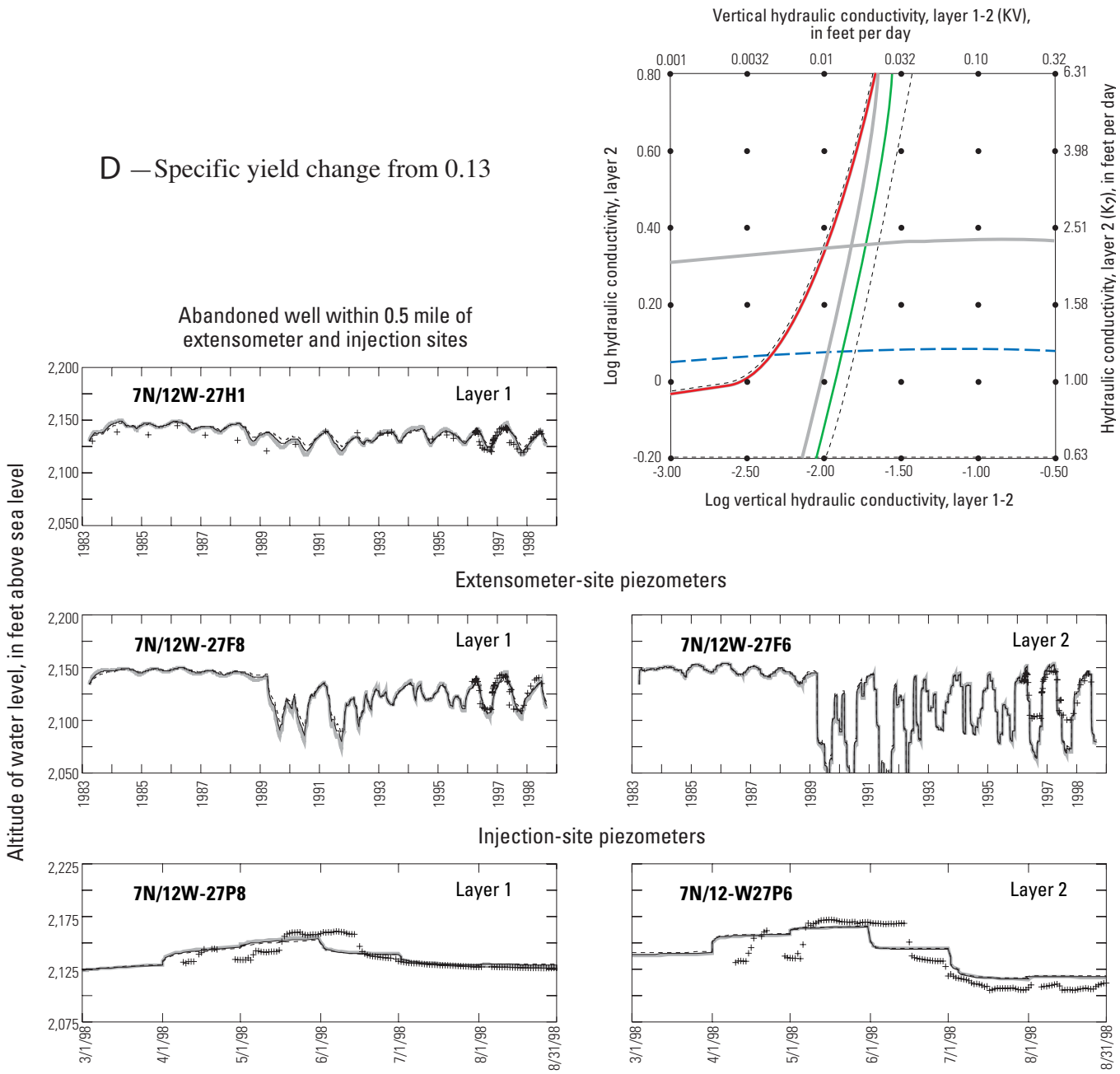

EXPLANATION

Specific yield change from 0.13:

- Calibrated model (0.13)
- Decreased to 0.09
- Increased to 0.19
- \+ Measured water levels

Lines of zero error between simulated and measured:

- Water-table peak (during injection)
- Vertical gradient during water-table peak
- Vertical gradient during water-table low (extraction)

Figure 50.—*Continued.*

The model results were sensitive to changes in S_y. The effects of changing S_y from 0.13 to 0.09 and 0.19 are shown on the hydrographs and sensitivity plot, respectively (fig. 50*D*). The long-term hydrograph was not affected because long-term water-level changes were small; however, the amplitude of simulated water levels was sensitive to the S_y, particularly in layer 1. The sensitivity plot shows that the estimated hydraulic conductivities were relatively sensitive to S_y; for example, the reduction of S_y resulted in larger estimates of K_2 and *KV* by factors of about 1.9 and 1.4, respectively. The value of S_y determined from coupled gravity and water-level measurements (0.13) provided reasonable results and was well-bracketed by the sensitivity analysis.

Model results and parameter estimates clearly are variably sensitive to changes in storage properties and various sources of recharge; however, there are consistent patterns in the responses to these changes. Decreases in recharge or S_y resulted in lower simulated water levels and greater seasonal water-level change. The sensitivity plots indicate that the calibrated K_2 and *KV* values would have to be increased to compensate for these effects. Although the decreases in recharge or S_y would allow better simultaneous simulation of vertical gradients during peak and low water-level conditions, there are negative consequences with respect to long-term trends and (or) the magnitude of seasonal changes. This is also true for increases in recharge or S_y, but in the opposite sense. Model results and parameters estimates for the central part of the model were most sensitive to changes in local storage properties and local recharge and essentially were insensitive to changes in remote sources of recharge.

Appropriate Use and Improvement of the Ground-Water-Flow Model

The ground-water-flow model of the Lancaster area (the LAN model) was designed for estimating aquifer-system properties in the vicinity of the injection site and as the basis for a simulation/optimization model for planning and managing a larger scale injection program. Limitations of numerical models, assumptions made during model development, and results of model calibration and sensitivity analysis are factors that constrain the appropriate use of the model and highlight potential improvements.

Limitations of Numerical Models

Results from this model should be interpreted generally in time and space, and are best suited for comparative analysis rather than for prediction of absolute changes. A numerical model is a means for portraying and testing one's conceptual view of a system. Because ground-water flow systems are inherently complex, simplifying assumptions are made during the development and application of such model codes (Wang and Anderson, 1982; McDonald and Harbaugh, 1988; Anderson and Woessner, 1992). Models solve for average conditions within each model cell for which the parameters are interpolated or extrapolated from measured values and (or) values estimated during calibration. In light of this, the intent in developing this ground-water flow model was not to reproduce the natural system exactly, but rather to portray its general characteristics.

The accuracy of model results for time and space is strongly related to the availability and accuracy of temporal and spatial input data and calibration criteria (for example, ground-water levels) for comparison with simulation results during model calibration. The central part of the LAN model area was the only part for which multi-depth time-series data were available for model calibration and had excellent records of ground-water extraction and injection. The south-central Lancaster area also is relatively isolated from known sources of recharge. A user should have relatively high confidence in model results for the central part of the model area, but less confidence in the results for other areas of the model.

Other Factors that Constrain Appropriate Use of the Model

The vertical distribution of pumpage between model layers was assumed to be the same for extraction and injection because accounting for temporal changes in the distribution would require prior knowledge of future head responses. If all aquifer materials adjacent to the well screen are saturated during extraction, this is a reasonable assumption; however, any change in the length of saturated well screen constitutes a change in the relative equivalent transmissivities. This limitation, which was previously discussed with respect to anomalous head responses, needs to be recognized because it may affect the ability of the model to accurately simulate head responses to both injection and extraction at some sites.

The areal distribution of aquifer-system storage was assumed constant for both confined and unconfined conditions. Geodetic data, however, showed spatial variability in both elastic and inelastic deformation, which is associated with variability in skeletal storage properties. Simulation of the confined middle aquifer may be affected significantly by this limitation, which would be manifested as excess drawdown, particularly within areas susceptible to subsidence. Simulation of the unconfined part of the system would not be affected significantly if aquifer-system compaction is accounted for because the specific yield is much greater than the inelastic skeletal storage, but it may be affected somewhat by changes in the simulated vertical gradient between layers. Model results for the upper aquifer are relatively sensitive to changes in the specific yield. Significant changes in specific yield in a given area of the model may require re-evaluation of hydraulic conductivities in that area.

The northern specified-head boundary provides significant recharge to the model area. This recharge was required to reasonably match measured water levels in the northernmost wells, which are very sensitive to this boundary condition. Because there are limited potential sources of recharge in that area of the valley, it was assumed that the source of this recharge probably is due to a change in storage owing to the slow growth of a cone of depression at Lancaster and to the associated northward retreat of the ground-water divide. Because this process cannot be simulated explicitly at the subregional scale, a user needs to consider the long-term effects of this boundary condition, to monitor water levels in that area, and to adjust the boundary condition accordingly.

It was assumed that no flow occurred between the middle and lower aquifers across the lacustrine unit. Where measured, vertical gradients were upward when the wells were inactive, which indicates that the lower aquifer is a source of water—particularly where wells screened in both aquifers can act as free-flowing conduits. Results of the phase I calibration indicate that the simulated heads are relatively sensitive to this source of water. Volumetrically, the lower aquifer likely is a relatively small component of total recharge because the vertical gradients are small and there is a strong contrast in water chemistry across the lacustrine unit; however, it may have local effects, particularly in the middle aquifer.

Potential Improvements

Limitations of the current flow model can be addressed by technical improvements in model capabilities and by new and continued monitoring activities coupled with data analysis. Potential technical improvements include simulation of aquifer-system compaction, simulation of the lower aquifer, and better accounting for variability in the vertical distribution of stresses. Subsidence could be simulated in future models if water supplies become too limited to halt water-level declines. Use of the IBS1 package (Leake and Prudic, 1991) allows simultaneous simulation of ground-water flow and vertical aquifer-system compaction in MODFLOW. Key inputs to this package, including elastic and inelastic storage values, and information for estimating the areal distribution of these values are included in this report. Although current versions of the optimization tools used for this study cannot make direct use of IBS1 output, the head response in the middle aquifer within the subsidence area may be improved substantially.

Flow between the middle and lower aquifers across the lacustrine unit is poorly understood; however, it may have important local effects, as discussed previously. Simulation of the lower aquifer using the LAN model is presently not a viable option, but it may be in the future if new data allow reasonable definition of the boundary conditions in that aquifer.

For wells screened in both the upper and middle aquifers, as are most of the wells, the variability in the vertical distribution of extraction and injection generally is governed by changes in the water level in the well. If the water level in the well is within the screened interval, any change in the water level is a change in the effective transmissivity of that portion of the well within the upper aquifer. During extraction, the water level declines, as does the effective transmissivity of the upper aquifer; the opposite occurs during injection. The effective transmissivity of the middle aquifer is constant and, therefore, the vertical distribution of the extracted or injected water is subject to change. Ideally, the changing distribution would be accounted for within the flow model for each time step. This capability recently was developed for MODFLOW (Halford and Hanson, 2002).

Monitoring activities can help address several of the uncertainties in the current model. Standard monitoring at each potential injection site would likely include continuous measurement of water levels in nested piezometers; continuous and (or) periodic measurement of land-surface deformation; continuous recording of injection and extraction rates; and periodic chemical analyses. A monitoring program also would include areas distant from the injection sites, but within their zone of influence. This information is essential for documenting the effects of an injection program, but also is needed for calibration of the flow model in these areas.

Water-level and stress histories are vital for improved estimation of the hydraulic properties of the aquifer system in the vicinity of each injection site. Measurement of land-surface deformation in the subsidence-prone areas is equally vital for determination of storage properties required for simulation of land subsidence and the associated effects on water levels. These measurements would also serve to extend the calibration period, providing a more challenging history to match while further minimizing any long-term error associated with mis-specification of initial conditions.

The sensitivity analysis showed that the model results were most sensitive to changes in nearby sources of recharge (Amargosa Creek and the northern boundary condition) and the specific yield. Gaging Amargosa Creek, which is currently ungaged, would provide information necessary for improving estimates of recharge from that stream. A series of two or more gages and monitoring of inflows and diversions between the gages may be an effective way to measure recharge from this source. Monitoring the water table in the vicinity of the northern boundary would allow adjustment of the specified heads as needed to reflect long-term decreases in the southward hydraulic gradient.

Specific yield is relatively difficult to determine, but can be estimated using microgravity, simulation, or aquifer-test methods. Each of these techniques requires periodic to continuous measurement of water-table change. Coupled, precise measurements of water levels and gravity can be used to generate relatively accurate estimates of specific yield, particularly where the water-level change is large. Simulation of water-table changes during extraction and (or) injection can be used to estimate specific yield; however, simulation results depend on multiple variables. The likely outcome from simulation methods is a range of values of specific yield associated with ranges of other variables. The same holds for aquifer-test methods.

DEVELOPMENT OF A SIMULATION/OPTIMIZATION MODEL

A simulation/optimization model (LANOPT) was developed as an adaptable tool for use in planning and managing a larger scale injection program. The simulation model (LAN) was modified and incorporated into a linear-programming problem to determine optimal means for managing an injection program given an objective and a set of constraints. Thus, the LANOPT model considers simultaneously the physics of the aquifer system (built into the simulation model) and any physical or institutional considerations (in the form of constraints) in determining the optimal way to meet an objective.

The primary objective of the injection program for the Lancaster area is to halt the long-term decline of ground-water levels and associated land subsidence while meeting growing water demand. Overdraft of local ground-water resources has caused water-level declines, land subsidence, diminished well capacities, and increased dependence on deeper, lower quality ground water. A primary constraint of the program is that LACDPW must continue to meet water demand using existing and new wells and pipelines (as provided for in their 5-year development plan) and imported water of unknown reliability and for which cost and availability are affected seasonally. Additional constraints include maintaining minimum heads to avoid subsidence, staying 100 ft below land surface to avoid high water-table conditions, and using a set of specifications that constrain well performance and the vertical distribution of pumpage/injection.

Model Objective

The long-term decline of ground-water levels is the key issue to be addressed. The objective that was used to address this was to maximize the lowest value of head. This objective has associated head constraints, and the objective function has the form:

$$\max(\min h)$$

subject to

$$h - h_{it} \leq 0 \qquad (7)$$

where

h is the minimum head and

h_{it} is the head in the cell containing well i (i = 1, number of wells) during stress period t (t = 1, number of stress periods).

Given this objective function, the LANOPT model would seek to increase the head value at the location (within a set of specified locations) with the lowest head in each stress period by varying injection and extraction rates (the decision variables) in specified wells. The location with the lowest head value may change during a simulation; the optimization seeks equal heads at all specified locations, which is not always possible.

This solution, however, may not always result in a desirable outcome. If, for example, heads were relatively high in a subsidence-prone area, the optimal solution may result in significant drawdown in that area as heads in other areas recover to the same level; thus, land subsidence may be a negative consequence of this model objective. In this study, the measured heads, and presumably the preconsolidation heads, in the subsidence-prone areas are indeed higher than or equal to those in other areas; therefore, constraints on the minimum head in the subsidence area were added to the model to ensure that the optimal solution did not result in subsidence.

Another way to state the model objective, in this circumstance, is "to minimize the loss of well capacity." The target of the optimization is always the area with the lowest water table, which is also the area where water-table altitudes and associated extraction capability of wells are decreasing.

Constraints on Water Supply and Demand

Several physical, institutional, and economic factors limit the acquisition of imported water and the supply of ground water. Some of these factors are included in the LANOPT model in the form of constraints. Future water demand, which drives the need for supplies, is also included as a constraint.

Imported Water-Supply Constraint

Availability and cost of imported water are controlled largely by climatic conditions and competing demands for water from the SWP. During seasonal low-demand periods (generally late autumn to early spring) in nondrought years, AVEK often purchases SWP water at reduced rates and sells the treated water at a discount which is ideal timing for the LACDPW with respect to artificial recharge because their demand also is low during that period (fig. 41*C*). Because of the low water demand, including that for ground water, existing production wells can be used for injection.

AVEK's historical purchases from the SWP are far below their entitlement of 138,400 acre-ft/yr (fig. 51). The future capability of the SWP to deliver full entitlements, however, is unknown. Currently, the SWP does not have the facilities to deliver full entitlements, and the reliability of the SWP annual deliveries historically has been affected by drought conditions (see 1991 deliveries, fig. 51). Recent environmental legislation has designated more SWP water for protection of wildlife, and talks continue at the Federal, State, and local levels regarding future allocations of SWP water in California.

Effects of future decisions on AVEK's ability to obtain additional SWP water are difficult to predict. For planning purposes, AVEK estimates that their long-term average potential yield from the SWP will be 91,400 acre-ft/yr (Russell Fuller, General Manager, Antelope Valley–East Kern Water Agency, oral commun., 2000). Assuming that the growth in deliveries from 1989 to 1999 will continue for another 10 years, deliveries would reach about 97,000 acre-ft/yr by 2009, which slightly exceeds the projected yield. For the purpose of this study, however, it is assumed that AVEK will be able to deliver the additional water needed for injection during the 10-year planning horizon. The primary reason for this assumption is that injection water would be purchased

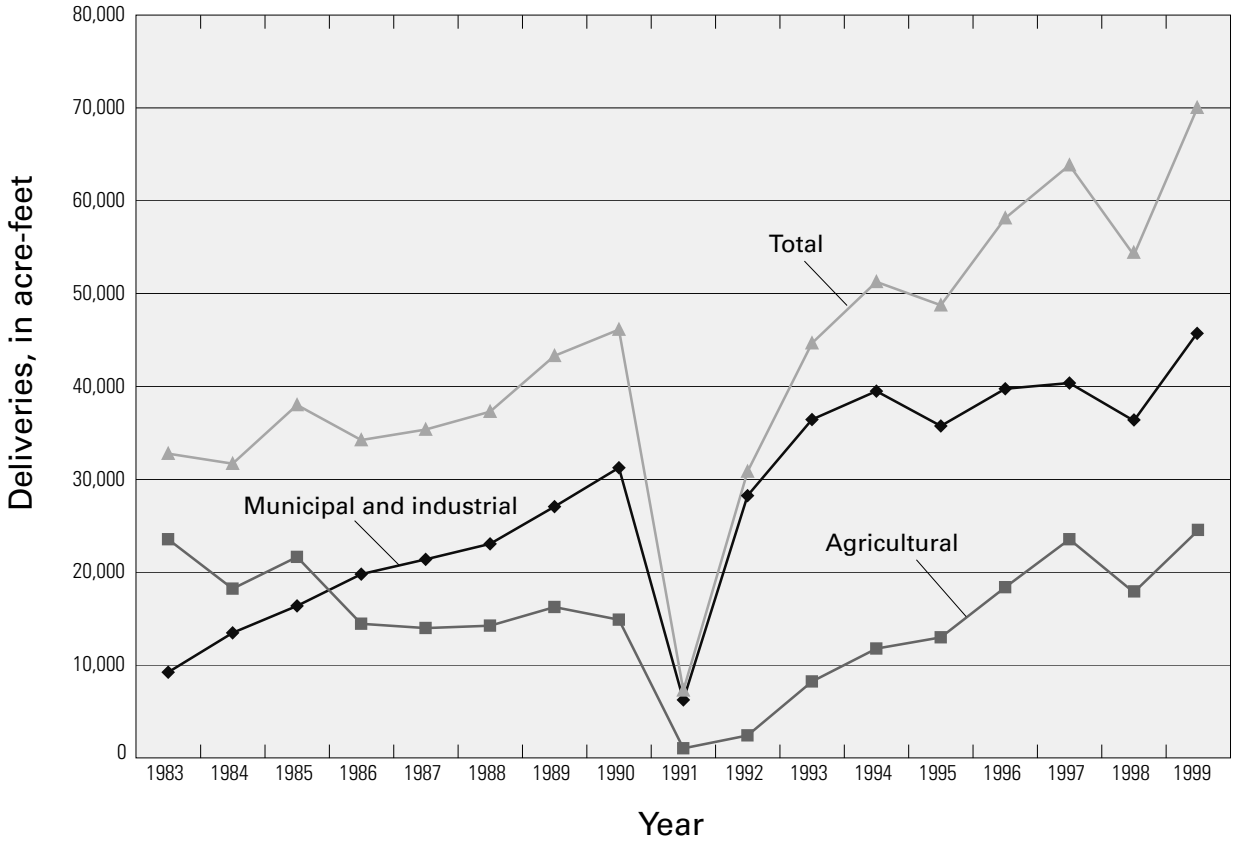

Figure 51. Historical deliveries of State Water Project water by the Antelope Valley–East Kern Water Agency (AVEK), Lancaster, Antelope Valley, California.

(Russell Fuller, General Manager, Antelope Valley–East Kern Water Agency, written commun., 2000)

from AVEK from late autumn through early spring when competition and prices for SWP water are lowest. Accordingly, injection was constrained to occur only during the late autumn/early spring period (stress periods 1, 5–7, 11–13, and so forth):

$$Q_{\text{inj}}^{t} = 0 \qquad (8)$$

where

Q^{t}_{inj} is the water injected during high-demand stress period t.

Ground-Water-Supply Constraints

The ground-water-supply constraints define physical limits on the way water is pumped from and injected into wells. These constraints were based on the extraction capacities and vertical distribution of pumpage from each well selected as a potential injection well. Figure 52 shows the 16 existing and 13 proposed wells considered in the optimization, which are in the central, well-calibrated part of the LAN model. Only the LACDPW production wells that are, or will be, screened within the upper and middle aquifers (table 1) were considered for injection purposes because of the high arsenic concentrations and the low transmissivity and storativity in the lower aquifer. These conditions do not preclude the use of the lower aquifer for these purposes, but use of the lower aquifer for injection was not considered in this study.

All the selected injection/production wells are, or will be, connected to a network of pipelines that allow routing of AVEK water to the wells for injection and widespread distribution of pumped water to LACDWP customers. The locations of these wells were predetermined; well placement was not a goal in the optimization problem.

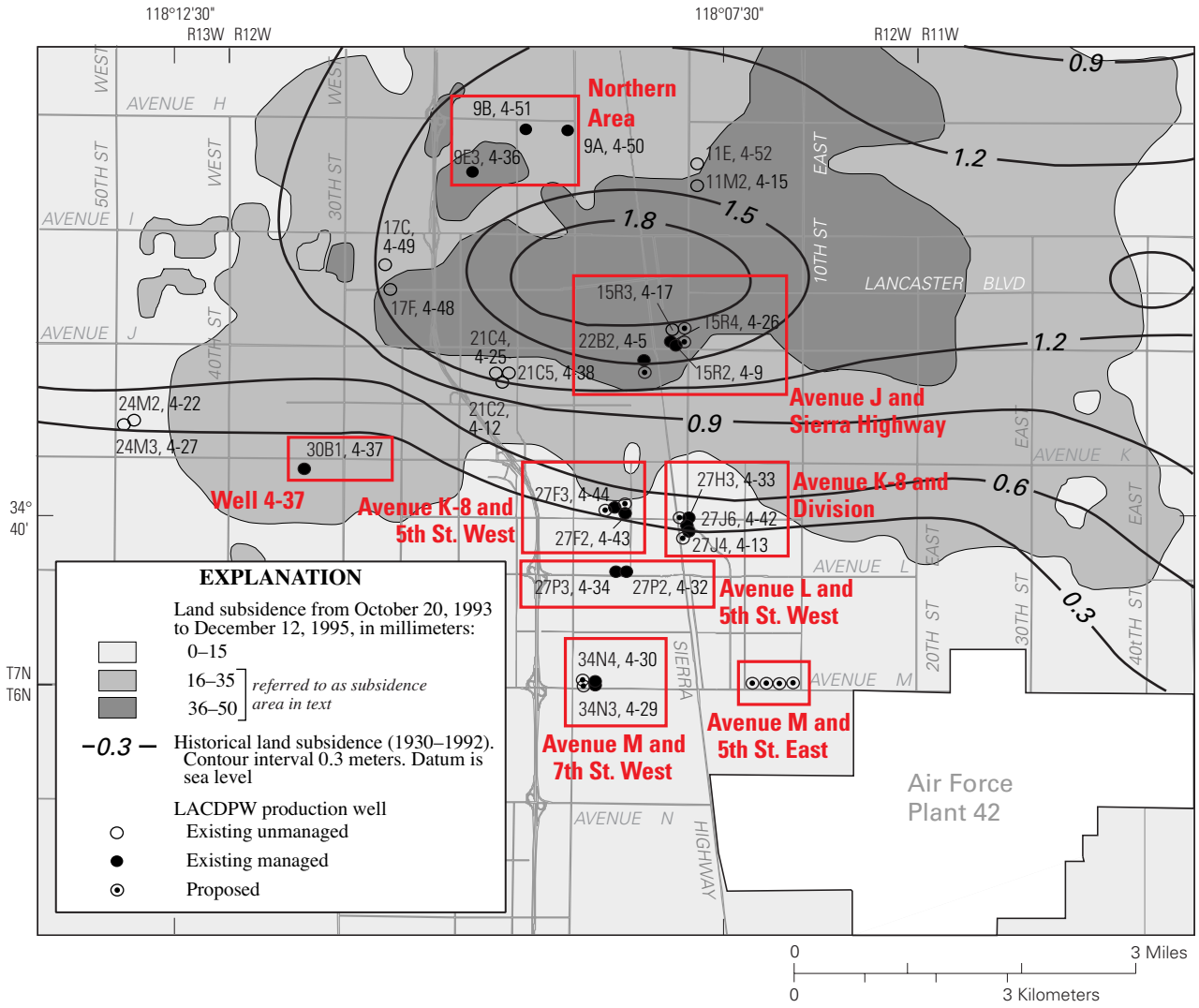

Figure 52. Historical and recent land subsidence, and locations of Los Angeles County Department of Public Works (LACDPW) wells, Lancaster, Antelope Valley, California.

Wells include existing and proposed wells with variable rates of injection and extraction in the simulation/optimization model (managed wells) and existing wells with fixed rates of extraction in the model (unmanaged wells).

Because of the proximity of some of the injection/extraction wells to one another and the size of the model cells, some groups of nearby LACDWP injection/production wells are represented in the LANOPT model collectively. Each well, or group of nearby wells, was simulated as four wells; different wells were used for injection and extraction, and for the upper and middle aquifers. For the purposes of this report, these injection/production wells will be considered single wells, except where discussion requires they be considered separately.

The maximum extraction capacity of each well (expressed herein as a volumetric rate) (table 3) was determined from a combination of existing capacity-test data, maximum measured monthly pumpage in 1997, and anecdotal information from LACDPW employees who maintain these wells. Because these wells may be used for long periods, their long-term capacities were assumed to be 80 percent of the maximum to allow for the effects of long-term drawdown and occasional maintenance.

Table 3. Estimated maximum and long-term capacities of existing and proposed potential injection/extraction wells in Lancaster, Antelope Valley, California

[See figure 52 for location of wells. Long-term estimates, which were 80 and 72 percent of maximum for extraction and injection, respectively, were used in the simulation/optimization model. Well site designations are used to simplify presentation and discussion of model results. gal/min, gallon per minute; na, not applicable]

State well No. (7N/12W-)	Local well name	Well site designation	Maximum capacity (gal/min)	Long-term extraction capacity (gal/min)	Long-term injection capacity (gal/min)
9A	4-50	Northern Area	1,300	1,040	940
9B	4-51	Northern Area	1,090	870	780
9E3	4-36	Northern Area	880	700	630
15R2	4-9				
15R4	4-26	Avenue J and Sierra Highway	1,770	1,420	1,270
22B2	4-5	Avenue J and Sierra Highway	1,040	830	750
27F2	4-43				
27F3	4-44	Avenue K-8 and 5th West	[1]1,750	[1]1,400	na
27H3	4-33				
27J4	4-13	Avenue K-8 and Division	1,090	870	780
27J6	4-42	Avenue K-8 and Division	[2]840	[2]670	na
27P2	4-32				
27P3	4-34	Avenue L and 5th West	1,820	1,460	1,310
30B1	4-37	Well 4-37	1,040	830	750
34N3	4-29				
34N4	4-30	Avenue M and 7th West	2,080	1,660	1,500
Two proposed wells	near 4-13 and 4-33	Avenue K-8 and Division	1,450	1,160	1,040
Two proposed wells	near 4-29 and 4-30	Avenue M and 7th West	2,080	1,660	1,500
Two proposed wells	near 4-43 and 4-44	Avenue K-8 and 5th West	1,820	1,460	1,310
Four proposed wells	(new site)	Avenue M and 5th East	4,160	3,330	3,000
Two proposed wells	near 4-9 and 4-26	Avenue J and Sierra Highway	2,080	1,660	1,500
One proposed well	near 4-5	Avenue J and Sierra Highway	1,040	830	750

[1]Portion of capacity within upper and middle aquifers; total maximum extraction capacity is 3,680 gal/min.
[2]Portion of capacity within upper and middle aquifers; total maximum extraction capacity is 1,040 gal/min.

Results of the pilot injection test in wells 7N/12W-27P2 and 27P3 showed that the injection capacity in these wells may equal, and probably exceed, the extraction capacity. However, this may not be the case for all the wells considered for injection in the LANOPT model, nor may it be representative of the long-term performance of the wells. In practice, maintenance generally is required more frequently during injection periods than during extraction periods, and injection rates are typically less than those for extraction (Pyne, 1995); therefore, the long-term injection capacities were reduced to 72 percent of the maximum extraction capacity (table 3).

For all the periods that injection was allowed, extraction also was allowed for the same wells, which was required at times to meet water demand. The total well capacity for each stress period is calculated as a weighted sum of the injection and extraction during that period in which the weights are related to the respective capacities. Thus, the constrained flow in a well can range from the long-term injection capacity (72 percent of the maximum extraction capacity) to the long-term extraction capacity (table 3). If both injection and extraction occur, the constraint will limit flow in the well to some value between these limits:

$$c Q^t_{inj_i} - Q^t_{ext_i} \leq C_i \qquad (9)$$

where

c is the ratio of extraction capacity to injection capacity,

$Q^t_{inj_i}$ is the injection (positive) in well i during stress period t,

$Q^t_{ext_i}$ is the extraction (negative) from well i during stress period t, and

C_i is the extraction capacity of well i.

Just as the extraction capacity limits ground-water supply, the hydraulic properties of the aquifer system and screened intervals of wells control the relative amount of water that can be withdrawn from or injected into different depths within the aquifer system. The distribution of stress among the aquifers in the LANOPT model was constrained by the relative effective transmissivity within each aquifer:

$$-Q_{i_1} + cQ_{i_2} = 0 \qquad (10)$$

where

Q_{i_1} is the flux in well i, model layer 1,

Q_{i_2} is the flux in well i, model layer 2, and

c is the ratio of effective transmissivity of layer 1 to effective transmissivity of layer 2.

This effective transmissivity was calculated for the flow model on the basis of hydraulic conductivity and length of screened interval in each aquifer and was assumed to be constant with time.

Ground-Water Demand Constraint

Future demand for ground water is difficult to predict because it is dependent on many variables. These variables include the future availability of SWP water and ground water, for which there are many competing interests; the financial costs of these and other sources of water; potential effects of future local ground-water-management legislation or adjudications; the potential effects of water-conservation efforts or development of new water sources; and potential growth in water demand. It was assumed for this study that growth in residential demand will be the dominant factor on ground-water demand within the model area and that this demand will be met by some combination of native ground water and injected water.

Several estimates of future population growth have been made for Lancaster, Palmdale, and other parts of Antelope Valley. In 1993, the Southern California Association of Governments (SCAG) projected a population growth of 56.5 percent for Lancaster for 1990 to 2000 (Templin and others, 1995). This agrees well with the growth of 57 percent calculated using data from the California Department of Finance (1999) for the same period, extrapolating to the year 2000 from the 1989 to 1999 trend (fig. 2). In 1994, the Los Angeles County Department of Regional Planning estimated a population growth of about 68 percent from 1990 to 2000 in District 4, the LACDPW district that serves Lancaster (Los Angeles County Department of Power and Water, written commun., 1999). Owing to the close agreement between the SCAG estimates and data from the California Department of Finance (1999), their estimates for the 2000–2010 population growth in Lancaster (essentially the same increase as 1990–2000) were used for the 10-year projections. The equivalent population growth for this period was about 37 percent, or an annual rate of about 3.2 percent.

The city of Palmdale experienced a much more rapid rate of growth from 1990 to 2000: 118 percent, calculated using data from the California Department of Finance (1999). SCAG and the California Department of Finance project a 2000–2010 population growth in Palmdale of over 50 percent. However, the LAN model indicated that at the constant (no growth) 1995 rate of extraction, the simulated water table in Palmdale declined into the middle aquifer within this 10-year period. It was assumed for this study that such a condition would not be reached because alternative sources of water would be used and (or) pumping would be redistributed to keep the water table within the upper aquifer thereby maintaining reasonable extraction capacities. Through trial and error, the pumpage for Palmdale was reduced in the model by an annual rate of 0.5 percent, which kept the water table within the upper aquifer. This reduction in pumping acted as a surrogate for combinations of future conservation, alternative water sources, and redistribution of pumping in the Palmdale area.

The population growth rate for areas outside the cities of Lancaster and Palmdale was assumed to be the same rate as that for Lancaster. The increase in urban water demand for this rate of population growth was applied to all non-agricultural wells in these areas except those at Air Force Plant 42 where no growth was assumed. Agricultural demand was assumed to be steady at the 1995 level. There is evidence of increased agricultural activity since 1995, but little information on the amount and distribution of increased ground-water extraction. The little information that was available suggests that most of the agricultural areas with increased activity as of 1998 are outside the LAN model area (Carlson and Phillips, 1998).

The initial ground-water demand in 2000 was assumed to be that during 1995, the year prior to injection testing; it appears to be representative of the overall ground-water use during recent nondrought periods (fig. 41*B*). The initial demand was increased linearly with time in accordance with the assumed growth rates. Figure 53 shows the estimated effect of population growth on ground-water demand in the Lancaster area during the 2000–2010 period relative to that in the recent past. Because 1995 through 2000 was assumed a no-growth period, the estimated water demands for the 10-year management period are considered conservative.

Ground-water demand (pumpage) was constrained in the optimization problem by specifying the total pumpage for all managed wells, incorporating the projected growth rate for Lancaster. The demand constraint has the form

$$\sum_t \sum_i -Q^t_{\mathrm{extr}_i} = D^t \tag{11}$$

where

$Q^t_{extr_i}$ is the extraction (negative) from well *i* during stress period *t* and

D^t is the total ground-water demand during stress period *t*.

Constraints on Hydraulic Head

The upper and lower bounds on hydraulic head were specified for all cells containing wells considered in the optimization (fig. 52). The upper bound was set at an elevation of 100 ft below land surface to avoid waterlogging, mobilization of near-surface contaminants, and susceptibility to liquefaction during an earthquake. For the 10-year management period, these upper bounds were required only in the northernmost wells where initial heads were within 150 ft of the land surface. The upper head constraints have the form

$$h_{it} \le h_{\max} \tag{12}$$

where

h_{it} is the head at the cell containing well *i* in stress period t, and

h_{max} is the maximum allowable head (land surface -100 ft) at the cell containing well *i*.

The lower bounds were specified for wells in areas that are more susceptible to land subsidence; areas outside the subsidence area were unbounded. These constraints have the form

$$h_{it} \ge h_{min} \tag{13}$$

where

h_{it} is the head at the cell containing well *i* in stress period *t* and

h_{min} is the minimum allowable head at the cell containing well *i*.

Ideally, the lower bound is set at the preconsolidation head to ensure that no subsidence could occur; however, the magnitude and distribution of the preconsolidation head is complex and poorly understood. Comparisons of water-level and land-surface time-series data from Antelope Valley indicate that subsidence can continue for a decade or longer despite significant recovery in water levels (Galloway and others, 1998a), thus delayed drainage of aquitards may be a significant component of subsidence in this area, and the spatial and temporal distribution of the preconsolidation head is difficult to determine and to express in the context of an optimization constraint.

Given the difficulty of determining preconsolidation head, the selection of lower bounds was somewhat subjective; selection, therefore, was partly based on the feasibility of obtaining an optimal solution. The range considered for the lower bound was between the initial (spring) conditions and the lowest water level recorded at or near the wells. The former would concede the amount of subsidence associated with delayed drainage from historical water-level changes, but not that caused by additional drawdown. The latter is what one would specify if compaction was essentially an instantaneous response to drawdown beyond the preconsolidation head, and delayed drainage did not occur. Because delayed drainage is known to occur in this aquifer system, it was considered important to be near the upper end of this range.

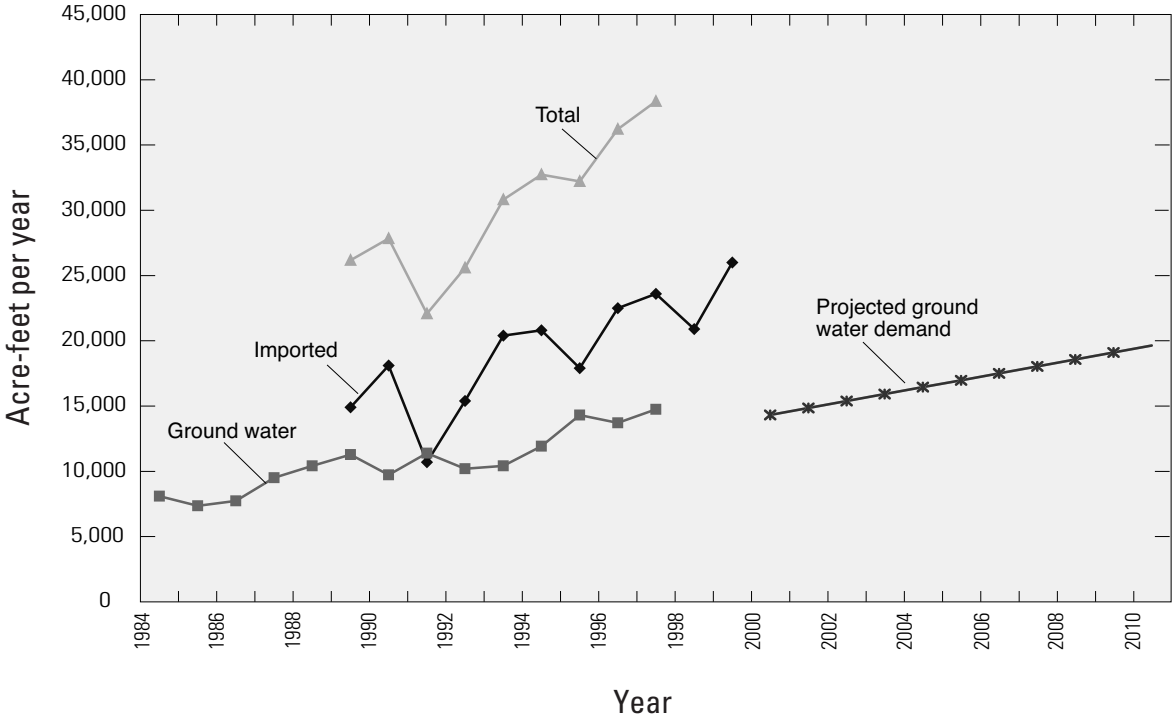

Figure 53. Water delivered in Lancaster by the Los Angeles County Department of Public Works (LACDPW) and projected ground-water demand used in the simulation/optimization model, Lancaster, Antelope Valley, California.

Initial runs of the LANOPT model indicated that the upper end of the range of lower bounds (the water-table peak in 1995) was not going to result in feasible solutions. Ground-water demand could not be met without pumping from wells within the subsidence area and violating the lower bounds, particularly early in the simulation before injection had much of an effect. Thus, these bounds were decreased until the model consistently reached a feasible solution for a variety of conditions. For all wells within about 0.25 mi of the area where subsidence was about 16 mm/yr or greater from 1993 to 1995 (fig. 52), the lower bounds were set 10 ft lower than the starting head for the 10-year management period. An exception was made for the first pumping season; the lower bounds were decreased by an additional 10 ft to obtain a feasible solution. This set of lower bounds for the subsidence area represents a conservative assumption of the preconsolidation head that should limit additional land subsidence to that primarily caused by delayed drainage from the thick aquitards.

Model Components and Conversion to Uniform Grid

The LANOPT model was constructed using three software programs: MODMAN, version 3.0 (Greenwald, 1993), LINDO (Schrage, 1991), and MODFLOW (McDonald and Harbaugh, 1988). MODMAN facilitates the formulation of an optimization problem and runs a MODFLOW-based ground-water-flow model multiple times to generate a response matrix. This response matrix contains the transient head response at specified locations in the model (in the form of a response coefficient) to a stress (extraction or injection) imposed by any single managed well. LINDO was then used to solve the linear optimization problem given the response matrix and specified constraints. Assuming the system reacts linearly and using the principle of superposition (Bear, 1972; Ahlfeld and Mulligan, 2000), the response at the specified locations can be calculated by adding the responses caused by any combination of managed wells that are extracting/injecting at any rate. This general approach of using response coefficients is discussed in greater detail by Gorelick and others (1993).

MODFLOW is the software used to develop the ground-water-flow model (LAN) described earlier in this report. A significant change was made to this model for use in the LANOPT model: the variable model grid was converted to a uniform, fairly coarse grid. The primary reason for this conversion was that a uniform grid was required to avoid introducing bias into the optimization results owing to the different-size cells containing the managed wells. Simulated water levels in cones of depression, or impression, would be more exaggerated for wells in small cells than for those in large cells, so the constraints would not be equally applied. A secondary reason for this conversion was to reduce the execution time for the LANOPT model.

The new uniform grid was 37 rows by 60 columns (fig. 54) with a 0.33-mi spacing. Rows 1 and 35 through 37, and columns 1 through 3 and 59 and 60 were inactive. This newly configured model was used to simulate the calibration period to determine the effects of re-discretization on model results. Figure 55 shows hydrographs of measured and simulated hydraulic heads for the variable and uniform grids, which have essentially identical long-term trends. Seasonal and injection-related fluctuations, though, are reduced with the uniform grid because the response to stresses that may be affecting water levels for a small area is distributed across a larger area. For this reason, and the fact that simulated heads do not perfectly match the measured water levels even in the variable-grid model, the initial (simulated) heads, rather than measured water levels, were used to specify the lower head constraints in the subsidence area.

The length of the stress period was increased to 2 months (60.875 days) in the LANOPT model, double that used to calibrate the LAN model. This greatly reduced the execution time of the LANOPT model, and reflects more appropriately the role of this model as a management tool—as a general guide, not a blueprint for short-term well management.

The initial condition for the 2000–2010 management period was generated by extending the LAN model from August 1998 through April 2000 using measured pumpage values for months without pumpage in 1995 (prior to injection testing). The 10-year management period ended in October 2010, the end of the final summer pumping season, for a total of 58 stress periods, each 2 months in length. All other input for the simulation component of the LANOPT model is identical to that in the LAN model.

The above approach emphasizes regional spatial and temporal changes in hydraulic head, not local, short-term changes. This approach is consistent with that of the uniform-grid model in matching long-term trends compared with short-term fluctuations. Some of the head constraints, however, are based on real world values, and may, in reality, be violated close to the wells. For example, the upper head limit of 100 ft below land surface may, in practice, be exceeded near injection wells.

Nonlinear Effects

The LANOPT model uses a response matrix approach to solve a linear optimization problem. This approach assumes a linear response in hydraulic head to changes in extraction/injection rates; however, the upper aquifer is simulated as unconfined, which introduces a nonlinearity. In a confined aquifer, the saturated thickness and associated transmissivity are constant; changes in head are proportional to changes in stress. In an unconfined aquifer, the saturated thickness and associated transmissivity vary as the water table rises or declines in response to changes in stress; the head response, therefore, is a nonlinear function of extraction or injection.

The effect of this nonlinearity on the solution depends on the magnitude of the simulated head changes relative to the initial saturated thickness. If simulated head changes are small compared to the saturated thickness, the change in transmissivity and associated error from nonlinearity will be small; using relatively large model cells helps to reduce this source of error. The error was measured by comparing optimal heads at the managed wells (LINDO output generated from the response matrix) to those generated using the optimal extraction/injection rates in the LAN model. The results of this comparison are shown later in this report.

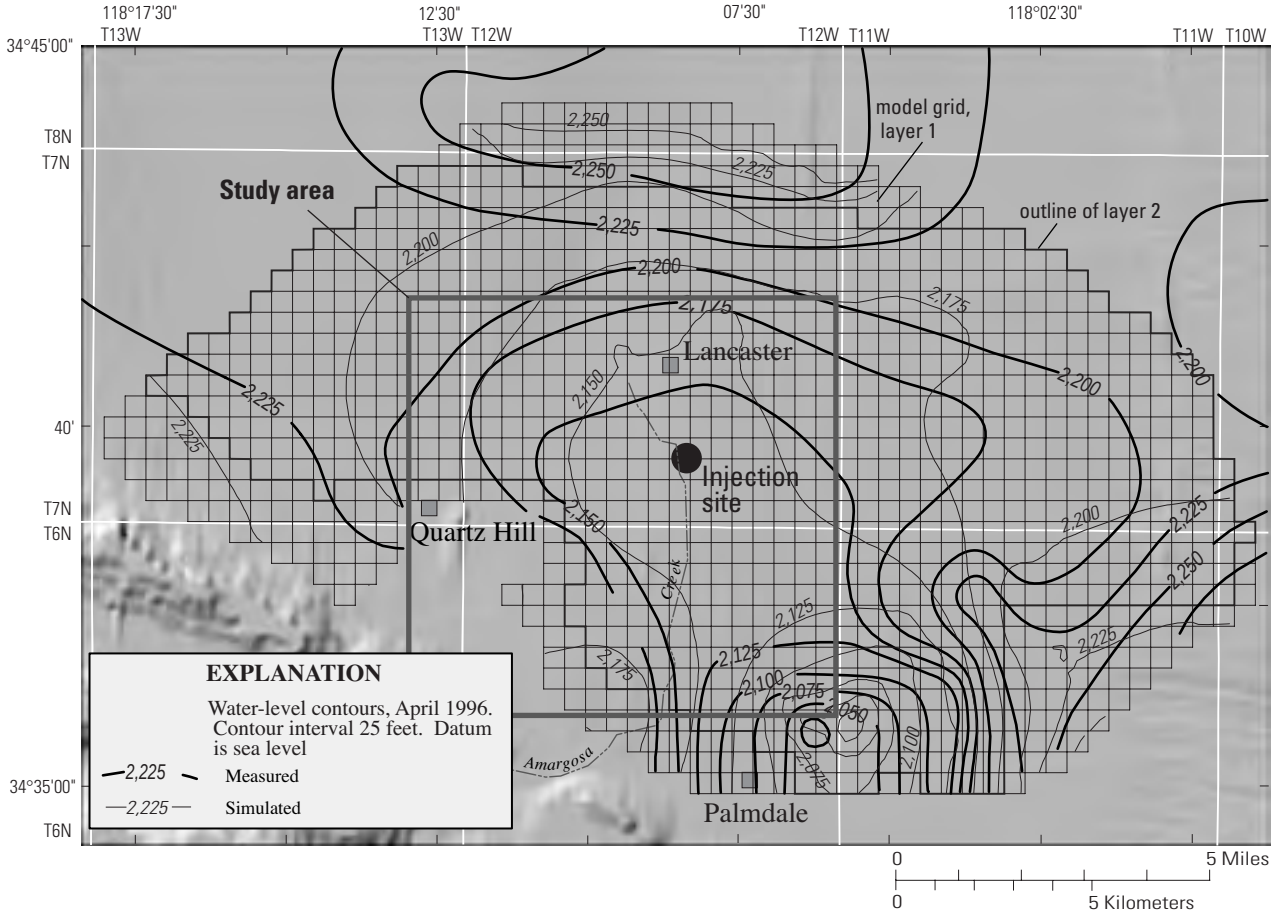

Figure 54. Location and dimensions of uniformly spaced model grid used in the simulation/optimization model, and simulated and measured water levels for April 1996, Lancaster, Antelope Valley, California.

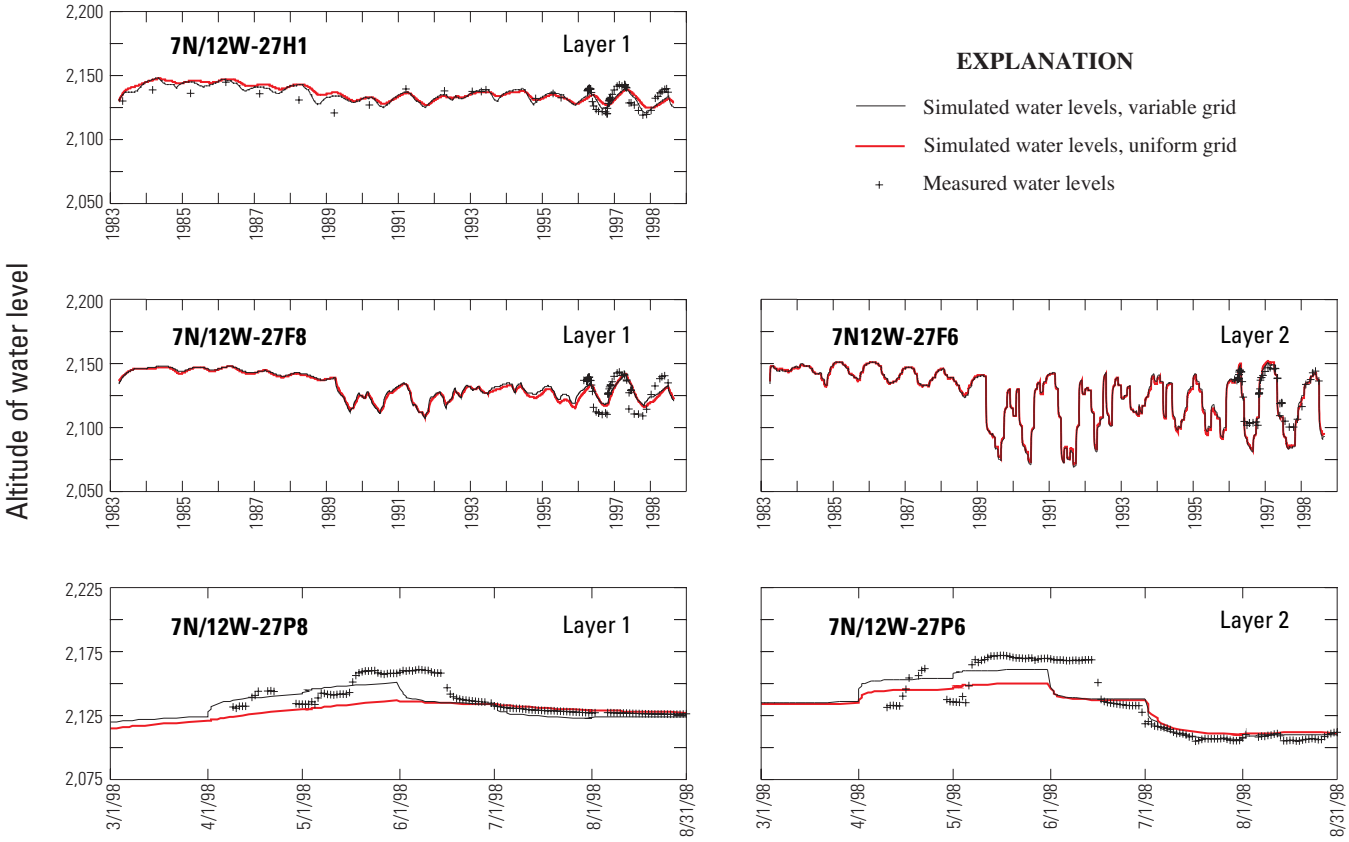

Figure 55. Variable- versus uniform-grid results, Lancaster, Antelope Valley, California.

Preliminary Simulation/Optimization (LANOPT) Model Results

The LANOPT model was used to compare results from maintaining present management practices (without injection) for a 10-year management period with those for three other injection-program scenarios. For reference, the current objective and constraints are summarized in table 4.

Scenario 1, which was not an optimization problem, represents maintenance of present management practices (without injection). Present practices were represented using the 1995 pumping distribution for existing wells assuming no growth in ground-water demand (fig. 53).

Scenario 2 represents extraction and injection using only the existing wells, assuming a feasible solution and allows injection for 6 months of the year, which is considered the maximum possible injection period. This scenario represents the best achievable result for the existing wells and the current constraints.

Scenarios 3 and 4 represent extraction and injection using existing and proposed wells. Scenario 3 allows injection for 6 months; this scenario represents the best achievable result overall for the existing and proposed wells and the current constraints. Scenario 4 restricted the injection period to 4 months of the year to allow for variability in SWP supply and other factors that may limit the length of an injection season.

Table 4. Summary of simulation/optimization model objective and constraints, Lancaster, Antelope Valley, California

		Description
Objective:	Maximize lowest value of head	Seeks the highest value possible for the lowest value of head.
Constraints:	No injection during high-demand period	Injection was not allowed from late spring through early fall, when State Water Project water is less available, more expensive, and competing demands are greater. Availability of well capacity is at a minimum during this period.
	Well use cannot exceed capacity	For each well and stress period, the sum of injection and extraction cannot exceed the total capacity of the well. The total capacity was adjusted for the difference between injection and extraction capacities.
	Injected and extracted water is distributed by aquifer	For each well, injected and extracted water was partitioned to aquifers by the ratio of effective transmissivity within each aquifer (on the basis of hydraulic conductivity and length of perforated interval in that aquifer) to the total effective transmissivity.
	Must meet ground-water demand	The sum of extraction from all managed wells must equal ground-water demand. Demand was total extraction from these wells during 1995, and an annual growth rate was applied.
	Upper head limits	Limits were placed on the maximum head at all managed wells to avoid high water-table conditions.
	Lower head limits	Limits were placed on the minimum head at all managed wells within the subsidence area to avoid drawdown and associated land subsidence.

Comparison of Simulation/Optimization (LANOPT) Model Results for Scenarios

Results of the four management scenarios are summarized in figure 56. Included in this figure are hydrographs showing the water-table responses to the scenarios and bar charts depicting the optimal injection/extraction rates during the 10-year management period. The optimal rates are expressed in the form of percentage well capacity used; the long-term capacities are shown in table 3. The bar charts were simplified by combining these rates for 6-month periods representing the high- and low-demand periods. The first stress period, however, represents only a 2-month period, March and April 2000, during which injection was allowed prior to the first high-demand period. Nearby wells are grouped by site designation for clarity (table 3). Optimal extraction rates for the three deep wells (7N/12W-27J6, 7N/12W-27F2, and 7N/12W-27F3) for which injection was not allowed were combined and included with the rates for the Avenue K–8 and 5th Street West site where two of the three wells are located.

Numerical comparisons also are made, including comparisons of the objective value, average simulated water levels (directly related to average well capacity) at managed wells within and outside the subsidence areas (fig. 52) during the 10-yr management period, and total injection volumes (table 5). The average water levels were important because the minimum heads (optimal values) occurred near the beginning of the simulated scenarios that included the proposed wells; thus, the objective value was not always as sensitive as the average heads (outside the subsidence area).

When present practices were maintained (scenario 1) the average simulated water-table altitude at the existing wells during the 10-year management period was 2,131 ft in the subsidence area and 2,097 ft elsewhere. This reflects water-level declines of about 15 to 65 ft at individual sites (fig. 56). Simulated drawdowns were greatest at Avenue J and Sierra Highway, Avenue K–8 and 5th Street West, and Avenue L and 5th Street West sites, followed by the Avenue K–8 and Division Street and Avenue M and 7th Street West sites, the northern area, well 4-37, and the Avenue M and 7th Street East site (no existing wells at this site). Optimization constraints did not apply for this scenario; however, the minimum heads specified for the other scenarios in the subsidence area were violated in every case and ranged from less than 15 ft at well 4-37 to about 100 ft at the Avenue J and Sierra Highway site (fig. 56). Although there is considerable uncertainty associated with the magnitude of these estimates, the trends strongly suggest that maintaining present practices would result in continued drawdowns and associated loss in well capacities, and increased land subsidence.

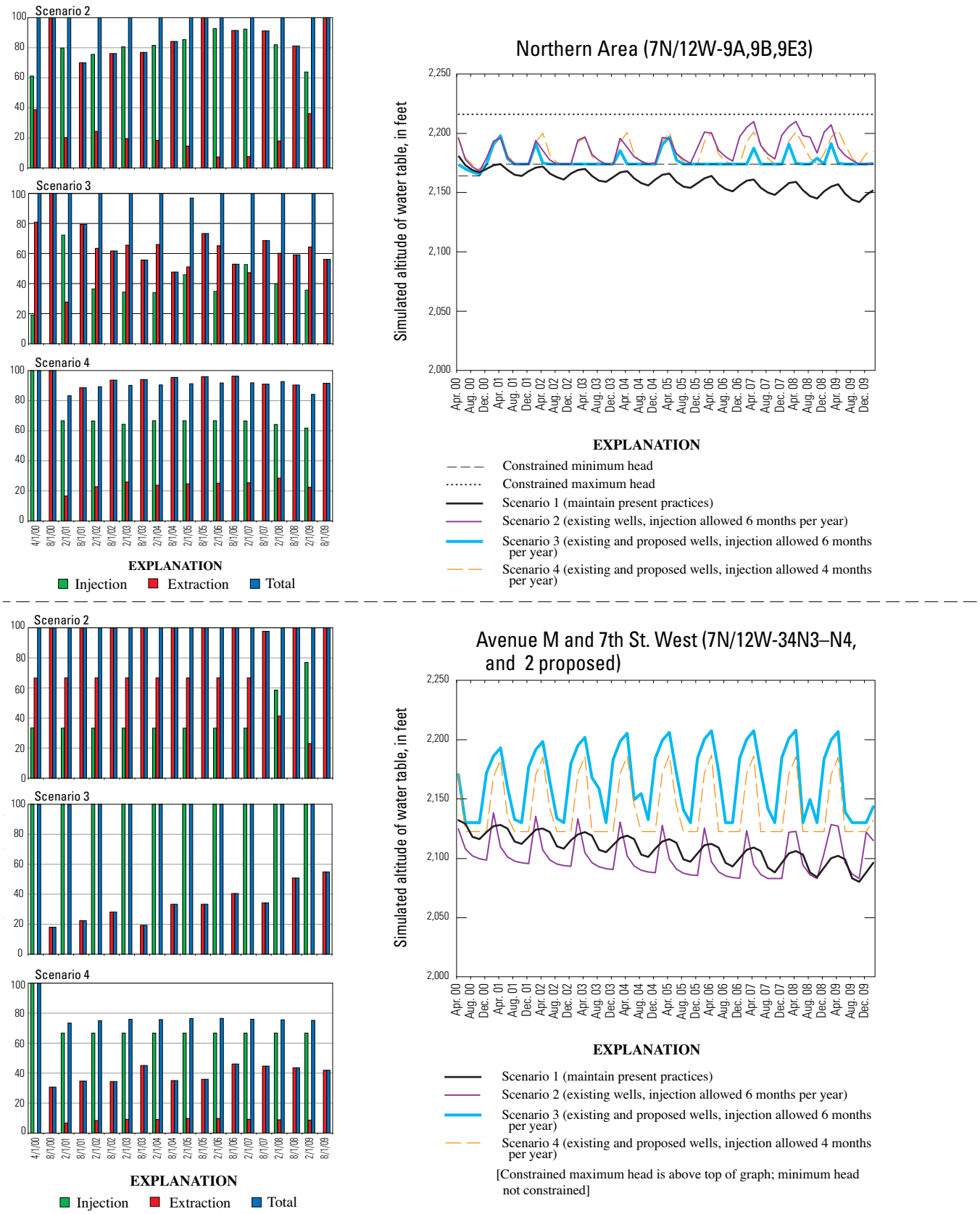

Figure 56. Graphical results from simulation/optimization (LANOPT) model for four hypothetical management scenarios, Lancaster, Antelope Valley, California.

Optimal well rates and associated water-table altitudes are shown for eight sites (table 4) representing all managed wells for the 10-year management period.

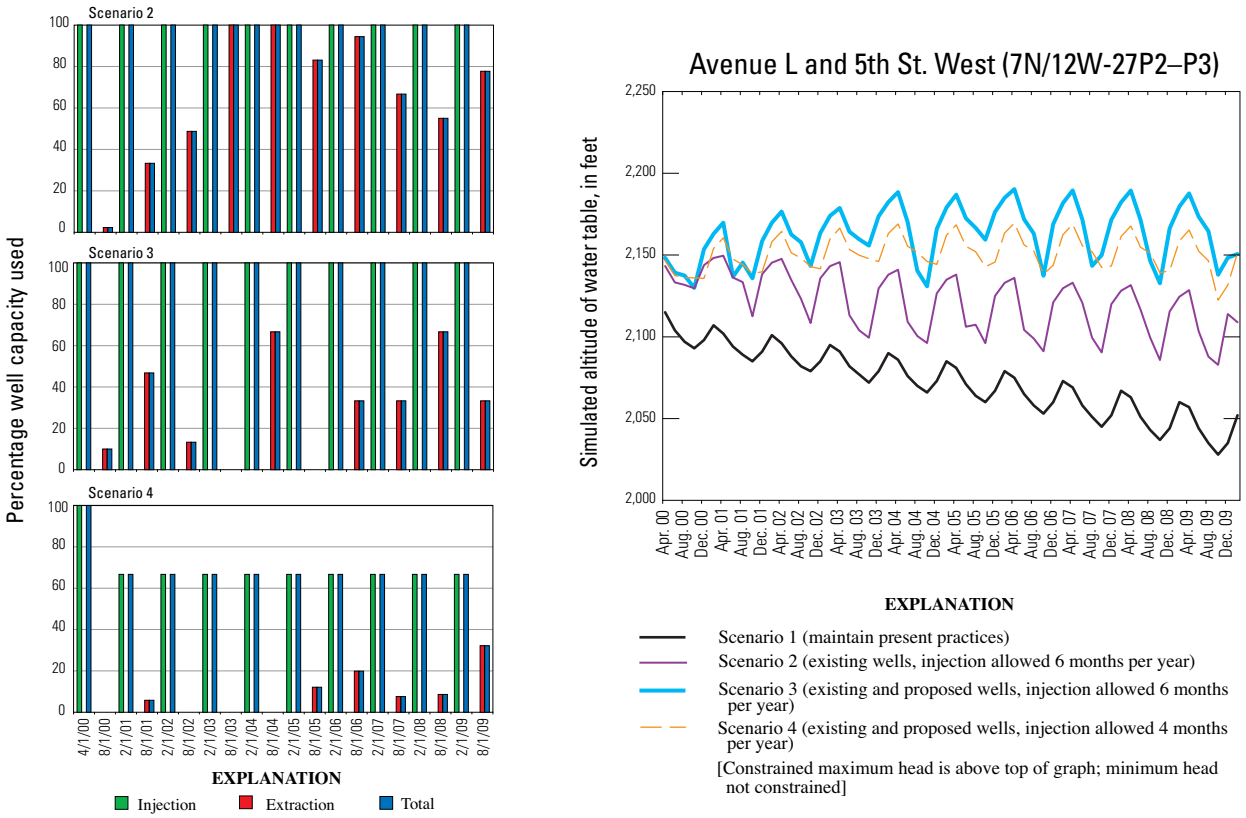

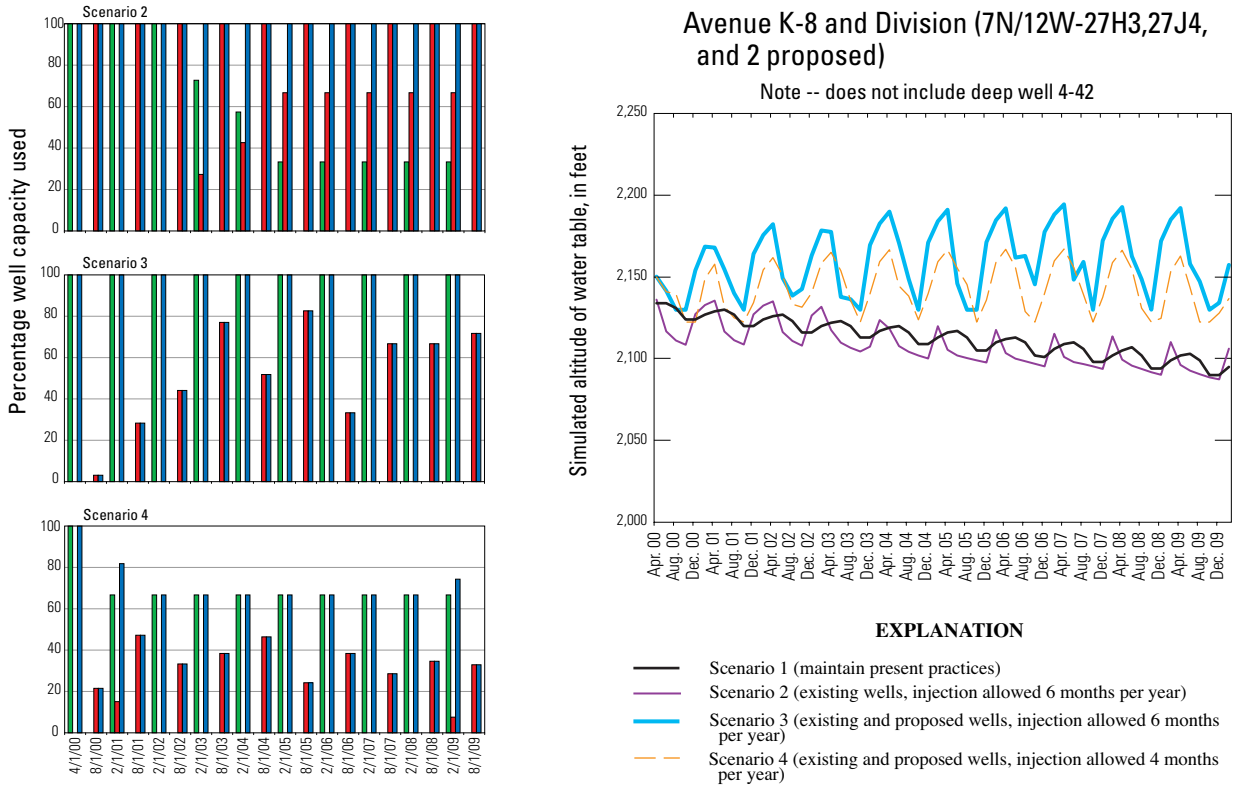

Figure 56.—*Continued.*

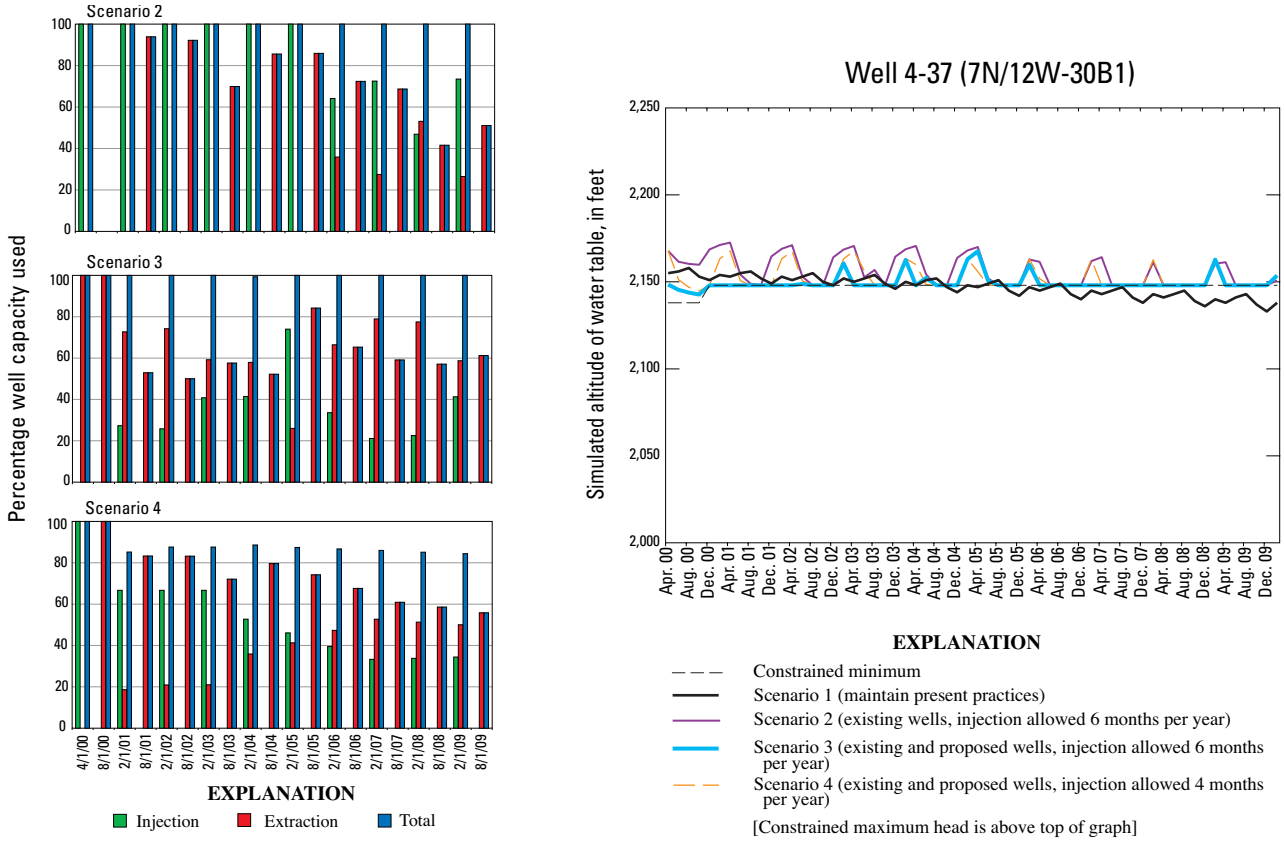

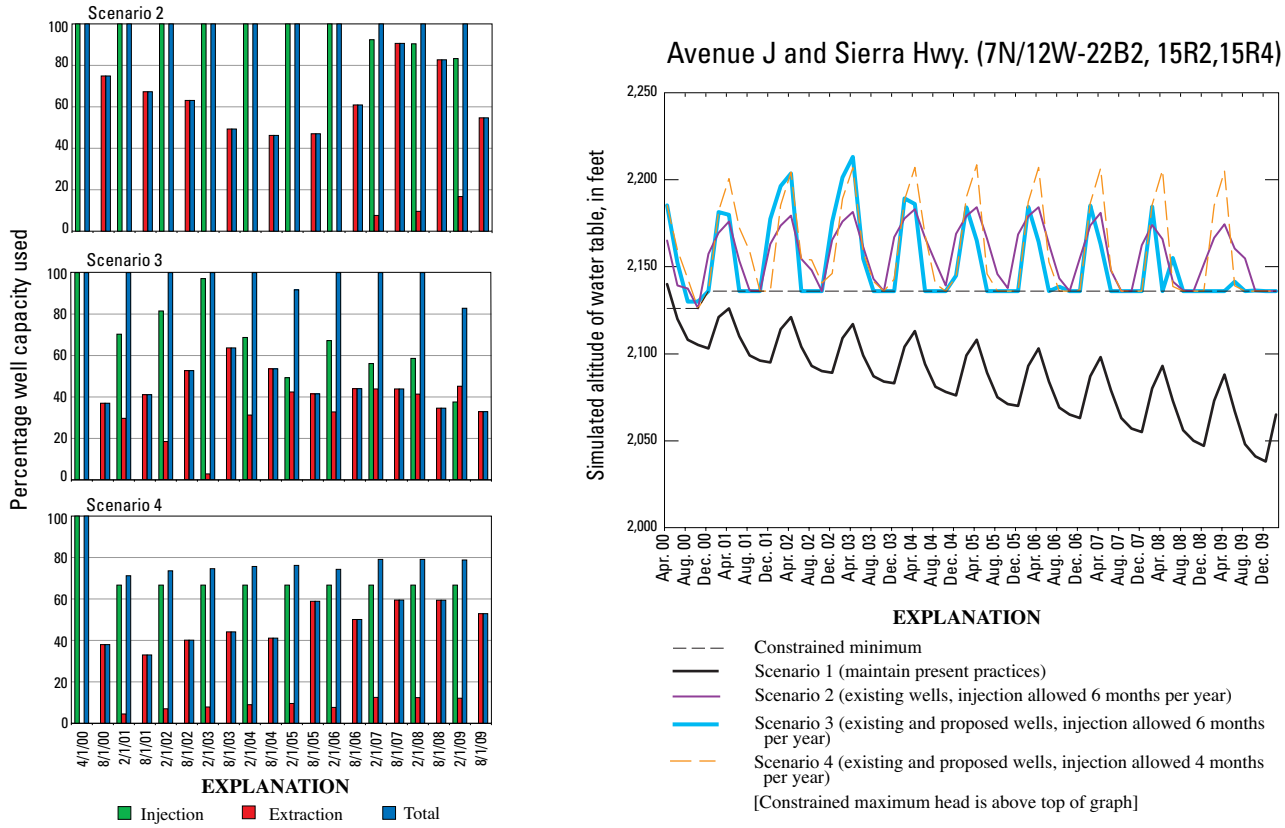

Figure 56.—*Continued.*

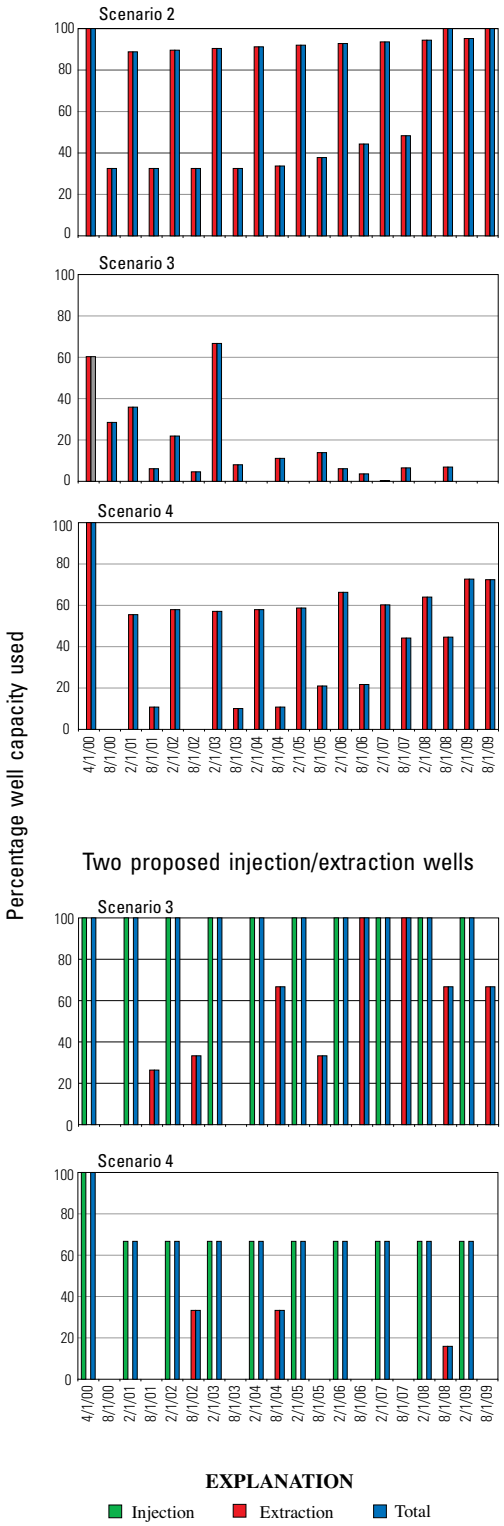

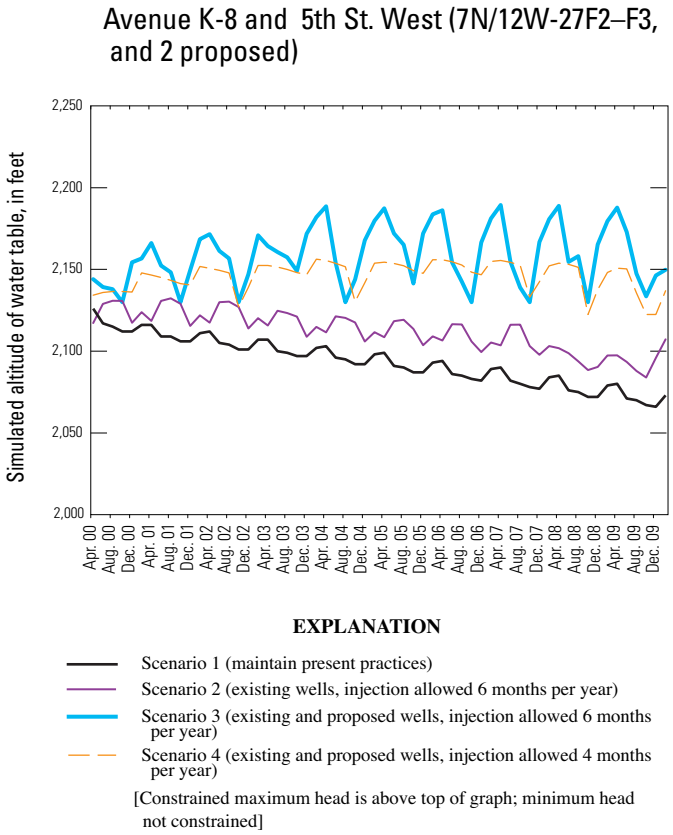

Figure 56.—*Continued.*

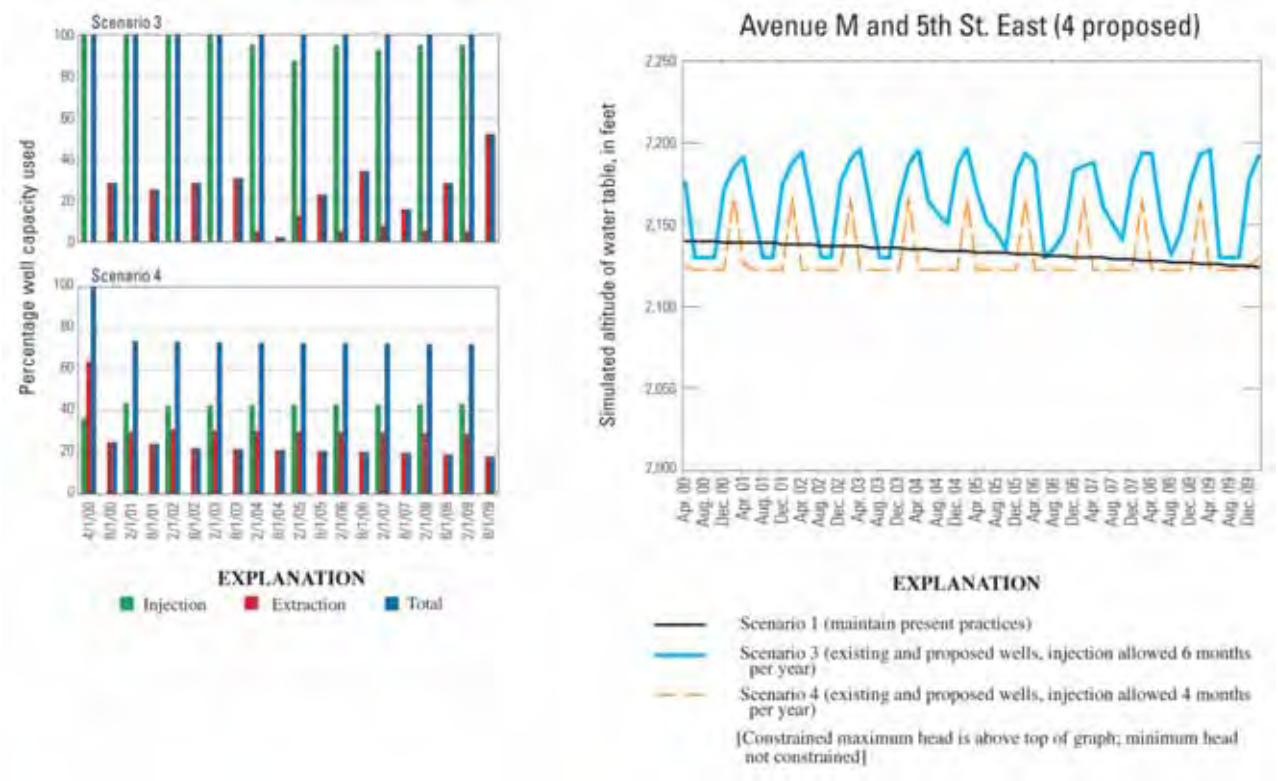

Figure 56.—*Continued.*

Table 5. Results from the simulation/optimization model for four hypothetical management scenarios for Lancaster, Antelope Valley, California for management period 2000–2010

[na, not available]

Scenario	Objective value, minimum head (feet)	Average simulated water level during management period at managed well locations		Total injection management period (acre-feet)
		Within subsidence area (feet)	Outside of subsidence area (feet)	
Scenario 1: Maintain present practices	na	2,131.4	[1]2,096.9	0
Scenario 2: Existing wells, 6 months injection	2,082.9	2,166.3	[1]2,110.5	52,480
Scenario 3: Existing and proposed wells, 6 months injection	2,129.9	2,159.2	2,162.0	110,520
Scenario 4: Existing and proposedwells, 4 months injection	2,122.4	2,165.0	2,142.1	84,621

[1] Does not include Avenue M and 5th Street East, a proposed site having no existing wells.

The LANOPT model was used to test the feasibility of meeting the constraints while maintaining present practices (scenario 1), but allowing the pumping distribution to vary in time and space. No feasible solution was found, which was expected owing to the large drawdowns in the subsidence area. Feasible solutions were found, however, for the other three scenarios.

The optimal solution for managing injection and extraction in the 16 existing wells (three of which are extraction-only wells) (scenario 2) required extensive injection in the subsidence area to maintain water levels above the constrained minimum (fig. 56). Injection into the wells in the subsidence area during the low-demand period (6 months) provided for continued use of these wells during the high-demand period. At least 50 percent of the extraction capacity of these wells was used for more than 86 percent of the high-demand periods during the 10-year simulation. Outside the subsidence area, extraction was dominant at the Avenue K–8 and 5th Street West, Avenue K–8 and Division Street, and Avenue M and 7th Street West sites, where the spring water table (the seasonal maximum head) declined by about 10 to 28 ft. Injection exceeded extraction at Avenue L and 5th Street West, the site of the pilot injection tests, which resulted in an increase in water-table elevation of 12 ft. Overall, the annual amount of water injected decreased from about 5,800 to 5,200 acre-ft during the management period, which represented 40 to 31 percent, respectively, of total well use. This decrease in injection with time is correlated to the constrained increase in ground-water demand.

The objective value (the minimum head) for managing the existing wells was 2,082.9 ft (table 5), which occurred in the final stress period at Avenue L and 5th Street West and Avenue M and 7th Street West. Heads at Avenue K–8 and 5th Street West and Avenue K–8 and Division Street were within 6 ft of the objective value indicating essentially equal heads at all the managed sites outside the subsidence area. The average simulated water-table altitude at the existing wells during the 10-year management period was 2,166 ft in the subsidence area and 2,110 ft elsewhere (table 5). The average simulated water-table altitudes for scenario 2 improved about 35 and 14 ft, respectively, within and outside the areas of subsidence over maintaining present practices (scenario 1).

The addition of 13 proposed wells (scenario 3) constitutes a large increase in both injection and extraction capacity, which was reflected by the 47-ft increase in the objective value, to 2,130 ft and by a similar increase in average water levels outside the subsidence area (table 5). The average simulated water levels for all the managed locations outside the subsidence area were within 8 ft of the objective value, which remained above the minimum head constraints within the subsidence area. The injection volumes for scenario 3 about doubled those of scenario 2 and decreased during the 10-year management period from 12,400 acre-ft/yr to 10,500 acre-ft/yr. The injection volumes for scenario 3 represented 58 to 48 percent of total well use. Extraction exceeded injection in the subsidence areas (while meeting subsidence constraints), but injection exceeded extraction elsewhere, resulting in substantial increases in water-table altitude (fig. 56). The spring water table outside the subsidence area rose 54 to 73 ft during the management period; the maximum increase was at the Avenue L and 5th Street West and Avenue M and 7th Street West sites. The deep wells, in which no injection was allowed, seldom were used, particularly during the latter two-thirds of the management period.

The 6-month period of injection allowed for scenario 3 was reduced to 4 months for scenario 4 to determine the effects of a substantial reduction in injection volume. Injection volumes may be reduced for a variety of reasons, including availability of SWP water, overestimation of injection capacities, underestimation of maintenance requirements during injection, and potential water-quality considerations. The objective value for scenario 4 decreased by 7.5 ft to 2,122.4 ft, but the average water level outside the subsidence area declined 20 ft, to 32 ft higher than that for scenario 2. The water table at all the managed locations during the last stress period of scenario 4 was equal to the objective value or the lower head constraint. Injection volumes decreased to about 8,700 to 9,000 acre-ft/yr within and outside the subsidence area, respectively; the injected water represented 43 to 50 percent of total well use, both decreasing with growth in demand. Extraction approximately equaled injection in the subsidence areas, and injection exceeded extraction elsewhere, except at the proposed site at Avenue M and 5th Street West. Unlike scenario 3, extraction from the deep wells was extensive, exceeding 50 percent of capacity during more than half of the simulation. The spring water table outside the subsidence area rose by 23 to 55 ft during the 10-year management period, with the maximum increases at Avenue L and 5th Street West and Avenue M and 7th Street West, as in scenario 3 (fig. 56).

Another means for comparing the results of managements scenarios and for judging their relative feasibilities is evaluating the percentage of total well capacity used for injection and extraction. Figure 57 shows total well capacities and the combined totals for the management period. Note that for scenario 2 (only the existing wells used), growth in spring/summer demand resulted in extraction volumes that required an increase in well use from less than 65 percent at the beginning of the management period to 85 percent at the end. It may not be feasible to pump all the existing wells 85 percent of the time with the current infrastructure because additional storage and rigorous management of that storage may be required to allow for continued extraction during daily and (or) extended periods of low demand. The addition of the proposed wells (scenarios 3 and 4) reduces the maximum well use during high-demand periods to only 46 percent of long-term capacity to allow down time.

All wells operate at full capacity in all scenarios when injection is allowed, with the exception of the deep extraction-only wells (figs. 56, 57) and two other minor exceptions. This indicates that injection capacity is the binding constraint for this optimization problem. Thus, added capacity would improve the solution until another constraint becomes dominant.

Figure 58 shows the annual volumes of injected and extracted water for management scenarios 2, 3, and 4, which represent a wide range of injection volumes and associated net stresses. The variability of the injection curve for scenario 4 is due primarily to the large annual variability in volumes extracted from the deep extraction-only wells, which was not the case for the other scenarios (fig. 56). When extraction decreased from these deep wells, the other wells switched from injection to extraction to compensate; the opposite occurred when extraction from the deep wells was increased. This sporadic extraction from the deep wells resulted in high variability in the totals for injection.

The accuracy of results from the LANOPT model depends on many factors, and one should not have too much confidence in the details—for example, the exact mix of injection and extraction at a specific site. The strength in this type of model is the ability to compare alternate scenarios knowing that one is comparing the optimal case for each scenario. The results for management scenarios 1–4 suggest that an injection program with existing wells would be a substantial improvement over no injection at all, although the water-table would continue to decline outside of the subsidence area. The high rates of well usage associated with this scenario may not be sustainable in practice. The results also indicate that installation and inclusion of all the proposed wells into the injection program would result in a significant water-table rise outside the subsidence area and average rates of well usage far below current values.

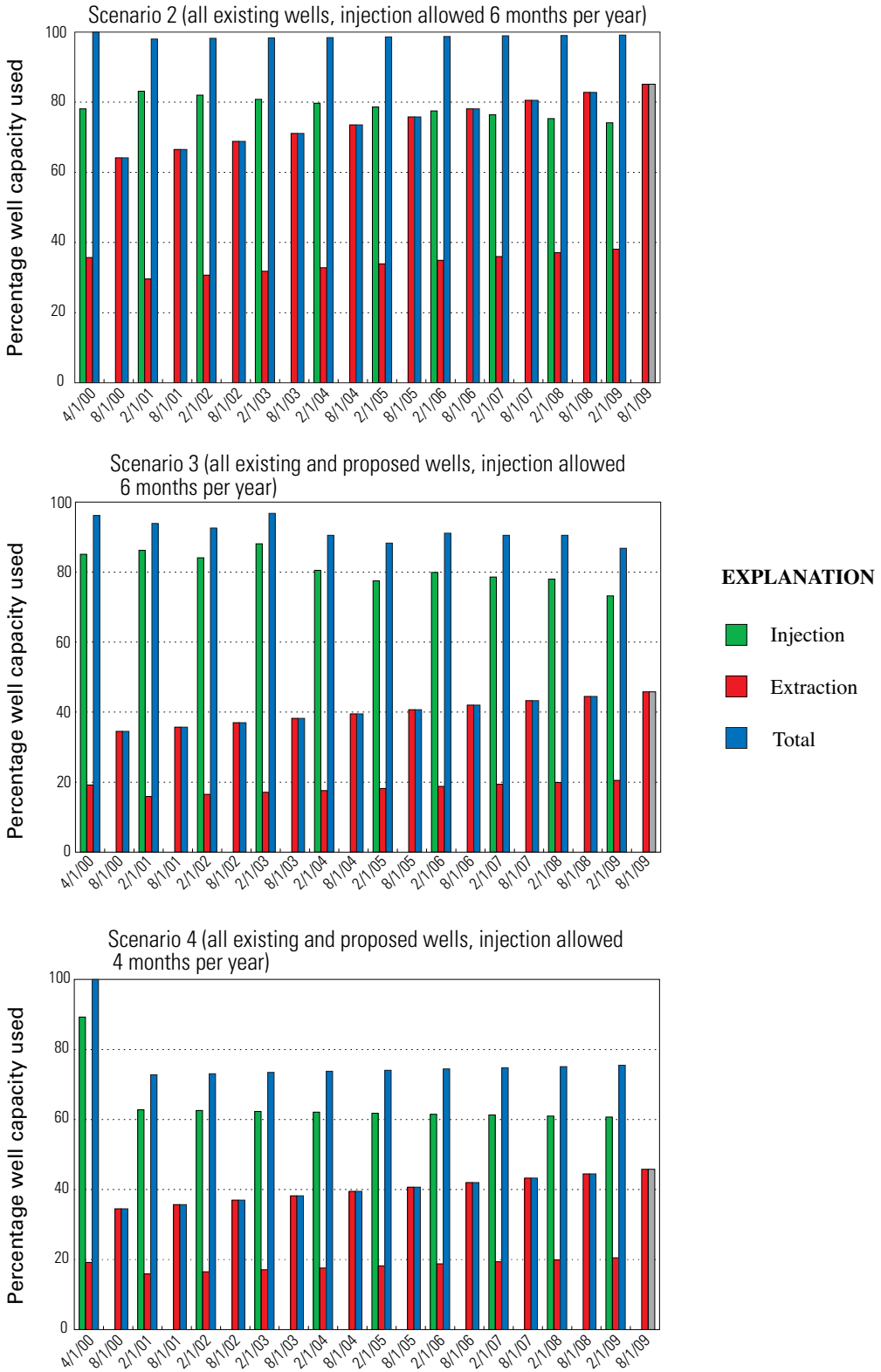

Figure 57. Optimal well capacity used for injection and extraction for three hypothetical management scenarios for Lancaster, Antelope Valley, California.

Totals were adjusted to compensate for the difference in capacities for injection and extraction and are less than the sum of these components.

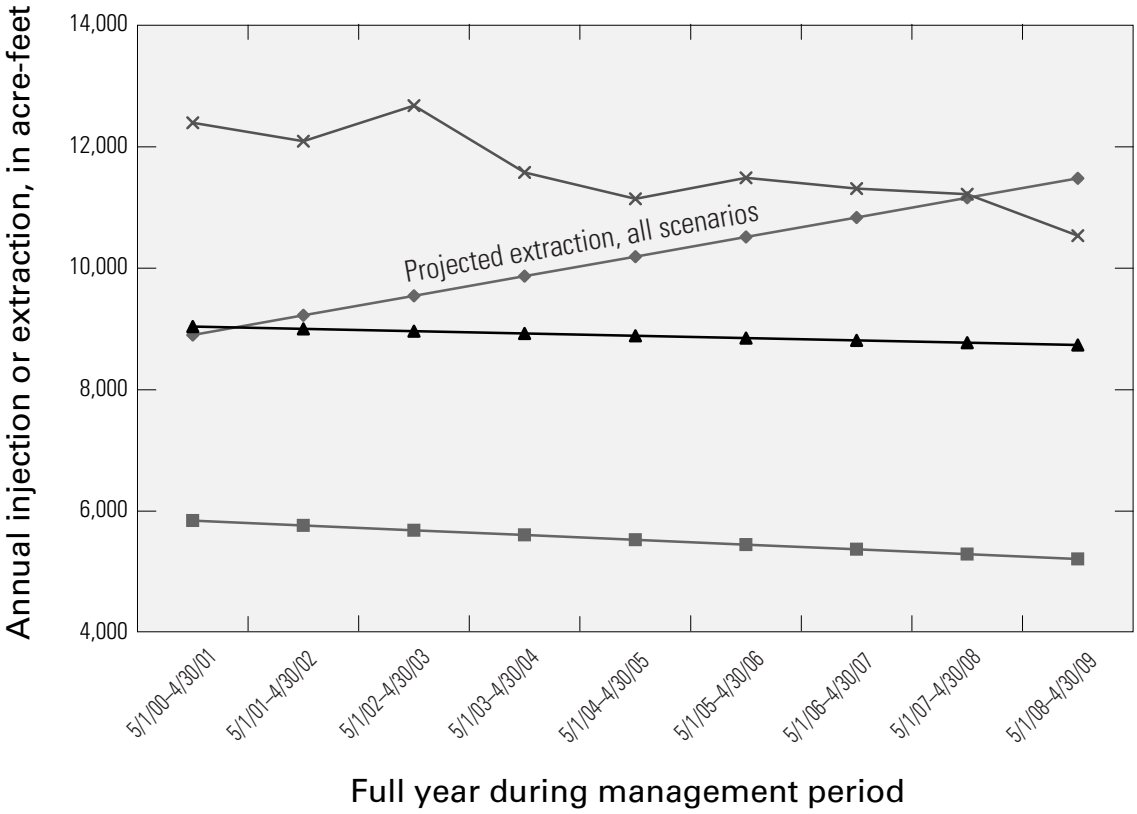

EXPLANATION

- Extraction, all scenarios
- Scenario 2 (injection in existing wells, allowed 6 months per year)
- Scenario 3 (injection in existing and proposed wells, allowed 6 months per year)
- Scenario 4 (injection in existing and proposed wells, allowed 4 months per year)

Figure 58. Optimal volumes of injection and extraction during the management period for three hypothetical management scenarios, Lancaster, Antelope Valley, California.

This dichotomy suggests that a more moderate, or phased-in approach to the addition of the proposed wells may accomplish the objective of avoiding additional land subsidence while maintaining, or even improving, extraction capacities outside the subsidence area. If a phased-in installation of the proposed wells is desired, the LANOPT model can be used to help decide the logical order of well installation. Although integer methods and other more complex techniques may be applied to answer this question more rigorously, a simple approach is to include groups of proposed wells into the problem and to compare the objective value to that without the proposed wells (scenario 2). The results of this approach are given in table 6.

The improvement in the objective value for individual proposed wells is generally correlated with the injection capacity (table 6). Assuming that the injection (and extraction) capacities are accurate in a relative sense, this analysis suggests that the Avenue M and 5th Street East site, where no wells presently exist, may be the most effective site for the proposed wells. Although there are twice as many proposed wells at this site than at most of the other sites, the improvement in the objective value exceeds that at the other sites by more than a factor of two. To ensure this result was not overly influenced by the large capacity at this site, a simulation was run using the wells at the Avenue M and 5th Street East site at half capacity. The resulting improvement in the objective value was 24 ft,

Table 6. Effect of proposed wells on the objective value (2,083 feet without proposed wells), Lancaster, Antelope Valley, California

[ft, foot; ft^3/d, cubic foot per second]

Proposed well site	Number of proposed wells	Objective value (ft)	Improvement in objective value (ft)	Injection capacity (ft^3/d)
Avenue M and 5th Street East	4	2112.9	29.9	576,000
Avenue J and Sierra Highway	2	2094.9	11.9	288,000
Avenue K-8 and 5th Street West	2	2094.9	11.9	252,000
Avenue M and 7th Street West	2	2094.7	11.7	288,000
Avenue K-8 and Division Street	2	2093.8	10.8	205,200
Avenue J and Sierra Highway, near well 4-5	1	2090.2	7.2	144,000

about twice that of any other site, and only 6 ft less than the objective value at the original capacity. This result strengthens the conclusion that the Avenue M and 5th Street East site may be the most effective site for the proposed wells, and it indicates that it may be more effective to install only two wells at that site in the early stages (four are proposed).

Sensitivity Analysis of Simulation/Optimization (LANOPT) Model

As with the LAN model, a sensitivity analysis was done for the LANOPT model to determine the sensitivity of model results to key variables. The following optimization constraints were considered in the sensitivity analysis: ground-water demand, injection capacity, minimum hydraulic heads, and the limit on summer injection. The estimated growth in ground-water demand was adjusted upward and downward by 50 percent (18 percent of the 2000 population) because population forecasts and other assumptions (for example, no change in conservation practices) have a large potential for error. Injection capacities were changed from 72 to 64 and 80 percent of the estimated long-term capacity. Minimum heads in the subsidence area were increased and decreased by 10 ft, except for the first four stress periods (through the end of the first summer). The limit on injection during the summer was raised from 0 to 3,000 acre-ft for a 6-month period, which represents about 25 percent of the average injection during the winter period.

Management scenario 3, which included all the wells and 6 months of injection, was used for the sensitivity analysis and as a basis for comparison. The objective value for this scenario is relatively insensitive to fluctuations in most of the variables because the minimum head occurs during the first summer stress period; therefore, average changes in the heads at the managed wells within and outside the subsidence areas during the 10-year management period and changes in total injection were used as the primary indicators of sensitivity (table 7).

The optimal solution for scenario 3 required full usage of well capacity throughout the 10-year management period, except at the deep wells for which injection was not allowed and at two locations within the subsidence area (Avenue J and Sierra Highway and the northern area) where well usage dropped to 83 to 97 percent on two occasions (fig. 56). If the constraints are tightened, the unused well capacity will decrease, which may not be feasible; and if the constraints are relaxed, the unused capacity will increase.

Tightening the constraints results in lower water levels outside the subsidence area and generally causes increased use of wells in the subsidence area, which is a somewhat counterintuitive result. This occurs because the optimization procedure shifts as much extraction as possible to the subsidence area, allowing maximum injection outside the subsidence area (where the lowest heads are). Additional extraction in the subsidence area is achieved by increasing injection in that area during periods when injection is allowed. This shift in stresses with the tightening of constraints generally results in an increase in average water levels within the subsidence area and an accompanying increase in total injection. The opposite responses generally are observed when constraints are loosened (table 7).

Table 7. Effect of changes in optimization constraints on results from simulation/optimization (LANOPT) model of Lancaster, Antelope Valley, California, for management period, 2000–2010

Change in optimization constraint	Change in average simulated water level during management period at managed well locations, compared to scenario (all wells with 6 months injection allowed)		Change in total injection, management period (percent)
	Within subsidence area (feet)	Outside of subsidence area (feet)	
Increase growth in ground-water demand 50 percent	10.0	−8.6	6.3
Reduce growth in ground-water demand 50 percent	−0.3	1.4	−11.1
Increase injection capacity from 72 to 80 percent of long-term extraction capacity	−0.6	3.2	3.2
Reduce injection capacity from 72 to 80 percent of long-term extraction capacity	3.1	−7.7	−10.0
Increase minimum heads in subsidence area by 10 feet	11.7	−9.1	4.3
Reduce minimum heads in subsidence area by 10 feet	−8.5	3.5	−12.3
Allow 3,000 acre-feet of injection during late spring through early fall	−1.6	0.7	−3.2

A limited amount of injection during the summer was slightly more effective than that during the winter; essentially the same average water levels were achieved using about 97 percent of the injection. However, increased cost and decreased reliability of SWP water during the summer were not taken into account in the LANOPT model.

Appropriate Use and Improvement of the Simulation/Optimization (LANOPT) Model

The LANOPT model described in this report was conceived as an adaptable tool for use in designing, and later managing, an injection program. It is best suited for comparative analysis of alternative scenarios. Potential sources of error and limitations associated with the optimization component of the LANOPT model are discussed here, but those associated with the simulation component also apply. Assumptions made during model development and limitations associated with the software should be kept in mind with respect to appropriate use and improvement of the model.

Assumptions Made during Model Development

Assumptions made during model development include those associated with well capacities, future availability of SWP water, future ground-water demand, water conveyance and storage, and the linearity of the optimization problem. The extraction capacity of existing wells was estimated for 1-month periods of full-time operation, but that for longer periods is unknown; it was arbitrarily assumed to be 80 percent of the 1-month capacity. Injection capacity is known only for the wells at the injection site. Actual injection capacities may differ substantially, and may decline with time regardless of changes in water-table elevation. The estimated capacities for the proposed wells may have significant error, particularly the estimates for the new site (Avenue M and 5th Street East). Sensitivity analysis showed that the optimal solution is sensitive to small changes in injection capacities, which suggests a similar sensitivity to those for extraction.

An unlimited volume of SWP water was assumed to be available every year from November through April; in reality, this may not be the case. A combination of conservation efforts and alternative water supplies successfully averted large increases in ground-water use during the 1987–92 drought and the associated low availability of SWP water. SWP water would not have been water available for injection during some of those years and most likely will not be available in the future when drought conditions recur.

Ground-water demand was assumed to increase at the same rate as the projected growth in population. Population forecasts are associated with high potential error because unexpected changes in socioeconomic conditions can cause dramatic changes. Other factors that can affect ground-water demand include development of alternative water sources, increased conservation efforts, and contaminant issues. The sensitivity analysis of the LANOPT model showed that the model results were sensitive to large changes in ground-water demand.

Conveyance and storage facilities were assumed to be adequate for moving and storing water for all the management scenarios. All the managed wells are connected by a network of pipelines, which also connects a number of above-ground storage tanks and taps the AVEK pipeline. It is possible that additional storage and (or) connections would be required to implement a given scenario.

The presence of an unconfined aquifer in the flow model violates the assumption of linearity between stress and response; it should be noted that simulation/optimization results may be sensitive to this violation. Recall that the response matrix is built by applying stress at one managed well at a time and recording the transient head response at all the specified locations. The linear optimization procedure assumes these responses are additive for multiple wells; however, the change in transmissivity resulting from a change in water-table elevation is not taken into account.

Figure 59 shows linear (optimization results) and nonlinear (results from LAN model using optimal injection and extraction) water-table elevations during the management period (2000–2010) at two sites where hydraulic head changes, and associated errors, were greatest. The seasonal fluctuations of the water-table altitudes, based on the assumption of linearity, were greater than those simulated by the LAN model because the water table generally was higher than the initial condition; hence the transmissivity generally was greater. Although there clearly was some error associated with the assumption of linearity, that error was very small relative to the magnitude of seasonal head changes for the scenarios considered (fig. 59). If the errors associated with nonlinearity increase to unacceptable levels, an iterative linear approach may be affective in reducing these errors (Danskin and Gorelick, 1985; Greenwald, 1993; Nishikawa, 1998; Ahlfeld and Mulligan, 2000); otherwise, nonlinear methods may be required.

Limitations Associated with the Software

The optimization software used for this work has limitations, the effects of which should be understood by the user. The primary limitations include the inability of the software to account for various effects of changing water-table conditions, and no explicit means for addressing land subsidence. Changing water-table conditions not only introduce error between simulated and optimal hydraulic head response, but also introduce potentially large changes in constraints that are assumed to remain constant. Well capacity and the vertical distribution of extraction and injection between the upper and middle aquifers sometimes are, in reality, functions of water-table elevation. If heads decline below the top of the screened interval, well capacity decreases, as does the percentage of extracted water from the upper aquifer (the opposite occurs as heads rise within the screened interval). Neither the optimization software nor the LAN model account for these changes, which can result in significant error. This error is proportional to water-table change within screened intervals during the management period.

MODMAN (Greenwald, 1993) does provide for manual specification of well capacity and vertical distribution of stresses. Specification of these changes, however, would require prior knowledge of the optimal solution or the development of a complex iterative approach that would be time consuming and computationally expensive.

The version of MODMAN used for this investigation (Greenwald, 1993) does not accommodate use of the IBS1 package (Leake and Prudic, 1991), which enables simulation of aquifer-system compaction in MODFLOW. A newer version of MODMAN (Greenwald, 1998) does allow the use of the IBS1 package in the simulation model, but it does not allow use of compaction or subsidence within the objective or constraint set.

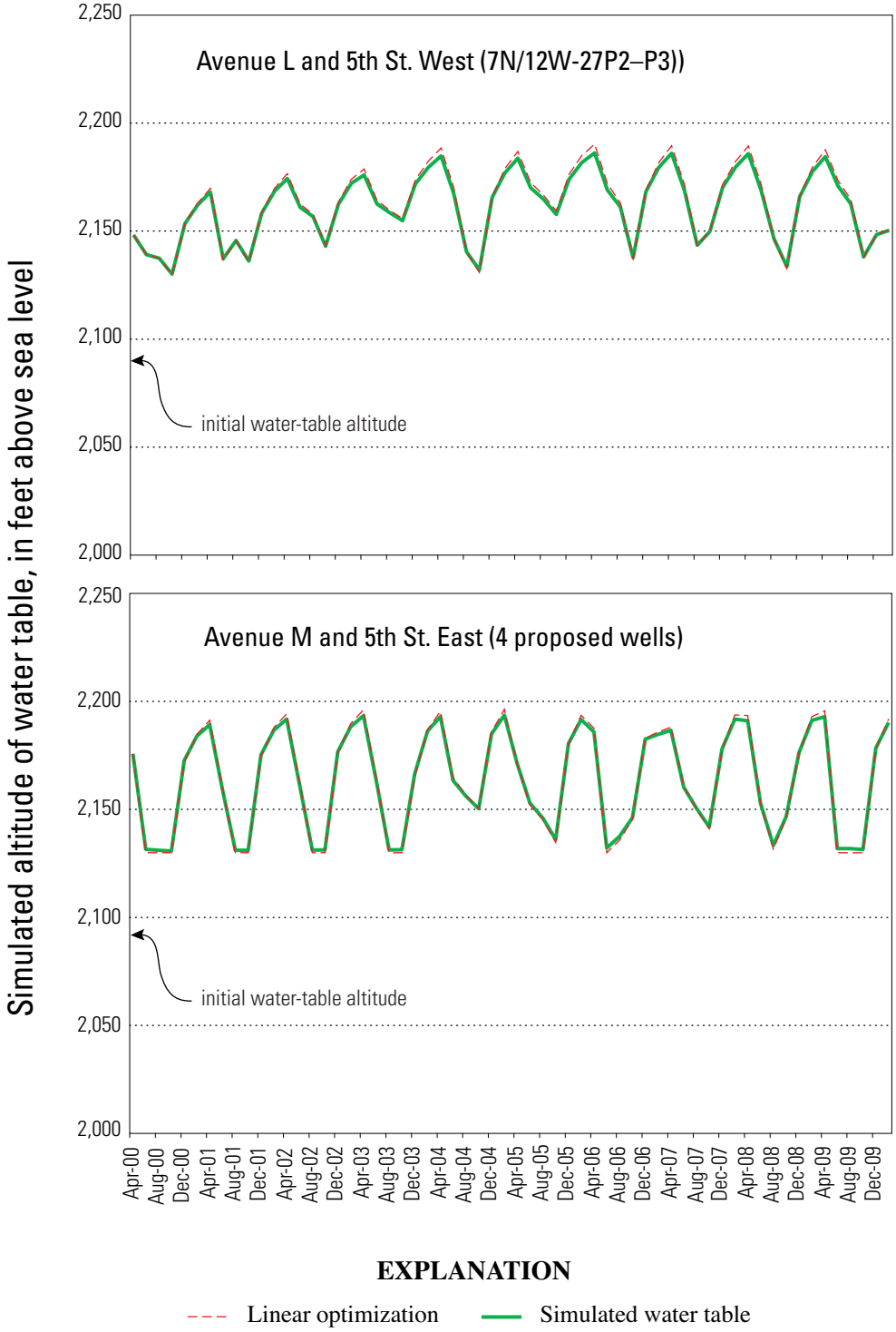

Figure 59. Water-table results from linear optimization and the ground-water-flow model using optimal injection and pumping rates for scenario 4 (all existing and proposed wells for injection during six months of the year), Lancaster, Antelope Valley, California.

Potential Improvements

The LANOPT model is useful for planning purposes, but its usefulness for management purposes is currently limited. This limitation is directly related to the assumptions and limitations discussed above, but it can be addressed by monitoring of injection sites, selecting appropriate optimization objectives, and improving the model, as needed. New information can be used to improve simulation results in areas that are currently poorly understood, and the objective and (or) constraints can be adjusted to better represent site conditions and future goals.

Monitoring the hydraulic and subsidence-related response to measured injection and extraction rates at each injection site would provide critical information needed to reduce model uncertainty. The water-level response would guide meaningful adjustment of the head constraints, which are highly subjective. If, for example, the water table rises too close to the land surface under optimal stresses, the upper head constraint should be adjusted downward and a new solution generated. Similarly, simultaneous monitoring of aquifer-system deformation and (or) land-surface elevation would allow determination of the preconsolidation head, on which the lower head constraint is based.

Improvement or adaptation of the LANOPT model may require changing the discretization of the model grid. Simulated water-level changes are sensitive to the size of model cells, particularly those cells in which stresses occur. Because simulated head changes represent the average change within a cell, large cells containing wells show a relatively muted response compared with smaller cells containing the same wells. Care must be taken to adjust head constraints appropriately.

Periodic evaluation of the availability of SWP water and any changes in ground-water demand is needed for development and maintenance of realistic constraints. No expanded monitoring is necessary, as these data are routinely gathered. The current constraints associated with these values are subject to significant short- and long-term error.

The conveyance, mixing, and storage of injected and extracted water was not accounted for in the LANOPT model. Difficulties may arise in implementing optimal strategies that do not take these aspects into account. In such cases, constraints could be added or modified to restrict capacities of individual or multiple wells sharing pipelines and (or) storage facilities.

The current optimization objective, to maximize the lowest value of head, is not the only approach to this problem, and may not be appropriate for future applications. Suppose, for example, that field measurements result in a minimum head for each well, below which capacity drops to unacceptable levels. One could then use these heads, or their equivalent, as minimum head constraints and the objective could be changed to maximize injection (if interested in using as much SWP water as possible) or to minimize injection (if costs are a concern). There is a wide range of objectives to choose from, and any change in focus or arrival of new information should result a re-evaluation of the objective.

The combination of measured stresses and water-level response is key to determining the magnitude and variability of well capacities. Long-term average injection and extraction capacities determined from field measurements would be an improvement from the current estimates. More importantly, perhaps, is the determination of the critical head below which extraction capacity will decrease rapidly. A combination of velocity logging within the well and simultaneous measurement of extraction and drawdown would provide an accurate means for determining this threshold. Once determined, the minimum head can be constrained at that well to avoid large losses in capacity.

If future management goals are changed to allow some subsidence to occur, the LANOPT model could be improved with respect to subsidence control and predicted head changes by simulating inelastic compaction. Future versions of optimization software likely will allow direct use of results from existing subsidence simulation tools. Note that because aquifer-system compaction and associated subsidence is not a linear function of head, nonlinearity would be introduced which may require an iterative linear or nonlinear approach.

SUMMARY AND CONCLUSIONS

This report documents the monitoring and analysis of the hydraulic, subsidence-related, and general chemical effects of a series of freshwater injection tests in Lancaster, California, and the development of the LAN and LANOPT models for use in planning and managing, respectively, a larger scale injection program. It is one of five U.S. Geological Survey reports describing this series of tests, which were designed to assess the feasibility of implementing an injection program as part of a management strategy to halt the depletion of ground-water resources and avoid future land subsidence.

Treated water from the State Water Project, which is potable, was gravity-fed at a rate of about 750 gal/min into one or two existing wells in Lancaster for as much as 5 months, stored for 2 to 4 weeks, and extracted at about the same rate. The wells used for injection fully penetrate the upper unconfined aquifer and penetrate most of the middle confined aquifer above the lacustrine unit. A flow analysis (velocity log) for one of the injection wells showed that much of the flow between the well and the aquifer system took place in the upper aquifer.

Monitoring during the tests fell into three primary categories: hydraulic (water levels), subsidence-related (aquifer-system and land-surface deformation), and chemical. Hydraulic monitoring included electronic and periodic measurements in nested piezometers and wells and microgravity surveys. The direct measurements showed that the hydraulic response to injection was significant within about a 1-mi radius of the injection wells. Coupled water-level and gravity measurements were used to estimate the specific yield (0.13). This value was then used to estimate the shape of the injection mound using the distributed measurements of gravity change.

Aquifer-system deformation was measured directly using a dual borehole extensometer located about 0.5 mi north of the injection site, and indirectly using first-order leveling, continuous GPS (Global Positioning System), and high-precision tiltmeters. The extensometer showed expansion of the aquifer system during injection and compaction during extraction. A portion of this compaction (for example, about 0.01 ft at the extensometer site from 1996 to 1997) was inelastic (permanent). Leveling results showed the range of deformation increased to the north, which is consistent with measurements from previous studies of Antelope Valley made using static GPS and InSAR (interferometric synthetic aperture radar). Leveling and tiltmeter measurements indicated that about 6 to 11 mm (about 0.02 to 0.04 ft) of uplift of the land surface at the injection site occurred during injection. Uplift may have exceeded this estimate, but it was not areally extensive, concentrated within several hundred feet of the well. Coupled measurements of water levels and aquifer-system deformation were used to estimate the elastic (1.2×10^{-6}/ft) and inelastic (4.0×10^{-5}/ft) skeletal specific storage values.

Major ions, selected trace metals, and trihalomethanes samples were analyzed, and field parameters were measured periodically in injected and extracted water. Constituent concentrations in injected water, including those for chloride and trihalomethanes, generally exceeded those in native ground water. Trihalomethanes were not detected in native ground water, but concentrations increased substantially between injection and extraction. Chloride concentrations did not exhibit this behavior, suggesting that trihalomethanes formed within the aquifer system after injection. Mass balance calculations for the second injection cycle using chloride suggested that the water extracted, which was 156 percent of the injected volume, contained 51 percent of the injected water, indicating a significant residual effect on ground-water chemistry.

A three-dimensional numerical model of ground-water flow (LAN model) was developed to estimate the hydraulic properties of the aquifer system in the Lancaster area, which is a subset of the area covered by a regional model for Antelope Valley. Results of calibration of the model showed there is an infinite, but predictable, set of hydraulic conductivity values (horizontal hydraulic conductivity of the upper and middle aquifers and vertical hydraulic conductivity between the aquifers) that result in reasonable simulation of long-term and seasonal water levels. Combined with independent information (the velocity log and microgravity results), a unique combination of these values was chosen from this set (17, 1.7, and 0.006 ft/d, respectively). The calibrated model closely simulated measured conditions in the vicinity of the injection wells, and reasonably simulated conditions elsewhere.

A simulation/optimization model (the LANOPT model) was developed using a modified version of the LAN model and commercially available optimization tools. The LANOPT model was used to estimate the relative effectiveness of four hypothetical management scenarios for halting the decline of ground-water levels in the southern Lancaster area and avoiding future land subsidence in the northern Lancaster area while meeting increasing ground-water demand. The scenarios consisted of maintaining present practices with no injection (scenario 1); injection allowed in 16 existing wells during a 6-month period (scenario 2); and injection allowed in the existing wells and the 13 proposed wells during 6- or 4-month periods (scenarios 3 and 4). Results of the LANOPT model indicate that a phased-in installation of the proposed wells will be required over a 10-year management period to maintain ground-water levels in the southern area of Lancaster while avoiding land subsidence in the northern area.

REFERENCES CITED

Ahlfeld, D.P., and Mulligan, A.E., 2000, Optimal management of flow in groundwater systems: San Diego, Calif., Academic Press, 185 p.

Anderson, M.P., and Woessner, W.W., 1992, Applied groundwater modeling—simulation of flow and advective transport: San Diego, Calif., Academic Press, 381 p.

Bear, J., 1972, Dynamics of fluids in porous media: New York, Elsevier Publishing Company, 764 p.

Behr, J.A., Hudnut, K.W., and King, N.E., 1998, Monitoring structural deformation at Pacoima Dam, California using continuous GPS: Satellite Division of the Institute of Navigation, 11th International Technical Meeting, Proceedings, ION GPS-98, Nashville, Tenn., p. 59–68.

Beutler, G., and Neilan, R., 1997, International GPS Service for Geodynamics: International Association of Geodesy General Assembly, Rio de Janeiro, Brazil, September 3–9, 1997.

Blissenbach, Erich, 1954, Geology of alluvial fans in semiarid regions: Geological Society of America Bulletin, v. 65, no. 2, p. 175–189.

Blodgett, J.C., and Williams, J.S., 1992, Land subsidence and problems affecting land use at Edwards Air Force Base and vicinity, California, 1990: U.S. Geological Survey Water-Resource Investigations Report 92–4035, 25 p.

Bloyd, R.M., Jr., 1967, Water resources of the Antelope Valley–East Kern Water Agency area, California: U.S. Geological Survey Open-File Report, 69 p.

California Department of Finance, Historical Census Populations of Places, towns, and cities in California, 1970–1980, 1980–1990, 1990–2000: accessed 1999, at URL http://www.dof.ca.gov/HTML/DEMOGRAP/E-1table.xls

Carlson, C.S., and Phillips, S.P., 1998, Water-level changes (1975–98) in the Antelope Valley, California: U.S. Geological Survey Water-Resource Investigations Report 98–561, 2 sheets.

Carlson, C.S., Leighton, D.A., Phillips, S.P., and Metzger, L.F., 1998, Regional water table (1996) and water-table changes in the Antelope Valley ground-water basin, California: U.S. Geological Survey Water-Resource Investigations Report 98-4022, 2 sheets

Danskin, W.R., and Freckleton, J.R., 1992, Ground-water-flow modeling and optimization techniques applied to high-ground-water problems in San Bernardino, California, *in* Subitzky, Seymour, ed., Selected papers in the hydrologic sciences 1988–92: U.S. Geological Survey Water-Supply Paper 2340, p. 165–177.

Danskin, W.R., and Gorelick, S.M., 1985, A policy evaluation tool: Management of a multiaquifer system using controlled stream recharge: Water Resources Research, v. 21, no. 11, p. 1731–1747.

Dibblee, T.W., Jr., 1967, Areal geology of the western Mojave Desert, California: U.S. Geological Survey Professional Paper 522, 153 p.

_____ 1981, Regional structure of the Mojave Desert, *in* Howard, K.A., and others, eds., Tectonic framework of the Mojave and Sonoran Deserts, California and Arizona: U.S. Geological Survey Open-File Report 81-0503, p. 26–28.

Dinehart, R.L., and McPherson, K.R., 1998, Topography, surface features, and flooding of Rogers Lake Playa, California: U.S. Geological Survey Water Resources Investigations Report 98-4093, 30 p.

Durbin, T.J., 1978, Calibration of a mathematical model of the Antelope Valley ground-water basin, California: U.S. Geological Survey Water-Supply Paper 2046, 51 p.

Dutcher, L.C., and Worts, G.F., Jr., 1963, Geology, hydrology, and water supply of Edwards Air Force Base, Kern County, California: U.S. Geological Survey Open-File Report, 225 p.

Federal Geodetic Control Subcommittee, 1984, Standards and specifications for geodetic control networks: Rockville, Maryland, National Oceanic and Atmospheric Administration, 29 p.

Fetter, C.W., 1994, Applied hydrogeology, third edition: New Jersey, Prentice-Hall, 691 p.

Fram, M.S., Bergamaschi, B.A., Goodwin, K.D., Fujii, Roger, and Clark, J.F., 2003, Processes affecting the trihalomethane concentrations associated with the third injection, storage, and recovery test at Lancaster, Antelope Valley, California, March 1988 through April 1999: U.S. Geological Survey Water Resources Investigations Report 03-4062, 72 p.

Fram, M.S., Berghouse, J.K., Bergamaschi, B.A., Fujii, Roger, Goodwin, K.D., and Clark, J.F., 2002, Water-quality monitoring and studies of the formation and fate of trihalomethanes during the third injection, storage, and recovery test at Lancaster, Antelope Valley, California, March 1998 through April 1999; U.S. Geological Survey Open-File Report 02-02, 48 p.

Fujii, Roger, Ranalli, A.J., Aiken, G.R., and Bergamaschi, B.A., 1998, Dissolved organic carbon concentrations and compositions, and trihalomethane formation potentials in waters from agricultural peat soils, Sacramento–San Joaquin Delta, California: Implications for drinking-water quality: U.S. Geological Survey Water-Resources Investigations Report 98-4147, 75 p.

Galloway, D.L., Hudnut, K.W., Ingebritsen, S.E., Phillips, S.P., Peltzer, G., Rogez, F., and Rosen, P.A., 1998a, Detection of aquifer-system compaction and land subsidence using interferometric synthetic aperture radar, Antelope Valley, Mojave Desert, California: Water Resources Research, v. 34, no. 10, p. 2573–2585.

Galloway, D.L., Jones, D.R., and Ingebritsen, S.E. (eds.), 1999, Land subsidence in the United States: U.S. Geological Survey Circular 1182, 175 p.

Galloway, D.L., Phillips, S.P., and Ikehara, M.E., 1998b, Land subsidence and its relation to past and future water supplies in Antelope Valley, California, *in* Borchers, J., ed., Land Subsidence—Case Studies and Current Research: Proceedings of the Dr. Joseph F. Poland Symposium on Land Subsidence, Association of Engineering Geologists Special Publication 8, p. 529–539.

Gorelick, S.M., Freeze, R.A., Donohue, David, and Keely, J.F., 1993, Groundwater contamination: Optimal capture and containment: Lewis, Boca Raton, FA, 385 p.

Greenwald, R.M., 1993, Documentation and user's guide: MODMAN and optimization module for MODFLOW, Version 3.0: Sterling, Va., GeoTrans, variously paged.

———1998, Documentation and user's guide: MODMAN and optimization module for MODFLOW, Version 4.0: HSI GeoTrans, Freehold, N.J., variously paged.

Halford, K.J., and Hanson, R.T., 2002, User guide for the drawdown-limited, multi-node well (MNW) package for the U.S. Geological Survey's modular three-dimensional finite-difference ground-water flow model, versions MODFLOW-96 and MODFLOW-2000: U.S. Geological Survey Open-File Report 02-293, 33 p.

Hanson, R.T., and Leake, S.A., 1999, Documentation for HYDMOD, a program for extracting and processing time-series data from the U.S. Geological Survey's modular three-dimensional finite-difference ground-water flow model: U.S. Geological Survey Open-File Report 98–564, 57 p.

Herring, T. A., 1998, GLOBK: Global Kalman Filter VLBI and GPS analysis program: Mass. Institute of Technology, Cambridge.

Hewett, D.F., 1954, General geology of the Mojave Desert region California, *in* Jahns, R.H., ed., Geology of Southern California: California Department of Mines and Geology, Bulletin 170, chap. 2, p. 5–20.

———1954b, A fault map of the Mojave Desert, California, *in* Geology of Southern California: California Division of Mines Bulletin 170, chap. 4, contribution 2, pl. 1, scale 1:630,000.

Hill, M.C., 1990, Preconditioned Conjugate-Gradient 2 (PCG2), a computer program for solving ground-water flow equations: U.S. Geological Survey Water-Resources Investigations Report 90–4048, 43 p.

Howle, J.F., Phillips, S.P., Denlinger, R.P., and Metzger, L.F., 2003, Determination of specific yield and water table changes using temporal microgravity surveys collected during the second injection storage and recovery test at Lancaster, Antelope Valley, California, November 1996 through April 1997: U.S. Geological Survey Water-Resources Investigations Report 03–4019, 28 p.

Ikehara, M.E., and Phillips, S.P., 1994, Determination of land subsidence related to ground-water level declines using Global Positioning System and leveling surveys in Antelope Valley, Los Angeles and Kern Counties, California, 1992: U.S. Geological Survey Water-Resources Investigations Report 94–4184, 101 p.

Izbicki, J.A., 1999, Transition Probability/Markov Chain analysis of the subsurface geology of the Victorville Fan in the western part of the Mojave Desert, southern California, *in* Reynolds, R.E., and Reynolds J., eds., Tracks along the Mojave; a field guide from Cajon Pass to the Calico Mountains and Coyote Lake, p. 55–63.

Izbicki, J.A., Christensen, A.H., and Hanson, R.T., 1999, U.S. Geological Survey combined well-bore flow and depth-dependent water sampler: U.S. Geological Survey Fact Sheet 196-99, 1 p.

Izbicki, J.A., Michel, R.L., and Martin, Peter, 1998, chloride and tritium concentrations in a thick unsaturated zone underlying an intermittent stream in the Mojave Desert, southern California, USA, *in* Brahana and others, eds., Gambling with groundwater—physical, chemical, and biological aspects of aquifer-stream relations: Proceedings of the Joint Conference of the International Association of Hydrogeologists and the American Institute of Hydrology, Las Vegas, Nev., September 28–October 2, 1998, p. 81–88.

Johnson, H.R., 1911, Water resources of Antelope Valley, California: U.S. Geological Survey Water-Supply Paper 278, 92 p.

Kennedy/Jenks Consultants, 1995, Antelope Valley water resource study—final report for the Antelope Valley Water Group: Ventura, Calif., variously paged [available from Kennedy/Jenks Consultants, 1000 Hill Rd., Suite 200, Ventura, California 93003].

King, R.W., and Bock, Y., 1998, Documentation for the MIT GPS analysis software: GAMIT: Mass. Institute of Technology, Cambridge.

Leake, S.A., and Prudic, D.E., 1991, Documentation of a computer program to simulate aquifer-system compaction using the modular finite-difference ground-water flow model: U.S. Geological Survey Techniques of Water Resources Investigations, book 6, chap. A2, 68 p.

Leighton, D.A., and Phillips, S.P., 2003, Simulation of ground-water flow and land subsidence in the Antelope Valley ground-water basin, California: U.S. Geological Survey Water-Resources Investigations Report 03-4016, 107 p.

Londquist, C.J., Rewis, D.L., Galloway, D.L., and McCaffrey, W.F., 1993, Hydrogeology and land subsidence, Edwards Air Force Base, Antelope Valley, California, January 1989–December 1991: U.S. Geological Survey Water-Resources Investigations Report 93-4144, 74 p.

Mabey, D.R., 1960, Gravity survey of the western Mojave Desert, California: U.S. Geological Survey Professional Paper 316-D, p. 51–73.

McDonald, M.G., and Harbaugh, A.W., 1988, A modular three-dimensional finite-difference ground-water flow model: U.S. Geological Survey Techniques of Water Resources Investigations, Book 6, Chapter A1, 586 p.

Metzger, L.F., Ikehara, M.E., and Howle, J.F., 2002, Vertical-deformation, water-level, microgravity, geodetic, water-chemistry, and flow-rate data collected during injection, storage, and recovery tests at Lancaster, Antelope Valley, California, September 1995 through September 1998: U.S. Geological Survey Open-File Report 01-414, 149 p.

Morin, Robert L., Mariano, John, and Jachens, Robert C., 1990, Isostatic residual gravity map of Edwards Air Force Base and vicinity, Kern, Los Angeles, and San Bernardino counties, California: U.S. Geological Survey Open-File Report 90-664, scale 1:62,500, 1 sheet.

Munsell Color, 1975, Munsell soil color charts: Baltimore, Md., Munsell Color, Macbeth Division of Kollmorgen Corporation.

Nishikawa, Tracy, 1998, A simulation/optimization model for water-resources management, Santa Barbara, California: U.S. Geological Survey Water-Resources Investigations Report 97-4246, 99 p.

Nishikawa, Tracy, Rewis, D.L., and Martin, Peter, 2001, Numerical simulation of ground-water flow and land subsidence at Edwards Air Force Base, Antelope Valley, California: U.S. Geological Survey Water-Resources Investigations Report 01-4038, 111 p.

Parkhurst, D.L., Thorstenson, D.C., and Plummer, L.N., 1980, PHREEQE—a computer program for geochemical calculations: U.S. Geological Survey Water-Resources Investigations Report 80-96, 216 p.

Phillips, S.P., Hamlin, S.N., and Yates, E.B., 1993, Geohydrology, water quality, and estimation of ground-water recharge in San Francisco, California, 1987–92: U.S. Geological Survey Water-Resources Investigations Report 93-4019, 69 p.

Poland, J.F., ed., 1984, Guidebook to studies of land subsidence due to ground-water withdrawal: United Nations Educational, Scientific and Cultural Organization, Paris, Studies and reports in hydrology 40, 305 p.

Ponti, D.J., 1985, The Quaternary alluvial sequence of the Antelope Valley, California: Geological Society of America Special Paper 203, p. 79–96.

Pool, D.R., and Eychaner, J.H., 1995, Measurements of aquifer-storage change and specific yield using gravity surveys: Ground Water, v. 33, no. 3, p. 425–432.

Pool, D.R., and Hatch, M., 1991, Gravity response to storage change in the vicinity of infiltration basins: Proceedings of the Fifth Biennial Symposium on Artificial Recharge of Groundwater, Tucson, Ariz., p. 171.

Prince, K.R., Galloway, D.L., and Leake, S.A., eds., 1995, U.S. Geological Survey Subsidence Interest Group Conference, Edwards Air Force Base, Antelope Valley, California, November 18–19, 1992: abstracts and summary: U.S. Geological Survey Open-File Report 94-532, 84 p.

Pyne, R.D.G., 1995, Groundwater recharge and wells—a guide to aquifer storage recovery: Boca Raton, Fla., CRC Press, Inc., 376 p.

Rantz, S.E., 1969, Mean annual precipitation in the California region: U.S. Geological Survey Open-File Report, 2 sheets, scale 1:1,000,000.

Reed, R.D., 1933, Geology of California: Tulsa, Okla., American Association of Petroleum Geologists, 355 p.

Reineck, H.E., and Singh, I.B., 1980, Depositional sedimentary environments: New York, Springer-Verlag, 552 p.

Rewis, D.L., 1993, Drilling, construction, and subsurface data for piezometers on Edwards Air Force Base, Antelope Valley, California, 1991–92: U.S. Geological Survey Open-File Report 93-148, 35 p.

Riley, F.S., 1969, Analysis of borehole extensometer data from central California, *in* Tison, L.J., Land Subsidence: International Association of Hydrological Sciences Publication 89, v. 2, p. 423–431.

———1998, Mechanics of aquifer systems—the scientific legacy of Joseph F. Poland, *in* Borchers, J., ed., Land Subsidence—Case Studies and Current Research: Proceedings of the Dr. Joseph F. Poland Symposium on Land Subsidence, Association of Engineering Geologists Special Publication 8, p. 13–27.

Schrage, Linus, 1991, LINDO user's manual release 5.3: Boyd and Fraser, New York, 132 p.

Sneed, Michelle, and Galloway, D.L., 2000, Aquifer-system compaction and land subsidence: measurements, analyses, and simulations—the Holly site, Edwards Air Force Base, Antelope Valley, California: U.S. Geological Survey Water- Resources Investigations Report 00-4015, 65 p.

Snyder, J.H., 1955, Ground water in California—The experience of Antelope Valley: Berkeley, California, University of California, Division of Agriculture Science, Giannini Foundation Ground-Water Studies No. 2, 171 p.

Templin, W.E., Phillips, S.P., Cherry, D.E., DeBortoli, M.L., and others, 1995, Land and water use in the Antelope Valley, California: U.S. Geological Survey Water-Resources Investigations Report 94-4208, 97 p.

Terzaghi, Karl, 1925, Principles of soil mechanics: IV; settlement and consolidation of clay: Erdbaummechanic, 95, 3, p. 874–878.

Thayer, W.N., 1946, Geologic features of Antelope Valley, California: Los Angeles County Flood Control District Report, 20 p.

Thompson, D.G., 1929, The Mohave Desert region, California, a geographic, geologic, and hydrologic reconnaissance: U.S. Geological Survey Water-Supply Paper 578, 759 p.

University of California Cooperative Extension, 1994, Using reference evapotranspiration (ETo) and crop coefficients to estimate crop evapotranspiration for agronomic crops, grasses, and vegetable crops: University of California Cooperative Extension, Division of Agriculture and Natural Resources Leaflet 21427, 12 p.

U.S. Environmental Protection Agency, National Primary Drinking Water Regulations: Accessed October 2, 2002, at URL http://oaspub.epa.gov/ogwdw/mcl.html

Wang, H.F., and Anderson, M.P., 1982, Introduction to groundwater modeling—finite difference and finite element methods: W.H. Freeman and Company, New York, 237 p.

Ward, A.W., Dixon, G.L., and Jachens, R.L., 1993, Geologic setting of the East Antelope Basin, with emphasis on fissuring on Rogers Lake, Edwards AFB, Mojave Desert, California: U.S. Geological Survey Open-File Report 93-263, 9 p.

Western Regional Climate Center, Southern California Climate Summaries: accessed July 10, 1999, at URL http://www.wrcc.dri.edu/summary/climsmsca.html